The IMPACT *of* CLIMATE CHANGE *and* Population Growth *on the* National Flood Insurance Program *through* 2100

prepared for

Federal Insurance and Mitigation Administration
Federal Emergency Management Agency

prepared by

AECOM

in association with

Michael Baker Jr., Inc.
Deloitte Consulting, LLP

June 2013

The Impact of Climate Change and Population Growth on the National Flood Insurance Program Through 2100

June 2013

prepared for

Federal Insurance and Mitigation Administration
Federal Emergency Management Agency

prepared by

AECOM

in association with

Michael Baker Jr., Inc.
Deloitte Consulting, LLP

IMPORTANT NOTE: All results in this report showing projected flood conditions (Section 4) should be interpreted for national averages only. Owing to inherent variability, projections should not be interpreted locally.

This report is dedicated to the memory of David Divoky, who was the originator of the technical approach and project leader for this study. Dave distinguished himself amongst some of the most intellectual technical experts in the world with his unpretentious methods of scientific investigations. Sadly, Dave passed away on February 4, 2012.

Dave was the guiding force throughout the project; he provided counsel to both senior and junior team members. He played a pivotal role in getting the team to collaborate creatively and develop innovative, simple solutions to carry out the analysis. The degree to which Dave challenged the younger team members was particularly impressive; he urged them to speak freely of their thoughts, ultimately facilitating a culture of innovative thinking with an open dialog fostering new ideas among the entire team. His keen sense of humor, intellectual wit, and academic brilliance will be greatly missed by his many friends and colleagues, but never forgotten.

About the FEMA Climate Change and Coastal Studies Project

This report presents the findings of one of three components of a project entitled *The Impact of Climate Change and Population Growth on the National Flood Insurance Program Through 2100 & Improving Coastal Floodplain Mapping*. Initiated in the fall of 2008, the project is sponsored by the Federal Emergency Management Agency (FEMA) and performed under a contract with AECOM. The project has significant implications for the protection of life and property nationwide, with three primary objectives:

- The first and most complex objective was to evaluate the likely impact of climate change and population growth on the National Flood Insurance Program (NFIP).
- The second objective was to evaluate FEMA's Primary Frontal Dune (PFD) regulations and policies. This involved evaluating current flood insurance and hazard identification regulations, policies, and guidelines that require the PFD to be included entirely within the coastal high hazard area (VE Zone).
- The third objective was evaluation of a new coastal flood insurance zone, the Coastal A Zone, to better account for the increased risk to property and life in areas subject to wave hazards below the 3-foot wave height threshold of the established VE Zone.

These three components of the project were addressed in three distinct studies and are presented individually in separate reports.

The present volume addresses the impact of climate change and population growth on the NFIP. The work was undertaken in November 2008 to provide an estimate of the likely financial impact on the NFIP associated with climate change and population growth through the year 2100. The work did not attempt a detailed site-by-site evaluation of conditions throughout the United States, but was based upon regional methods and engineering inference designed to produce a realistic estimate within limited time and budget constraints. No new climate modeling or projections were developed. Instead, the work plan specified that estimates should be based upon available material published through the *United States Climate Change Science Program* (CCSP) (now the United States Global Change Research Program) and the *Intergovernmental Panel on Climate Change* (IPCC) established by the World Meteorological Organization and the United Nations Environment Programme. Since the understanding of climate change is in a state of rapid development, the tools created during the work were developed so as to allow updates to be made with relative ease as the reliability of climate forecasts improves.

Contacts

Federal Emergency Management Agency (FEMA)

Mark Crowell, Contracting Officer's Technical Representative, Task Leader
500 C Street, SW
Washington, DC 20472
Phone: 202-646-3432
Email: mark.crowell@dhs.gov

AECOM

Perry Rhodes, Project Manager
3101 Wilson Blvd.
Arlington, VA 22201
Phone: 703-682-4914
Email: perry.rhodes@aecom.com

AECOM

David Divoky, Project Technical Leader (deceased)
One Midtown Plaza
1360 Peachtree Street NE, Suite 500
Atlanta, GA 30309
Phone: 404-861-8515
Email: david.divoky@aecom.com

Senior Review Panel Members

Federal Agency Representatives

Margaret Davidson, National Oceanic and Atmospheric Administration (NOAA) Coastal Services Center
Maria Honeycutt, on behalf of Margaret Davidson, NOAA Coastal Services Center
David Levinson, NOAA National Climatic Data Center
Kathleen White, U.S. Army Corps of Engineers, Institute for Water Resources
Howard Leikin, retired, formerly U.S. Department of the Treasury, Terrorism Risk Insurance Program

State Floodplain Representative

Tony Pratt, Delaware Department of Natural Resources & Environmental Control

Independent Members

Robert Dean, Professor Emeritus, University of Florida
William Gutowski, Professor, Iowa State University

Project Staff

AECOM

Scott Edelman, Principal-in-Charge
Perry Rhodes, Project Manager
Manas Borah, Assistant Project Manager
David Divoky, Project Technical Leader, Senior Scientist (deceased)
Josh Kollat, H&H Engineer, Assistant Technical Leader
Art Miller, Senior H&H Engineer
Joe Kasprzyk, H&H Engineer
Ray Yost, GIS Specialist
David Markwood, H&H Engineer
Kevin Coulton, Senior Coastal Scientist
Ben Pope, Senior H&H Engineer
Alisha Fernandez, H&H Engineer
Andy Wohlsperger, GIS Specialist
Susan Phelps, GIS Team Leader
Vivian Lee, Senior Environmental Engineer
David Manz, Senior Environmental Engineer

Michael Baker Jr., Inc.

Wilbert O. Thomas, Jr., Senior Hydrologist
Senanu Agbley, Coastal Scientist
Krista Conner, Coastal Scientist
Steve Eberbach, Coastal Scientist
Mark Osler, Senior Coastal Engineer
Lisa Winter, Coastal Engineer

Deloitte Consulting, LLP

Susan Pino, Economic/Actuarial Director
Joshua Merck, Economic/Actuarial Manager

Acknowledgments

The project team wishes to acknowledge the assistance provided by FEMA Headquarters staff, especially Mark Crowell, the FEMA Task Leader, who oversaw the entire project and provided critical review and guidance throughout; and Jonathan Westcott, who supported both this study and its companion study of primary frontal dunes and coastal mapping. We also wish to thank Sandra Knight, Roy Wright, Doug Bellomo, Emily Hirsch, Lois Forster, Nancy Steinberger, Tom Hayes, Andy Neal, and Dan Spafford of FEMA for their detailed reviews of the report and substantive comments and suggestions. Special thanks are due to Linda Bernhardt of CreativePages, LLC, who provided editorial support, and to Shannon Slobodien of AECOM, who contributed in many ways to the study, the logistics of meetings, and preparation of the report. Mary Miller of AECOM played an essential role in coordinating the work of the several project team offices and the organization of interim technical workshops.

We also wish to acknowledge the *Program for Climate Model Diagnosis and Intercomparison*, and the World Climate Research Programme (WCRP) *Working Group on Coupled Modelling* for their help in making available the WCRP CMIP3 multi-model dataset, supported by the Office of Science, U.S. Department of Energy; Bruce Douglas for his clarifying discussions of the implications of sea level rise and erosion; and Thomas Knutson, Geophysical Fluid Dynamics Laboratory/NOAA, for his timely help in obtaining updated tropical storm data.

We also thank the U.S. Global Change Research Program (USGCRP) for helping to arrange and facilitate reviews of this report from their member agencies and thank the Subcommittee on Water Availability and Quality (SWAQ) for their review of the report. Both groups are under Executive Office of the President, the National Science and Technology Council's Committee on Environment, Natural Resources and Sustainability.

Role of the Senior Review Panel

The project team especially wishes to acknowledge the Senior Review Panel, which played a key role in the study through a process of methodology and report review and comment, assistance identifying and obtaining data, and general encouragement. Their project reviews included participation in a two-day kick-off meeting in November 2008 to outline the proposed study plan, four online WebEx meetings to discuss interim progress and findings, and a final review meeting held in

AECOM's Arlington, Virginia, office in April 2010 prior to preparation of the draft report. Following distribution of the draft report, the panelists provided written comments and suggestions. The panel's efforts, however, should not be in any way construed as an endorsement of the study's findings by them or by their several agencies and organizations; their role was solely advisory, and responsibility for the work remains with the project team. Several suggestions for improvement of the study offered by the panelists were beyond the scope of this initial effort and have been incorporated in the recommendations that accompany the report.

Foreword

At the request of the Government Accountability Office (GAO), the Federal Emergency Management Agency (FEMA) funded a study in November 2008 on the effects of climate change and population growth on the National Flood Insurance Program (NFIP). Through the study, FEMA hopes to understand the potential impact of climate change on the financial strength of the NFIP and recommend options to increase the NFIP's viability. FEMA contracted with AECOM, in partnership with Michael Baker Jr., Inc. and Deloitte Consulting, LLP, to conduct an independent study and present the findings and recommendations to FEMA.

The study looked at both riverine and coastal flooding throughout the U.S. with estimates at 20-year intervals through the year 2100. AECOM relied on existing data, studies, reports, and research, including information from the *United States Climate Change Science Program* (now the United States Global Change Research Program), the *Intergovernmental Panel on Climate Change* (IPCC), and relevant papers contained in peer-reviewed academic journals. Although no new climate modeling was performed, the methods used to evaluate the data were innovative.

The study used a probabilistic approach to capture expected values and the important uncertainties around those expectations. After gathering the samplings, the projected flood estimates were interpreted for their NFIP implications through development of population-weighted averages of both flood elevation changes and floodplain area changes. These changes allowed for an economic assessment that includes the viability of the program, growth in policies, growth in premium and annual expected loss levels, and possible administrative considerations.

The study is groundbreaking in two major ways. First, it demonstrates innovative methods to capture the influence of climate change and population growth on the nation's flood hazards through the century, accounting for both riverine and coastal processes. Second, the study provides not only a median projection, but also important insight regarding the associated uncertainty inherent in the current state of climate modeling.

The study finds that over the next 90 years, there will likely be (50-percent chance) a significant increase in coastal and riverine flooding in our nation, which will have a

significant impact on the NFIP. The Federal Insurance and Mitigation Administration (FIMA) supports the findings in this study and is committed to increase public awareness of flood risk and promote action that reduces risk to life and property. If the risk of flooding increases as described in this report, there will be a need for FEMA to directly incorporate the effects of these changes into various aspects of the NFIP. As a nation, we need to acknowledge our risk, establish our roles, and work together to prepare for the future.

Table of Contents

List of Figures

List of Tables

Appendices

Executive Summary

Executive Summary

Origin and Purpose of the Study

This Climate Change Study was recommended by the *Government Accountability Office* (GAO) to assess the likely influence of climate change on the National Flood Insurance Program (NFIP). The recommendation further stated that FEMA should use assessments from the *United States Climate Change Science Program* (US CCSP) and the *Intergovernmental Panel on Climate Change* (IPCC) in conducting the analysis, rather than undertaking any independent climate modeling effort. The GAO recommendation was stated as follows (directed to both FEMA and the U.S. Department of Agriculture):

> *We recommend that the Secretary of Agriculture and the Secretary of Homeland Security direct the Administrator of the Risk Management Agency and the Under Secretary for Emergency Preparedness to analyze the potential long-term implications of climate change for the Federal Crop Insurance Corporation and the National Flood Insurance Program and report their findings to the Congress. This analysis should use forthcoming assessments from the Climate Change Science Program and the Intergovernmental Panel on Climate Change to establish sound estimates of expected future conditions. Key components of this analysis may include: (1) realistic scenarios of future losses under anticipated climatic conditions and expected exposure levels, including both potential budgetary implications and consequences for continued operation, and (2) potential mitigation options that each program might use to reduce their exposure to loss.*

The GAO recommendation addressed "climate change" in general terms, indicating that FEMA should perform a comprehensive analysis of potential changes in precipitation intensity and patterns, coastal storms, sea level rise, and other natural processes affecting both riverine and coastal flooding.

Aspects of the Study

- *Scope of the Effort* – The climate change and population growth impact assessment considered all 50 states and U.S. territories. However, since the concern is impact on the NFIP as a whole, it was recognized that not all national regions have the same relative significance. A detailed region-by-region assessment of climate change was not intended. Primary attention was to be given to areas of greatest population and largest inventory of at-risk properties. The study considered climate change and population growth projections through the year 2100, with interim estimates at 20-year intervals, or epochs.
- *Source Data* – It was not within the scope of the study to perform any new or independent climate research or climate modeling. Instead, the findings and source materials of the US CCSP and the IPCC (Fourth Assessment Report) were

relied upon to the greatest extent possible, with other necessary information, such as population projections, based upon the work of authoritative sources, especially official government sources where available.

- *Measures of Flood Hazards* – The NFIP characterizes the flood hazard at any place, in part, by the floodwater surface elevation having a 1% chance of being equaled or exceeded in any given year. This elevation is identified as the *Base Flood Elevation* (BFE) and is the primary basis for flood insurance and floodplain management requirements within communities participating in the NFIP. Areas of higher risk associated with coastal wave action are identified where appropriate. In addition to the BFE, the community flood hazards are also characterized by the 10%, 2%, and 0.2% annual chance water levels. The sources of flooding include precipitation runoff in riverine areas throughout the nation's interior and coastal storm effects on all U.S. coastlines. Areas affected by the BFE are identified as lying within the *Special Flood Hazard Area* (SFHA) and are usually denoted as being within AE and VE Zones on flood insurance rate maps.

Technical Approach

The technical engineering approach for this study was based on the fact that the BFE and other flood factors are statistical or probabilistic in nature. Consequently, a probabilistic approach was used in which a range of climate changes was considered. In general, the climate factors of interest include both the *frequency* and the *intensity* of storms that influence flooding. In riverine areas, intensity is primarily associated with the amount of rainfall during storm episodes, whereas in coastal areas, storm intensity is primarily characterized by winds and pressures that produce large waves and storm surge. The riverine and coastal approaches are briefly summarized below. All engineering analyses were based on equal consideration of three greenhouse gas emissions scenarios: A2, A1B, and B2. These scenarios, as defined in Appendix A.3, depend upon assumed population growth, and represent a balanced range between low and high climate change impact.

The report is a scoping-level study and as such, the results can be further enhanced as new and more robust climate change predictions become available. The study gives a first order prediction of the impact of climate change and population growth on the NFIP.

Riverine Flooding – Changes in riverine BFEs may be caused by regionally varying increases or decreases in precipitation frequency and quantity as the controlling storms become more or less frequent, and more or less intense. Riverine floods also depend upon the rate of runoff from a watershed, and so depend upon factors such as urbanization (promoting more rapid and abundant runoff from a particular storm), which, in turn, depends upon changes in population and population distribution patterns.

The approach taken in the study was based on well-established methods of riverine hydrology, chiefly the concept of a *regression equation* to relate flood discharges to watershed or basin characteristics. Watershed characteristics that are commonly represented in a regression model include such things as drainage area, channel slope, percentage of impervious area, and storage area. In order to incorporate climate change into the approach, this study expanded the list of candidate regression factors to include a set of *extreme climate indices* reported in climate model projections. These several indices include such factors as the annual maximum five-day precipitation (R5D), the number of days per year with rainfall exceeding 10 mm (R10), the maximum number of consecutive dry days (CDD) per year, the total number of frost days (FD) per year, and so forth. In order to establish which indices are significant, and to establish appropriate regression relationships incorporating those indices, regression analyses were performed with data taken from 2,357 stream gage stations across the United States. The flood discharges at these stations were not affected by regulation from flood detention structures upstream of the gages. The analysis determined the relative statistical importance of each climate index in explaining the variability of unregulated stream flows, and led to specification of simple expressions from which stream flow can be estimated for given values of the indices. Then, using climate modeling results through the year 2100, stream flow response was determined accordingly. The projected future discharges from this analysis do not reflect the effects of constructing flood detention structures to mitigate the future impacts of climate change.

In addition to changes in climate, there will be changes in population. Those changes influence riverine flooding since developed land promotes more rapid runoff. Consequently, projected changes in population are used to estimate changes in basin impervious area, one of the non-climate regression factors. Other factors such as drainage area and channel slope do not, of course, change with changing climate. There are a number of different population assumptions that could be assumed; the population assumptions used in this study were consistent with the assumptions made in the basic emissions scenarios used in the climate modeling.

The regression equations provide estimates of stream flow. From projected changes in flow, the study estimated the associated changes in flood depths and in floodplain areas. Taken together, these changes in the BFE and SFHA are the key factors needed to complete the financial and insurance assessment portion of the study.

Coastal Flooding: Sea Level Rise – The important flood mechanisms are quite different in coastal regions, and include both gradual sea level rise (SLR) and the effects of storms. The consideration of SLR in this study is broadly similar to an earlier FEMA study (1991) of the impact of SLR, but based upon more recent

projections. Projections of the rate of global SLR (the *eustatic* rise) are available from climate studies and are adjusted to account for local variability along U.S. coastlines. *Relative* SLR may also be partly caused by regional land subsidence, which must be separately considered.

For this study, the U.S. coast was divided into 13 zones in such a way that the projected SLR within each zone is approximately uniform. Associated with SLR is the likelihood of enhanced long-term shoreline erosion and recession, which is a significant process since its effect may be to move the coastal SFHA substantially inland by 2100.

The SLR estimates used in the study were based upon the recent work of Vermeer and Rahmstorf (2009) which is widely quoted in the recent literature. Depending upon the emissions scenario being considered, they estimated that the global rise at 2100 would average approximately 1.2 meters (4 feet) over the three emissions scenarios adopted here, with still higher levels possible owing to variability or uncertainty of the estimates. It has been noted by Nicholls, et al. (2010), however, that while these projections are a pragmatic range of possibility, it is unlikely that values in the upper portion of the range will actually occur. The study team recognizes the presence of uncertainty inherent to the SLR projections applied in this study, yet considers the projections used appropriate given the agreement found in existing climate science literature that the range of sea level increases applied are possible. In addition, the average eustatic sea level increase applied in the study is approximately consistent with the conclusion made by the U.S. Global Change Research Program's Synthesis and Assessment Product 4.1, which states: "thoughtful precaution suggests that a global sea level rise of 1 meter to the year 2100 should be considered for future planning and policy decisions" (CCSP, 2009). The range of SLR projections applied in the study could be revisited following release of Assessment Report 5 from the Intergovernmental Panel on Climate Change.

Coastal Flooding: Storms – As with riverine flooding, coastal flood hazards depend upon both storm frequency and intensity. The most significant coastal flood hazard, nationally, is associated with tropical storms and hurricanes. In this study, the influence of changes in tropical storm and hurricane frequency was accounted for in a straightforward manner, based upon data taken from existing coastal flood insurance studies on a county basis. Flood stage-frequency curves taken from the existing FEMA flood studies were adjusted for both projected changes in storm frequency and projected changes in storm intensity. A similar approach was used in other areas such as the Pacific Coast where the flood mechanisms are somewhat different from those of hurricane regions.

As with riverine flooding, it was necessary to estimate the change in the affected SFHA. For coastal regions, this was done in two ways. In the first, it was assumed that existing shorelines would be maintained through 2100, despite sea level rise and erosive forces tending to cause shoreline recession. In the second, similar to the assumption made in FEMA's 1991 sea level rise study, it was assumed that shorelines will retreat so as to compensate for sea level rise.

The Monte Carlo Approach –The general statistical computational approach for both riverine and coastal areas was based on Monte Carlo simulations drawn from a range of projected possibilities. The approach involves random sampling of that range for each parameter of interest. Each sample represents a possible future, with the entirety of the computations giving an estimate of the range of uncertainty or variability in the future estimates. The median values were taken to be the projections of interest for subsequent interpretation.

Demographic Analysis

The engineering analysis was followed by a demographic analysis to determine the projected population, number of insurance policies, and related factors within flood hazard areas through 2100. This work was based on county-level data, developed from Census Block and other data, including insurance and loss data. Existing SFHA information was projected forward according to the engineering findings, as were population densities, numbers of structures, numbers of policies, and other parameters, categorized according to flood hazard zone.

Insurance and Economic Aspects

The insurance and economic analyses were based on the information generated as described above. The growth in the number of policies estimated for the program was based on the growth in overall population and on the change in the percentage of the population within the riverine and coastal floodplain areas. It is noted, then, that part of the economic projections are independent of climate change, and will occur owing to normal population growth during the century.

The results were developed from county-based demographic information, and then aggregated to the national level. As with the engineering evaluations, the results should not be interpreted as plausible projections at the local level owing to the inherent variability introduced by the methodology. Results at the national scale, however, are deemed representative within the fundamental assumptions of the technical approach and the present limitations of climate projections.

The ratio of number of current policies to the current population was determined (the concentration factor) separately for riverine and coastal areas inside and outside the floodplains. In addition to the concentration factor, the proportions of policies within

different categories were also determined (e.g., policies at "grandfathered" rates). The future populations within and outside the floodplains were estimated based on the results of the climate change analysis, and were further subdivided into components due to population growth and to floodplain area growth. Assuming constant concentration factors and other simple proportionalities, future policy counts were estimated. The program premium at each future epoch was estimated by multiplying the policy counts by current average premiums, considered separately by:

- County;
- Subsidized or actuarially rated risks; and
- Riverine floodplain, coastal floodplain, riverine non-floodplain, and coastal non-floodplain.

The economic analysis first developed a baseline loss cost at the county level, based on an assumed average distribution of structure types and heights relative to the BFE. At each future epoch, future loss cost was determined by accounting for the shift in the location of structures relative to the BFE. The shift in the BFE was based on the percentage change in floodplain depth determined by the climate change analysis and the average floodplain depth of the county.

At each future epoch, policies added incrementally since the prior epoch were added at the new risk classification or at the prior risk classification if they resulted from population growth. At each epoch, the overall indicated change in loss cost was weighted based on the amount of premium at each risk classification.

From these analyses, results are presented tabularly by epoch for growth in policies and premiums; changes in premiums by risk classification; changes in loss cost by risk classification; and changes in risk classification and loss cost under different re-build assumptions.

General Findings

For the riverine environment, the typical 1% annual chance floodplain area nationally is projected to grow by about 45%, with very large regional variations. The 45% growth rate is a median estimate implying there is a 50% chance of this occurring. Floodplain areas in the Northwest and around the Great Lakes region may increase more, while areas through the central portions of the country and along the Gulf of Mexico are expected to increase somewhat less. No significant decreases in floodplain depth or area are anticipated for any region of the nation at the median estimates; median flood flows may increase even in areas that are expected to become drier on average. Within typical developed areas of primary interest for the NFIP, approximately 30% of these increases in flood discharge, SFHA, and base floodplain depth may be attributed to normal population growth, while approximately

70% of the changes may be attributed to the influence of climate change. The implication is that on a national basis approximately 30% of the 45% (or 13.5%) growth in the 1% annual chance floodplain is due solely to population growth and would occur even if there is no climate change. Conversely, approximately 70% of the 45% (or 31.5%) growth in the 1% annual chance floodplain is due solely to climate change and would occur even if there is no population growth. The split is highly variable from place to place, and so should not be taken as a definitive value; the relative importance of population growth will be much less in undeveloped areas, but will be greater than the national average in densely populated centers.

For the coastal environment, under the assumption of a fixed shoreline, the typical increase in the coastal SFHA is projected to also be about 55% by the year 2100, again with very wide regional variability. The 55% increase is a median estimate so there is a 50-percent chance of this occurring. The subsequent projections in this section are all median estimates implying there is a 50% chance of them occurring. The typical increase may be less along the Pacific Coast and more for portions of the Gulf of Mexico and the Atlantic coasts. Under the receding shoreline assumption, negligible change in the coastal SFHA is projected. This is due to the fact that recession serves to reduce the size of the SFHA and so reduces chronic exposure. The sporadic losses incurred during recession are also accounted for in the analysis.

Nationally, considering riverine and coastal floods together, the average increase in the SFHA by the year 2100 is projected to be about 40% or 45%, according to whether coastal recession is assumed or is not assumed.

For the economic analysis under the assumption of a receding shoreline, the total number of NFIP insurance policies was projected to increase by approximately 80% by 2100. The number of riverine policies may increase by about 100%, and the number of coastal policies may increase by approximately 60%. The increase in the number of polices is due in part to normal population growth and in part to the effect of climate change on the size of the SFHA.

The average loss cost per policy in today's dollars under this assumption may increase approximately 50% by the year 2100, with cumulative increases of about 10% to 15% through the year 2020 and 20% to 40% through the year 2080.

Average premium per policy for the receding shoreline scenario are projected to increase as much as 40% in today's U.S. dollars by the year 2100 in order to offset the projected increase in loss cost.

Under the assumption of a fixed shoreline, the total number of NFIP policies may increase by approximately 100% by the year 2100, with number of riverine policies increasing by about 80% and the number of coastal policies increase by as much as

130%. The greater number of coastal policies is the result of the enlargement of the SFHA caused by sea level rise.

The average loss cost per policy under this assumption may increase approximately 90% by the year 2100, with cumulative increases of about 10% to 15% through the year 2020 and 20% to 60% through the year 2080.

Average premium per policy for the fixed shoreline scenario would increase as much as 70% in today's U.S. dollars by the year 2100 in order to offset the projected increase in loss cost, corresponding to a cumulative increase of about 0.6% per year.

Organization of the Report

Section 1 of the report presents a general introduction regarding the study approach, while Sections 2 and 3 discuss the engineering methodology. Major findings (projections for the riverine and coastal environments) are presented graphically in Section 4 using national maps, while the economic and insurance analyses are discussed in Section 5. Section 6 provides a somewhat more detailed summary of the generalized findings than is presented in this Executive Summary, as well as a list of technical issues that should be considered and addressed in any future refinement of the work.

1.0
General Introduction

1.0 General Introduction

1.1 Origin of the Study

This study was initiated in November 2008 in response to a request from the Government Accountability Office (GAO) in its report *CLIMATE CHANGE: Financial Risks to Federal and Private Insurers in Coming Decades Are Potentially Significant* (March 2007). In that report, the GAO recommended that the Secretaries of Agriculture and Homeland Security analyze the potential long-term fiscal implications of climate change for the Federal Crop Insurance Corporation's crop insurance and for the National Flood Insurance Program (NFIP) flood insurance programs, respectively, and report their findings to Congress. The study reported here was performed for FEMA to assess the implications for the NFIP.

1.2 Study Objectives and Scope

The objective of the work was to evaluate the potential sensitivity of flood severity and extent throughout the United States to climate change and population change, and to assess the consequent financial and insurance implications. Both interior riverine flooding caused by rainfall runoff, and coastal flooding caused by ocean storms and sea level rise were considered. The study considered change through the 21st century, with findings given at 20-year intervals. These 20-year snapshots are referred to as the study *epochs* throughout the report. They should not be construed as precise predictions, but simply as estimates based on physically plausible assumptions. This is an initial, scoping-level assessment of the potential for significant vulnerabilities of the NFIP, at the national scale, across a range of scientifically plausible future climate change (i.e., it is a first order treatment). As such, it provides a foundation for future, more detailed and regionally relevant studies that would be appropriate for informing specific management decisions.

Although the study is national in scope, some areas were not addressed in detail. Areas outside the contiguous 48 states do not contribute significantly to the national flood hazard assessment and so are included in the analysis only by extension; that is, the relatively small climate change implications of those areas are assumed to obey the same trends established in the detailed study. It is noted, for example, that over 75% of the nation's flood losses since 1978 have occurred in the coastal states on the Gulf of Mexico and the Atlantic. The three mainland Pacific states account for another 3.5%, so that nearly 80% of the loss experience has occurred in the mainland coastal states. This is not to say, however, that those losses have all been coastal in nature – the loss numbers include both riverine and coastal floods.

1.3 Data Sources

This work did not include any independent climate change analysis as such. Instead, in accordance with guidance from FEMA and GAO, the evaluation is based primarily upon information published by the *U.S. Global Change Research Program* (USGCRP), their *Climate Change Science Program* (CCSP) reports, and by the *Intergovernmental Panel on Climate Change* (IPCC), including their supporting papers and Fourth Assessment Report. Additional, more recent information has been used where appropriate. Appendix A details the key literature that was identified to provide pertinent data; a bibliography of sources categorized by topic, can be found in supplementary materials provided to FEMA. Additional references are summarized in Appendix G.

1.4 Intended Use of the Findings

It is important at the outset to clarify the intended use of this scoping-level study, and to caution against inappropriate uses. It is a first order approximation for the assessment of the impact of climate change and population growth on the NFIP. The findings are based upon climate projections with several sources of uncertainty, ranging from natural, but unpredictable factors, to uncertainties in human behavior, to climate model simulation error. The study does not address or include how adaptation might take place; rather it focuses on what impacts are caused by climate and population changes. Although the methods are necessarily approximate owing to the large geographic scale of the analysis, they have been developed in an effort to avoid systematic bias and so to provide reasonable estimates at the aggregate national level. That is, although the climate and engineering uncertainties are significant locally, they tend to cancel out the national aggregate, with the result that national totals remain acceptable.

For this reason, the study findings are intended only for guidance regarding national policy evaluations for the National Flood Insurance Program. Although determination of the required nationwide numbers inevitably proceeded through a cumulative sequence of calculations for individual local regions, it is only the aggregate average of those local estimates that are deemed appropriate for consideration.

In particular, nothing presented here should be construed as a projection of conditions at any particular location appropriate for local planning or engineering design purposes. The findings in this report should not be and are not intended for use in any update of flood insurance rate maps. The intended uses are restricted to providing NFIP policymakers with a first-order estimate of the possible significance of climate change, and to serve as the foundation for more refined analysis as the science of climate change advances.

1.5 Structure of the Report and Associated Materials

This report consists of two major portions: 1) the main text material contained in Sections 1.0 through 5.0, and the technical recommendations for future studies summarized in Section 6.0; and 2) seven appendices. The front text section presents the study methods and findings in overview, with most of the technical detail being presented in the appendices. It is hoped that this approach provides a clear exposition of the nature and findings of the study, unimpeded by excessive technical detail. Where the details of the methods are of interest, the reader will refer to the appropriate appendix.

In addition to the report itself, the study documentation includes a great deal of supporting information in the form of digital files provided separately to FEMA on DVD. That material includes raw and working data files, additional results of a secondary nature, computer codes, and other items of a specialized nature not suited to the primary report document.

2.0
Engineering Methods

2.0 Engineering Methods

2.1 Accounting for Uncertainty

Projections of future climatic conditions are inherently uncertain for two major reasons. First, although great progress has been made in understanding the physics of climate and in the ability to simulate likely changes by using powerful numerical models, much research and analysis still remains to be done. Second, climate change will depend to some degree upon human choices and actions over the next decades, and these cannot be known with any certainty. Therefore, no scenarios of policy change were investigated because there will likely be a wide range of regional policy changes.

Several approaches to characterizing the uncertainty of future climate simulations are found in the literature; (see, for example, Carter et al., 2007). Approaches vary in the level of physical detail and in the manner in which the *likelihood* or the *probability* of an outcome is addressed. The *scenario* method is the approach commonly encountered, and consists of postulating particular values for governing factors; for example, sea level might rise by some amount if a postulated event occurs in Greenland; approaches based on storylines are plausible sequences of scenarios.

For the present study, the goal is to better understand the vulnerability of potential future climate change on the financial and insurance aspects of the NFIP, based on current scientific understanding. To achieve (or approach) this goal requires a method of analysis that can account for the range of possible futures as partly influenced by the range of possible human actions and by the estimated response of the global climate system.

Furthermore, the method should provide measures of the likelihood of those futures, covering a range between low and high extremes of possible impacts, with a best estimate somewhere in between. The approach that has been adopted in this study seeks to provide quantitative estimates of the possible degree of variability around median values. For this scoping-level study, the median values based on national averages form the basis of the economic analyses.

2.1.1 Types of Uncertainty

There are two fundamentally different types of uncertainty that are confronted in this study: *epistemic* and *aleatory.*

Epistemic uncertainty is the uncertainty caused by lack of knowledge; aleatory uncertainty is associated with an inherent randomness of a natural process. For example, human response to climate change is unknown, and so epistemic. There will be some response; it will not be random – just unknown at this time. Similarly,

the accuracy of computer models and physical assumptions introduce epistemic uncertainties. Aleatory uncertainty remains the irreducible minimum in the reliability of the projections. For example, even if climate change could be forecast perfectly, the random nature of the day-to-day *weather* occurring within a given climate ensures that the flood process remains highly variable. This sort of variability is recognized in the definition of the Base Flood Elevation (BFE) as the flood elevation having a 1% chance of being exceeded in any given year.

For this study, it is important to recognize that there is a very great deal of epistemic uncertainty in the currently available climate change forecasts. One important product of this work is the set of computational tools that have been developed, and which can be applied at a future time to new ranges of climate futures to better illuminate the range of potential risk to the NFIP.

2.1.2 Uncertainties of Input Data

There are two major levels of uncertainty in the climate data used for the study. First, there are numerous global climate models that have been constructed by independent researchers, and numerous assumptions regarding future greenhouse gas emissions that go into those models. For a given emissions assumption (an emissions scenario) each model yields a different forecast. For a given model, each emissions scenario yields a different forecast. Second, even with a given model and a given emissions scenario, forecasts can still be uncertain, perhaps with defined ranges of variability – for example, that some parameter is expected to lie within a stated range with a defined chance.

An additional broad class of uncertainty has to do with societal change. Examples of this include possible changes in relative population density owing to unknown future migration patterns, or a community's response to sea level rise. For the former, the study has assumed that population density patterns will not change over time because any assumption of population migration would be very speculative; for the latter, two bracketing analyses have been done with the assumptions of shorelines held fixed or allowed to recede.

2.1.3 The Monte Carlo Method

The method used in this study to capture uncertainties is the *Monte Carlo* method. This is one of many approaches, but was selected here for its simplicity as an initial approach. More refined methods, including Bayesian techniques, could be used in future studies. In a Monte Carlo analysis, a large number of simulations are performed, making random choices for each controlling factor in proportion to that factor's likelihood, or weight. Among the important factors are the emissions scenarios representing various assumptions for the levels of future emissions, the global climate model used to make climate projections for a particular emissions

scenario, the manner in which population growth influences rainfall runoff rate, and so forth. Other factors can be identified as pertinent to the flood change forecast and added to this list, each with an associated estimate of uncertainty or variability reflected in a weight. For the present work, however, emissions scenarios and global climate models have not been weighted, but have been taken as equally plausible.

With these assumptions, the Monte Carlo method proceeds by performing a very large number of simulations, for each, choosing a set of input parameters (one emissions scenario, one model, one population growth assumption, and so forth), and assigning each set a relative weight. The choices are made so that the several parameters within a simulation are mutually consistent (based on the same population growth assumption, for example). The watershed characteristics such as drainage area, channel slope, and storage were not varied, as they do not change with time. The result might be an estimate of change in the BFE at some site in the year 2060. This estimate is saved and the process is repeated many times.

The full set of results will show wide variation, because sometimes the random choices will combine so as to produce a result toward one extreme or the other, although the majority of the results will tend to peak in a middle zone corresponding to the most likely input choices. In this study, the middle of the range, the median of the sample results, is assumed to be representative of the estimate of the BFE change, while the upper and lower portions of the results indicate possibilities around the median. Knowledge of this variability is important for assessing the influence of climate change on the NFIP, since it provides a measure of the relative reliability of the median. If the upper and lower values (at the upper and lower quartiles, for example) are not too different from the median, then the median can be judged relatively more reliable than if the upper and lower values are widely different. It must be kept in mind, however, that the study was performed using representative but unweighted emissions scenarios, with the assumption that all of the considered climate models are equally skillful. Consequently, the results at this time are qualified, and should be construed as plausible projections based on the assumptions, not as precise forecasts.

The technical details of the Monte Carlo analyses are provided in Appendices B and C for the riverine and the coastal flood calculations. As discussed in Appendix B, the regression equations for the riverine analysis were defined on a national basis in order to have sufficient variation in the climatic indicators. Therefore, the Monte Carlo simulations were performed on a national basis.

Three emissions scenarios were used in all of the Monte Carlo simulations: A2, A1B, and B1. These three scenarios cover a range of future assumptions regarding emissions, and are also directly related to assumptions regarding global population

growth. Appendix A.3 gives a discussion of these fundamental choices. They represent possible responses of the global community to climate change, and have been treated equally.

2.2 Riverine Floods

The method used for the riverine areas of the nation involves the use of *regression equations*, following traditional hydrologic techniques, to estimate 1% annual chance flood flows. The conventional approach has been extended here to include climate parameters among the explanatory variables. In a traditional study, the flood discharge (commonly represented by the symbol *Q*) flowing through a stream is taken to depend upon a number of physical factors including the rainfall, the basin area, the basin slope and surface characteristics, and so forth. If the discharge flowing through the stream is known, one can also determine the depth of flow, or the elevation of the water surface, using hydraulic computer models.

The simple form of a traditional riverine regression equation (see Appendix B for more detailed discussion) is:

$$Q_{1\%} = k(DA)^{P1}(SL)^{P2}(IA+1)^{P3}$$

where $Q_{1\%}$ is the 1% annual chance (or 100-year return period) discharge, *k* is a coefficient, *DA* is the area of the drainage basin, *SL* is the channel slope, and *IA* is the impervious area of the basin. The similar notation $Q_{10\%}$ is used for the 10% annual chance discharge, corresponding to the 10-year return period. The coefficient and the powers are determined through an analysis that relates observed *Q*s to the observed parameters, and finds the set of values that provides the best statistical agreement between the two sides of the equation. Other frequencies of discharge give different sets of coefficients and powers. Note that any number of parameters thought to be significant for the estimation of *Q* could be included in the expression, not just the three parameters shown in this simplified example. Part of the effort of a regression analysis is to determine whether such parameters are significant or not – that is, whether their inclusion significantly improves the predictions of the equation. If a parameter is not found to be important, it is eliminated from the expression. The parameters on the right-hand side of the expression are called the *explanatory variables* for the dependent parameter on the left.

It is emphasized that regression expressions such as these do not express physical laws as do most equations of engineering and physics. Instead, they are strictly statistical constructs providing approximate fits to observations although, of course, the explanatory variables are not chosen arbitrarily, but are based on physical knowledge of basins and flood processes. Their usefulness depends upon the

adequacy of the fits, expressed as the amount of variability of the observations around the simplified regression expressions.

The approach used in this study was to generalize the traditional regression equation shown above to also account for climate change and population growth factors. This was done by adding additional climate-related explanatory variables and population-related factors, and fitting the generalized expression to observed values of *Q* using corresponding values of the climate and population factors as obtained from observations. The following section summarizes the approach and findings, which are described in detail in Appendix B.

2.2.1 Extreme Climate Indices

A set of base climate parameters, the *extreme climate indices* or *indicators,* have been commonly identified in the climate literature. For example, Frich et al. (2002) reported on ten extreme climate indices (five based on temperature and five based on precipitation) that were determined to be statistically robust indicators of world-climate extremes. Eight of these extreme climate indices were chosen for consideration in this study and are specified in Table 2-1 derived from Tebaldi et al. (2006). The extreme climate indices describe a range of climate characteristics.

Table 2-1. Descriptions of the eight climate indices considered in this study (based on Tebaldi et al., 2006).

Indicator	Description	Units
FD	Total number of frost days, defined as the annual total number of days with absolute minimum temperature below 0◦ C.	days
GSL	Growing season length, defined as the length of the period between the first spell of five consecutive days with mean temperature above 5◦ C and the last such spell of the year.	days
TN90	Warm nights, defined as the percentage of times in the year when minimum temperature is above the 90th percentile of the climatological distribution for that calendar day.	%
R10	Number of days with precipitation greater than 10mm per year.	days
CDD	Annual maximum number of consecutive dry days.	days
R5d	Annual maximum 5-day precipitation total.	mm
SDII	Simple daily intensity index, defined as the annual total precipitation divided by the number of wet days.	mm d^{-1}
R95T	Fraction of total precipitation due to events exceeding the 95th percentile of the climatological distribution for wet day amounts.	%

The manner in which the new regression analysis was performed is detailed in Appendix B. The first step was to obtain values for the climate indices over a regular grid covering the nation. A typical example is shown in Figure 2-1 for the case of

climate indicator R10. (See Appendix B for a discussion of data sources and methods that were used for this analysis.) Baseline information to define current conditions included streamflow studies extending back to the 1950s. As noted by Lins and Slack (2005), while some upward flow trends are seen over the baseline period, they are primarily in the low flows and are not evident in the larger magnitude flood flows. Consequently, stationarity was assumed to be a sufficient approximation for the present study over the baseline period.

Figure 2-1. Gridded R10 observed climate indicator for the U.S. in 1951. The black dots represent the stations used to derive the gridded climate data (Alexander et al., 2005). The scale units are number of days annually with precipitation greater than 10mm, as shown in Table 2-1.

The second step was to estimate values for each of the climate parameters, at each of 2,357 stream gaging stations (not affected by flood detention structures) throughout the United States, as shown in Figure 2-2. This was done by interpolating from the gridded climate cells to each stream gage site. A regression analysis incorporating these indices could then be performed.

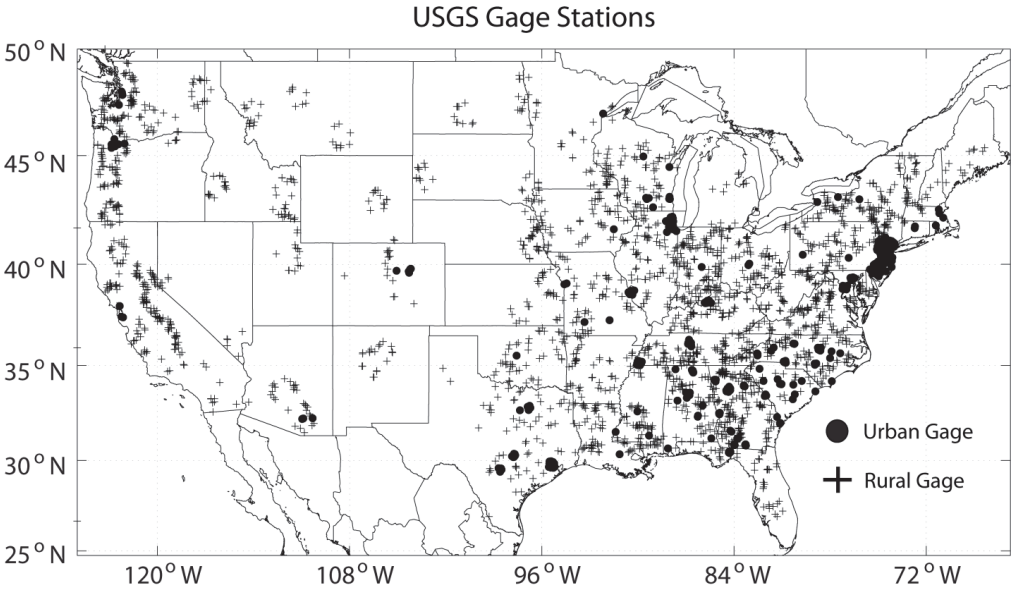

Figure 2-2. Locations of 2,357 USGS gaging stations – 384 urban (circles) and 1,973 rural (crosses) – used to develop the generalized regression relationship between $Q_{1\%}$, $Q_{10\%,}$ and watershed characteristics, and climate indicators for observed conditions.

2.2.2 New Climate Dependent Regression Equations

The flood estimates to be shown subsequently depend upon both the 10%-annual chance (10-year) conditions and the more extreme 1%-annual chance (100-year) conditions. Consequently, a regression analysis was performed at both of these frequency levels. The method is detailed in Appendix B. As explained there, the statistical procedure determines a best exponent for each candidate variable in an augmented expression, and assesses the degree to which that variable improves the prediction. Variables that do not improve the regression prediction to a statistically significant degree are dropped from consideration.

The following equation was established for $Q_{10\%,}$ and involves three climate indicators:

$$Q_{10\%} = 0.1093 DA^{0.723} SL^{0.158} (ST+1)^{-0.339} (IA+1)^{0.222} (MFD+1)^{-0.044} (MCDD+1)^{-0.395} (MR5D+1)^{1.812}$$

where the variables are as previously defined. The set of explanatory variables was expanded to include FD (the annual number of frost days), CDD (the maximum number of consecutive dry days per year), and R5D (the annual maximum five-day precipitation). The prefix *M* for each of these climate indices denotes mean values of the observed data used to establish the expression.

For $Q_{1\%}$ the similar result is:

$$Q_{1\%} = 0.321 DA^{0.711} SL^{0.169} (ST+1)^{-0.332} (IA+1)^{0.188} (MFD+1)^{-0.206} (MCDD+1)^{-0.177} (MR5D+1)^{1.440}$$

The annual maximum five-day precipitation (R5D) was found to be the sole precipitation predictor of the effects of climate change for this data set because:

- MR5D is the climatic index found to be most correlated with the flood discharges.
- MR5D has a correlation of 0.98 with MSDII, so the latter precipitation variable is effectively redundant and need not be included separately in the regression equation.
- MR5D has a correlation of 0.61 with MR10, the number of days per year with precipitation greater than 10 mm, and so partially accounts for the latter precipitation variable. MR10 is mildly significant when included in the regression equation, but does not improve the standard error significantly.
- From a hydrologic perspective, the annual maximum five-day precipitation is a reasonable predictor of the flood discharge because future changes in maximum precipitation should be directly related to changes in maximum (or flood) discharges. The five-day precipitation is the most reasonable precipitation predictor that is available from the GCM analyses. The five-day precipitation is correlated with short-term precipitation data making this variable applicable to small and large watersheds.

Two other climatic indices not directly measuring precipitation were also found to be statistically significant: the mean annual number of frost days (FD) and the mean number of consecutive dry days (CDD) per year. The full analysis and final regression forms incorporating all statistically significant explanatory variables are presented in Appendix B. Additional details on the regression analysis are also given in Kollat et al. (2012). The discharges computed from the two equations shown above form the basis of the riverine flood change estimates for this study.

2.2.3 Dependence of Water Surface Elevation on *Q*

Once the discharges are known, the next step is to determine water depths. In a typical engineering or flood insurance study, this is done using detailed and site-specific hydraulic models – an approach not practical for a nationwide study. Instead, it is necessary to adopt simplified rules relating water depth to discharge that can be easily applied at a national scale.

Burkham (1978) presented a regression expression relating the water depth in a channel to the discharge, *Q*. The present study has adopted this idea and developed it with additional data (see Appendix B). It is a practical approach that meets the needs of the study well. The expression is of the form:

$$h = aQ^b$$

where h denotes water depth from the channel bottom, and a and b are constants chosen to best fit the available data. If Q1% changes from a present value, Qp, to a future value, Qf, then the water depth h – and the BFE – changes by the amount:

$$\Delta h = BFE_f - BFE_p = a(Q_f^b - Q_p^b)$$

where the symbol Δ denotes the change of a parameter. This relationship, using the expressions for *Q* discussed in the previous section, provides the first of two essential measures of the impact of climate change on flooding: the change in flood depth. For this national scoping-level study, the channel geometry or flood depth was assumed to be constant with time, that is, no allowance for erosion or sedimentation. The second measure, discussed in the next section, is a measure of how much the corresponding floodplain area (the *Special Flood Hazard Area*, or SFHA) changes as a result of this change of depth. For use in the financial and insurance analyses, information regarding changes in water depth and floodplain area will be coupled with demographic information (projected according to emissions scenarios at each 20-year study epoch) to provide estimates of changes in the pertinent flood insurance factors.

2.2.4 Dependence of Floodplain Area on *Q*

Having established the method to estimate changes in flood flow, *Q*, and the associated changes in depth, the remaining hydraulic problem is to estimate how those changes will alter the size of the flooded areas. Again, this study has adopted a very simple assumption based on the idea that small to moderate changes in flood depth will result in proportional changes of flooded area.

In FEMA flood studies, the primary regulatory flood hazard area is called the *Special Flood Hazard Area* (SFHA) and is defined to be the area inundated by the 1% annual chance flood. Consequently, the SFHA will change in response to changes in the 1% annual chance flood depth discussed in the preceding section. Note that a change in the 1% annual chance flood depth measured from the bottom of the channel equals the change in the BFE usually measured with respect to NAVD (the North American Vertical Datum), since the datum is not relevant for *changes* of level. The procedure is encapsulated in Figure 2-3.

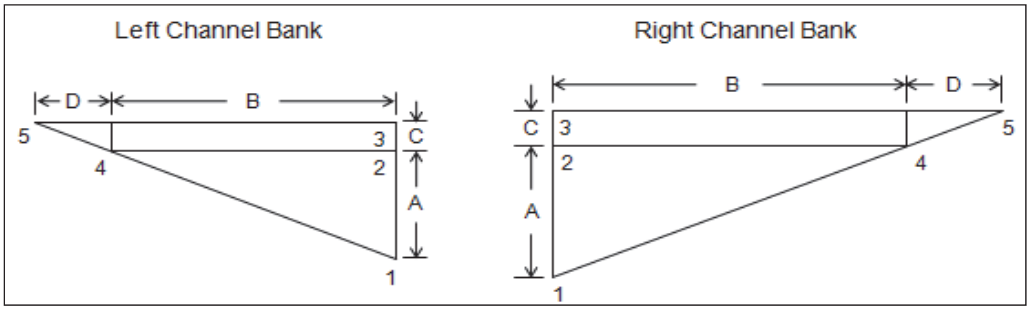

Figure 2-3. Defining sketch of overbanks and the method to estimate the change of the SFHA. See text for explanation of symbols.

In this sketch, a typical flood zone is represented by the reach *B* defined by the intersection of the current flood level *A* with the rising overbank regions at the points denoted *4*. The overbank zone is idealized as a triangular wedge defined by a mean slope between the effective *bank* denoted by *1* and the limit of flooding at *4*. Note, too, that the two overbank regions are not assumed to have equal slopes.

If climate change causes discharges to change so that the BFE increases by the amount *C*, then the SFHA on each side will change proportionally, by the amounts labeled *D*. As noted, the overbanks need not be similar, so that the two values of *D* will generally be different. However, the *percentage* changes for the overbanks will be equal, and it is only the percentage change that enters into the subsequent economic analysis.

An essential feature is the bank level, *1*, above which the similar left and right triangles are defined. The physical assumption is made that bank levels approximate the elevation of a stream surface flowing somewhat higher than a typical annual level (for which the banks would contain the flow) but below an extreme level (such as the BFE) for which the flow would produce an overbank flood condition.

As discussed in Appendix B.6, adopting the 10% annual chance flow depth derived from $Q_{10\%}$ through the simple regression expression of Section 2.2.3 was an adequate proxy for the unknown bank levels, 1. That is, adopting $D_{10\%}$ derived from $Q_{10\%}$ produced estimates of floodplain top width, B, in sufficient agreement with a large number of comparison values that were obtained from an inspection of detailed hydraulic modeling from past FEMA flood studies.

2.3 Coastal Floods

The methodology used for coastal regions was quite different from that just described for riverine regions. Whereas riverine changes were characterized indirectly by changes in the climate indicators, coastal flood changes are related directly to the characteristics of storms and sea level rise. Detailed analysis is found in Appendix C. The states bordering the Great Lakes have been included in the riverine analysis, but not in the coastal analysis. It is highly uncertain whether the lake levels might decline or rise slightly over time (whereas global sea level rise affects all outer coasts). In a recent study, Wuebbles et al. (2009) projected Great Lakes water levels to fall by as much as 1 foot by the end of the century under the SRES B1 scenario; under A2 emissions scenarios, the levels were projected to fall between 1 to 2 feet. These emissions scenarios will be discussed later in this report, and are two of three used in the present analysis. It is noted that the lake levels are also subject to a degree of unforeseeable human control and, in any case, coastal losses in the affected states represent only a very small fraction of the national exposure.

2.3.1 Sea Level Rise Regionalization

In this study, sea level rise (SLR) was considered regionally dependent, based in part upon the Coastal Vulnerability Index (CVI) defined by the U.S. Geological Survey (USGS) (Thieler, et al. 1999–2000), and upon data obtained from the National Oceanic and Atmospheric Administration's (NOAA) Center for Operational Oceanographic Products and Services (CO-OPS) (data available online). In all, the U.S. coastline was divided into 13 regions. Finer regionalization was neither feasible nor necessary within the scope of this nationwide study. In addition, it provided a means of parameterization within the Monte Carlo simulations. The goal was to define regions exhibiting relatively uniform historical sea level trends, although considerable variability remains, especially in the Pacific Northwest.

The ten mainland regions are shown in Figures 2-4 through 2-6; additional regions outside the mainland area are not shown. The historical trends shown in these figures were derived from the USGS CVI data set by length-weighted averaging of values at hundreds to thousands of shoreline segments within a region. There is a great deal of variability within and between regions. Region 6, for example, reflects local subsidence effects leading to a large relative SLR rate, while Region 9 reflects tectonic uplift, leading to a negative relative rate. The trends shown in Region 9 are especially generalized, with many sub-segments having positive rather than negative trends. This lack of spatial resolution might be addressed in future refinements of this study if better local projections are needed; it is not thought to be of significance to the national averages of interest here since the coastal flood hazard is dominated by the conditions on the Gulf and Atlantic coasts.

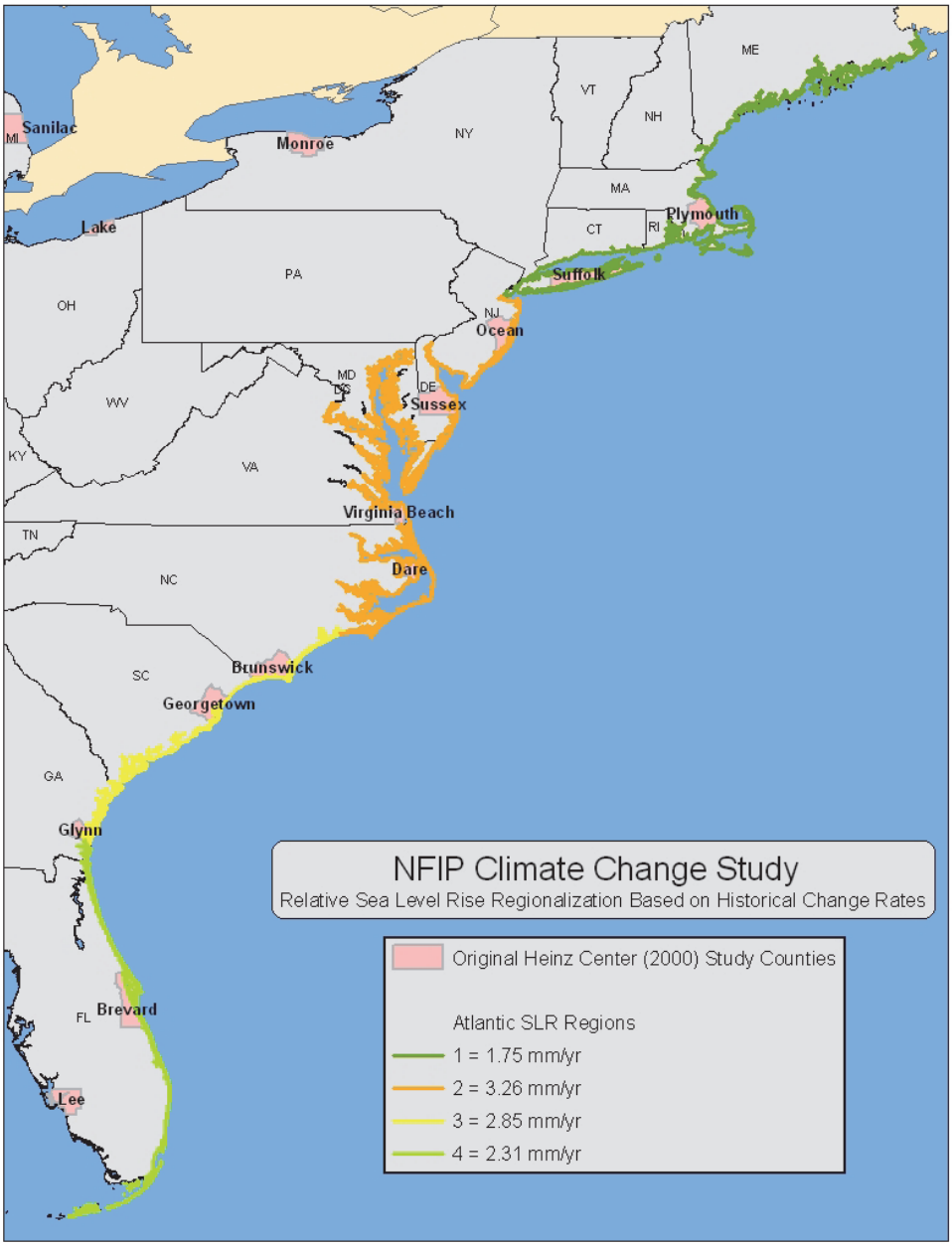

Figure 2-4. The four Atlantic SLR regions defined for this study.

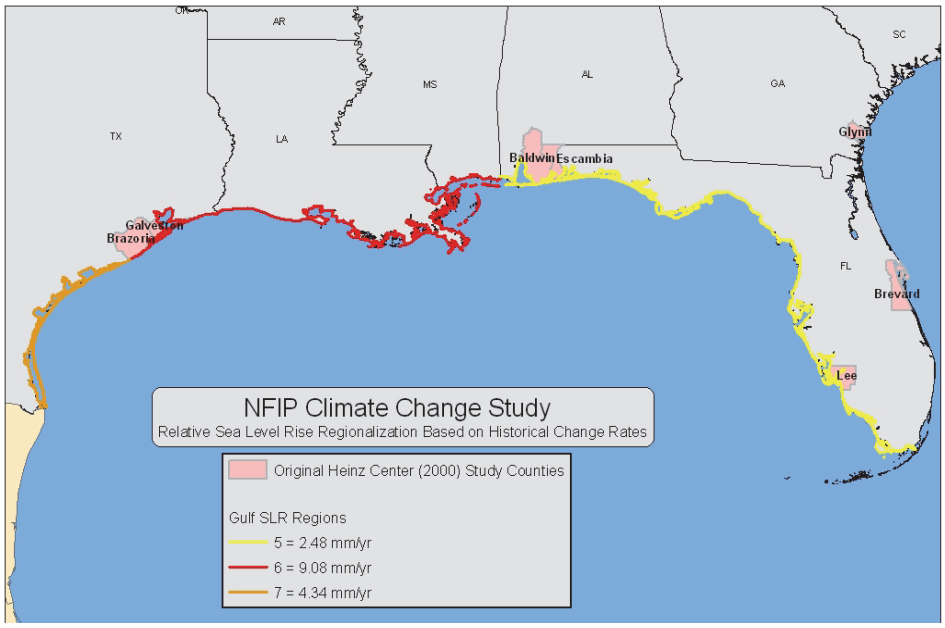

Figure 2-5. The three Gulf of Mexico SLR regions.

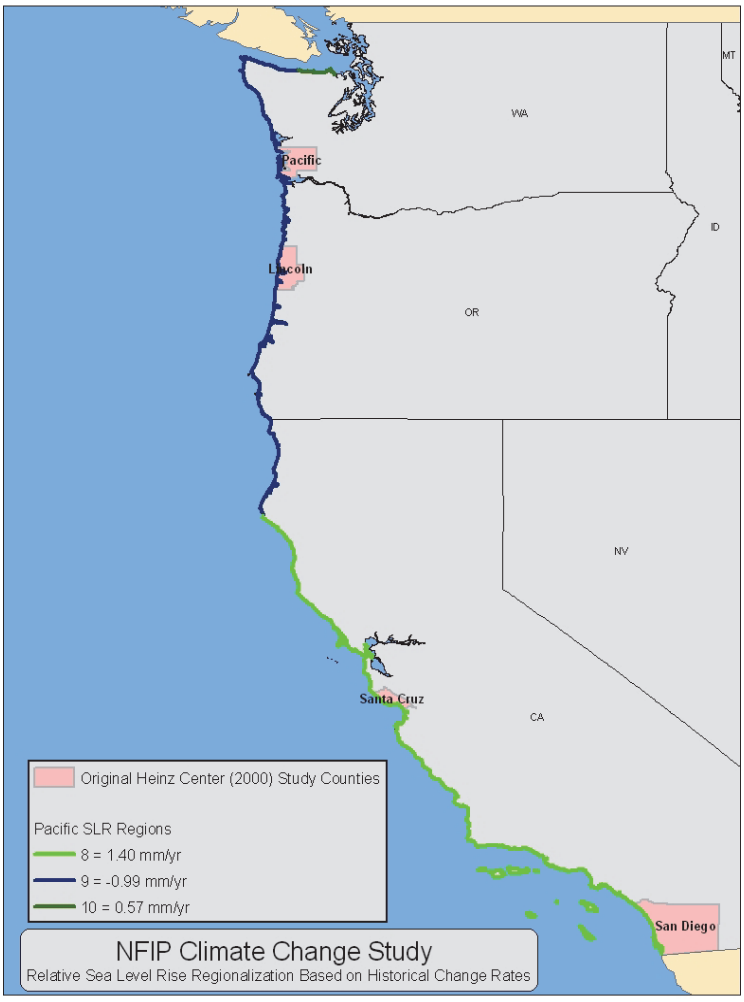

Figure 2-6. The three Pacific Coast SLR regions.

Future SLR is accounted for in the coastal methodology as a simple add-on to existing water levels (both normal and storm levels). The amount added within each of the defined regions at each of the epochs depends upon the climate forecasts adopted in the Monte Carlo sampling schemes discussed in later sections.

The projections used for future sea level rise in this study (based on Vermeer and Rahmstorf, 2009; see Appendix C) are consistent with the commonly considered possibilities, but are nonetheless highly uncertain. For example, the acceleration of sea level rise adopted in the present projections is tentative and, in fact, a small deceleration has been reported in some studies; see, for example, Douglas (1992) and a recent discussion in Houston and Dean (2011). A recent paper by Nicholls et al. (2010) suggests that while 0.5m to 2.0m of eustatic rise during the twenty-first century (consistent with the projections in this study) represents a pragmatic range of possibility, it is nevertheless unlikely that values in the upper portion of the range will actually occur.

The study team recognizes the presence of uncertainty inherent to the SLR projections applied in this study, yet considers the projections used appropriate given the agreement found in existing climate science literature that the range of sea level increases applied are possible. In addition, the average eustatic sea level increase applied in the study is approximately consistent with the conclusion made by the U.S. Global Change Research Program's Synthesis and Assessment Product 4.1 which states, "thoughtful precaution suggests that a global sea level rise of 1 meter to the year 2100 should be considered for future planning and policy decisions" (CCSP, 2009). The range of SLR projections applied in the study could be revisited following release of Assessment Report 5 from the Intergovernmental Panel on Climate Change.

2.3.2 Coastal Storms and Climate Change

The coastal flood analysis is, unlike the riverine case, based directly on the frequency and intensity of storms, most importantly tropical storms, including hurricanes. There are two key factors affecting coastal 1% annual chance flood levels: the frequencies and the intensities of storms.

Changes in storm frequency can be simply propagated through the analysis by adjusting the existing flood height vs. frequency information from existing flood insurance studies. That is, if storms at a site become 10% more frequent, then what is now the 1% annual chance flood (the 100-year flood) would be the 1.1% annual chance flood, or at about the 91-year level. The entire stage-frequency curve would scale in this same way.

Changes in storm intensity directly affect flood height. For tropical storms, storm intensity is measured by the central pressure deviation from normal, and it is known that flood elevation varies almost linearly with this pressure deviation. Other flood processes, such as wave runup, respond in a similar fashion to changes in storm intensity as measured by wind speed.

2.3.3 Changes in Coastal Flood Elevations

For tropical storms and hurricanes, it can be assumed that storm surge scales vary nearly linearly with storm intensity, as measured by the central pressure depression. An example of this, taken from the recent FEMA Hazard Mitigation Technical Assistance Program (HMTAP) study of Mississippi, is shown in Figure 2-7.

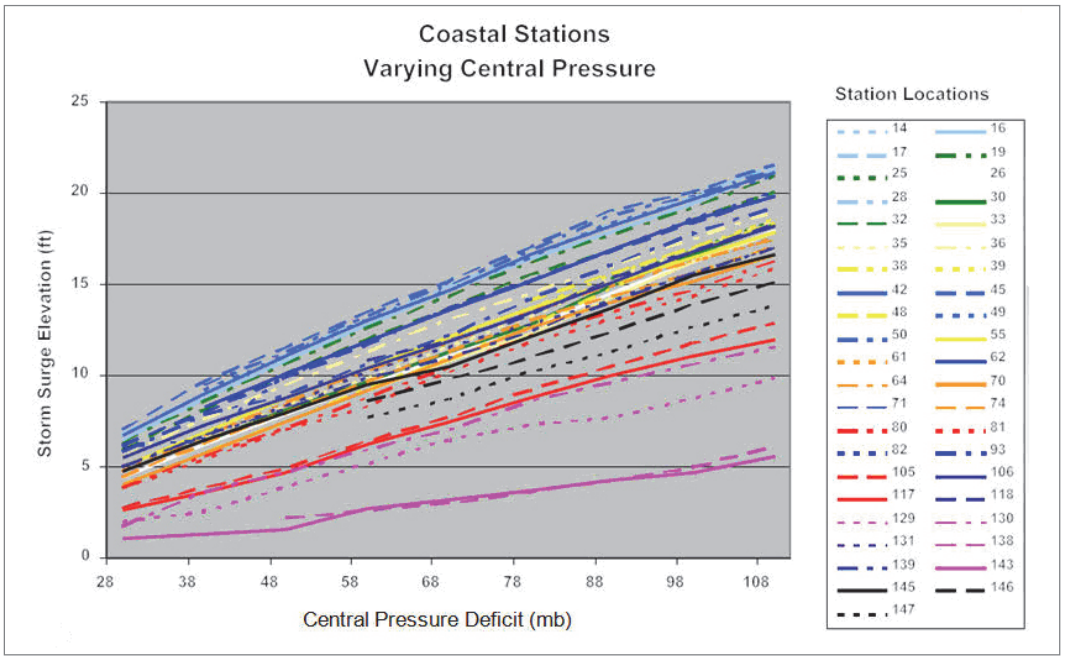

Figure 2-7. The variation of storm surge with central pressure depression for numerous coastal and inland stations in Mississippi (FEMA HMTAP Mississippi Coastal Study).

Each line in the figure corresponds to a site within the study area. The linearity of the surge response with storm intensity is clear. It is recognized that for the strongest storms there is an eventual flattening of these curves, but linearity prevails in the range most pertinent to 1% annual chance flood events. With storm frequency and intensity in mind, climate change can be related to a change in surge level by a two-step process of, first, adjusting for change in storm frequency, and second, adjusting for change in storm intensity. The slope of an existing surge vs. intensity curve can be determined from coastal flood insurance studies which include tables of data for all four FEMA basic flood levels established in FEMA studies: the 10%, 2%, 1%, and

0.2% annual chance (commonly referred to as the 10-, 50-, 100-, and 500-year flood levels, respectively). The procedure is illustrated in Appendix C.

2.3.4 Changes in Coastal Flood Hazard Areas

Figure 2-8 illustrates the simplified approach adopted in coastal areas for determination of changes of SFHA. Although this figure applies primarily to tropical storm surge environments, it is illustrative of other areas. Note that this approach resembles the riverine overbank assumptions discussed in an earlier section, and also the assumptions adopted in FEMA's 1991 Sea Level Rise study.

In the simplest assumption, the rising coastal floodplain is approximated by a plane slope, shown in green in Figure 2-8. The storm surge level obtained from the currently effective flood insurance study is indicated by the lighter blue horizontal line (horizontal by assumption). The existing stillwater surge intersects the rising land at the indicated Current Floodplain Width. The currently effective BFEs include a contribution from waves traveling on top of the surge level. In accordance with FEMA's standard methodology, the maximum wave addition is limited to 55% of the available water depth, which equals the difference between the (flat) surge level and the (rising) land level – this is shown by the sloping dashed blue line, intersecting the land surface at the same point as the surge (where waves must vanish). While waves contribute to the BFE, they do not ordinarily expand the SFHA, since wave breaking reduces wave height to zero at the inland limit of the SFHA.

The combined effects of storm frequency and intensity changes are suggested by the heavier horizontal blue line that intersects the land surface at a greater distance inland. Under 100-year hurricane conditions, the wave field at the open coast is assumed to be maximal, so that the same wave contribution is assumed: that is, an increase in the flood surface estimated to be 55% of available water depth. Then the adjusted BFE profile remains similar to the existing profile, but is shifted upward and extends farther inland. Note that in this simplified procedure, any increase associated with sea level rise is included as an additive term in the difference between current and future still water surge levels. Any changes in the astronomic tide are neglected.

2.4 Population and Land Use

2.4.1 Population and Impervious Area Projections

Population growth directly affects riverine flood hydraulics through modification of the terrain and landcover, such that the runoff rate in a watershed tends to increase with increasing population density. This is typically represented by the Impervious Area (IA) parameter in hydrologic models and regression relationships. Consequently, the financial influence of population growth consists both of population growth itself, and the increase in flood risk area caused by the secondary effects of population growth.

F = Surge Factor
- function of change in sea level & storm components

Slope Category	Profile Slope (M)
Very Highly Sloped	<0.2
Highly Sloped	0.2-0.07
Moderately Sloped	0.07-0.04
Low Sloped	0.04-0.025
Very Low Sloped	<0.025

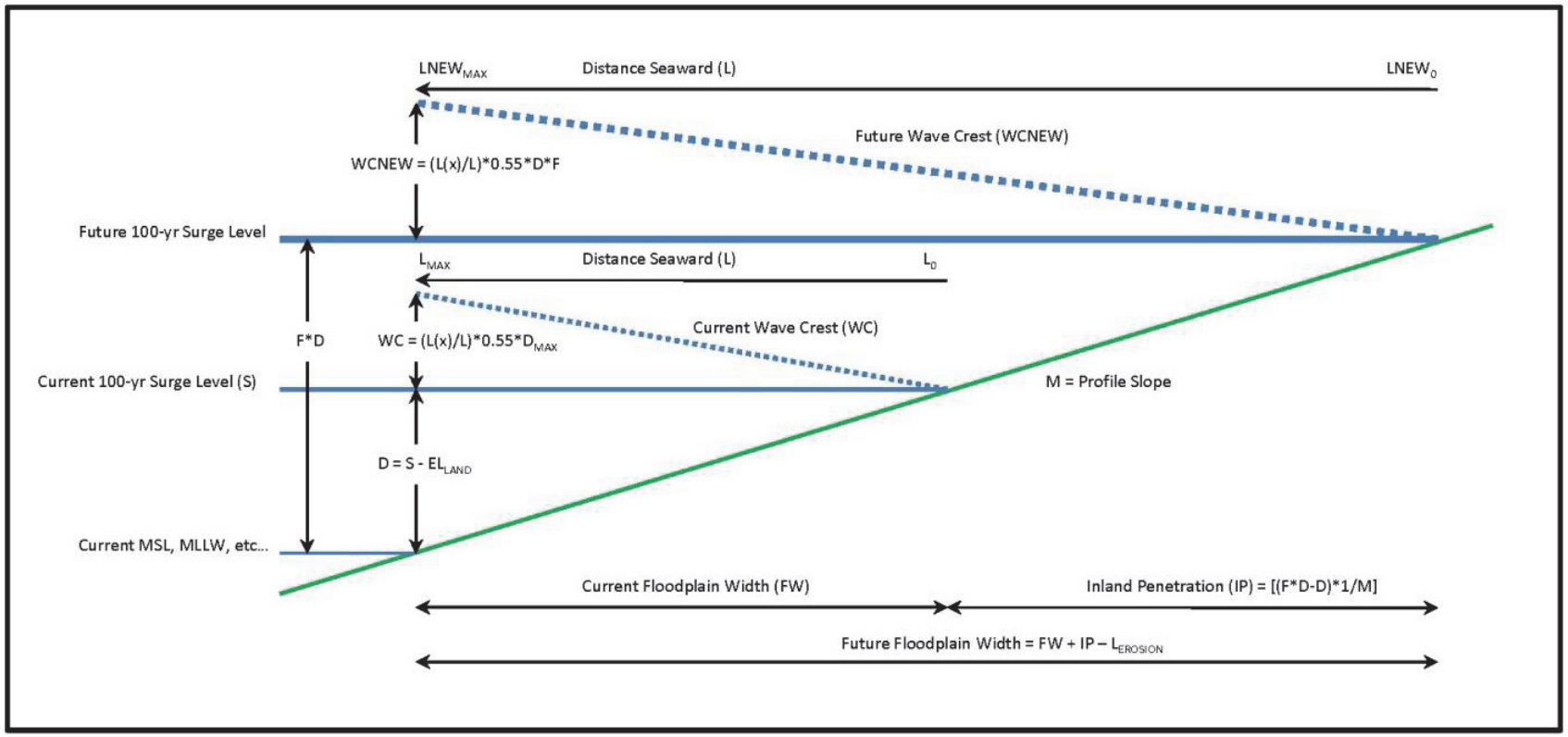

Figure 2-8. Schematic illustration of the coastal floodplain estimation procedure.

The IPCC's Special Report on Emissions Scenarios (SRES) forms the basis of the climate change projections used in this study, as discussed in Appendix A. In the analysis, the population growth assumptions implicit in those scenarios have been adopted in a consistent way with the projections of IA that are needed for flood discharge determinations. Although this discussion addresses IA estimates required by the riverine regression methodology discussed earlier, the same population projections are used for the coastal and economic aspects of the study. No attempt has been made to forecast the variability of population growth within the U.S. on a regional basis; instead, a uniform growth rate assumption has been adopted. Furthermore, no effort has been made to estimate local population saturation limits, since the spatial granularity of the later economic analysis (county level) is unlikely to be affected.

The SRES scenarios project a population growth rate for each country (available from the Center for International Earth Science Information Network, CIESIN, website at www.ciesin.org). Projections are provided at a country scale from 1990 to 2100 in 5-year increments consistent with the SRES B1, A1B, and A2 scenarios. In addition, this online resource also provides a gridded global population dataset at 0.5 deg. resolution for the years 1990 and 2025. To downscale the country-level SRES scenarios to a finer resolution, the common approach is to apply the uniform growth rate to each grid cell or area of interest (Bengtsson et al., 2006). This is the approach utilized in generating the projected gridded global population for the year 2025 mentioned above, and for longer term projections. Figure 2-9 illustrates this gridded global population dataset for the year 1990 and the corresponding projection out to the year 2100 for SRES scenario A2. Figure 2-10 shows the assumed U.S. population growth for the two emissions families considered.

The second part of the methodology is to identify the relationship between IA and population. IA is used in this study as an explanatory variable for extreme event flooding due to its strong effect on runoff, as discussed previously and in Appendix B. To obtain projections of IA, previously established regression relationships relating it to population density were adopted, as shown in Figure 2-11, and discussed in Appendix A. The Hicks curve identified in the figure was adopted for use since it represents a practical compromise among the data, giving a reasonable transition from low density to high density observations.

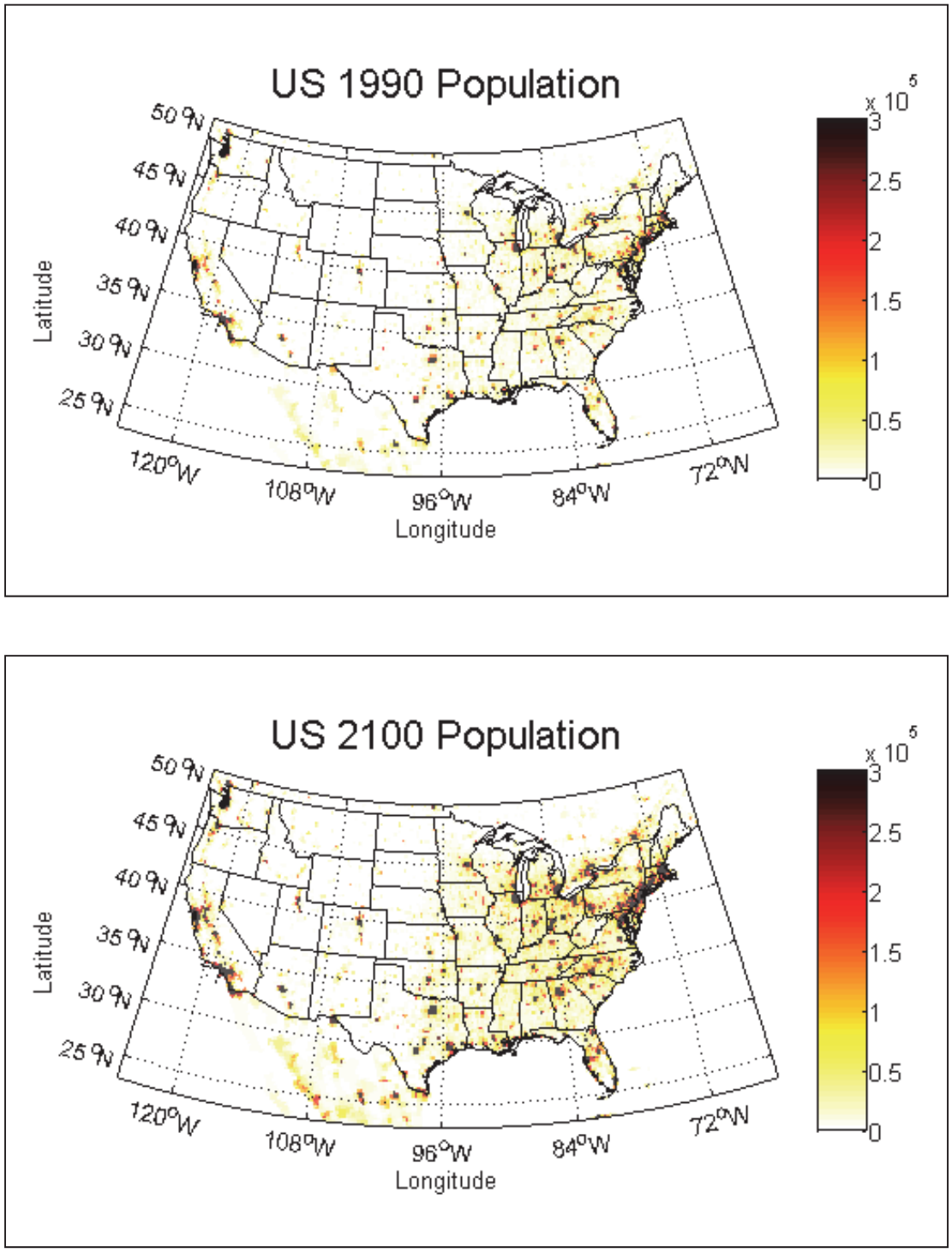

Figure 2-9. Gridded (0.25 deg. resolution) U.S. population data for years 1990 and 2100 (projected based on SRES A2 scenario). These projections are based on applying the population growth rate of the entire country for the A2 scenario to each individual grid cell over time.

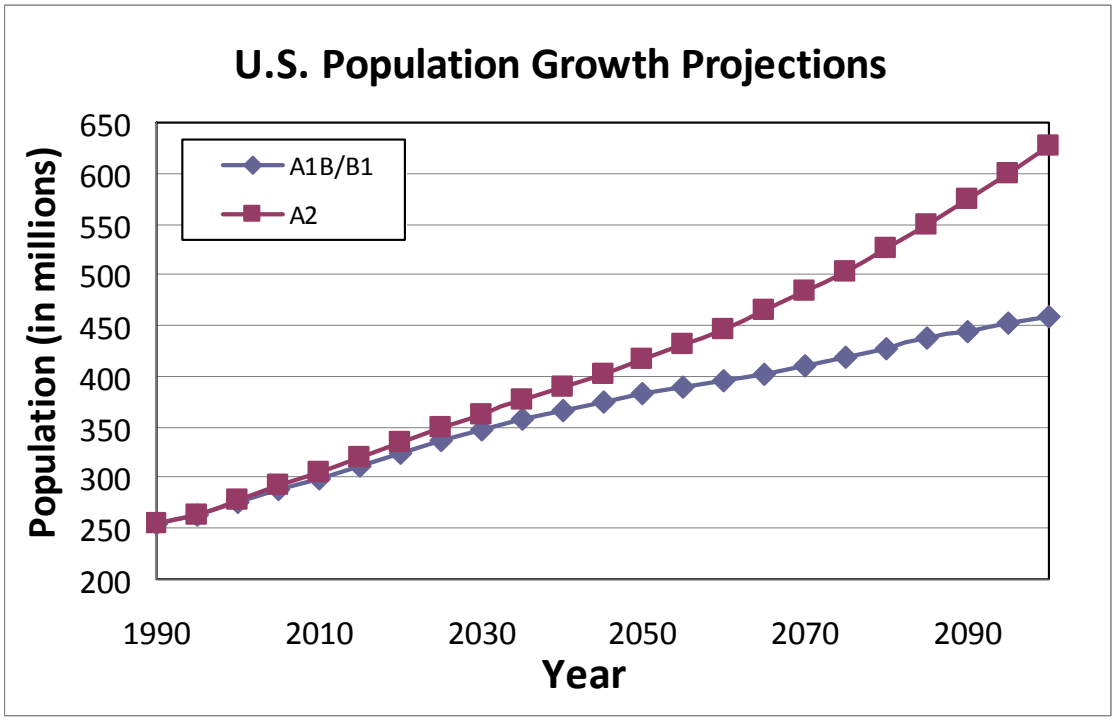

Figure 2-10. U.S. population growth assumptions for the two emissions families, based on Bengtsson et al. (2006); A SRES-based gridded population dataset for 1990–2100.

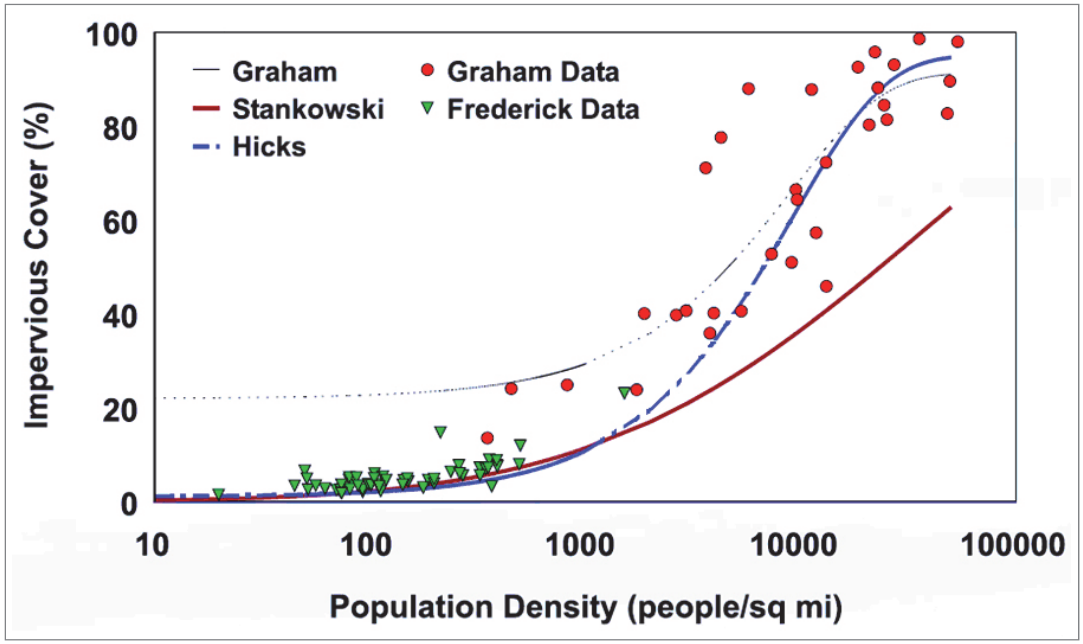

Figure 2-11. Impervious cover versus population density for several studies (Exum et al., 2005).

3.0
Additional Technical Considerations

3.0 Additional Technical Considerations

3.1 Erosion

Coastal erosion is a topic of considerable complexity that cannot be fully addressed within the scope of this study. FEMA undertook two prior studies that bear upon erosion. First, was a 1991 study entitled *Projected Impact of Relative Sea Level Rise on the National Flood Insurance Program* (FEMA, 1991) and second was *Evaluation of Erosion Hazards* (The Heinz Center, 2000). The Heinz study provides an in-depth analysis of erosion as a topic for possible FEMA mapping, through specification of long-term coastal erosion risk zones similar to coastal flood zones. Generalized estimates were made of numbers of structures at risk within a prescribed distance from the shoreline (500 feet) and within a candidate erosion hazard zone (defined by an estimate of the region subject to long-term erosion during a 60-year period).

The 1991 SLR study considered sea level rise and its effects on coastal flood insurance in a way similar to one method adopted here. Among the differences are the facts that the rate of sea level rise inferred in 1991 was less than that adopted here for long-term climate change projections, and that the combined effects of changing storm climate were not considered. The 1991 study adopted a similar assumption regarding the growth of the coastal SFHA vs. sea level rise when shoreline recession caused by erosion is not considered.

A difference between the 1991 study and this study concerns alternate assumptions regarding shoreline adaptation to sea level rise. For the rates considered in the prior work, it was found that natural shoreline recession was of the same general magnitude as the growth of the SFHA. This was based on the same assumption of local proportionality between changes of water level and changes of inland flood penetration as has been used in this study. Consequently, it was assumed that in the absence of human intervention, the two would offset each other with essentially no net growth of the SFHA, and little net impact on the flood insurance program. The slow inland migration of the shoreline was assumed to stay in approximate equilibrium with rises of sea level in such a way that periodic updates of the flood insurance rate maps would, on average, involve a simple migration of the SFHA.

In this study, a second, equally simple alternative assumption has also been considered: that the shoreline is held fixed by human action, so that the SFHA grows in response to sea level rise. This is an assumption that overestimates the growth of the SFHA, where the 1991 study underestimated it. Both assumptions will be valid in some areas, so that the truth will be somewhere between these extremes, requiring a

much more detailed investigation of the highly variable nature of site by site erosion potential. It is thought that many highly developed coastal areas might not be allowed to migrate inland, instead being protected or otherwise evolving in place in response to SLR and erosion. Areas of lesser development, such as rural or park areas, might be more readily allowed to adapt to erosion through retreat.

It is also noted that even if a shoreline migrates inland, such relocation would not be cost free, but would be reflected in a series of episodic flood losses. This is the case since major erosion would likely occur in a stair-step fashion as major storms periodically caused adjustment to the changing water levels.

As part of this study, coastal response has been estimated both with and without SLR, with the former being presented pictorially in Section 4.0, Projections. The results without SLR are only a rough approximation to the more complex case of SLR combined with offsetting erosion, as was assumed in the 1991 FEMA study; a much more detailed analysis accounting for erosion variability would be necessary to improve the receding shoreline estimate. The results without SLR show much smaller changes in coastal SFHAs, and are generally more consistent with the 1991 SLR study; they have been provided to FEMA as part of the package of supplementary materials.

Another approximate way to estimate the influence of erosion as it might fall between the extremes just discussed, is to consider the projection of historical observed rates, or to estimate rates from SLR through a rule such as the Bruun rule (Bruun, 1962). The Bruun rule has spurred much discussion in the years since it was proposed, but remains a useful and reasonable tool if considered in its simplest conceptual form: that for small changes in sea level, the shoreline response should be proportional. The difficulty is in specification of the constant of proportionality, since it must depend upon local conditions and will not remain valid over large variations. In essence, the rule is for a given sea level rise, R, the horizontal shoreline change, E, will approximate kR where k is a number requiring a local estimate, but, conceptually, being of order 100 (that is, within an order of magnitude; values on the order of 50 are commonly seen). Of course, this concept does not apply to hardened or stabilized shorelines.

The present study considered historical SLR and erosion rates (see Appendices A and B) for the adopted coastal study regions, and has not succeeded in finding an appropriate generalized Bruun coefficient applicable to an entire region that could be reliably used for projections, since variation within a region is very large. However, it is of interest to show the historical rates and to project them through 2100 to obtain an approximate notion of erosion magnitudes. This is shown in Table 3-1. The table shows this study's coastal regions as rows, with historical weighted mean SLR rate.

The mean rates were obtained from USGS CVS data by length-weighted averaging of hundreds to thousands of shoreline segments within each region. There is high variability around these means, owing to physical variability of the coast and the large size of the regions. Any future and more localized studies should adopt more refined data, although the large regional averaging done here is appropriate for national scale estimates. The region-averaged historical SLR rates are followed by the mean and range of historical erosion rates, and then by the mean erosion estimates (meters of recession) at each future study epoch. Note that some areas show mean accretion and that even in zones where the mean erosion estimates are consistently negative (recession) there are local values that, if projected through 2100, show large accretion. Other data sources, such as information summarized in Crowell and Leatherman (1999) show substantial erosion rate differences from the regionalized estimates in Table 3-1. In all, there is a very great deal of spatial variability within a region, making the choice of simple rules a vexed issue. It is recommended that any future refinement of this study requiring erosion estimates should undertake a more detailed and locally representative effort than has been possible here.

3.2 Special and Critical Event Scenarios

Additional issues that are sometimes encountered in discussions of the impact of climate change, but that are not addressed in this study, include special event scenarios. An example of such a scenario is the collapse of the West Antarctic Ice Sheet, a possibility that has received considerable attention. Many other important possibilities of this general nature could be identified. They have not been considered here since, unlike climate modeling projections, quantitative estimates of when they might occur and with what probability are not available. Nevertheless, they are important possibilities that might be entertained in a subsequent study by FEMA working in a “what if” mode not consistent with the approach used in this study.

Another topic that has not been considered, but that could be of significant importance to FEMA, is the sensitivity of certain vulnerable sites to small changes in flood hazards. The nationwide study described here has been based on the fundamental idea that changes in effects are roughly proportional to changes in causes, but this is not always the case. For example, a small increase in flood level could have a disproportionately large effect in an area that is protected by levees if those levees were suddenly to become overtopped and fail. This matter – somewhat like adaptation to sea level rise and erosion – may be foreseeable and possibly countered by levee improvements and enhanced freeboard requirements. Other

possibilities of a “tipping point” nature might be identified as potentially important to FEMA.

Description of Table 3-1 *(on the following page)*

Table 3-1 provides a summary of relative sea level rise and shoreline change rates contained within the Coastal Vulnerability Index (see Appendix C) dataset for each of the ten identified sea level rise regions. Both sea level rise rates and shoreline change rates are based on historical data. In each region, weighted-mean values were calculated based on shoreline segment lengths. Hundreds to thousands of shoreline segments of varying lengths exist within each region. Minimum and maximum values were also extracted from the dataset. Estimates of future land lost through 2100 are provided based on historical shoreline change rates. These values are not intended to be used as a predictor of shoreline change at individual locations, but rather as an overall assessment of the varying potential for land loss by sea level rise region. Historical sea level and shoreline change rates are generally consistent with those documented in other literature sources. However, the study recognizes that rates calculated for Regions 9 and 10 do not represent local conditions as well as respective rates calculated for other regions throughout the U.S. A recommendation is made to further refine the sea level rise regions identified. Improvements in regionalization should focus on the Pacific Northwest (Regions 9 and 10) in particular.

Table 3-1. Summary of relative sea level rise and shoreline change rates contained within the Coastal Vulnerability Index dataset for each of the ten identified sea level rise regions.

	HISTORICAL RELATIVE SEA LEVEL RISE (SLR)			SHORELINE CHANGE negative —> erosion positive —> accretion					
	Regional weighted-mean historical SLR mm/yr	Min historical relative SLR rate mm/yr	Max historical relative SLR rate mm/yr	Regional weighted-mean historical shoreline change rates m/yr (ft/yr)	Shoreline change estimates by epoch based on mean historical shoreline change rates (meters)				
					2020	2040	2060	2080	2100
ATLANTIC COAST									
Region 1	1.75	0.9	2.75	-0.43 (-1.41)	-4.3	-12.9	-21.5	-30.1	-38.7
Region 2	3.26	2.45	4.1	-1.48 (-4.85)	-14.8	-44.4	-74	-103.6	-133.2
Region 3	2.85	2.45	3.15	-0.79 (-2.59)	-7.9	-23.7	-39.5	-55.3	-71.1
Region 4	2.31	2.15	2.45	0.07 (0.23)	0.7	2.1	3.5	4.9	6.3
GULF OF MEXICO									
Region 5	2.48	1.8	4.4	-0.58 (-1.90)	-5.8	-17.4	-29	-40.6	-52.2
Region 6	9.08	4.49	10.9	-2.76 (-9.05)	-27.6	-82.8	-138	-193.2	-248.4
Region 7	4.34	3.7	6.89	-0.81 (-2.66)	-8.1	-24.3	-40.5	-56.7	-72.9
PACIFIC COAST									
Region 8	1.4	0.1	2.75	-0.12 (-0.39)	-1.2	-3.6	-6	-8.4	10.8
Region 9	-0.99	-1.9	0	0.31 (1.02)	3.1	9.3	15.5	21.7	27.9
Region 10	0.57	0.05	0.9	2.12 (6.95)	21.2	63.6	106	148.4	190.8

4.0
Projections

4.0 Projections

4.1 The Projected Impact of Climate Change on Riverine Flooding

The methods that have been developed to assess the impact of climate change on riverine flooding at a national scale have been described in Section 2.0, and are further detailed in Appendix B. Major assumptions regarding climate change are discussed in Appendix A. As noted in Appendix A, this study has been based throughout on the equal consideration of three climate emissions scenarios, A2, A1B, and B1. The fact that these scenarios have been assigned equal weight should be reconsidered in a future update of this work if improved information allows, or entirely new information might be adopted as the basis of updated estimates. For the present, it is not thought that a compelling argument can be given to weight these emissions assumptions differently. The same assumption has been made regarding the ten international global climate models (GCMs) and their 43 simulations enumerated in Appendix B.

Given the climate assumptions and engineering flood estimation techniques that have been described, projections of three flood parameters were made nationally at each of the five epochs. The three flood parameters include:

- Changes in the 1% annual chance stream discharge, $Q_{1\%}$.
- Changes in the 1% annual chance floodplain depth parameter, FPD; this is the depth of the flood at the stream bank. As discussed in a previous section, the stream bank elevations are approximated by the current 10% flood stage. Since the flood depth drops to zero across the floodplain, the percentage change away from the banks will be greater. Owing to the assumptions of the geometric floodplain model, the percent change in FPD is identically equal to the change in the floodplain area, FPA.
- Changes in a derived Flood Hazard Parameter, FHP, defined as the difference between the 1% annual chance and the 10% annual chance future flood levels. This is a supplementary parameter of significance for the economic and insurance analyses, since it is directly related to the Flood Hazard Factor, FHF, previously, but no longer identified on FEMA flood insurance rate maps. It is provided since it remains important in the selection and interpretation of the PELV curves (probability-elevation curves) used in FEMA's actuarial analyses.

The results for these three factors at each epoch are shown in Figures 4-1 through 4-15 (starting on page 4-8) for the median (50th percentile) of the Monte Carlo simulations. Note that in these and all similar figures, the indicated changes are cumulative from the present through the indicated date; they are not changes occurring between epochs. Figure 4-16 (on page 4-23) shows a sample of the

variability captured in the simulation of $Q_{1\%}$ at epoch 5; the 10th, 25th, 75th, and 90th percentiles are shown. Although the median results are a best estimate within the assumptions of the analysis, the other percentiles show the range of variability. For example, 10% of the Monte Carlo simulations produced values below the 10th percentile, while 10% produced values above the 90th percentile. Since estimates of *Q* are fundamental to estimates of the other two flood factors, this sample is indicative of the variability of those as well. It can be seen from Figure 4-16 that the uncertainty in the projections is quite large, an entirely expected result owing to the disparity of model projections and the uncertainties implicit in the engineering procedures. For example, the 25th percentile indicates that the 1% annual chance discharge would decrease in all areas of the country at Epoch 5.

Figures 4-1 through 4-15 show increased flooding throughout the nation at each epoch, based on median projections for the 1% annual chance discharges. However, this does not mean that average conditions will also become wetter; in fact, it is possible that some areas will become drier on the average, despite worsening floods. The text box on the following page provides some additional discussion regarding the variability of the projections.

4.2 Separating Population Effects from Climate Effects

Additional analysis was performed to permit separation of the changes dependent upon population growth from those dependent entirely on climate effects (the three identified significant climate indices); the climate effects, however, contain inherent population growth assumptions through the emissions scenarios, so they are ultimately linked with population. Population growth by itself, however, causes flood changes owing to increased impervious areas; this is the factor being separated. Figure 4-17 (on page 4-24) shows this separation for $Q_{1\%}$. The three columns of the upper block show the separate and combined effects of climate and population, while the first three rows additionally show the separation according to the emissions scenario. The lower block of figures shows population and all emissions scenarios combined at each epoch.

It can be seen that population change – influencing the IA parameter – is responsible for as much as about 50% of the total flood discharge change in densely populated areas. However, since most areas of the country are not densely populated, the combined maps display a strong similarity to the climate-change-only maps. As a very approximate conceptual estimate, about 30% of the projected changes might be attributed to population growth in developed areas of most interest to the NFIP.

Variability of the Projections

The reader will have seen that the median 1% annual chance flood projections presented in this study show increases everywhere across the nation, and at all epochs. While data have not been developed or shown here for average annual rainfall conditions, it is possible that some areas of the country could become drier on average than they now are. The possibility of experiencing both drier conditions and increased flooding might seem inconsistent or counterintuitive, and so merits clarification.

There are two aspects to consider: the statistical variability of the estimates, and the physical realism of the median projections. Regarding the former, recall that Monte Carlo sampling was used to generate a range of possible 1% annual chance flood discharges at each epoch, accounting for the uncertainties associated with the ten global climate models (GCMs) and the three adopted emission scenarios. In the course of that sampling, *reduced* flooding was frequently found, as is clearly shown in Figure 4-16, where both the 10^{th} and the 25^{th} percentile maps show *reduced* flooding over the entire nation at Epoch 5. This means that fully 25% (or more) of the Monte Carlo simulations in this study produced future flood estimates lower than present conditions. However, an even *greater* number of simulations produced projections of floods *higher* than present conditions. This is seen in the maps at the 75^{th} and 95^{th} percentiles. The net result was that the median – or 50^{th} percentile – estimates uniformly show greater floods.

Some additional insight into the statistical aspect can be gleaned from the form of the regression equation used to estimate the 1% annual chance flood. Recall that the equation is a function of fixed watershed characteristics, of impervious area (IA), and of three extreme climate indicators: annual total number of frost days (FD), maximum total 5-day precipitation (R5D), and maximum annual consecutive dry days (CDD). The following facts based on the three emissions scenarios and the ten GCMs are pertinent:

- IA will increase as population increases, contributing to an *increase* in the 1% annual chance discharge.
- FD is projected to decrease on average, implying an *increase* in the 1% annual chance discharge.
- R5D in most areas is projected to increase on average, implying an *increase* in the 1% annual chance discharge.
- CDD is projected to increase on average, implying a *decrease* in the 1% annual chance discharge.

Of the four explanatory variables in the regression equation that change with population and climate, three are associated with increases in the 1% annual chance discharge, and were found to dominate other factors including the opposing influence of more annual dry days.

In summary, the Monte Carlo sampling procedure of this study projected *both* decreases and increases in the 1% annual chance flood projections for all epochs throughout the nation, but those projections were not symmetrically balanced, with the majority favoring greater floods. As a direct result, the median estimates used here as the basis for the NFIP impact assessment also favor greater floods. The occurrence of greater floods despite overall drying conditions is a *physically* reasonable possibility, since longer dry intervals can be punctuated by storms of greater intensity.

– Discussion by Will Thomas and David Divoky

4.3 The Projected Impact of Climate Change on Coastal Flooding

Tropical and winter extra-tropical storms have been considered separately, following climate change assumptions summarized in Appendix A, and coupled with forecast SLR as discussed in Appendix C. For both types of storms, the range of frequency and intensity changes are assumed to have a Gaussian distribution with the means and variances provided by existing climate science literature. Varying frequency and intensity projections are applied using these distributions.

4.3.1 Tropical Storms

The key sources for information regarding changes in tropical storm frequency and intensity were the recent papers by Knutson et al. (2010) and Bender et al. (2010). The former provides a comprehensive overview of the literature, while the latter reports updated modeling that forms the basis for the projections given here. In particular, Bender et al. predict a change of +10% in storm intensity and a -33% change in storm frequency for the North Atlantic by the year 2100, based on emissions scenario A1B. The standard deviation for the storm frequency estimate is given as 22 percentage points; no standard deviation is given for the intensity estimate. Since the intensity change estimate is comparable to estimates reported in the Knutson et al. review, the latter paper's typical estimate of a 6 percentage point standard deviation has been adopted. Both variations are assumed Gaussian.

The Bender estimate is based on the A1B emissions scenario. In order to estimate changes in frequency and intensity for other scenarios, a two-step interpolation was adopted. First, a linear interpolation on A1B per epoch was assumed through 2100. Then estimates for the A2 and B1 scenarios were obtained by assuming an intermediate proportionality to the CO_2 abundances in those scenarios at each epoch. This is a simplified assumption implying that as the driving mechanism of climate change, small changes in CO_2 abundance will be reflected proportionally in small changes of dependent parameters, and is an assumption warranting further investigation in future updates of these estimates.

4.3.2 Extra-Tropical Storms

The primary data sources adopted for intensity and frequency changes of extra-tropical storms are the papers of Bengtsson et al. (2009) for intensity, and Lambert and Fyfe (2006) for frequencies. Lambert and Fyfe provide estimates of changes in frequency for all three fundamental emissions scenarios, with both means and standard deviations. Those estimates have been interpolated over time for each epoch. Bengtsson et al. provide estimates of intensity change only for A1B so, as

with tropical storms, a secondary interpolation vs. CO_2 abundance was adopted, with the same caveats as before.

4.3.3 Coastal Projections

Given the foregoing climate assumptions and the computational procedures detailed in Appendix C, the coastal projections for median changes of Special Flood Hazard Area, *SFHA* (identical to changes of depth at the coast, as with the riverine case) are shown in Figures 4-18 through 4-32 (starting on page 4-25) for the five epochs; the projections at each epoch are cumulative from the present, not incremental between epochs. Counties showing no results are characterized by steep shorelines with very small population, so that FEMA coastal flood insurance data had not been developed prior to this work. The projections are based on the assumption of a fixed shoreline, thereby maximizing the flood hazard area growth. It should be recalled that the large regionalization introduces uncertainties, especially in the Pacific Northwest. Many regions shown with negative historical response (falling relative sea level) actually show a positive trend. This reinforces the important point that the projections are not to be adopted locally, but nationally, with local variability being smoothed.

A possible pitfall in interpreting these figures is that where the existing flood levels are small (such as inside protective embayments), even a small rise of sea level may produce a very large *percentage* increase in flood zone size. A large percentage increase of a very small number remains a small number, so that large changes indicated on the maps should not necessarily be construed as large in absolute magnitude. In fact, where the existing flood levels are large, what might be shown as a small percentage increase could exceed what is shown as a large percentage increase elsewhere where the existing flood levels are small. Information regarding absolute values is contained in supporting archived files.

One other feature of these maps will be mentioned here as an example of why the study results should not be considered as locally valid, but are expected to be affected by a large local variability that, if not systematic, will tend to cancel in the national aggregate numbers. An example of interest is Baltimore County in the upper reaches of Chesapeake Bay. In 2020, for example, the change in coastal flood hazard area for that county is shown to be about -23%, while the adjacent counties are shown as about +6%. The reason for this apparent mismatch is found both in issues of data quality and in the simplified methods adopted for the analysis. In particular, at this county the existing flood insurance study stage-frequency curve is anomalous in that it is not approximately linear, causing irregularities in interpolations.

4.3.4 Coastal Projections – Implications of an Adapting Shoreline Position

As discussed earlier, coastal estimates have been made in two ways. One includes the assumption that the existing shoreline remains fixed over time. This results in a maximum estimate of the increase in the coastal flood plain width caused by sea level rise and changes in storm conditions. This is the opposite of the second assumption (also made in the prior FEMA 1991 sea level rise study), and is shown in subsequent figures as the conservative upper bound. Under the alternate assumption used in the 1991 study, the shoreline will tend to migrate in response to erosion and sea level rise so as to compensate for the sea level rise influence, resulting in much smaller growth of the flood hazard areas. However, even if the SFHA is not assumed to change, there will remain changes associated with storms and with population growth. The truth is somewhere between these two assumptions, since in many areas it is expected that the existing shoreline will be held in place through protection and elevation measures. Even where the coastline does migrate inland, that migration will most likely occur during a sequence of step-like episodes when large storms produce erosion and the coast adapts to the then-current sea level.

An additional set of Monte Carlo simulations were made ignoring sea level rise in order to reveal the extent of flood area change associated only with storm changes. As expected, the projected changes in flood areas are much smaller, and are more consistent with the fully adaptive assumption of the 1991 FEMA SLR study since the postulated changes of storm conditions are relatively small. Both of these alternatives are addressed in the economic analysis in Section 5.0, although the topic remains a matter requiring a much more refined analysis, including consideration of likely human response, improved projections of sea level rise, and a more detailed resolution of coastal erosion than the broad regional estimates provided in this report.

As will be presented in detail in Section 5, the economic implications for the NFIP are greater for the fixed-shoreline assumption than for the receding-shoreline alternative. The text box on the following page provides a sketch and a brief discussion illustrating why this is so.

Receding vs. Stabilized Shorelines

Rising sea level and changes in storm intensity and frequency will cause the inland limit of coastal flooding to move landward over time. On a simple beach slope, the action of sea level rise would also cause the SFHA to migrate landward without much change of size, as long as the shoreline was allowed to move freely in a corresponding way. This receding shoreline assumption was adopted in the 1991 FEMA Sea Level Rise Study. It must be expected, however, that many communities will take steps to hold their shorelines in place through stabilization measures of various sorts. In such cases, the SFHA must *grow* since the inland limit moves landward while the seaward limit does not. Consequently, the area with exposure to 1% annual chance flooding would grow, representing enhanced chronic risk to the NFIP. No attempt has been made in this study to predict how individual communities might respond over time; some will allow shoreline recession, while others will take steps to stabilize and hold their existing shorelines. It is worth noting, however, that as a general trend, densely developed, urban areas could represent the stabilization case while rural coastal communities could represent the recession case. The financial implications of these two limiting cases are evaluated in Section 5 of this report. These alternate assumptions are discussed and illustrated in more detail below.

The following sketch illustrates the concepts discussed above. Note that the sketch is idealized and not to scale, perhaps spanning 10 or 20 feet vertically, but spanning thousands of feet horizontally. Possible changes to the beach profile caused by erosion or stabilization are not shown.

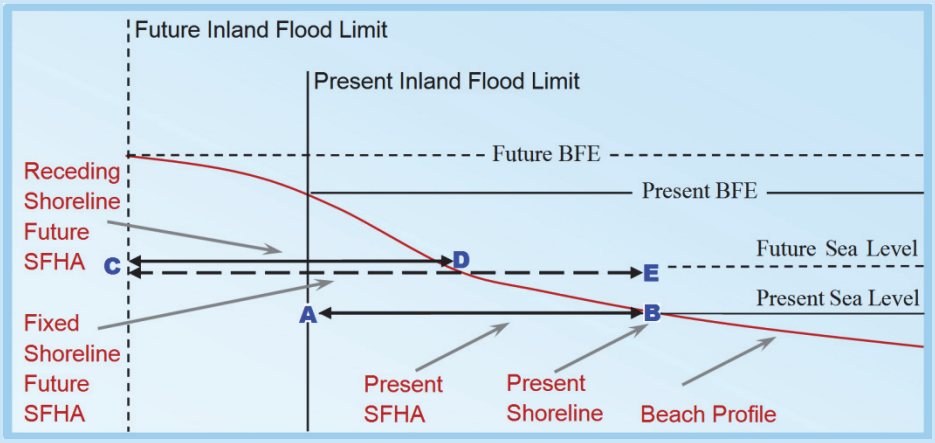

The lowest horizontal line represents present sea level, while the dashed line immediately above it represents future sea level. The upper two horizontal lines show present and future BFEs extending landward to the present and future inland flood limits. Point B is at the present shoreline, with the segment AB representing the present SFHA. Point D is a possible future position of the shoreline after landward migration caused by submergence and erosion; the segment CD represents the future SFHA for that receding shoreline case. Point E represents the future location of the shoreline if held near its present position at B. In this case, the future SFHA extends from C to E, exceeding the receding shoreline case CD. The sketch does not show the future beach profile, which could be stabilized (fixed) by seawalls, levees, beach fill, etc.

Since SFHA CE is larger than SFHA CD, it follows that there would be greater chronic exposure to flood losses in the fixed-shoreline case than in the migrating case, unless the fixed-shoreline case were exceptional, such as the Galveston Seawall or the Miami Beach nourishment. The encroachment area between D and E would be an area of transient losses as storms and sea level rise caused the shoreline to retreat from Point B to Point D; the costs of those transient losses are estimated separately in Section 5.

– Discussion by David Divoky and Robert Dean

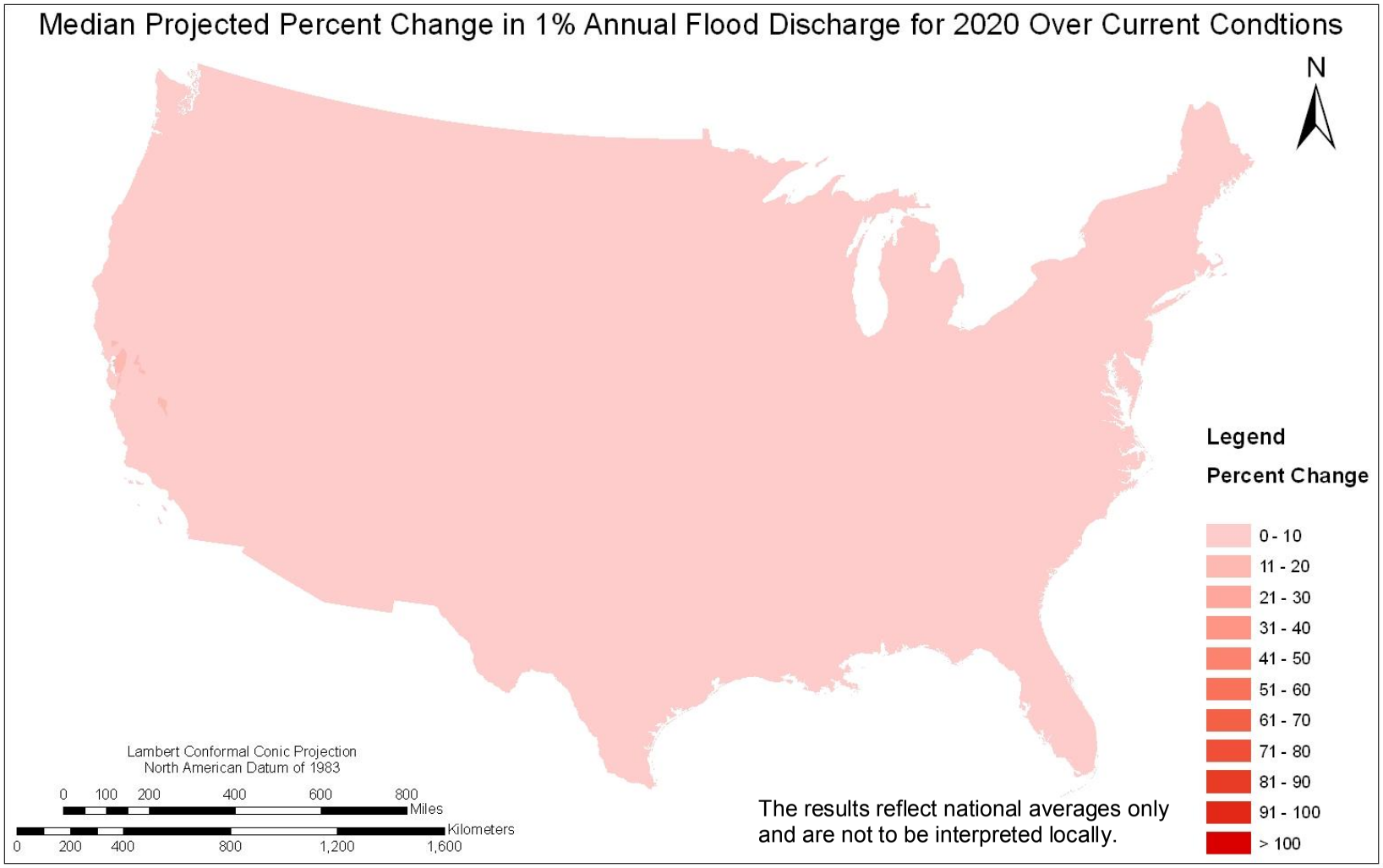

Figure 4-1. The median (50th percentile) relative change of the 1%-annual flood discharge at epoch 1 (2020). Changes are with respect to current conditions.

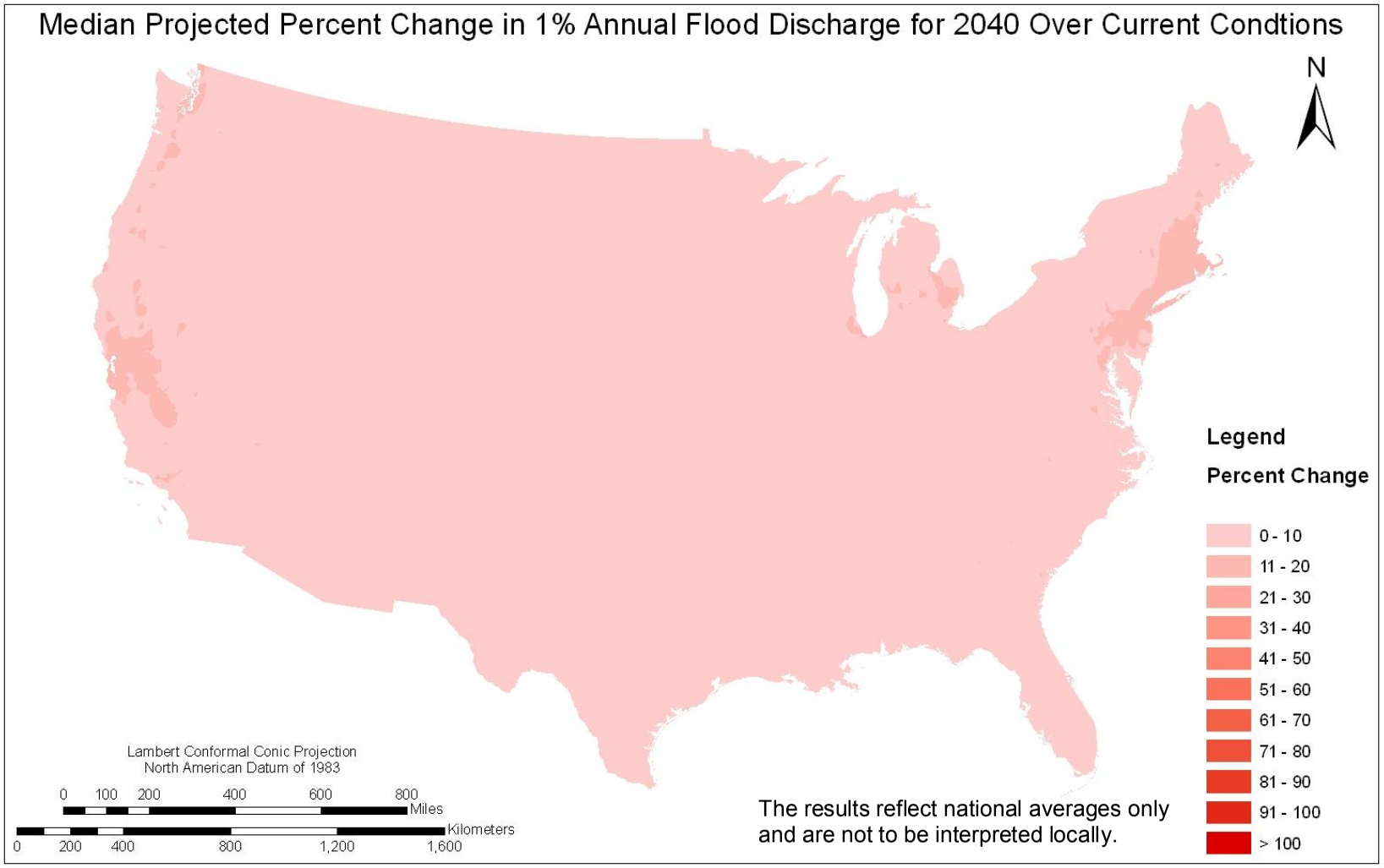

Figure 4-2. The median (50th percentile) relative change of the 1%-annual flood discharge at epoch 2 (2040). Changes are with respect to current conditions.

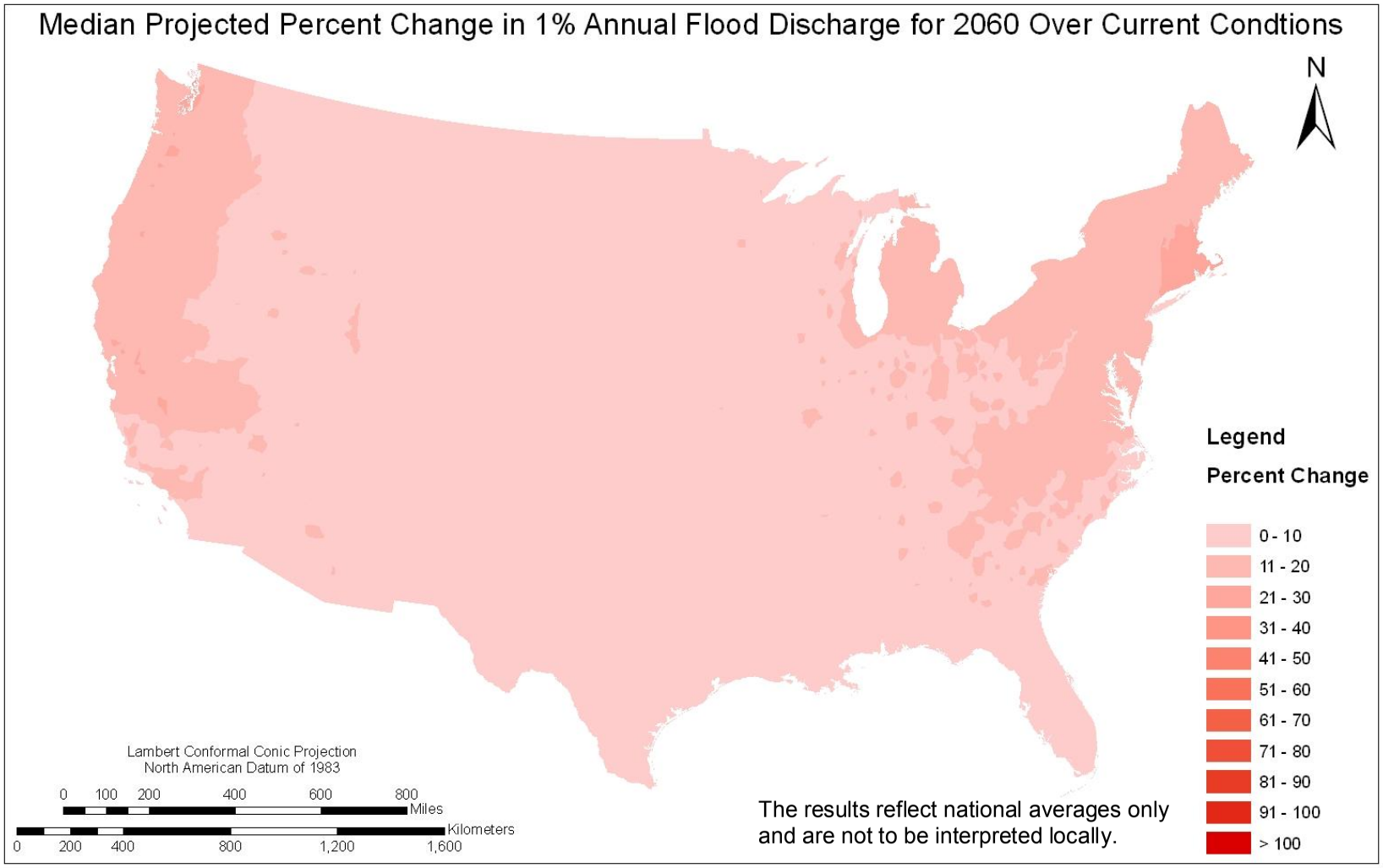

Figure 4-3. The median (50th percentile) relative change of the 1%-annual flood discharge at epoch 3 (2060). Changes are with respect to current conditions.

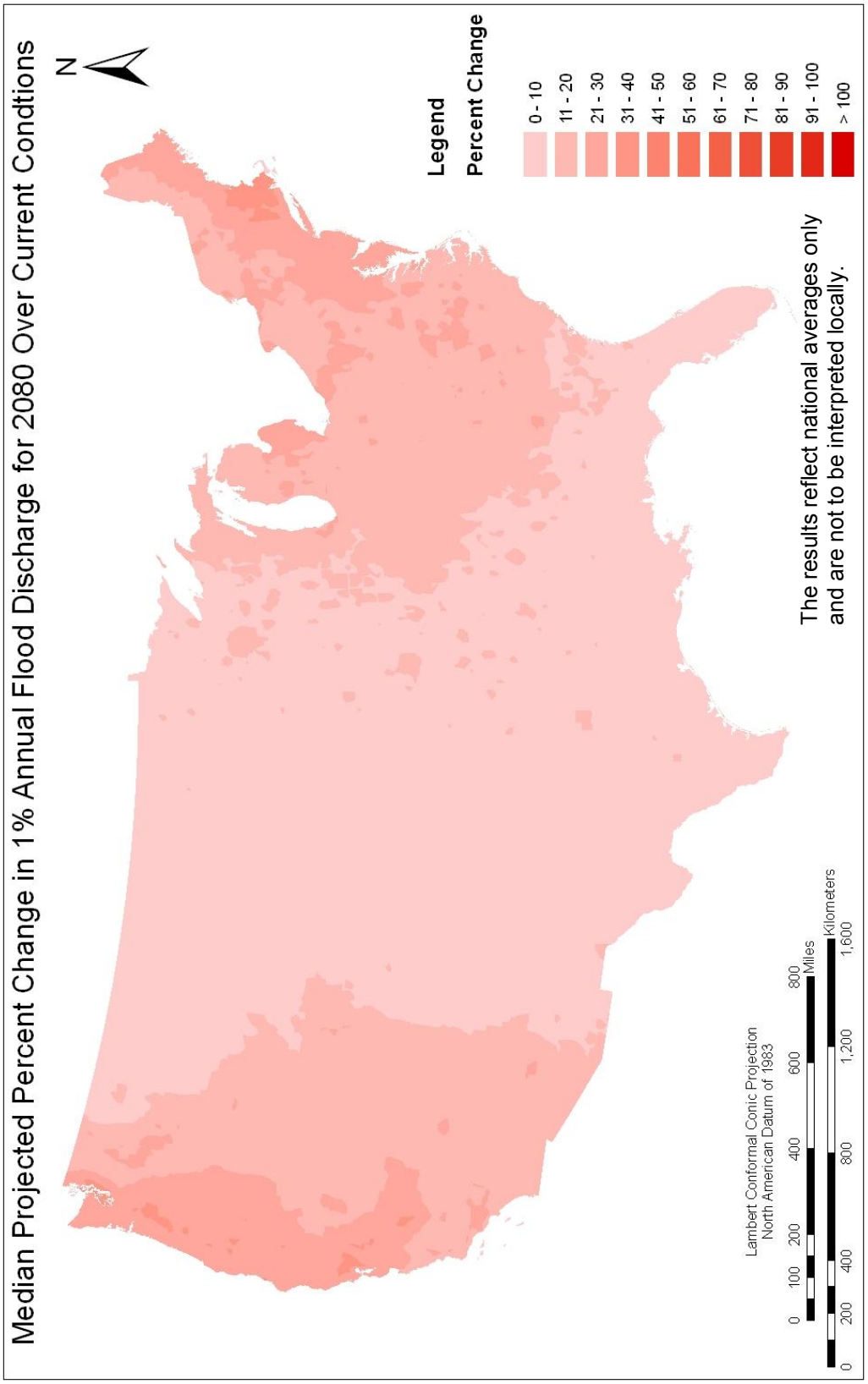

Figure 4-4. The median (50th percentile) relative change of the 1%-annual flood discharge at epoch 4 (2080). Changes are with respect to current conditions.

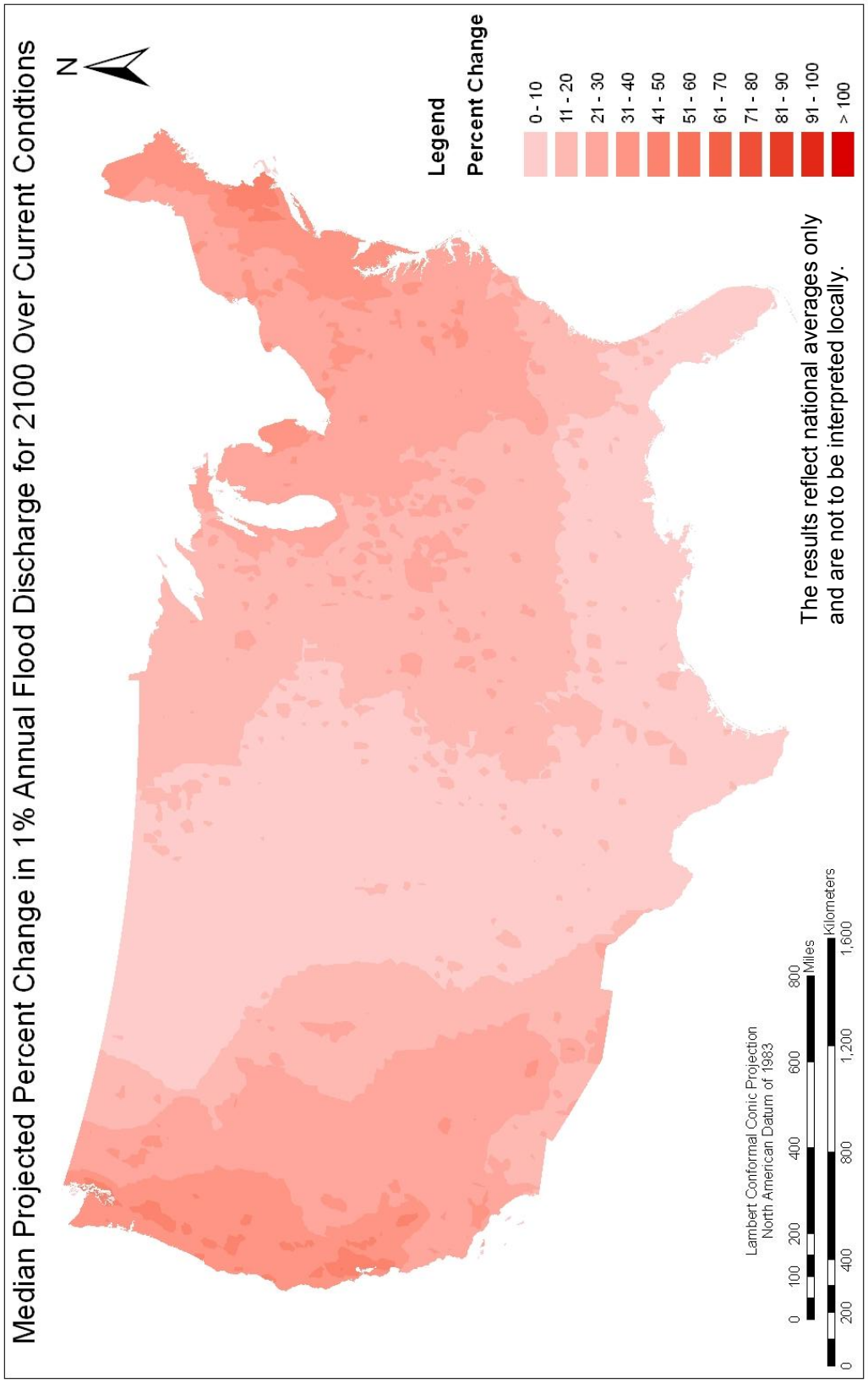

Figure 4-5. The median (50th percentile) relative change of the 1%-annual flood discharge at epoch 5 (2100). Changes are with respect to current conditions.

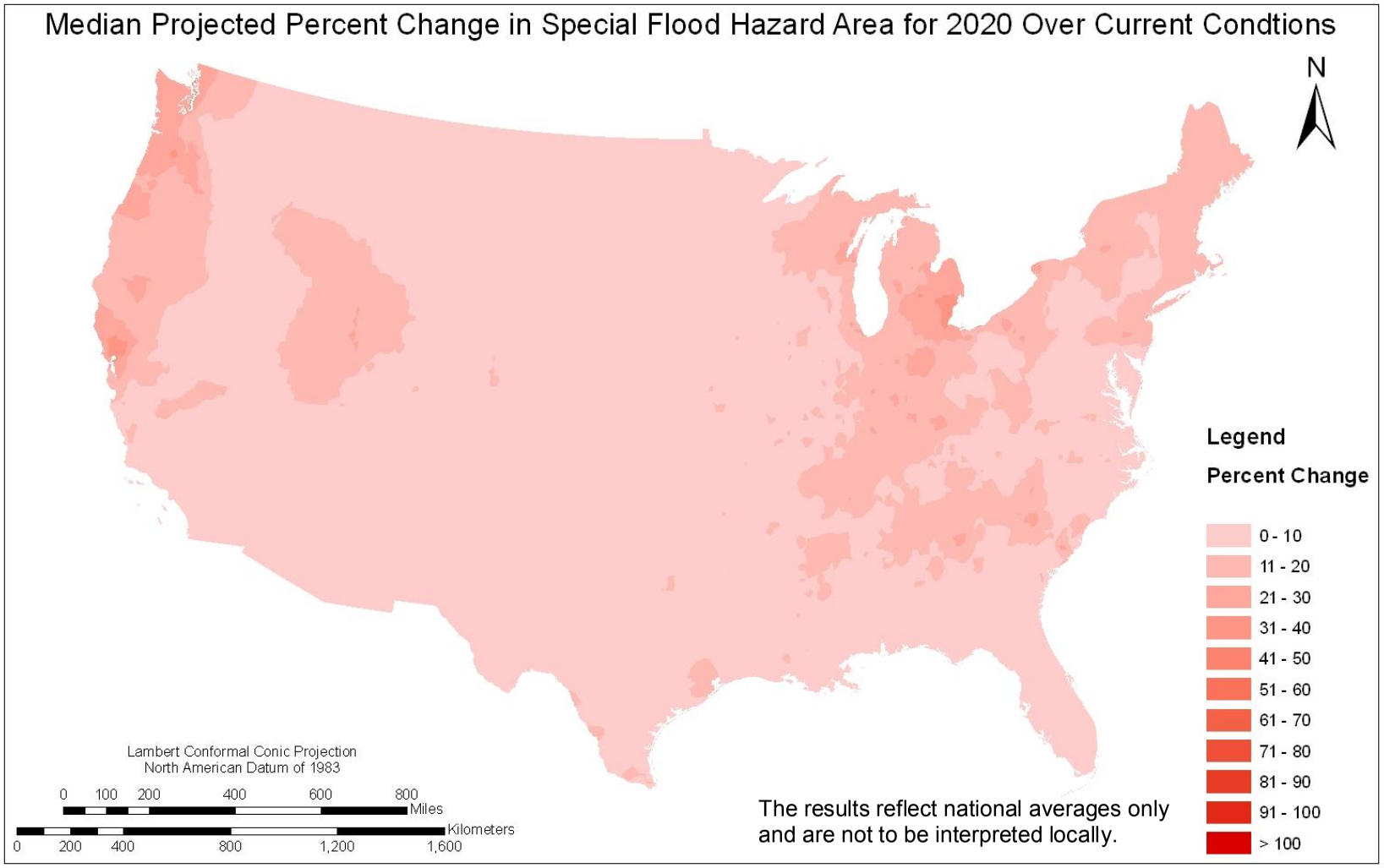

Figure 4-6. The median (50th percentile) relative change of the SFHA at epoch 1 (2020). Changes are with respect to current conditions.

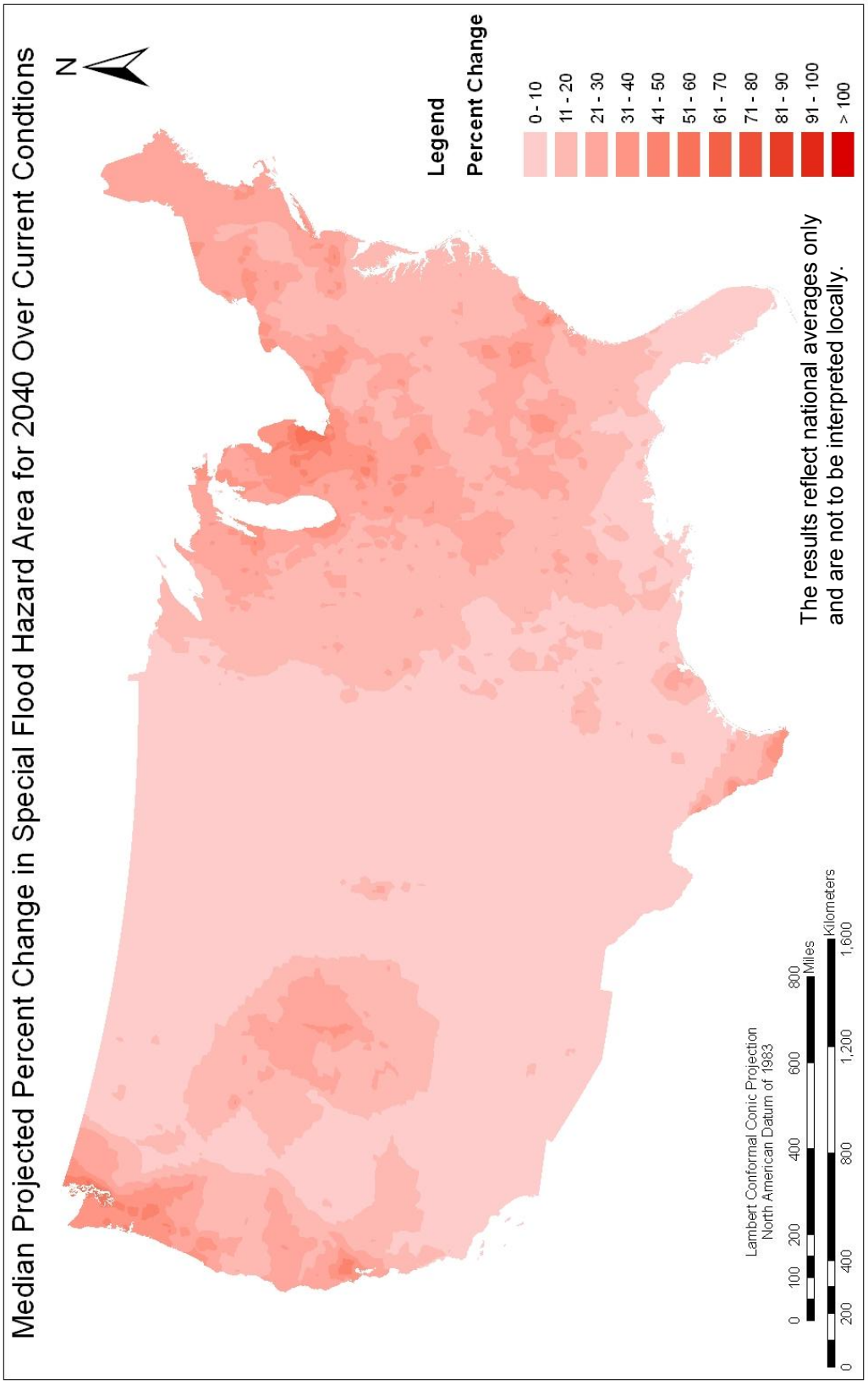

Figure 4-7. The median (50th percentile) relative change of the SFHA at epoch 2 (2040). Changes are with respect to current conditions.

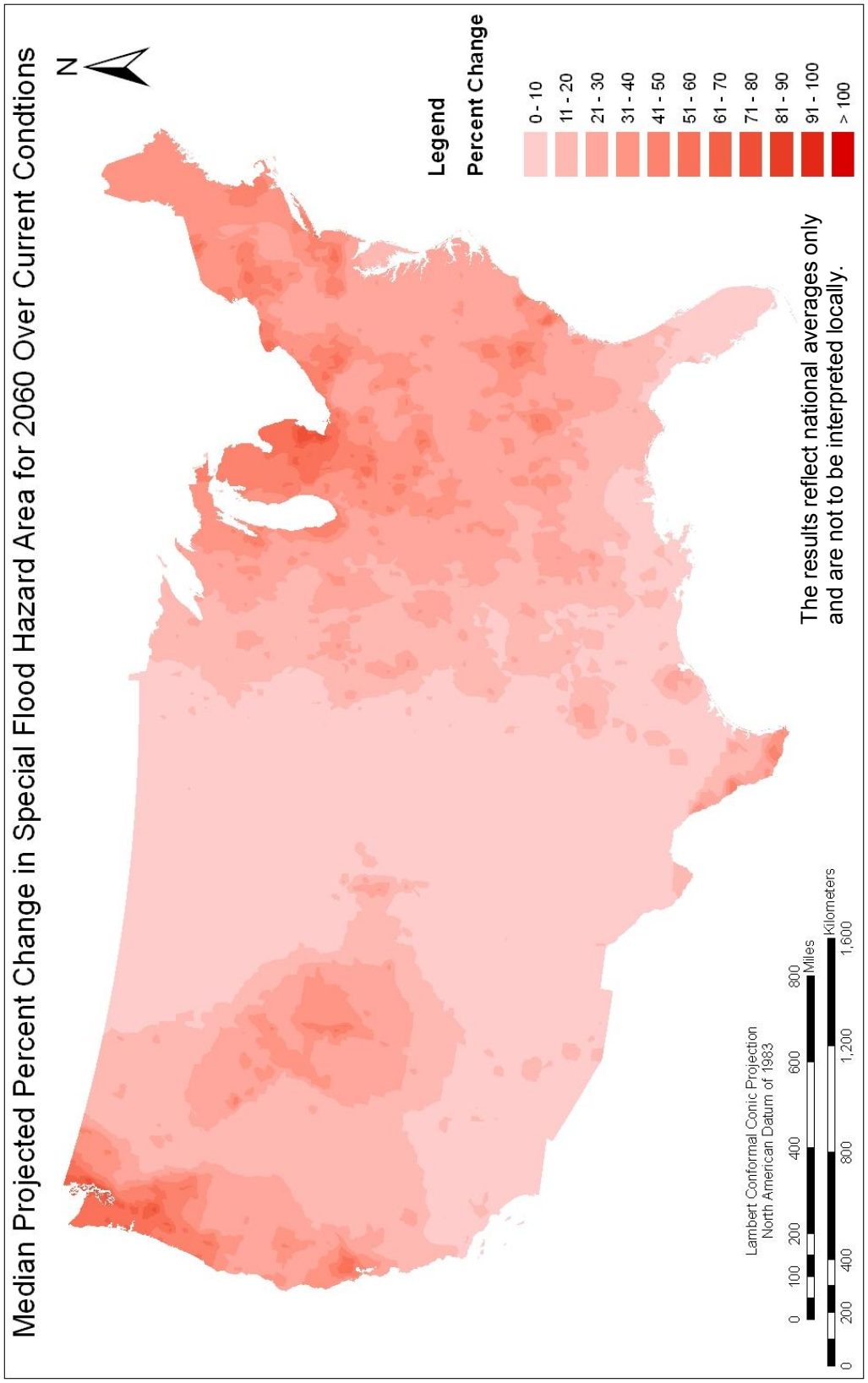

Figure 4-8. The median (50th percentile) relative change of the SFHA at epoch 3 (2060). Changes are with respect to current conditions.

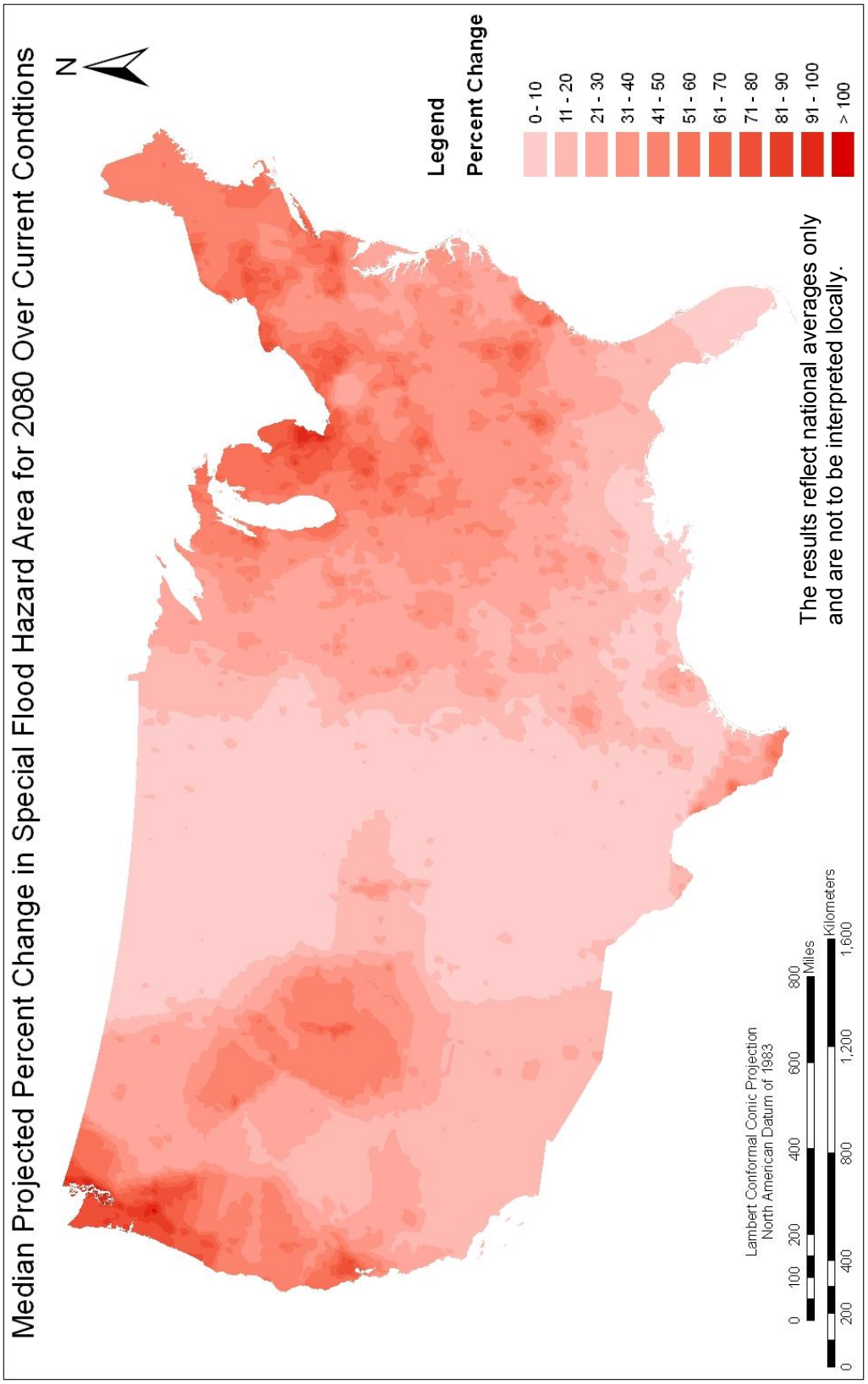

Figure 4-9. The median (50th percentile) relative change of the SFHA at epoch 4 (2080). Changes are with respect to current conditions.

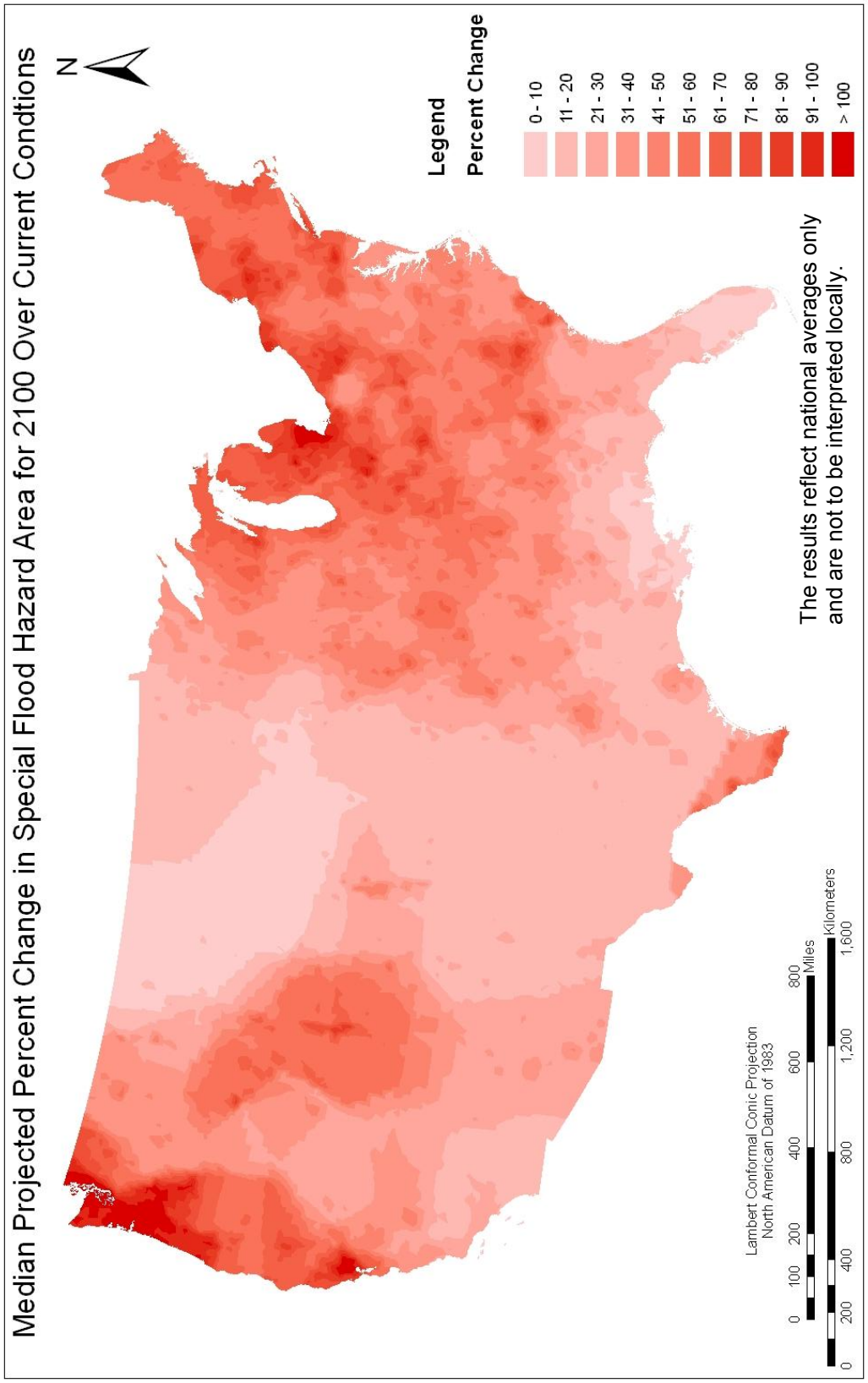

Figure 4-10. The median (50th percentile) relative change of the SFHA at epoch 5 (2100). Changes are with respect to current conditions.

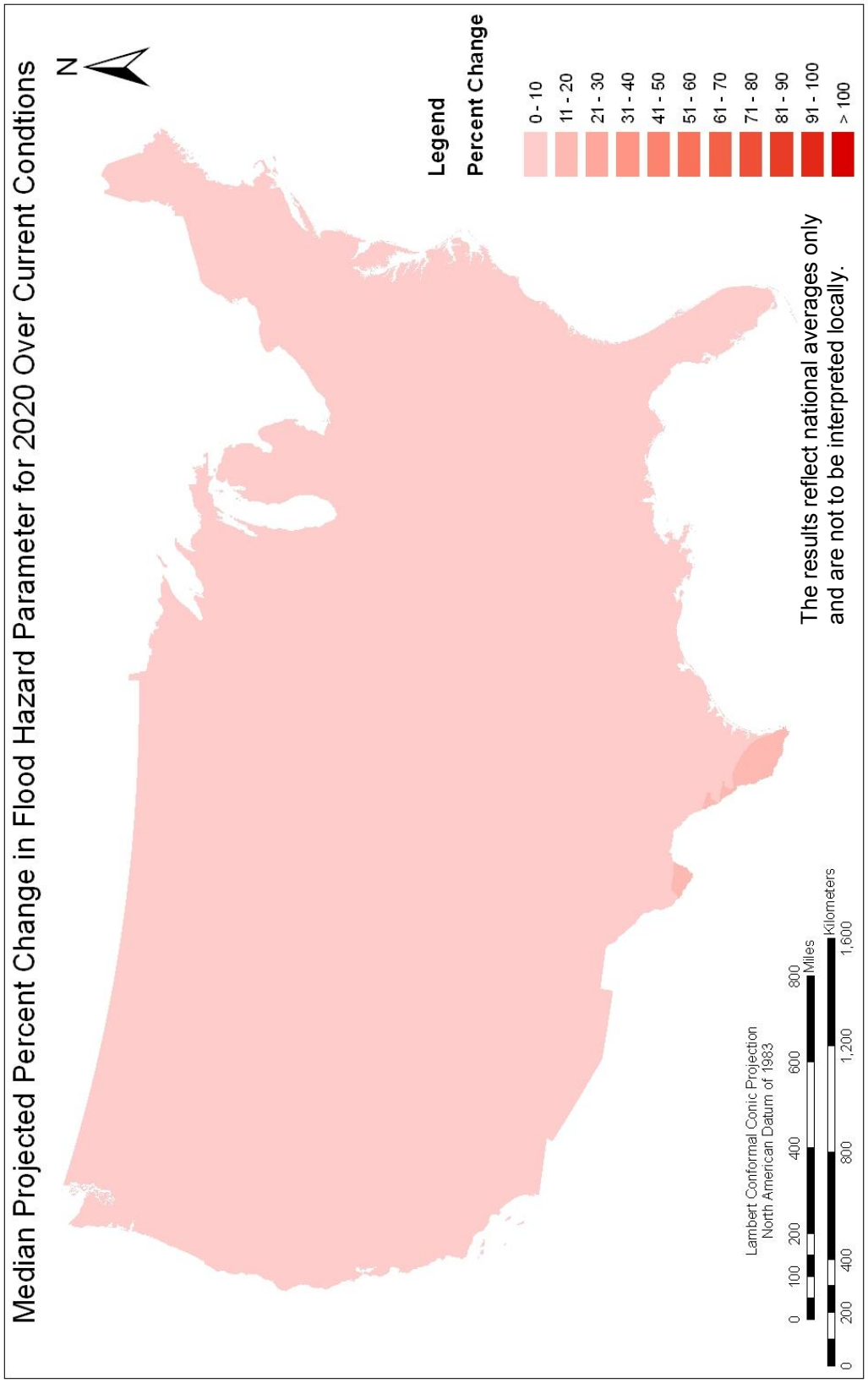

Figure 4-11. The median (50th percentile) relative change of the flood hazard parameter at epoch 1 (2020). Changes are with respect to current conditions.

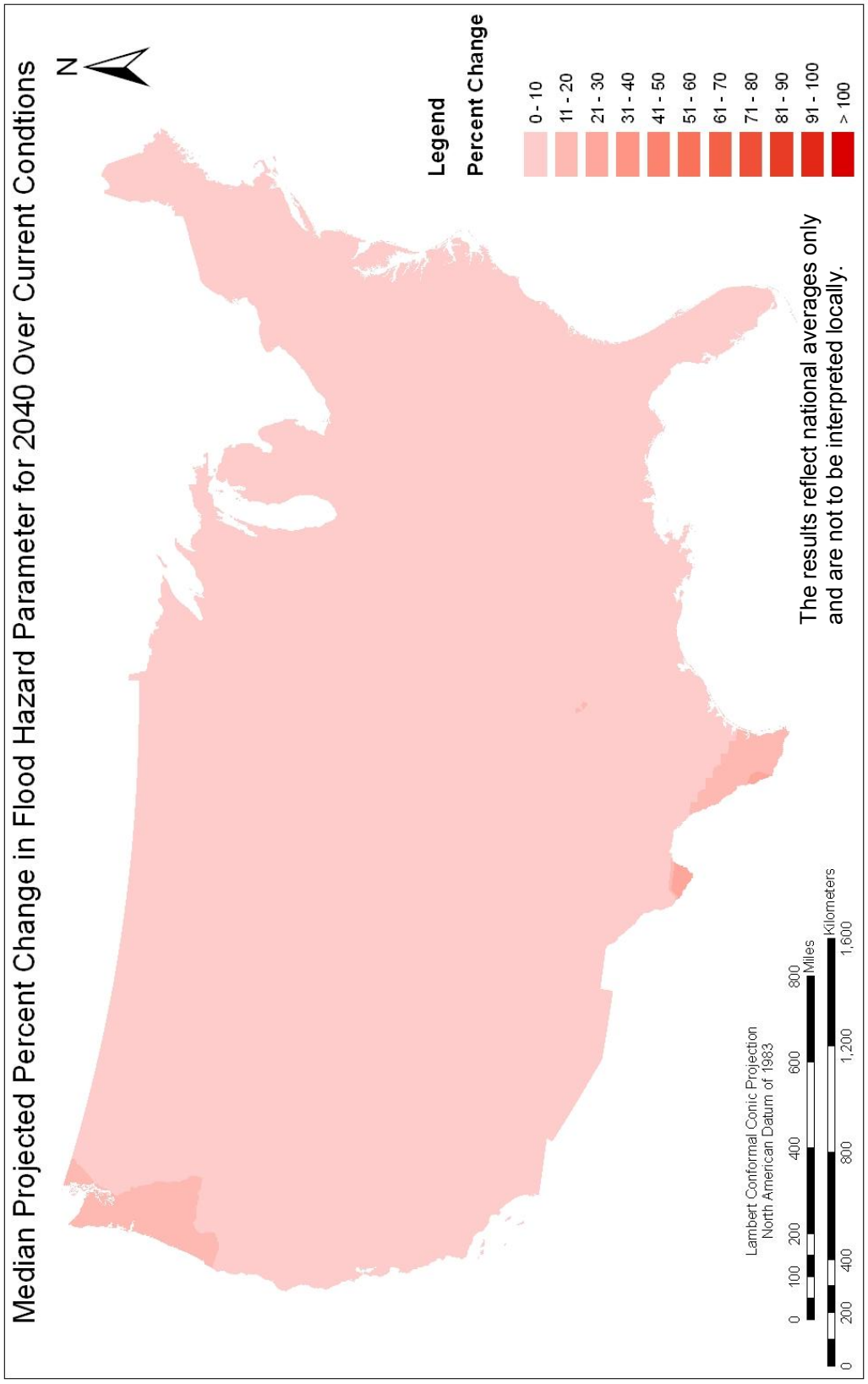

Figure 4-12. The median (50th percentile) relative change of the flood hazard parameter at epoch 2 (2040). Changes are with respect to current conditions.

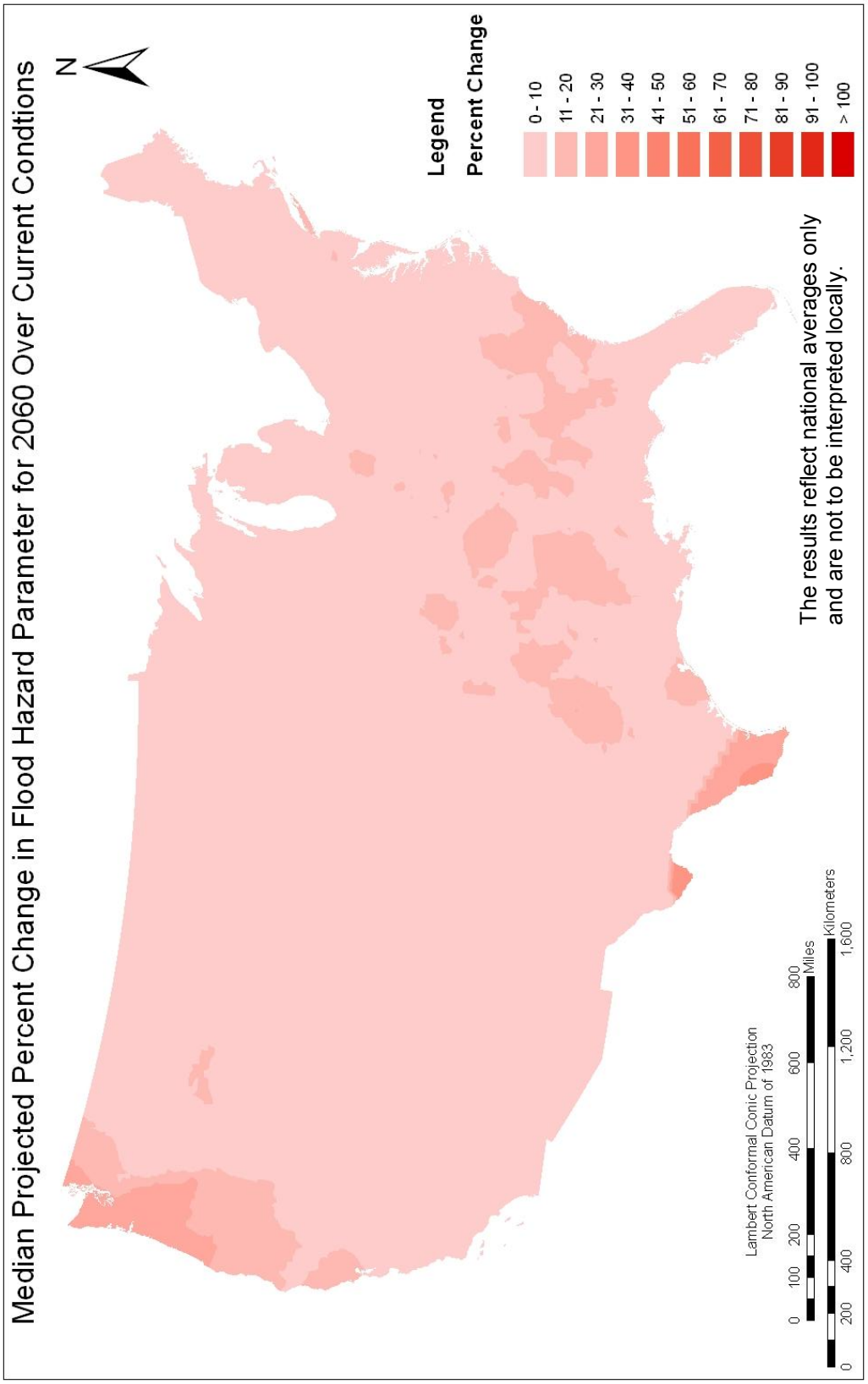

Figure 4-13. The median (50th percentile) relative change of the flood hazard parameter at epoch 3 (2060). Changes are with respect to current conditions.

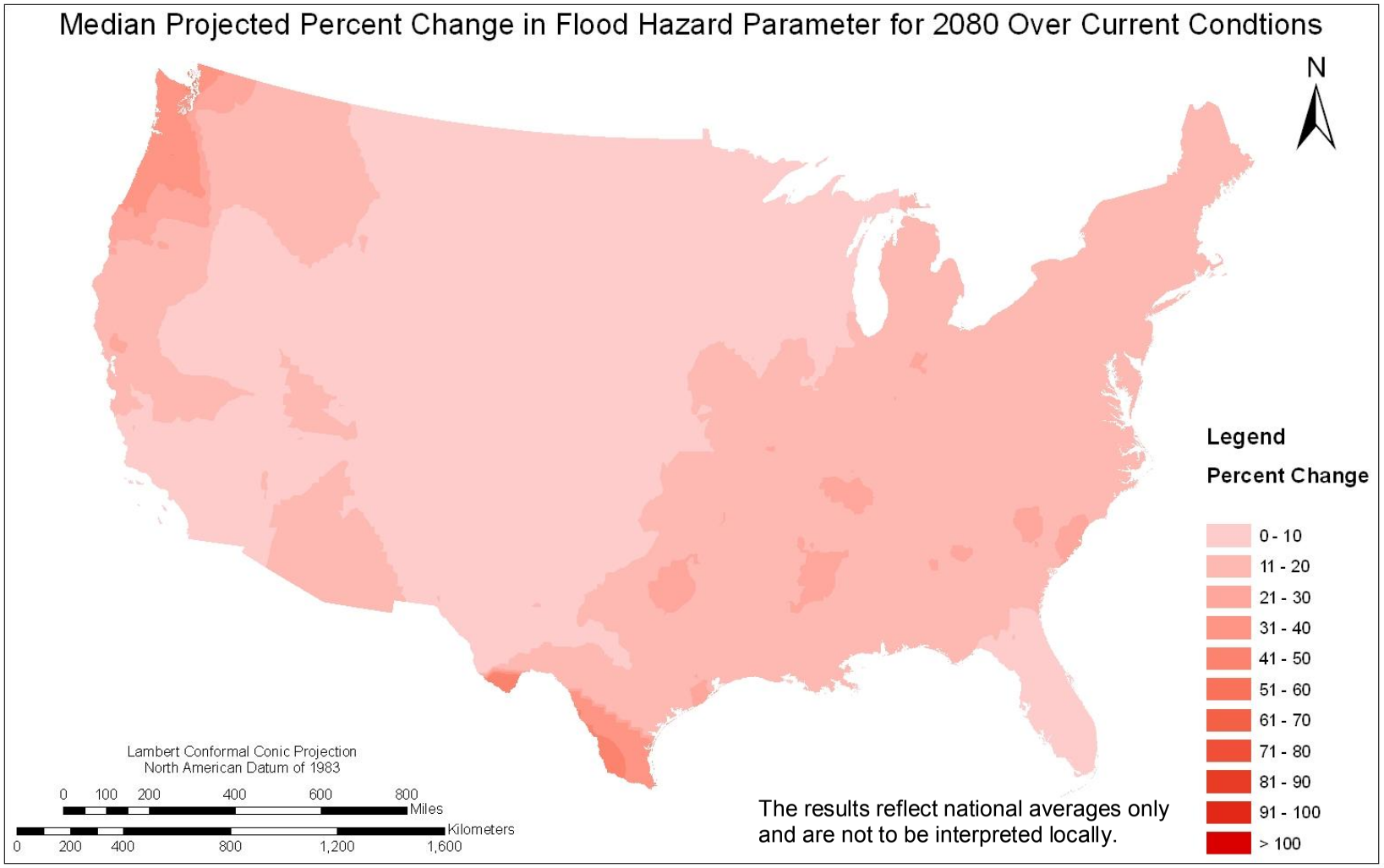

Figure 4-14. The median (50th percentile) relative change of the flood hazard parameter at epoch 4 (2080). Changes are with respect to current conditions.

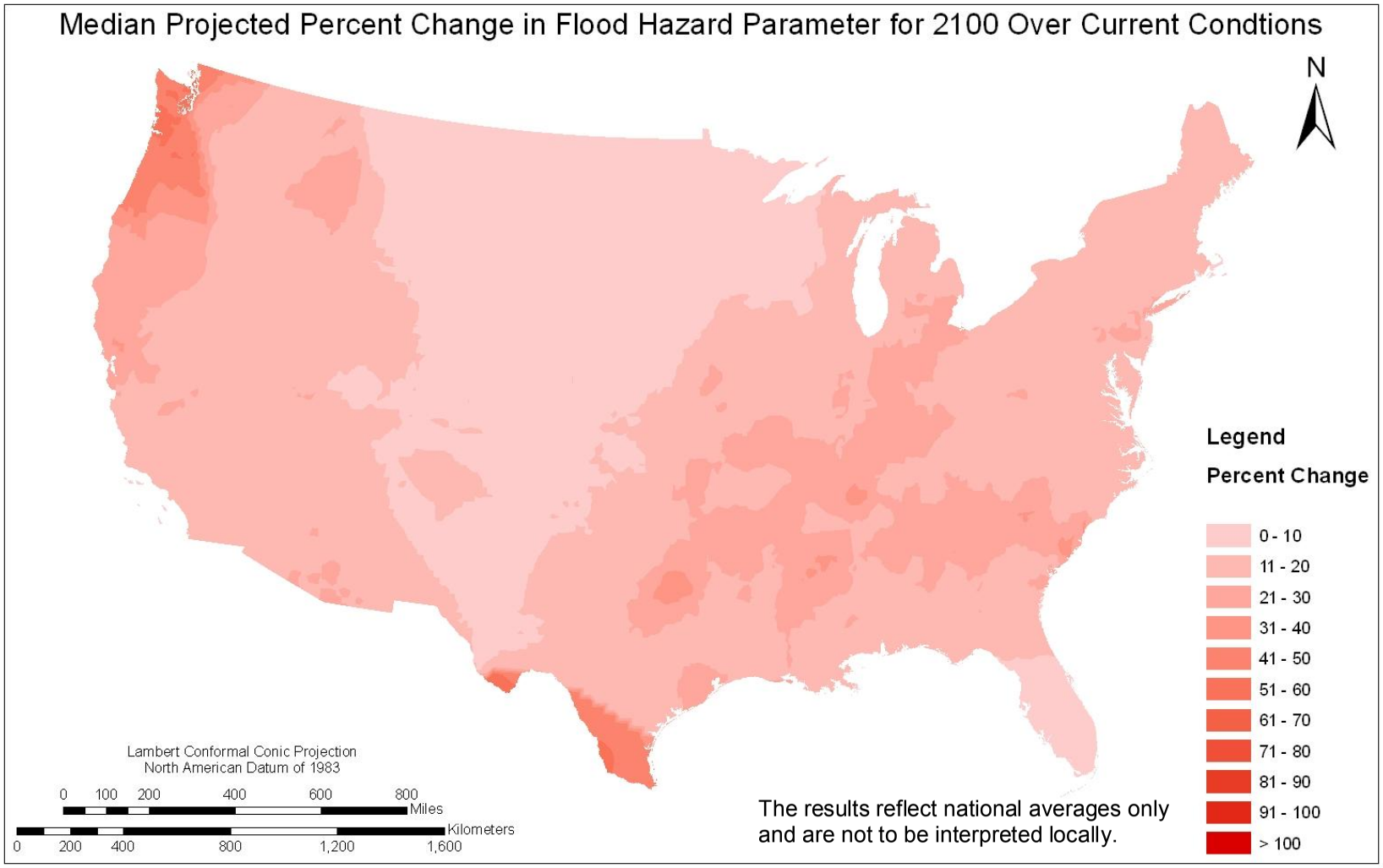

Figure 4-15. The median (50th percentile) relative change of the flood hazard parameter at epoch 5 (2100). Changes are with respect to current conditions.

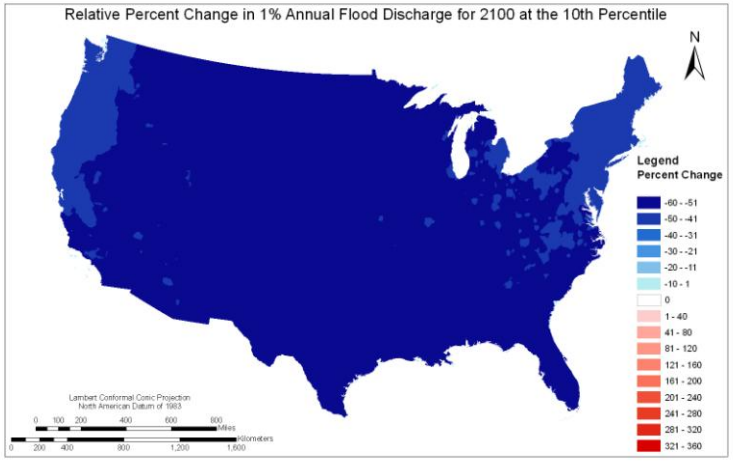

10th Percentile.

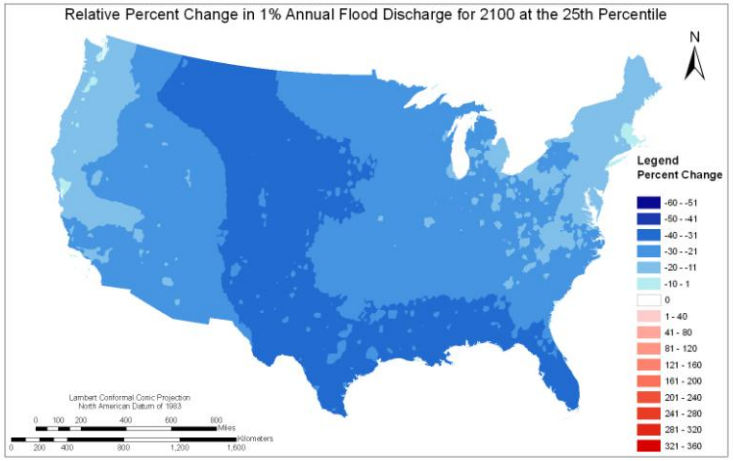

25th Percentile.

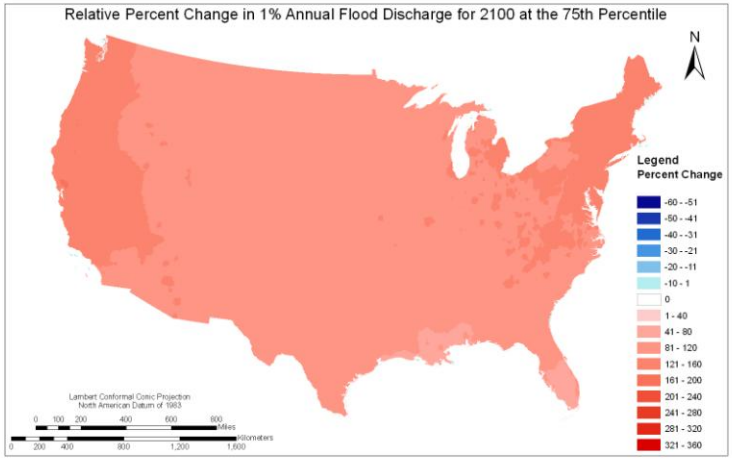

75th Percentile.

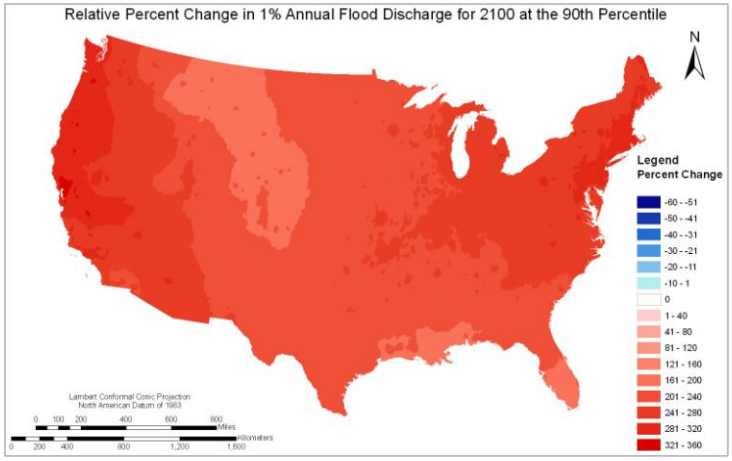

90th Percentile.

Figure 4-16. Relative change of the 1%-annual flood discharge at epoch 5 (2100) at the 10th, 25th, 75th, and 90th percentiles. The results reflect national averages only and are not to be interpreted locally. Changes are with respect to current conditions.

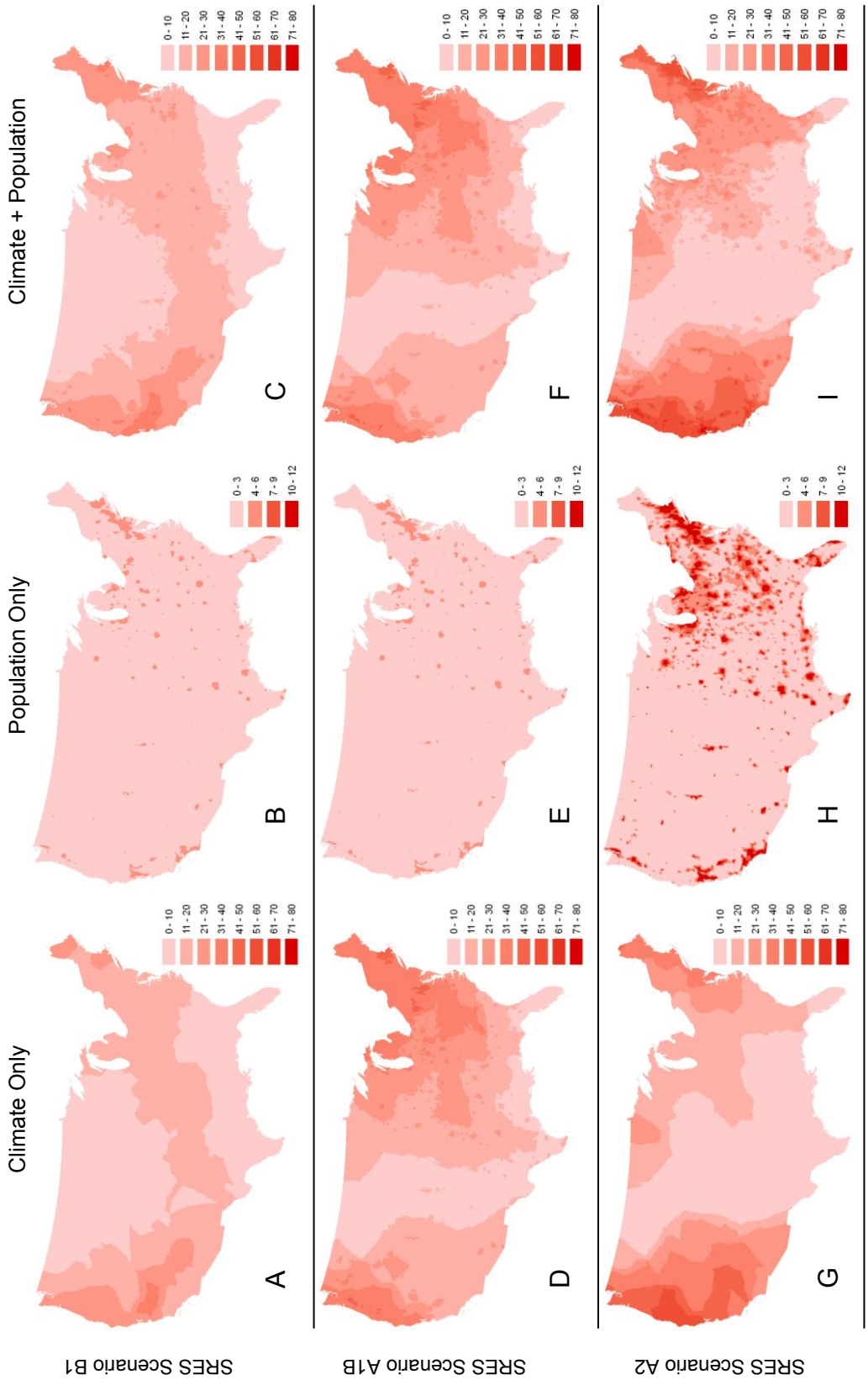

Figure 4-17. Median projected relative percent change in $Q_{1\%}$ due to climate change and population growth through the end of the 21st century; see the text for additional explanation of the maps. Note that the color scale for maps B, E, and H differs from the other maps in the figure.

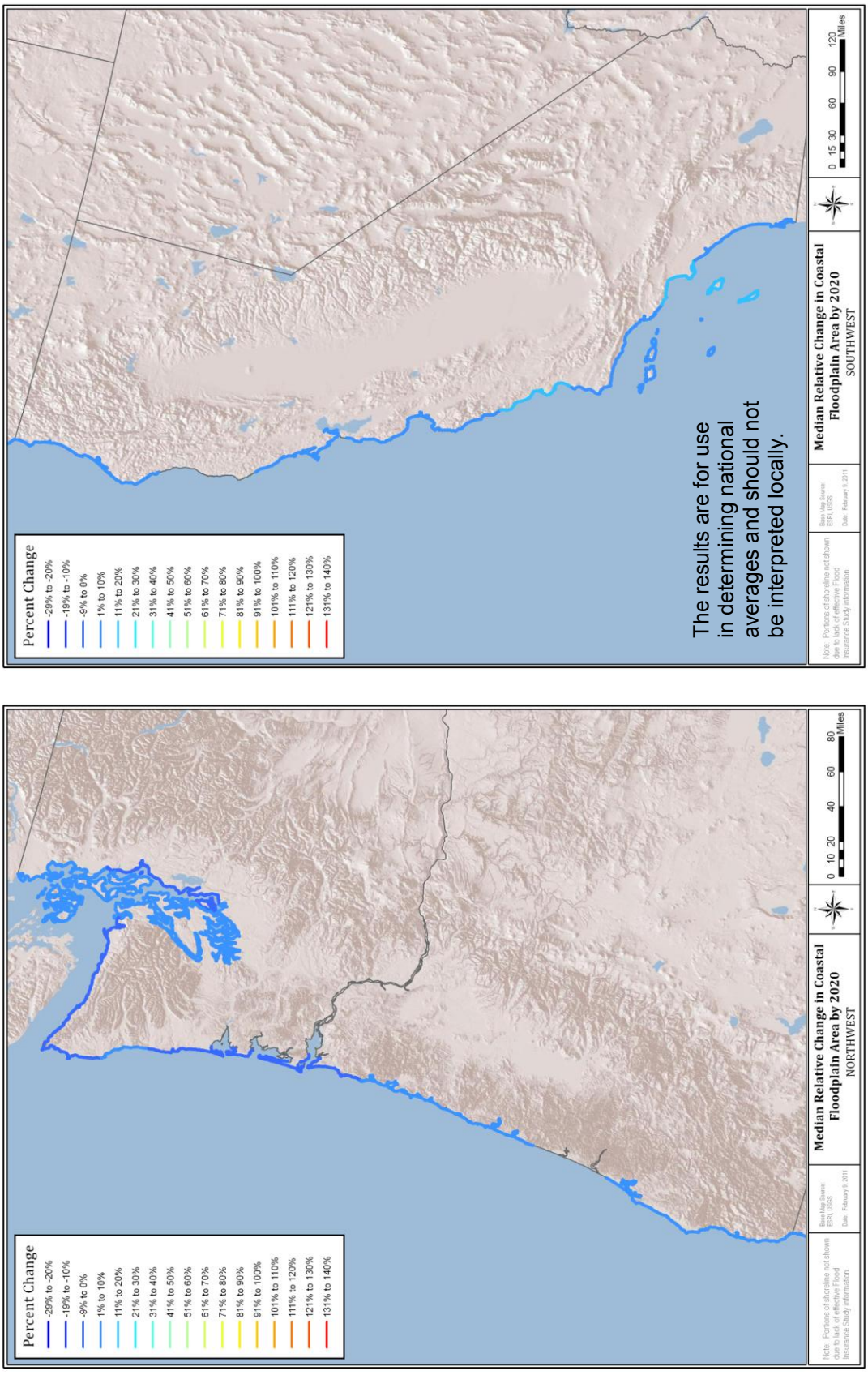

Figure 4-18. Estimated median (50th percentile) change in the coastal flood hazard area for the Northern Pacific Coast (left) and Southern Pacific Coast at epoch 1 (2020). Changes are with respect to current conditions for fixed shorelines.

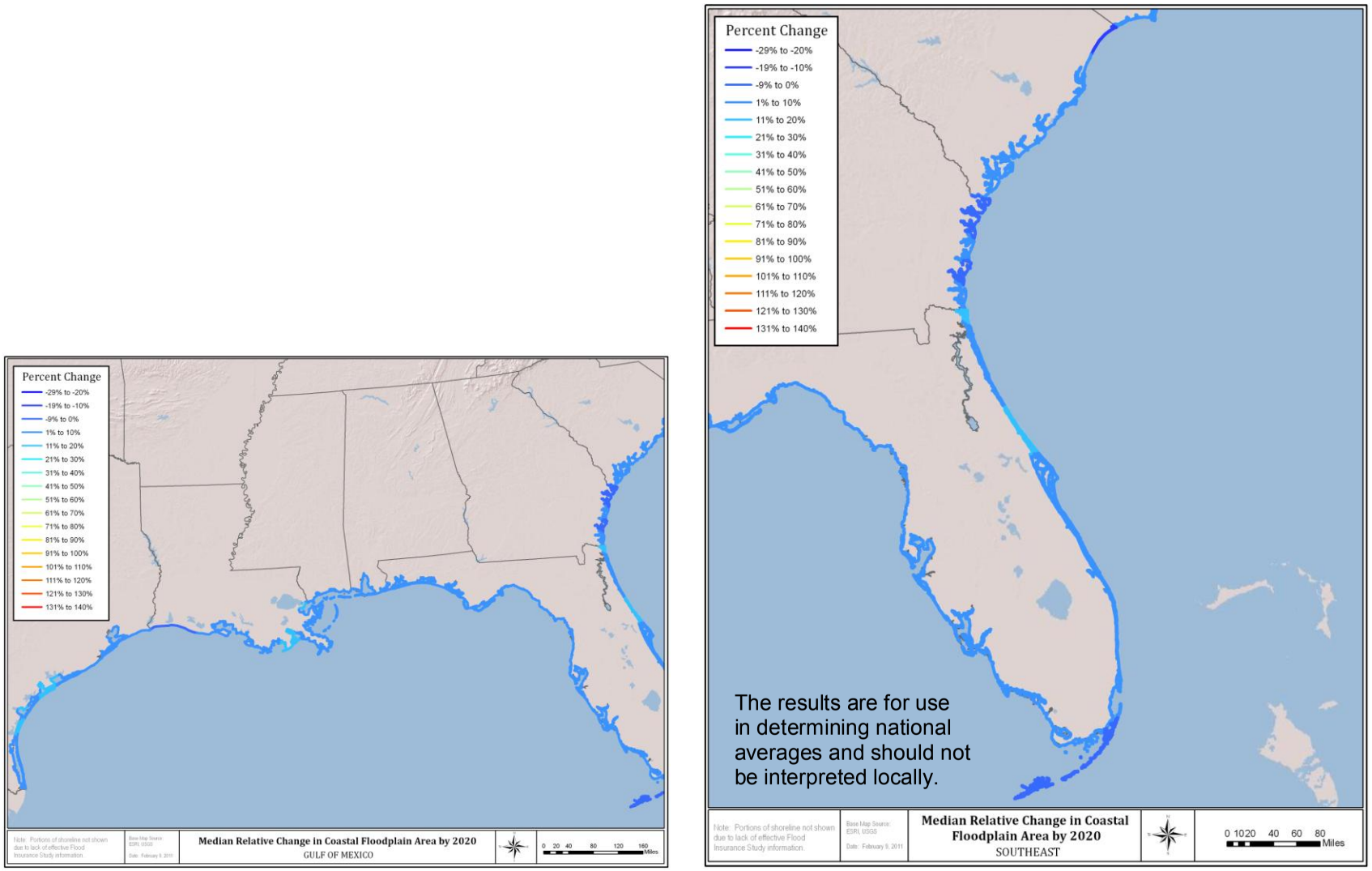

Figure 4-19. Estimated median (50th percentile) change in the coastal flood hazard area for the Gulf of Mexico (left) and South Atlantic Coast at epoch 1 (2020). Changes are with respect to current conditions for fixed shorelines.

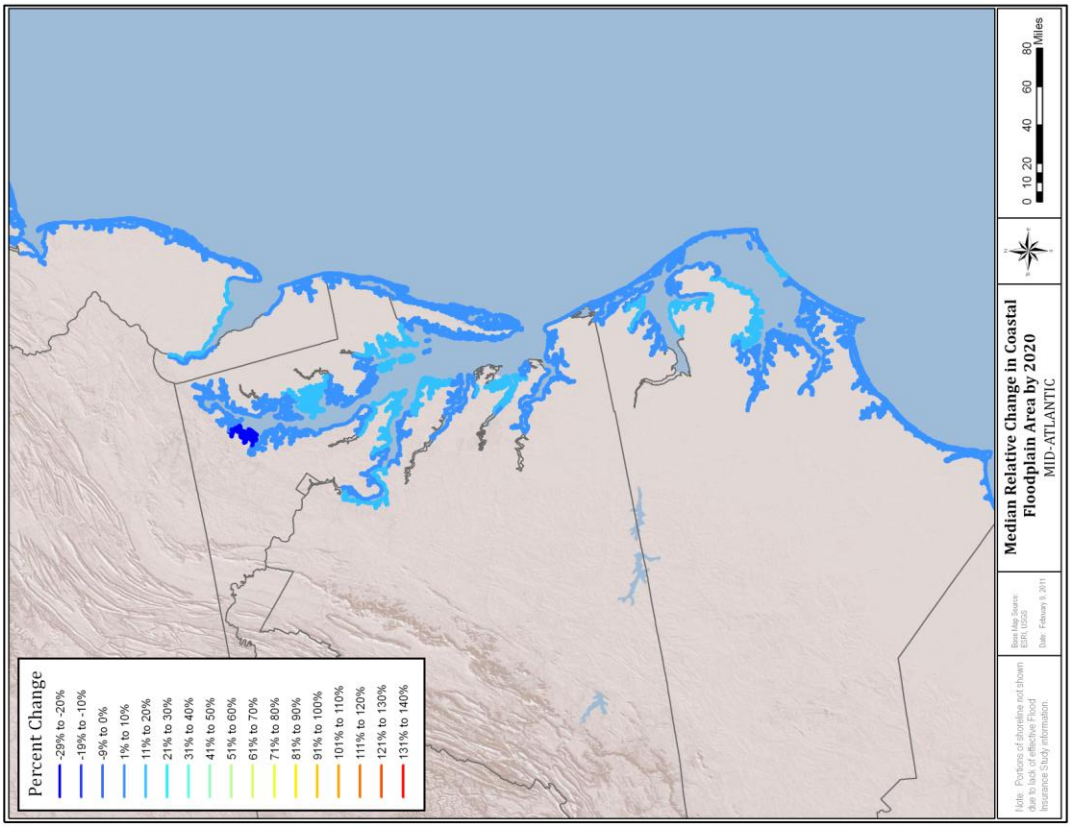

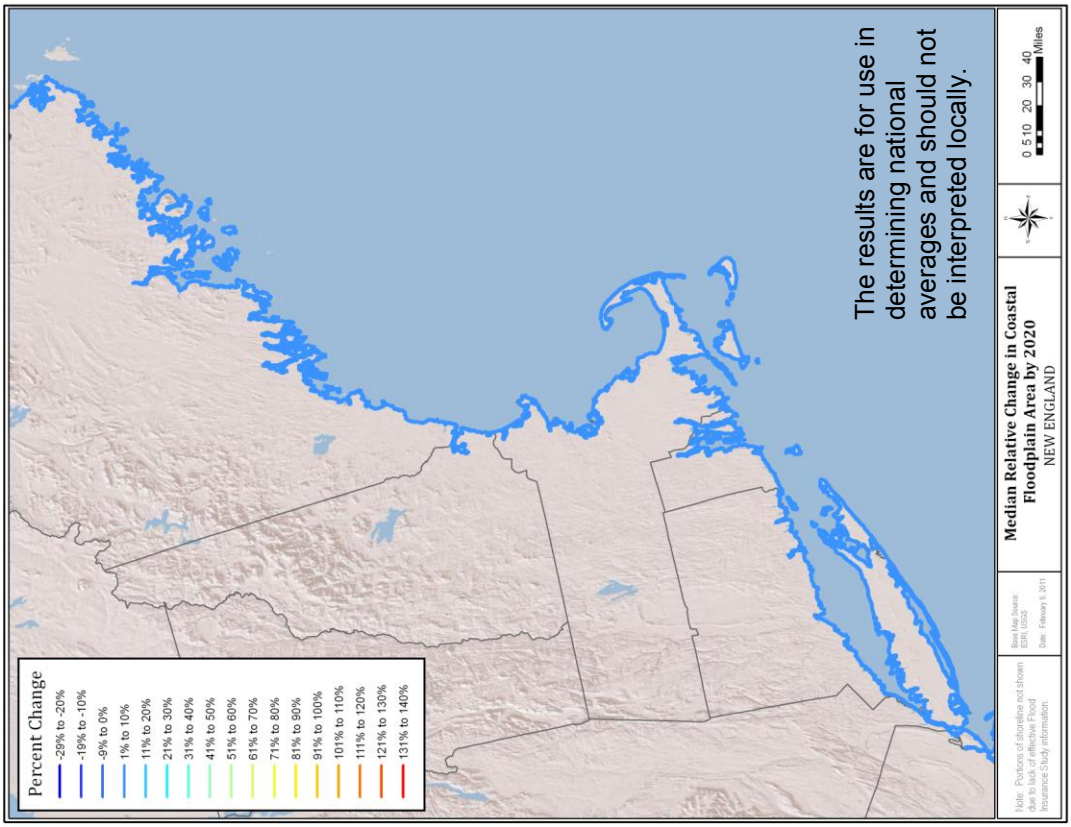

Figure 4-20. Estimated median (50th percentile) change in the coastal flood hazard area for the Mid-Atlantic Coast (left) and North Atlantic Coast at epoch 1 (2020). Changes are with respect to current conditions for fixed shorelines.

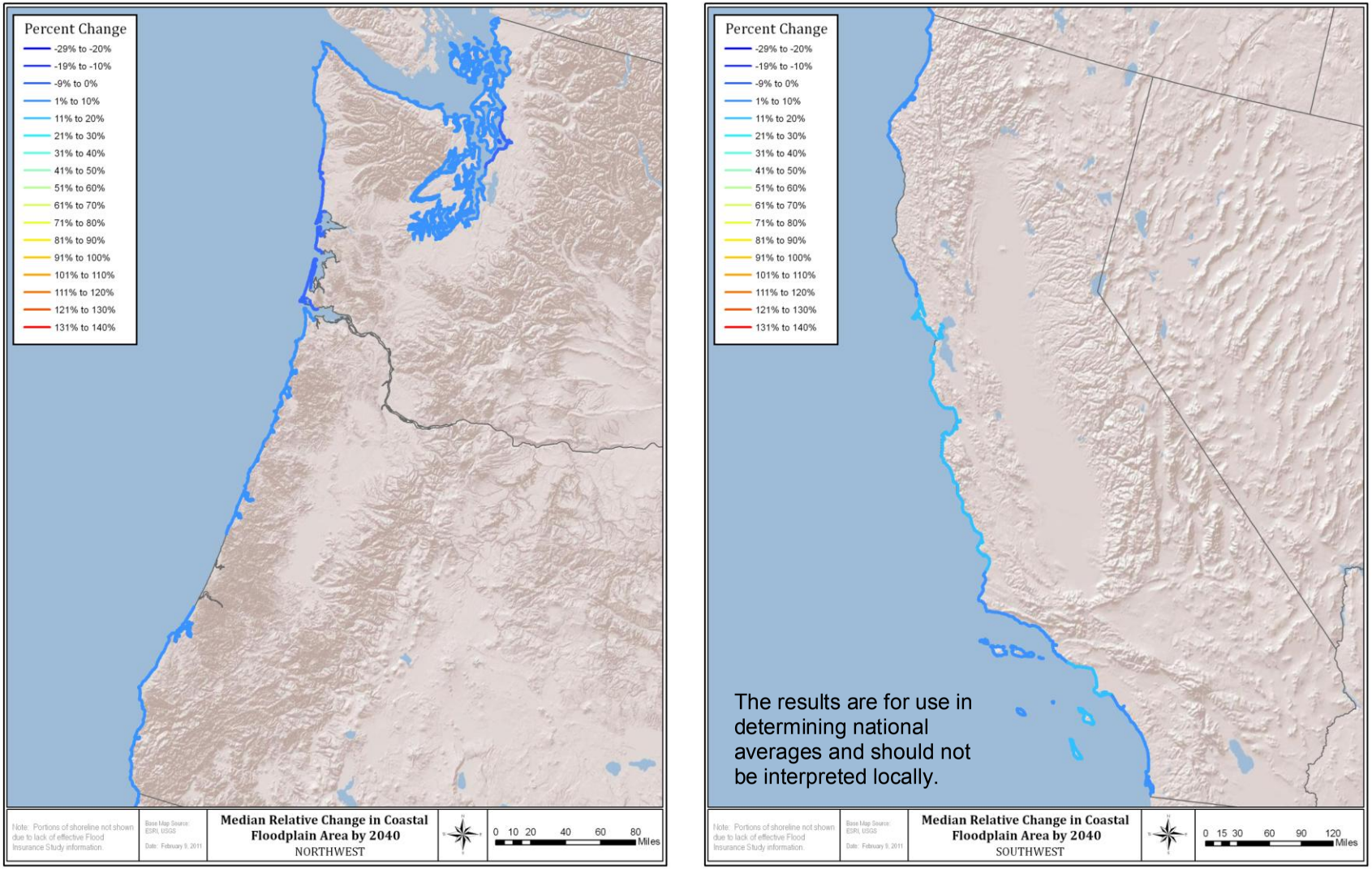

Figure 4-21. Estimated median (50th percentile) change in the coastal flood hazard area for the Northern Pacific Coast (left) and Southern Pacific Coast at epoch 2 (2040). Changes are with respect to current conditions for fixed shorelines.

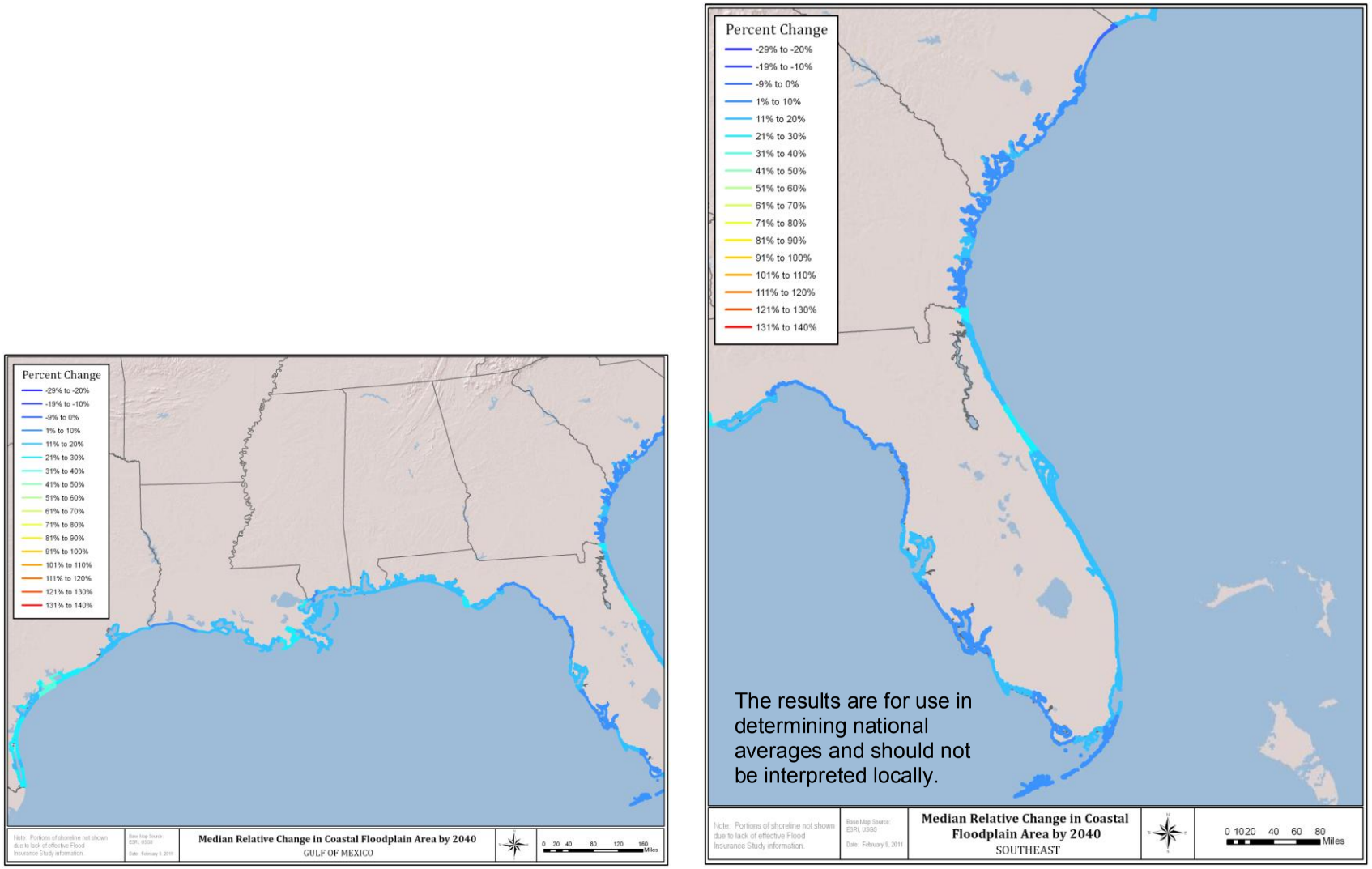

Figure 4-22. Estimated median (50th percentile) change in the coastal flood hazard area for the Gulf of Mexico (left) and South Atlantic Coast at epoch 2 (2040). Changes are with respect to current conditions for fixed shorelines.

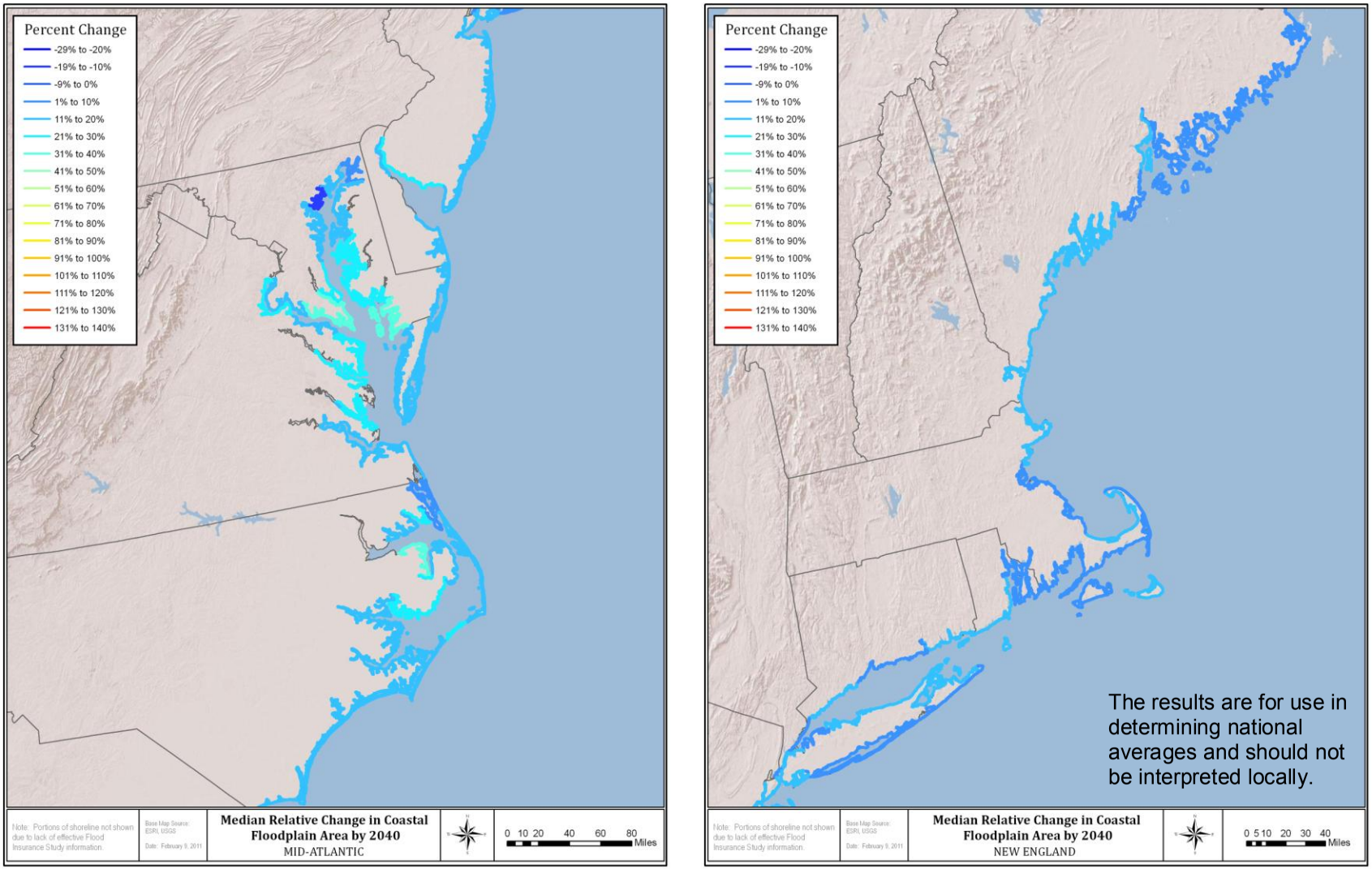

Figure 4-23. Estimated median (50th percentile) change in the coastal flood hazard area for the Mid-Atlantic Coast (left) and North Atlantic Coast at epoch 2 (2040). Changes are with respect to current conditions for fixed shorelines.

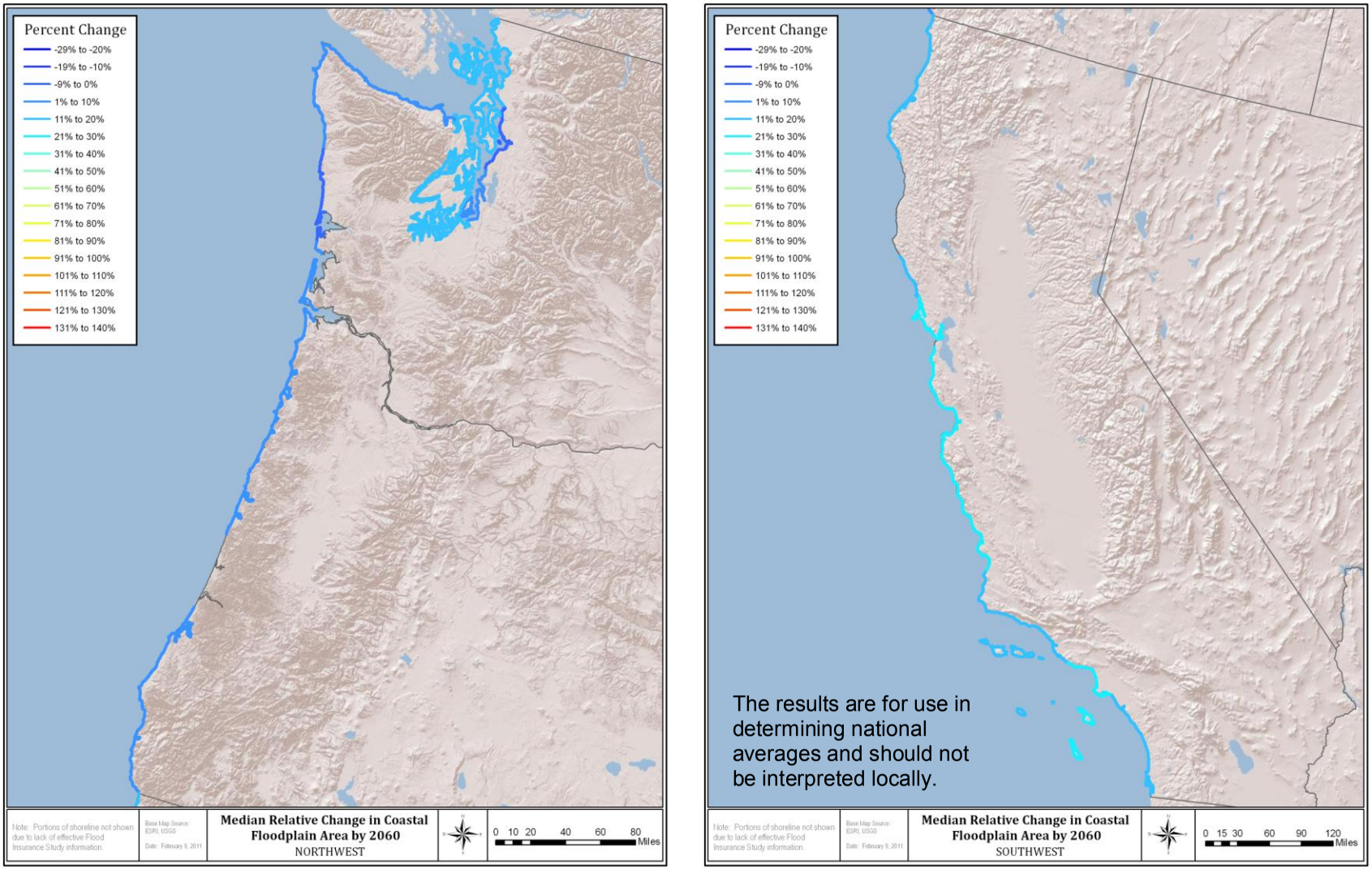

Figure 4-24. Estimated median (50th percentile) change in the coastal flood hazard area for the Northern Pacific Coast (left) and Southern Pacific Coast at epoch 3 (2060). Changes are with respect to current conditions for fixed shorelines.

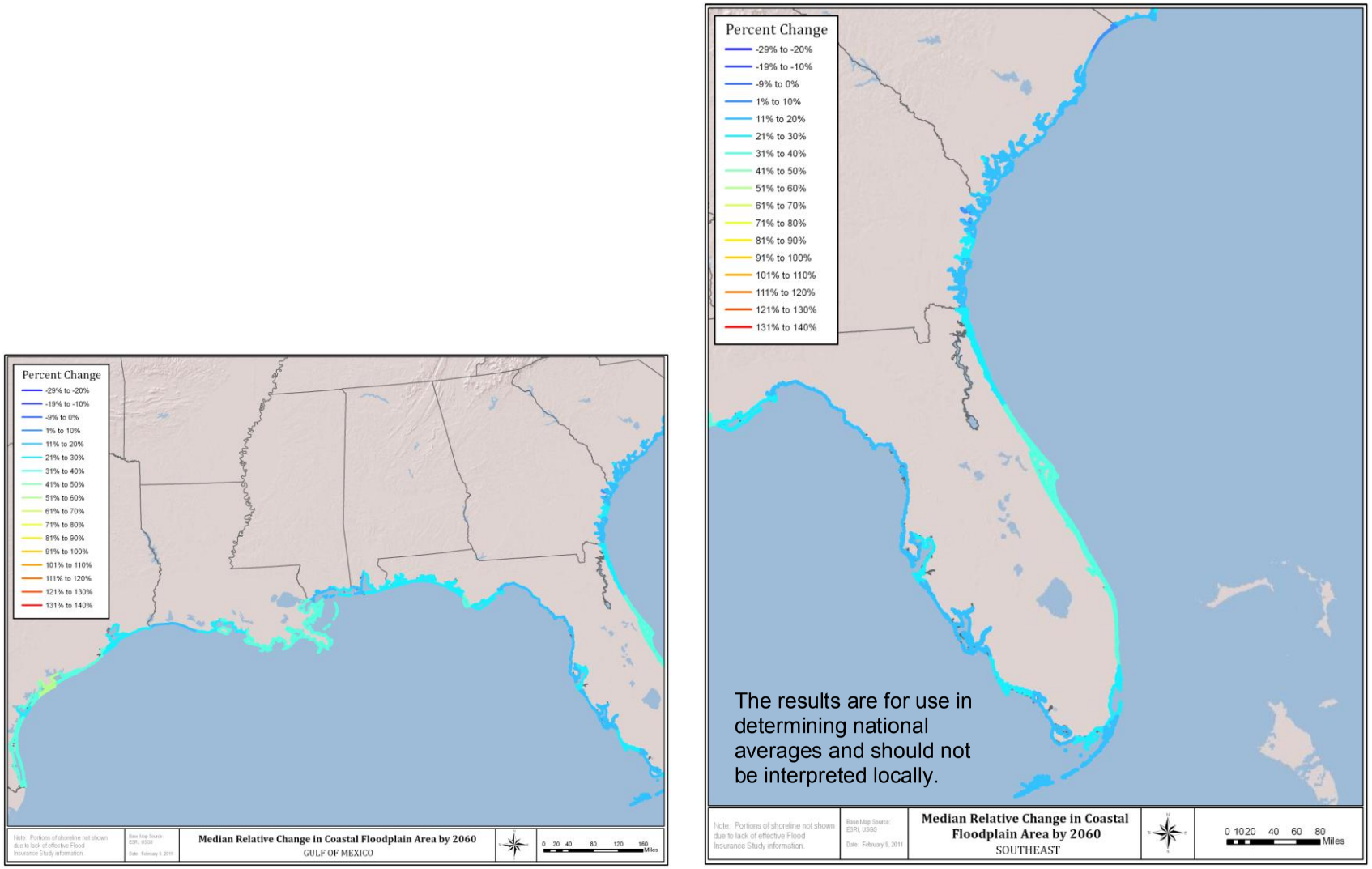

Figure 4-25. Estimated median (50th percentile) change in the coastal flood hazard area for the Gulf of Mexico (left) and South Atlantic Coast at epoch 3 (2060). Changes are with respect to current conditions for fixed shorelines.

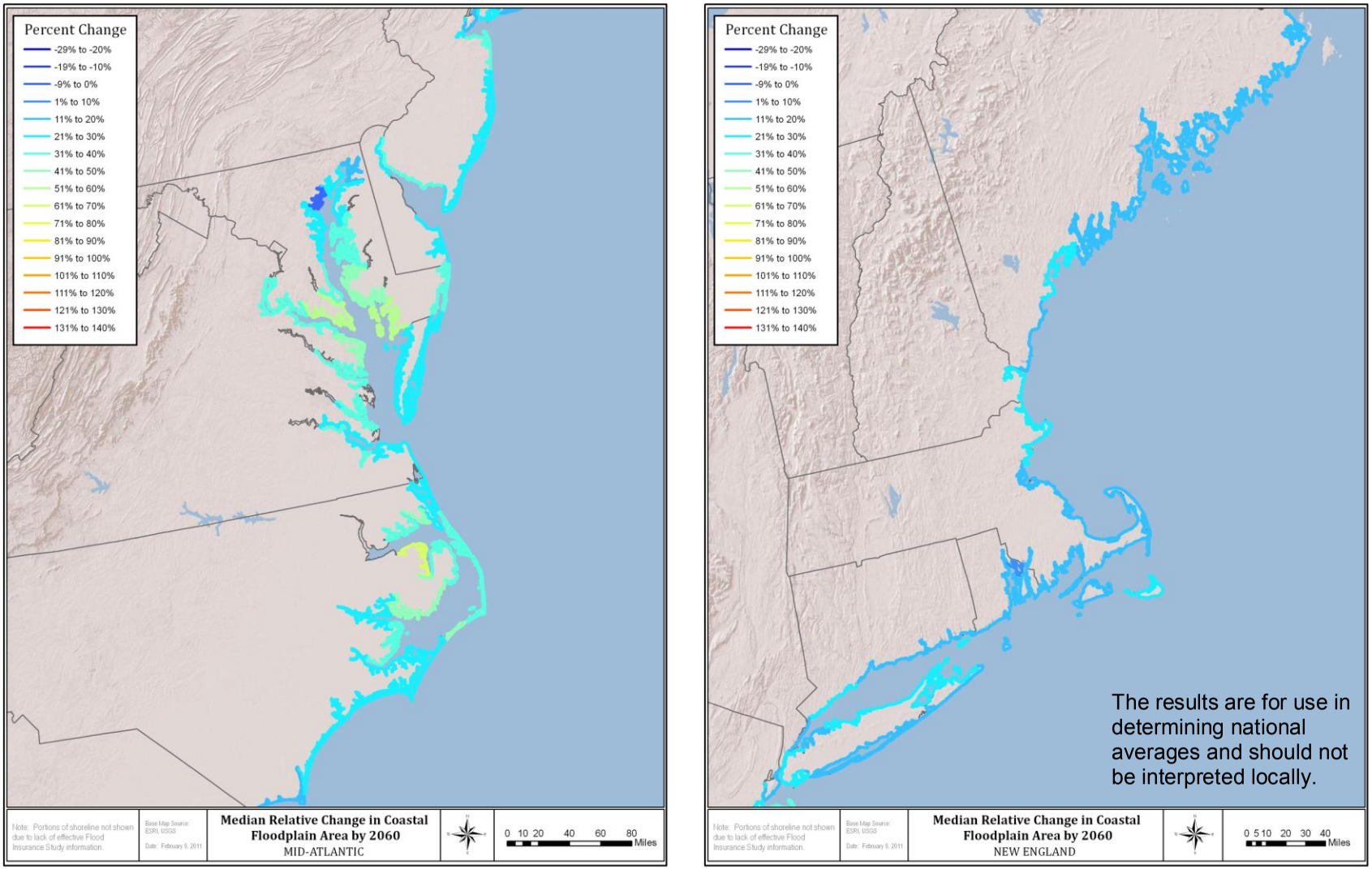

Figure 4-26. Estimated median (50th percentile) change in the coastal flood hazard area for the Mid-Atlantic Coast (left) and North Atlantic Coast at epoch 3 (2060). Changes are with respect to current conditions for fixed shorelines.

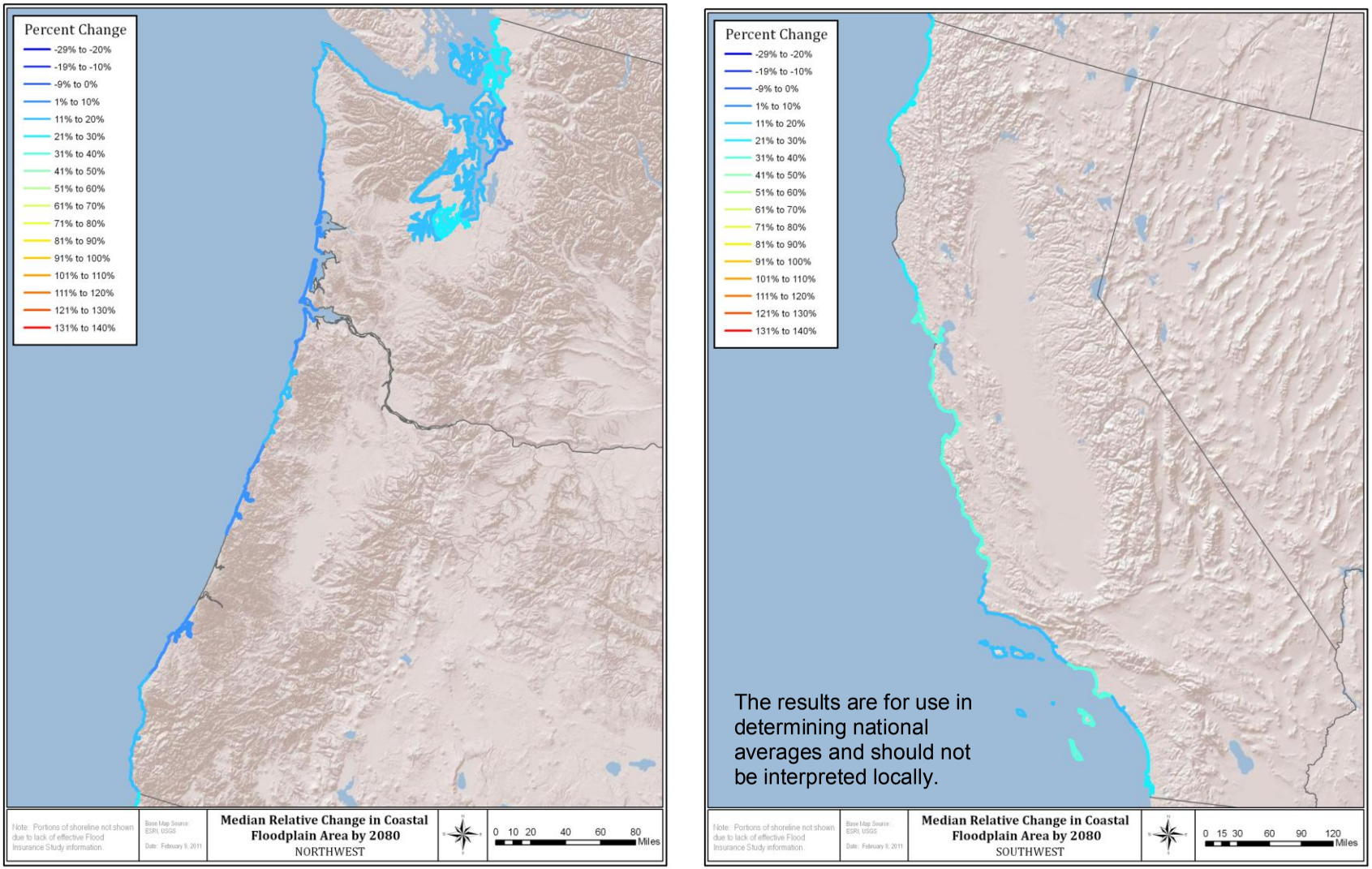

Figure 4-27. Estimated median (50th percentile) change in the coastal flood hazard area for the Northern Pacific Coast (left) and Southern Pacific Coast at epoch 4 (2080). Changes are with respect to current conditions for fixed shorelines.

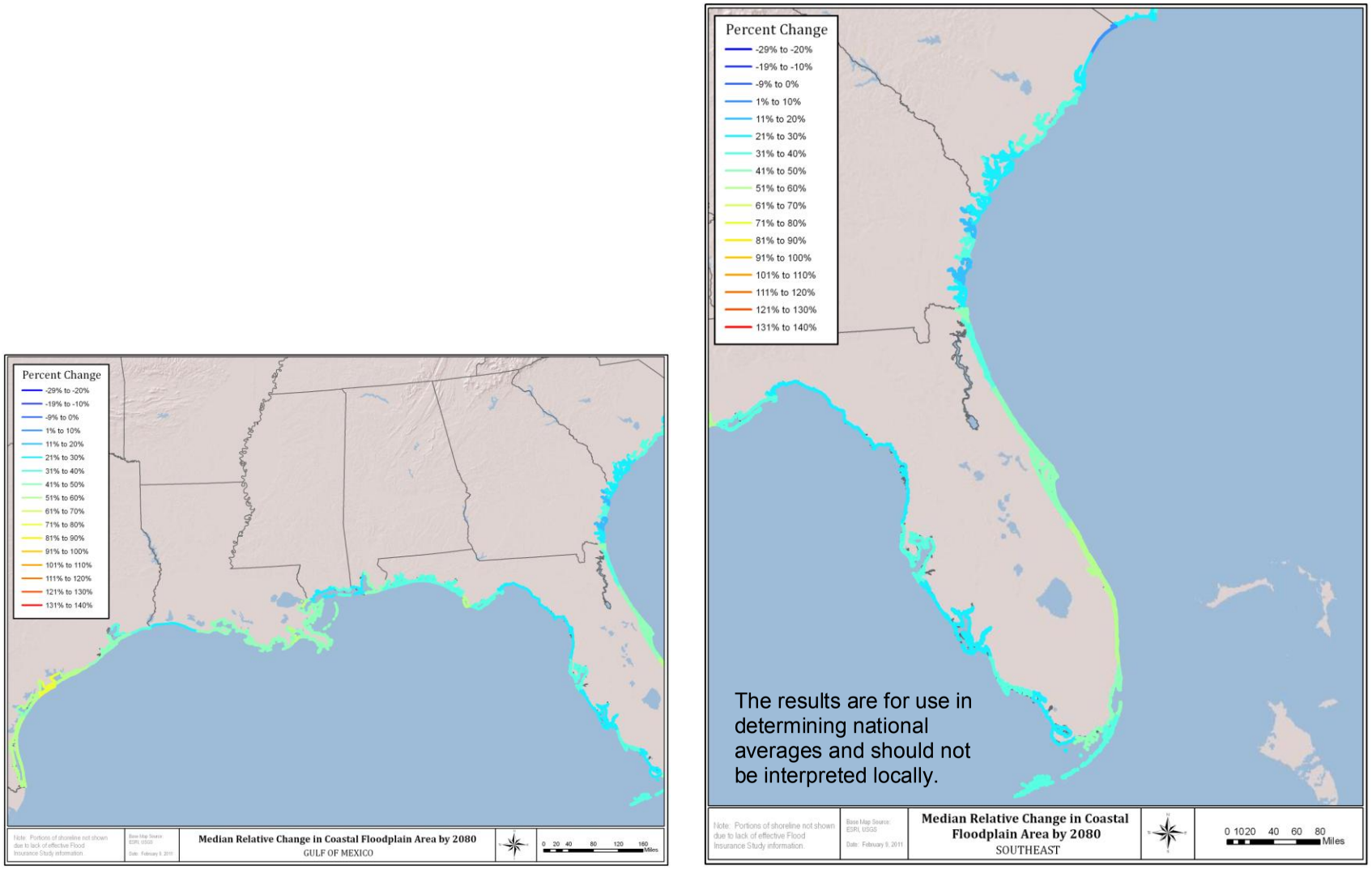

Figure 4-28. Estimated median (50th percentile) change in the coastal flood hazard area for the Gulf of Mexico (left) and South Atlantic Coast at epoch 4 (2080). Changes are with respect to current conditions for fixed shorelines.

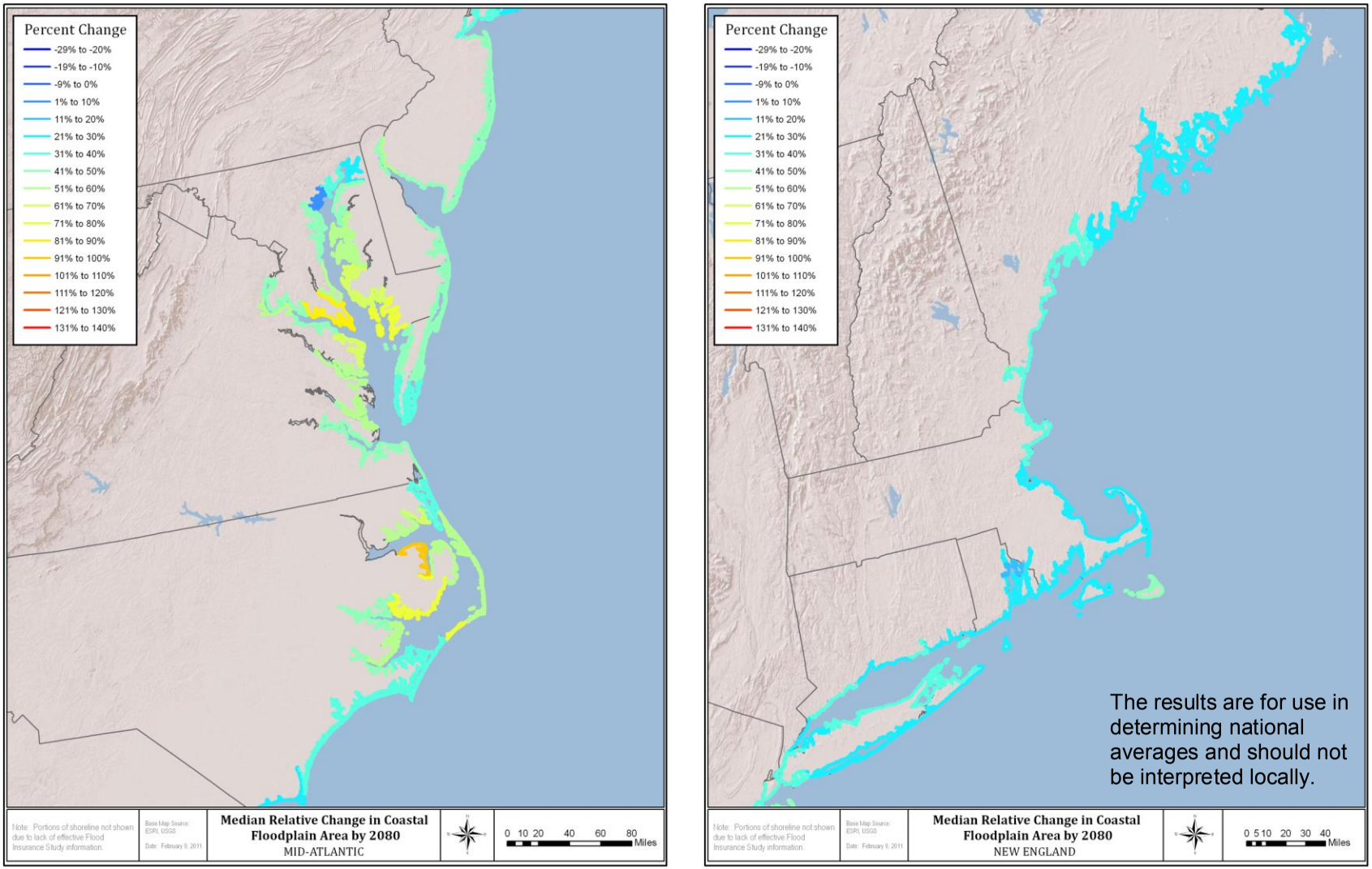

Figure 4-29. Estimated median (50th percentile) change in the coastal flood hazard area for the Mid-Atlantic Coast (left) and North Atlantic Coast at epoch 4 (2080). Changes are with respect to current conditions for fixed shorelines.

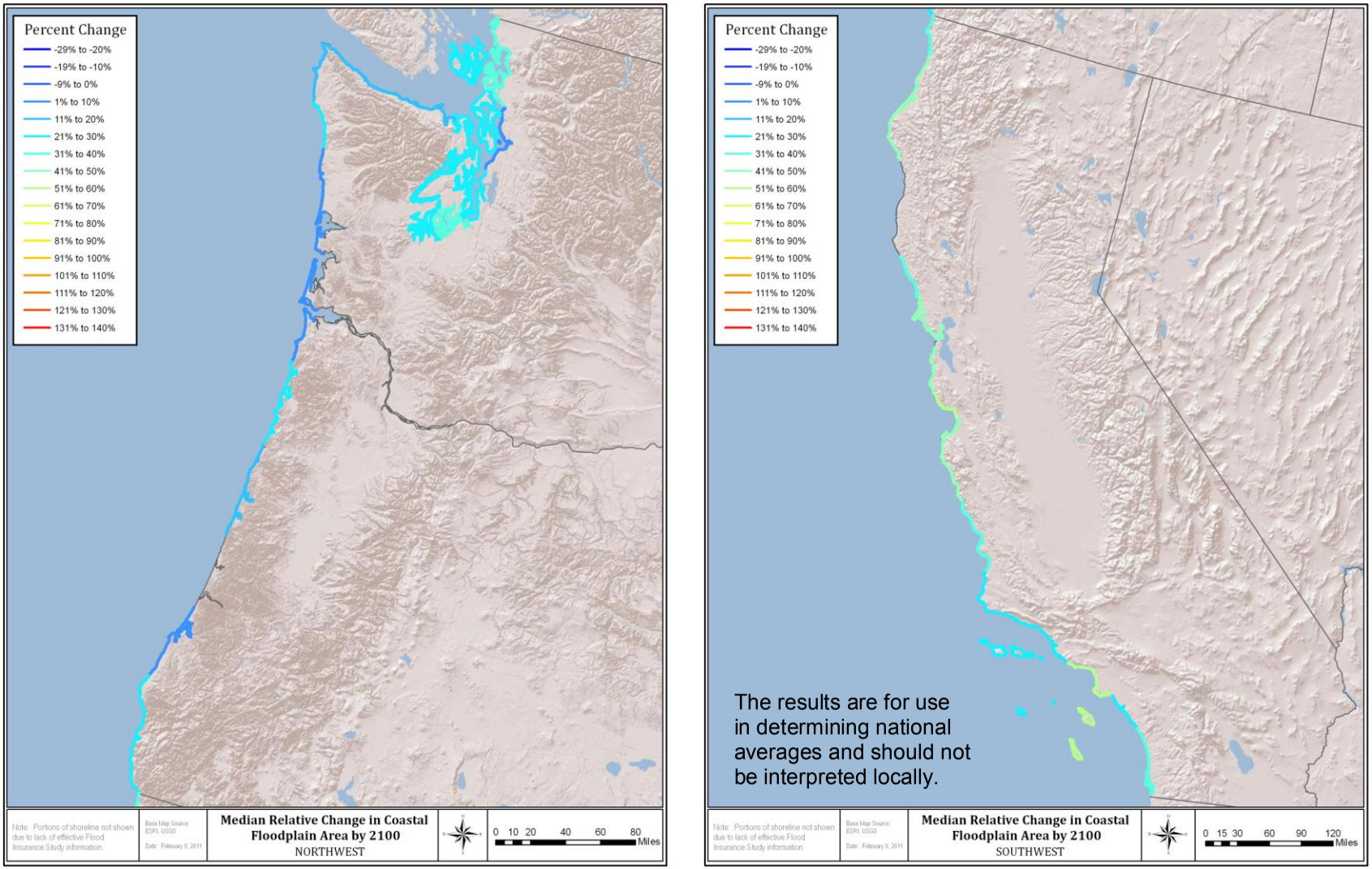

Figure 4-30. Estimated median (50th percentile) change in the coastal flood hazard area for the Northern Pacific Coast (left) and Southern Pacific Coast at epoch 5 (2100). Changes are with respect to current conditions for fixed shorelines.

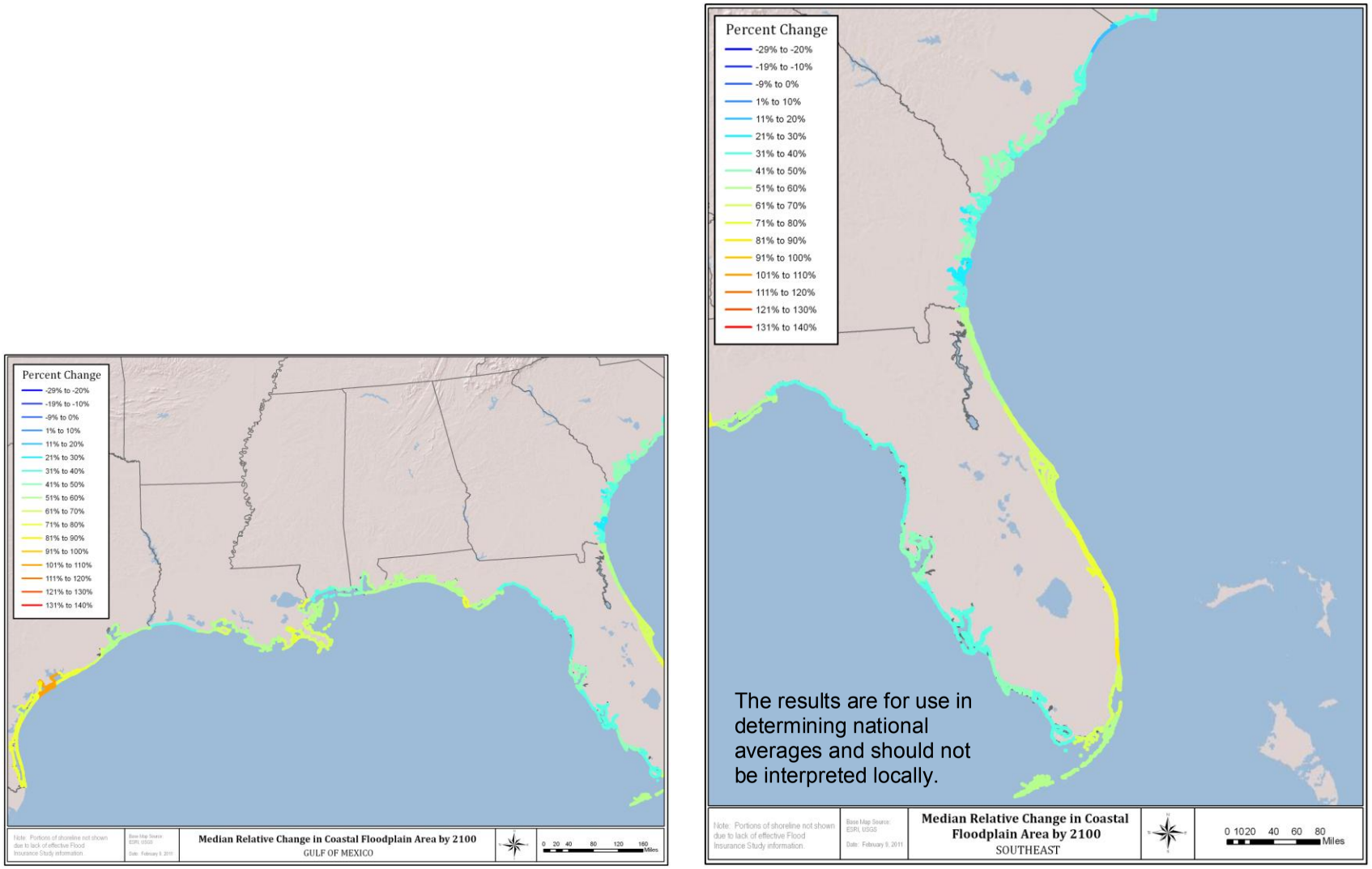

Figure 4-31. Estimated median (50th percentile) change in the coastal flood hazard area for the Gulf of Mexico (left) and South Atlantic Coast at epoch 5 (2100). Changes are with respect to current conditions for fixed shorelines.

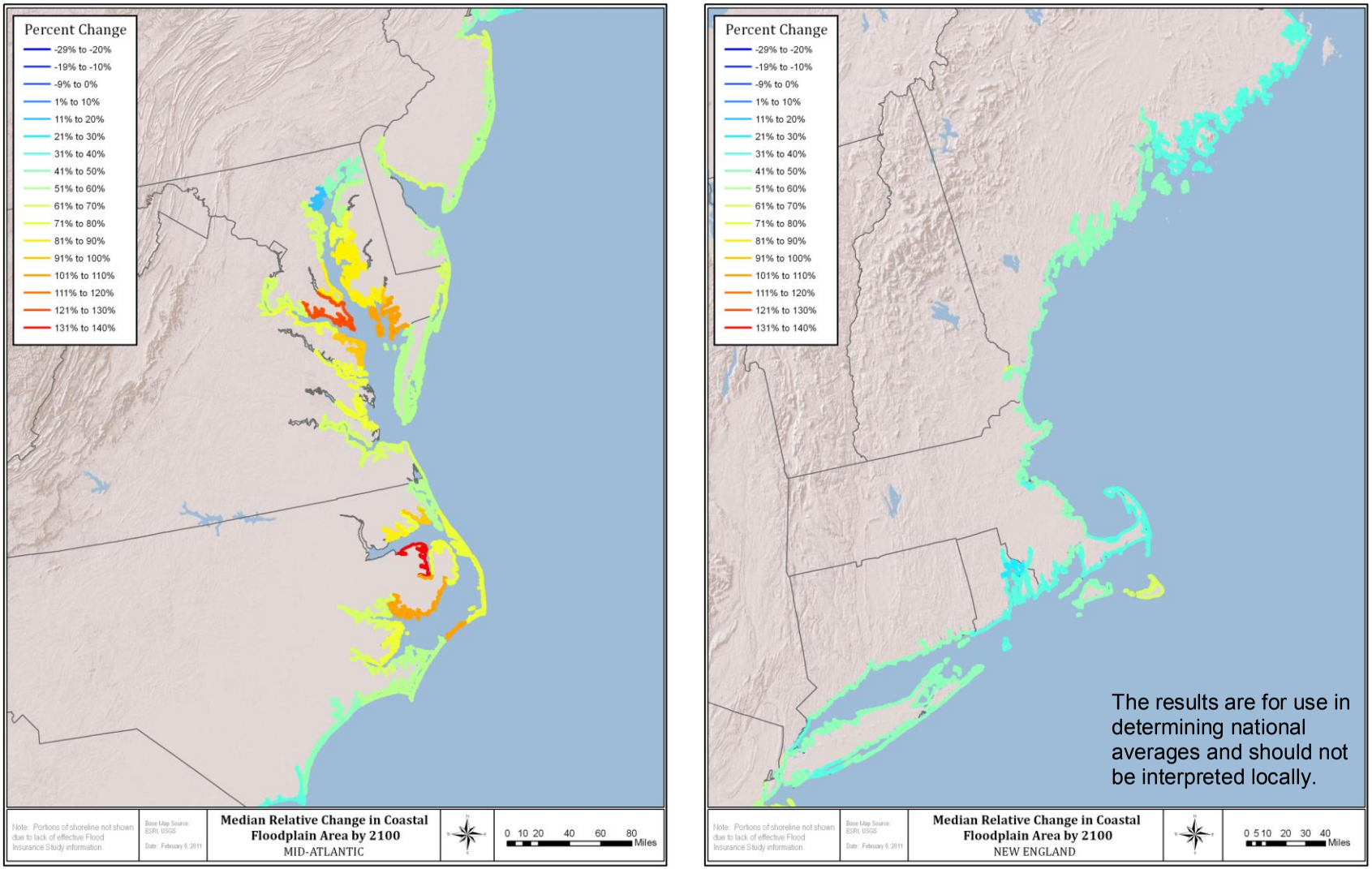

Figure 4-32. Estimated median (50th percentile) change in the coastal flood hazard area for the Mid-Atlantic Coast (left) and North Atlantic Coast at epoch 5 (2100). Changes are with respect to current conditions for fixed shorelines.

5.0
Economic Analysis

5.0 Economic Analysis

In this section, the climate change projections summarized in Section 4 are analyzed with respect to their impact on the NFIP, including estimated changes in numbers of policyholders, premium levels, and expected losses due to climate change and population growth impacts.

The results of this section are based on the following outputs from the climate change analysis:

- Change in population;
- Change in population within the flood hazard area (SFHA), which is impacted by the change in the footprint of the SFHA as well as by the overall change in population; and
- Change in depth of the flood hazard area.

The first two outputs are used to directly estimate the expected number of future NFIP policies and associated premium. The change in depth of the flood hazard area is used to estimate the change in future loss cost. The changes in future expected losses are estimated using elements of the NFIP's current ratemaking methodology and assumptions about the frequency and severity of flooding at different structure heights (relative to the base flood elevation) in combination with the change in depth of the flood hazard area.

5.1 Analysis Description

The methods used in this economic analysis are based on current methods and assumptions used by the NFIP. This section uses certain key terms, which are specific to the insurance discussion, including:

- **Loss(es)** – Amounts paid or payable to claimants under the terms of an insurance policy. With respect to NFIP policies, these amounts paid or payable relate to building or contents damages caused by floods.
- **Premium** – Dollars collected by the insurance program to pay for annual expected losses and expenses associated with the administration of the insurance program.
- **Exposure** – The basic unit underlying insurance premium. The selected measure usually relates directly to loss potential. For property coverages in general (and including flood), this is often expressed as the value insured.
- **Loss Cost** –The amount of loss per exposure. For the NFIP, it is measure of expected loss payments per $100 of insured building value. For example, if the expected loss cost for a structure is 1.25 and exposure represents $100 of insured value, the expected loss (i.e., annual payments) for a $100,000 structure is $1,250. Mathematically, it is also the product of the frequency of claims per unit of exposure and severity. The analysis measures the change in loss cost over the time period included in the study.

5.1.1 Background of NFIP Ratemaking

"The NFIP is a coordinated, three-pronged approach developed to (1) identify those areas within local communities that are most at risk of flooding, (2) reduce the impact of flooding through a combination of mitigation and floodplain management, and (3) make flood insurance available to help individuals and small businesses recover following a flood. The NFIP can provide the flexibility for flood insurance to be based on workable methods of pooling risks, minimizing costs, distributing burdens equitably among those protected by flood insurance and the general public, and structuring rates to support mitigation and floodplain management efforts." (Hayes and Neal, 2010).

NFIP underwriting, ratemaking, and claim processing were developed to support the mission of making flood insurance widely available. The NFIP is intended to (1) maintain a fiscally sound rating and coverage structure, and (2) generate premiums that at least cover expenses and losses for the average historical loss year. For these reasons, rates for flood insurance are reviewed annually by NFIP management.

FEMA actuaries consider both the professional standards for insurance ratemaking, as well as the unique public policy goals contained in the National Flood Insurance Act.

The premium structure of the NFIP consists of:

- Subsidized Premiums, or premiums that are less than actuarially estimated premiums, are available for structures:
    1. Constructed prior to the issuance of the local Flood Insurance Rate Map (FIRM), referred to as pre-FIRM structures; and
    2. Inside the Special Flood Hazard Area (SFHA).
- FEMA actuaries have estimated that the rate for subsidized structures as a group is approximately 40% of the indicated actuarial risk premium.
- Actuarially Estimated Risk Premiums, are charged to all other structures. Subsidized pre-FIRM structures may use actuarially estimated rates lower than the applicable subsidized rates by obtaining an elevation certificate, to take advantage of the lower rates allowed for structures elevated at or above the BFE, or 1% flood elevation.

FEMA uses the Actuarial Rate Model (ARM) to calculate the rate for insuring post-FIRM individual structures located in either an AE Zone or VE Zone. The ARM relies on a frequency-severity approach in which actual historical claims and the estimated flood damage for modeled event years are considered. Events are modeled based on their predicted frequency; larger events have a less frequent recurrence while smaller events have a relatively higher probability of occurring in a given year. The severity of an event is determined by modeling the water surface elevation. For

example, the specific water surface elevation that occurs in a storm event having a 1% chance of occurring in a given year (the BFE) is considered in the model.

5.1.2 Technical Overview of the Actuarial Rate Model

The ARM strives to develop actuarially sound rates, which by definition include a provision for catastrophic losses and loss adjustment expenses. The ARM relies on damage ratios derived using both actual historical claims paid by the NFIP and hydrologic data developed by the U.S. Army Corps of Engineers. The NFIP's ARM estimates the needed rate per $100 of insurance coverage purchased for individual post-FIRM structures located in either AE Zones or post-1981 VE Zones. All other zones are discussed later, but for the most part, they are reflective of the results of the ARM indications for AE rates as well as additional program considerations.

The model calculates the rates based on the following risk characteristics:

- Occupancy of the structure (i.e., single family, 2–4 family, other residential, and nonresidential);
- Building type (i.e., no basement, with basement, with enclosure, manufactured home);
- Contents location (for non-single family homes, the level of contents within the building, i.e., above ground level, etc.);
- Elevation of the structure relative to the BFE, and height of the lowest floor excluding the basement relative to the BFE; and
- Flood zone: Rating zones such as SFHA (AE, VE, etc.) and non-SFHA (X, B, and C).

The indicated rate per $100 of insurance for an individual post-FIRM structure is determined in two steps:

1. Determination of expected average annual flood damage as a percentage of the amount of insurance purchased; and
2. Conversion of the expected average annual flood damage into an insurance rate by applying other factors that adjust for the impact of deductibles, expenses, and other adjustments.

5.1.3 Probabilistic Components of the ARM

The national standard that was developed as the basis for assessing, managing, and rating flood risk is the 1% annual chance flood (sometimes referred to as the "100-year flood" or BFE). The 100-year flood is the level of water that has 1% statistical probability of being equaled or exceeded in any given year. The BFE represents the water surface elevation resulting from a flood that has a 1% chance of equaling or exceeding that level in any given year. The first step of ARM's rate calculation relies on the probability of a particular water surface elevation occurring relative to the BFE

(PELV), and on depth damage curves (DELV). These variables are further described below:

- PELV represents a series of curves that reflects the probability of a particular water surface elevation relative to the 100-year BFE over a range of topographies. There are two different sets of probability curves currently used by the NFIP:
  - The original set of curves (PELV) that was developed by the U.S. Army Corps of Engineers (USACE); and
  - The second set of curves (PELV 500) that was developed in the mid to late 1980s to reflect probability estimates for communities with limited engineering data available.
- DELV is a set of arrays that reflects the expected damage to the property, expressed as a percentage of the total property value, and is shown by occupancy, building type, and water depth. Initial DELV ratios are developed based on actual historical flood insurance loss data.

5.1.4 Ratemaking Process for Risks Not Determined Directly in ARM

As mentioned previously, ARM is used to estimate countrywide rates for post-FIRM AE and VE Zones, which account for approximately 30% of NFIP policies. Rates for the remaining 70% of polices are developed outside of the ARM. The NFIP develops the additional rates using historical loss experience in combination with the results produced from ARM. This process results in actuarially sound premium estimates for all post-FIRM structures in the zones described below:

1. X Zones are areas outside of the 1% annual chance SFHA and generally have low to moderate flood hazard. They comprise approximately 37% of NFIP policies and are typically rated as a percentage of AE rates. Elevation certificates in these zones are generally not available since the cost of developing credible certificates has been considered greater than the floodplain management and insurance benefits that would be derived. Due to the absence of the elevation certificates in X Zones, the relative risk for these zones cannot be determined consistently with zones using the BFE as the standard. In addition, certain other post-FIRM construction in the X Zones are “grandfathered” with respect to rates. In these cases, the flood hazard could be more significant. Another subset of the X Zone policies is known as Preferred Risk Policies (PRP). These policies are subject to stricter underwriting guidelines than standard X Zone policies and therefore receive discounted rates.
2. AO and AH Zones are areas subject to ponding and sheet flow flooding; these risks comprise approximately 10% of NFIP policies. Rates for these zones are judgmentally selected by comparing their relationship with similar AE Zone rates derived from the model.

The rates for the remaining 22% of NFIP policies are subsidized by statute.

5.1.5 Economic Analysis of Climate Change Data

The insurance and economic analysis uses the data developed in earlier sections of this study. The economic analysis uses this information to project future policyholders and the change in loss cost. Given this information, it is possible to estimate future annual premium and loss levels.

The growth in the number of policies for the program is based on the growth in overall population and on the change in the percentage of the population within the riverine and coastal SFHAs. Though all results are presented on a countrywide basis, the following process was performed at the county level and then aggregated.

The first step of the analysis was to determine the ratio of the number of current policies to the current population. For the purposes of the analysis, this ratio is referred to as the "concentration factor." The concentration factor is developed separately for riverine and coastal areas, and further, within the riverine and coastal areas the analysis tabulates results in four different groups. These groups represent different risk characteristics and are:

- Pre-FIRM (within the SFHA);
- Post-FIRM (within the SFHA);
- PRP (outside the SFHA); and
- Non-PRP (outside the SFHA).

The future population within the SFHA and outside the SFHA is estimated based on the results of the climate change analysis. The future population within the SFHA is further separated between growth due to population growth only and growth due to change in the SFHA. Specifically:

- The future expected population for each county multiplied by the future percentage of the population within the SFHA (separately for riverine and coastal) yields the total future population within the SFHA. This is broken down between the following two parts:
  - The growth in population within the SFHA as a result of population growth only (and not growth in the area of the SFHA) is estimated as the future population multiplied by the current percentage of the population within the SFHA.
  - The growth in population within the SFHA as a result of growth in the SFHA is the difference between the total future population in the SFHA and the future population within the SFHA as a result of population growth only.
- The growth in population in the non-SFHA is the difference between the total population growth and the growth of population within the SFHA.

For each area of population growth, the future population is multiplied by the calculated concentration factor to estimate the total number of policies. It is assumed that the concentration factor is constant in each future period. The future policies are then split between Pre-FIRM and Post-FIRM for policies within the SFHA, and PRP and Non-PRP for policies outside the SFHA.[1]

To determine the estimated program premium at each future epoch, the future estimated policy counts are multiplied by the current average premium, which is calculated separately by:

- County;
- Pre-FIRM, Post-FIRM, PRP, Non-PRP; and
- Riverine SFHA, coastal SFHA, riverine non-SFHA, and coastal non-SFHA.

As mentioned previously, the overall increase in premium does not consider any potential rate change or other inflation level increases (such as increase in home values) which affect total premium. However, the change has been separately estimated as the amount of expected loss per dollar of building value as a result of the shifting SFHA. Any indicated, and ultimately implemented, rate changes would likely be a function of the change in expected loss.

To estimate the change in future expected losses, the analysis will model the change in future loss cost. The loss cost is a measure of the expected claim payments per $100 dollars of building value. The use of the loss cost in the analysis is beneficial for several reasons, including:

- The average loss cost in a region makes it possible to standardize the expected losses over all insured structure types (single family, multi-family, condominium);
- It is inflation neutral; and
- The use of a loss cost is preferable to directly estimating future losses, due to significant variability of annual flood losses and the lack of enough credible historical flood claims. (Typically, for catastrophic events, insurance companies will use 50 to 100 years of data to model future losses).

The change in expected loss cost is based on the NFIP's current PELV curves and DELV arrays, which are used in the NFIP's ARM. The PELV curves represent the probability of water level reaching a certain height within a structure, given the structure's location relative to the BFE. The DELV arrays represent the expected percentage of damage caused to a structure, given the amount of water within the structure. The multiplication of the PELV curve and DELV array for a given structure

[1] A large amount of raw worksheet data have been archived for future FEMA reference, and have been submitted separately from this report. The details of this calculation as well as other calculations described in this section can be found in the auxiliary material provided separately to FEMA.

at a given height relative to the BFE provides an estimate of the loss cost for that structure.

The economic analysis first develops a baseline loss cost at the county level, based on an assumed average distribution of structure types and heights relative to the BFE. At each future epoch, future loss cost is determined by accounting for the shift in the location of structures relative to the BFE. For example, if the BFE within a county is estimated to move by 0.5 foot by 2020, then the loss cost is recalculated after adjusting the water level probabilities to account for the 0.5 foot change in the BFE. The shift in the BFE is based on the percentage change in SFHA depth determined by the climate change analysis and the average SFHA depth of the county indicated by the PELV curve for the county.

At each future epoch, those policies that have been added since the prior epoch because of growth in SFHA are added at the new risk classification, which assumes that they mimic today's distribution with respect to compliance of floodplain management standards, which more directly, for this analysis, means height relative to the BFE. Those policies added as a result of population growth are added at the prior risk classification, which assumes these policies reflect the elevation of existing structures relative to a BFE that is one epoch old. Those that existed as of the prior epoch are assumed to shift relative to the BFE as the SFHA changes and will have an assumed higher loss cost. At each epoch, the overall indicated change in loss cost is weighted based on the amount of premium at each risk classification (i.e., level relative to the BFE: current level, shifted once, shifted twice, etc).[2]

It is important to note that under the current guidelines of the NFIP, those policies that have a higher loss cost due to a shift in the SFHA will retain their original risk classification (as long as they were built in compliance with the NFIP at the time of construction). The NFIP, in total for a class of policies, is generally able to adjust the rates so that they reflect the change in loss cost for the class. For the purposes of this economic analysis, the main risk classification characteristic considered is the height relative to the BFE.

To estimate the total change in premium after the impact of the change in loss costs, the analysis multiplies the indicated change in loss cost by a "rate change factor" and then multiplies by the average premium estimated before the loss cost change. The "rate change factor" represents the portion of the change in loss cost that NFIP will be able to reflect in a rate change. For Pre-FIRM policies, this factor is assumed to be .50. For all other policies, the factor is assumed to be 1, which assumes NFIP will be able to increase rates on a basis consistent with the change in loss cost. The

[2] The details of these calculations can be found in the auxiliary material provided separately to FEMA.

Pre-FIRM rate change factor is assumed to be less than the factor of other policies due to additional rating restrictions on Pre-FIRM policies.

5.1.6 Structures Lost to Erosion

The cost for structures lost to erosion was estimated based on conclusions reached in the Heinz Center report (2000). The Heinz Center report estimated the annual cost of the erosion for four different coastal regions in the country. These data were used to calculate an annual cost of damage per foot of erosion. This rate was then applied to the estimated erosion rates in the Heinz Center study and those considered in this climate change analysis, through the period of time considered in this study (i.e., through 2100). These results indicated that the cost of paying claims on structures lost to erosion through 2100 is approximately 2% to 4% of the estimated premium earned through the same time period under the receded shoreline scenario.

5.1.7 Analysis Assumptions

The process described above includes several direct and indirect assumptions, which are necessary to perform this type of analysis. The assumptions made are reasonable given the scope of this analysis, which is to estimate the potential economic and insurance impact to the NFIP as a result of climate change. The analysis is based on the science and engineering data developed in Section 4 of this report, which are also based on a series of assumptions. Actual future results may not develop exactly as projected and may, in fact, vary significantly from the projections. The team believes, however, that the actuarial methods and assumptions used in the analysis are reasonable.

Each assumption, including its potential impact if modified, is discussed in detail below. To evaluate the impact of each assumption, it is important to understand that the overall analysis process is performed at the county level and then aggregated. Therefore, even though the process for developing an assumption is the same, the value of most assumptions is specific to each county (e.g., the concentration factor) and is representative of the current policy demographics of the county. This approach may mitigate some of the potential bias caused by assuming a nationally constant value for all counties.

- **Median Results from Climate Change Analysis:** As discussed above, the economic analysis is based on the results provided by the climate change analysis. Specifically used is the median (i.e., 50th percentile) of the results of the climate change analysis. This is the most appropriate assumption for this type of analysis. Relative to the results presented in this analysis, using a higher percentile of results from the climate change analysis would produce a faster growth rate of premium and policies. Similarly, using a lower percentile would result in a lower growth rate of premium and policies.

- **No Changes to Current Laws or Procedures:** The economic analysis is based on the current understanding of NFIP ratemaking policies and procedures. The analysis does not contemplate any changes to policies or procedures over the time period covered in this analysis.
- **Concentration Factor:** The concentration factor is estimated for each of the riverine SFHAs, coastal SFHAs, and non-SFHAs as the number of policies per population. This factor is multiplied by the future populations to determine the number of policies. No change in this factor is estimated through future points in time. An anticipated increase or decrease in this concentration factor would have a similar directional impact in the number of future policies. Though the NFIP has experienced growth in the concentration factor in recent years, an estimate of the change to this factor through 2100 is beyond the scope of this analysis.
- **Classification of Policies:** For Pre-FIRM and Post-FIRM policies (which are within the SFHA), all future policies are assumed to be added as Post-FIRM. In other words, the economic analysis has not considered any increase of Pre-FIRM policies from the policies existing today. For the PRP and Non-PRP policies (which are outside of the SFHA), future policies are added based on the current split of policies within the county. This relationship is assumed to remain constant in each county at each future epoch.
- **PELV Curves:** No change to the PELV curves that are currently used by the NFIP is anticipated. The analysis accounts only for the shift in the BFE, as described above, and does not attempt to redevelop the fit of the PELV curves at future points in time. This analysis used the original set of PELV curves developed by the USACE rather than the PELV500 curves. A single set of PELV curves was selected, rather than using both curves, as a simplifying assumption. Based on discussions regarding the NFIP, we do not believe there would have been a significant impact to the conclusions in this report if the PELV500 curves were used in the analysis.

  Additionally, each PELV curve is representative of the topography of a certain area. The topography, or shape of the SFHA, affects the probability of water level reaching a certain height relative to the BFE. Since the climate change analysis does not estimate changes in topography of different regions, the economic analysis has not changed in terms of which PELV curve applies to which region. Rather, the same PELV curve for a given region is used through each future epoch. Also, no change has been reflected in the PELV curve due to an increase in the floodplain footprint (i.e., the implied topography of the new floodplain area is the same as the existing floodplain area). This is consistent with the assumptions of the underlying climate change analysis, that the increase in the depth of the floodplain and the footprint of the floodplain is based on a consistent geometric assumption. Please refer to additional details included in the engineering analysis narrative.
- **DELV Arrays:** No change is anticipated to the current DELV arrays of damage to a structure, given an amount of water within the structure. The DELV arrays are

based on analysis performed by the NFIP and the USACE, and estimating change to the DELV arrays would be beyond the scope of this study.

- **Distribution of Structure Type:** The distribution of structure type is based on the distribution within each county or, in those cases where the county distribution is not available, on a countrywide distribution basis. This distribution is assumed to be representative for each county and to be the same in each future epoch. In other words, as policies are added to the program, they are added under the same distribution of structure type as the current group of policies. This is believed to be a reasonable assumption for purposes of this analysis.
- **Distribution of Structure Height Relative to the BFE:** The distribution of structure heights relative to the BFE is different for each of the four groups of policies:
  - **Pre-FIRM (within the SFHA):** It is assumed that structures are at a height of negative 4 relative to the BFE. This assumption is based on a review of an external study prepared by PricewaterhouseCoopers (1999).
  - **Post-FIRM (within the SFHA):** It is assumed that structures have a distribution based on the current actual distribution in each county (or on a countrywide average if county data are not available).
  - **PRP (outside the SFHA):** It is assumed that structures are at a height of positive 3 relative to the BFE. This assumption is based on the understanding that the PRP rate developed by NFIP as part of the annual rate review process is roughly equivalent to the positive 3 rate developed through ARM as part of that same process.
  - **Non-PRP (outside the SFHA):** It is assumed that structures are at a level equal to the BFE. This assumption is based on the understanding that the Non-PRP rate developed by NFIP as part of the annual rate review process is roughly equivalent to the 0 level rate developed through ARM as part of that same process.
- For each assumption above, the same distribution is assumed for each future epoch. In other words, as policies are added to the program, they are added under the same distribution of structure types and heights relative to the BFE at that epoch as the current group of policies. For example, PRP policies added in 2020 are added at a height of positive 3 relative to the BFE in 2020. This is believed to be a reasonable assumption for this analysis. Changes to the assumption could impact the overall loss cost analysis in either a positive or negative direction (the assumption would not impact the overall growth in policies). Specifically, assuming a more favorable height (higher) relative to the BFE would lower the results of the loss cost analysis, and assuming a lower height relative to the BFE would increase the results of the loss cost analysis.
- **Replacement Rate of Structures:** The loss cost portion of economic analysis does account for some rebuilding of structures and their corresponding policies. At each future epoch, a percentage of policies that existed at the start of the time period are assumed to have been rebuilt and therefore are added back to the analysis at the newer risk classification. It is likely that there would be a subset of

policies that are rebuilt during each epoch and re-rated under building standards and rating structure that reflect that they were rebuilt. However, credible data to estimate this rebuilding rate are not available. For the purpose of this analysis, three possible scenarios are assumed for this rebuild rate: 0%, 20%, and 30%. Specifically, a scenario where no structures are rebuilt, a scenario where 20% of the structures at the start of a time period are rebuilt by the end of the time period, and a scenario where 30% of the structures at of a time period are rebuilt by the end of the time period are considered. These rebuilding rates, in a simplified manner, account for any influences on the current policyholder base and any new policyholders that improve the risk classification from one epoch to the next. Inclusion of the rebuilding rates mitigates the worst-case scenario of holding all existing properties at current classification. It is also important to note that this assumption does not have an impact on the overall increase in policies. Rather, it has an impact only on the loss cost analysis.

- **Relationship of AE Zone Rates to Other Rating Zones:** As discussed previously, the NFIP currently uses the ARM to develop rates for the post-FIRM structures in the AE Zones, and bases the rates of other zones in part on a relationship to the AE Zone rates. This analysis uses components of the ARM to estimate the change in loss costs over time. It is assumed that this approximate change in the loss cost for AE Zone rates is a reasonable proxy for the change in all rates, because of the relationship used by the NFIP to develop all of the rates.

5.2 Detailed Results

The results presented in this chapter are based on the median climate change analysis outputs and are generally presented for two scenarios. These scenarios represent different assumptions underlying the impacts of climate change on the coast. Briefly, they are:

- **Receded shoreline:** Under this scenario, the flood hazard area on the coast recedes as the sea level rises and results in approximately the same size flood hazard area through each future epoch.
- **Fixed shoreline:** Under this scenario, the current shoreline remains fixed and the flood hazard area grows through each future epoch.

The results of the economic analysis are presented on a countrywide basis; however, consistent with the climate change analysis, all calculations were performed on a county-by-county level. This presentation of countrywide results is most appropriate given the variability and increased error in developing estimates for an individual county.

As noted elsewhere in this report, the results of an individual county could be subject to significant variation and thus not considered credible at that level of detail. However, it is believed that the process of aggregating the results on a countrywide basis has removed some of the variation inherent to an individual location or county.

Additionally, the NFIP currently produces rates on a countrywide basis, and as such, the results here are consistent with the process used by the NFIP.

The results presented in this section are shown to two significant digits to more directly display the differences between various values calculated under difference scenarios and through each epoch. As discussed throughout this report, there is a large amount of uncertainty and variability in the projections underlying the results of the climate change analysis, which were, in turn, used as inputs in the economic analysis. The future values estimated by this analysis will not develop exactly as projected and may, in fact, vary significantly from the projections. There is no expressed warranty or implication that such variance will not occur. However, we believe the assumptions and methods underlying the economic analysis are reasonable, and that results produced by this analysis are a reasonable illustration of the potential future results for the NFIP.

5.2.1 Demographic Results

As noted above, the results of the economic analysis are based on the results of the overall climate change analysis. The climate change results most significant to the economic analysis are discussed in this section.

Table 5-1 displays the growth in the Special Flood Hazard Area. The total area increases approximately 40% to 45% through 2100 (Column 5).

Table 5-1. Growth in Special Flood Hazard Area due to climate change and population.

	% of Total Land Area				Cumulative Growth Rate			
Epoch	Riverine SFHA	Coastal SFHA	Total SFHA	Non-SFHA	Area In Riverine SFHA	Area In Coastal SFHA	Total SFHA Area	Total Non-SFHA Area
	(1)	(2)	(3)	(4)	(5)	(6)	(7)	(8)
Receded Shoreline								
Current*	7%	1%	8%	92%				
2020	8%	1%	9%	91%	15%	-1%	13%	-1%
2040	9%	1%	10%	90%	22%	-1%	19%	-2%
2060	9%	1%	10%	90%	27%	-1%	23%	-2%
2080	9%	1%	10%	90%	33%	-1%	29%	-3%
2100	10%	1%	11%	89%	43%	-1%	38%	-3%
Fixed Shoreline								
Current*	7%	1%	8%	92%				
2020	8%	1%	9%	91%	15%	7%	14%	-1%
2040	9%	1%	10%	90%	22%	15%	21%	-2%
2060	9%	1%	10%	90%	27%	26%	26%	-2%
2080	9%	1%	11%	89%	33%	39%	34%	-3%
2100	10%	2%	12%	88%	43%	55%	45%	-4%

* 2009 estimates

Tables 5-2 and 5-3 display the cumulative population growth rates and percentage of population by area for each epoch, and under the two shoreline erosion scenarios. The results of Section 4 indicate the countrywide population will increase approximately 70% by 2100. Population within the flood hazard area increases approximately:

- 160% in the riverine SFHA,
- 60% in the coastal SFHA under the receded shoreline scenario, and
- 140% in the coastal SFHA under the fixed shoreline scenario.

Though population growth rates within the SFHA are higher than the general population, the portion of the total population within the SFHA is not significantly changed.

Table 5-2. Cumulative population growth rates.

Epoch	Total Population	Population In Riverine SFHA	Population In Coastal SFHA	Population Non-SFHA
	(1)	(2)	(3)	(4)
Receded Shoreline				
Current*				
2020	9%	30%	3%	8%
2040	25%	59%	18%	23%
2060	38%	83%	30%	34%
2080	53%	116%	45%	48%
2100	70%	160%	61%	64%
Fixed Shoreline				
Current*				
2020	9%	30%	10%	8%
2040	25%	59%	38%	22%
2060	38%	83%	66%	33%
2080	53%	116%	100%	47%
2100	70%	160%	143%	61%

5.2.2 Growth in Policyholders

The total number of policyholders will increase approximately 30% to 35% by the year 2040 and 80% to 100% through the year 2100. The range in this estimate is representative of the two scenarios for shoreline erosion. NFIP total annual premium, before consideration of changes to depth in the SFHA and resulting loss costs, will also increase by approximately 80% to 100% under the two shoreline scenarios, in today's dollars. The growth rate of policies and premium is faster than the growth of the general population. As the flood hazard area expands, a larger percentage of the population is included in the flood hazard area. In addition, population within this area is assumed to have a higher concentration of NFIP policyholders compared to areas outside of the flood hazard area.

Table 5-3. Portion of population by area.

Epoch	Percent In Riverine SFHA	Percent In Coastal SFHA	Percent In Non-SFHA
	(1)	(2)	(3)
Receded Shoreline			
Current*	7%	3%	90%
2020	9%	3%	89%
2040	9%	3%	88%
2060	10%	3%	88%
2080	10%	3%	87%
2100	11%	3%	86%
Fixed Shoreline			
Current*	7%	3%	90%
2020	9%	3%	88%
2040	9%	3%	88%
2060	10%	3%	87%
2080	10%	4%	86%
2100	11%	4%	85%

* 2009 estimates

Table 5-4. Cumulative growth in policyholders and premium.

Epoch	Cumulative Population Growth	Population Growth in SFHA	Cumulative Policyholder Growth	Cumulative Premium Growth
	(1)	(2)	(3)	(4)
Receded Shoreline				
2020	9%	22%	12%	11%
2040	25%	47%	30%	28%
2060	38%	68%	44%	42%
2080	53%	96%	63%	59%
2100	70%	132%	84%	80%
Fixed Shoreline				
2020	9%	24%	13%	13%
2040	25%	53%	33%	32%
2060	38%	78%	52%	50%
2080	53%	112%	74%	72%
2100	70%	155%	102%	99%

The estimated growth rates in premium and policies are also impacted by the shoreline erosion scenario selected. Under the receding shoreline scenario, the land area making up the coastal flood hazard area remains approximately the same size through each future epoch. However, under the fixed shoreline scenario, the coastal flood hazard area grows (in fact, at a much faster rate than the riverine SFHA). The growing coastal flood hazard area, combined with a higher concentration of policies and higher average premium per policy, compounds the expected increase in the number of future policies and the total program premium.

5.2.3 Change in Risk Classification

The relative risk classification of policies and the associated premium amounts is also tracked over time. "Risk Classification" in this context refers to the average height of a structure relative to the BFE. For example, the "current" risk classification refers to policies with height relative to the BFE based on the current or 2010 BFE (i.e., the BFE at the time of this study). Through each future epoch, the depth of the SFHA increases. However, all the structures classified as "current" risk classification have not moved; therefore, their heights relative to the new BFE have decreased. This results in an increase in expected loss for the risk class.

Table 5-5 shows the premium by risk classification at each epoch for the receded shoreline and fixed shoreline scenarios under a 0% rebuilding assumption. For illustration, as of epoch 2060 under a fixed shoreline scenario and 0% rebuilding assumption, 72% of the total premium will be from structures that are rated based on the current level of the BFE; 13% of the total premium will be from structures that are rated on the 2020 BFE level; 11% of the total premium will be from structures that are rated on the 2040 BFE level, and 4% of the total premium will be from structures that are rated on the 2060 BFE level (i.e., the level current at that epoch). Tables 5-6 and 5-7 show the same information under the 20% and 30% rebuilding assumptions. The 0% rebuilding assumption shown below, while perhaps not a realistic scenario, does illustrate the worst case scenario and provides a baseline for comparison to the results under the 20% or 30% assumptions. For the purposes of this comparison, the premium used in the calculation is shown before any expected rate changes, including any change in risk profile (climate change) or inflation.

In the above tables, the portion of premium in the right-most column of any row would be the premium at the risk classification consistent with that epoch. All other policies would be grandfathered with respect to their flood plain depth classification. This means, under the two rebuilding assumptions (and in either shoreline erosion scenario), approximately 70% of the structures insured as of 2100 will be grandfathered with respect to height relative to the BFE.

Table 5-5. Portion of premium by risk classification under a 0% rebuilding assumption.

Epoch	Current Classification	2020 Classification	2040 Classification	2060 Classification	2080 Classification	2100 Classification
	(1)	(2)	(3)	(4)	(5)	(6)
Receded Shoreline						
2020	97%	3%				
2040	85%	14%	2%			
2060	76%	12%	10%	1%		
2080	68%	11%	9%	10%	2%	
2100	60%	10%	8%	9%	11%	2%
Fixed Shoreline						
2020	96%	4%				
2040	82%	15%	4%			
2060	72%	13%	11%	4%		
2080	63%	11%	10%	12%	4%	
2100	54%	10%	9%	11%	12%	5%

Table 5-6. Portion of premium by risk classification under a 20% rebuilding assumption.

Epoch	Current Classification	2020 Classification	2040 Classification	2060 Classification	2080 Classification	2100 Classification
	(1)	(2)	(3)	(4)	(5)	(6)
Receded Shoreline						
2020	81%	19%				
2040	55%	25%	20%			
2060	36%	18%	23%	23%		
2080	19%	13%	17%	26%	25%	
2100	5%	9%	12%	19%	28%	28%
Fixed Shoreline						
2020	80%	20%				
2040	54%	25%	21%			
2060	34%	18%	24%	25%		
2080	17%	13%	17%	27%	27%	
2100	4%	9%	12%	19%	28%	29%

Table 5-7. Portion of premium by risk classification under a 30% rebuilding assumption.

Epoch	Current Classification	2020 Classification	2040 Classification	2060 Classification	2080 Classification	2100 Classification
	(1)	(2)	(3)	(4)	(5)	(6)
Receded Shoreline						
2020	73%	27%				
2040	40%	29%	31%			
2060	14%	18%	29%	38%		
2080	1%	11%	18%	34%	36%	
2100	0%	7%	11%	21%	32%	29%
Fixed Shoreline						
2020	71%	29%				
2040	39%	29%	33%			
2060	13%	18%	29%	40%		
2080	1%	11%	18%	34%	37%	
2100	0%	6%	11%	20%	32%	31%

The results of the climate change analysis, on average, show constant growth in the depth of the SFHA through 2100. Although new policies issued for new or rebuilt structures from one epoch to the next will be actuarially rated, the number of existing policies which now have a *rated* risk classification that understates their *actual* risk classification, with respect to their height relative to BFE, will increase. As a result, the majority of policies become rated on a grandfathered basis. For example, in terms of this analysis, a structure new to the program in 2020 might be built at one foot above the BFE. This structure is then considered to be rated at the one foot above the BFE level in 2020 and would keep the one foot above the BFE risk classification through 2100. However, as the depth of the SFHA increases through 2100, the actual height relative to the BFE would decrease by the amount of the SFHA depth increase. Therefore, in terms of this analysis, the policy would be rated on a grandfathered basis.

5.2.4 Change in Loss Cost

Policies for structures insured at a future epoch that are rated at a prior risk classification will have an increase in their expected loss cost due to the shift in the BFE. The estimated change in loss cost is shown in the following tables.

For example, as of the epoch 2060, under a receded shoreline scenario and a 30% rebuilding assumption, those policies that are built to a 2020 risk classification will have an expected loss approximately 32% higher than their expected loss when they entered the program in 2020.

By combining Tables 5-5 and 5-8, 5-6 and 5-9, and 5-7 and 5-10, the average increase in loss cost under various scenarios can be computed. For example, Tables 5-5 and 5-8 under the fixed shoreline scenario show that, as of 2100, approximately

54% of the total premium would be from risks that have experienced a 118% increase in their expected loss. Table 5-11 displays the sum of the product of each row of combined Tables 5-5 and 5-8, 5-6 and 5-9, and 5-7 and 5-10, to produce the overall weighted average estimate of the change in loss cost through each epoch under the six difference scenarios. Across the six scenarios, the change in loss cost ranges from approximately 15% to 30% through the year 2040 and 20% to 90% through the year 2100.

The changes in loss cost shown in Table 5-11 represent the increase in loss cost as a result of the climate change analysis, specifically the estimated changes in the size and depth of the SFHA. The portion of an individual policy premium that is developed based on the expected loss level (i.e., excluding fixed and variable expenses, etc.) would need to increase between 20% and 90% to account for the increase in expected loss cost. For most policies, specifically the actuarially rated ones, the NFIP would likely be able include this indicated change in loss cost in the overall total rate change for an entire class of policies. The NFIP's ability to consider the full change in loss cost for Pre-FIRM structures is limited based on current regulations. Under the scenarios that allow rebuilding, the number of Pre-FIRM structures gradually declines since this analysis does not allow for new policies to be considered as Pre-FIRM, or for rebuilt policies to remain as Pre-FIRM.

Though the NFIP is likely able to incorporate most, if not all, of the indicated loss cost change in future rates, the NFIP should be aware of the potentially increasing shift from policies rated at a "correct" risk classification, to those at a grandfathered risk classification.

It is also important to note that the increase in loss cost represents the change in amount of damage as a percent of total house value. For example, if, currently, the expected damage to a house is 0.1% of the total value and through a future epoch the loss cost increases by 20%, the expected damage would be 0.12%. The overall change in rate level will be a function of this change in loss cost. The change in loss cost does exclude other factors that impact the final rate charge on a policy. These factors include:

- **NFIP Policy Limits.** Currently, the NFIP has limits on the amount of insurance that can be purchased, and a claim to the NFIP cannot exceed the policy limit. The DELV arrays used by NFIP and by the economic analysis are not constrained by existing policy limits, since the limits are subject to change over time. If the policy limits were to remain the same through 2100 as they are today, expected loss to the NFIP may not increase as much as indicated by the analysis.

Table 5-8. Percentage change in expected loss cost by risk classification under a 0% rebuilding assumption.

Epoch	Current Classification	2020 Classification	2040 Classification	2060 Classification	2080 Classification	2100 Classification
	(1)	(2)	(3)	(4)	(5)	(6)
Receded Shoreline						
2020	16%	0%				
2040	25%	26%	0%			
2060	33%	40%	22%	0%		
2080	45%	53%	35%	22%	0%	
2100	63%	75%	47%	35%	23%	0%
Fixed Shoreline						
2020	19%	0%				
2040	34%	26%	0%			
2060	51%	45%	21%	0%		
2080	79%	67%	40%	21%	0%	
2100	118%	105%	62%	40%	22%	0%

Table 5-9. Percentage change in expected loss cost by risk classification under a 20% rebuilding assumption.

Epoch	Current Classification	2020 Classification	2040 Classification	2060 Classification	2080 Classification	2100 Classification
	(1)	(2)	(3)	(4)	(5)	(6)
Receded Shoreline						
2020	16%	0%				
2040	25%	21%	0%			
2060	33%	34%	20%	0%		
2080	46%	45%	31%	20%	0%	
2100	73%	64%	41%	31%	20%	0%
Fixed Shoreline						
2020	19%	0%				
2040	34%	23%	0%			
2060	51%	41%	21%	0%		
2080	82%	62%	39%	21%	0%	
2100	139%	100%	59%	39%	21%	0%

Table 5-10. Percentage change in expected loss cost by risk classification under a 30% rebuilding assumption.

Epoch	Current Classification	2020 Classification	2040 Classification	2060 Classification	2080 Classification	2100 Classification
	(1)	(2)	(3)	(4)	(5)	(6)
Receded Shoreline						
2020	16%	0%				
2040	25%	21%	0%			
2060	34%	32%	19%	0%		
2080	88%	43%	30%	19%	0%	
2100	176%	62%	40%	31%	20%	0%
Fixed Shoreline						
2020	19%	0%				
2040	34%	23%	0%			
2060	53%	41%	21%	0%		
2080	106%	61%	38%	21%	0%	
2100	178%	100%	59%	38%	21%	0%

Table 5-11. Overall estimated change in loss cost.

Epoch	No Rebuild	20% Rebuild	30% Rebuild
	(1)	(2)	(3)
Receded Shoreline			
2020	16%	13%	12%
2040	25%	19%	16%
2060	32%	23%	16%
2080	42%	25%	18%
2100	54%	26%	22%
Fixed Shoreline			
2020	18%	15%	13%
2040	31%	24%	20%
2060	45%	30%	20%
2080	64%	34%	21%
2100	86%	35%	27%

- **General Inflation Trends.** The economic analysis does not consider general inflationary trends, such as the increase in house values. The use of the DELV arrays is consistent with this approach. The damage percentages in the DELV arrays, as a percentage of house value, are inflation neutral. For example, house values may grow 3% per year due to general inflation, but the amount of damage as a percent of the value remains constant. In this case, the rate charged for a house could remain constant (e.g., $0.10 per dollar of value); however, final charged premium would reflect the increased house value.
- **Program Expense.** The final premium charged for a NFIP policy also includes various expense components, including, but not limited to: general program administration, claims service costs, marketing, and legal expenses associated with claims. The loss cost analysis has not considered any changes to the expense components included in the overall charged premium. Some of these components and their potential impact are discussed below:
  - Some claim expenses are considered "variable" and fluctuate with the loss cost. Changes to those expenses would proportionally follow changes to anticipated loss.
  - Other claim expenses are considered "fixed" and represent overall administrative costs of the program. These expenses are generally expected to be the same values year to year (except for inflation), regardless of the loss experience of the program. Projection of these expenses through 2100 would be difficult due to of the variety of factors impacting them. For example, the current program infrastructure may be able to handle the administration of future policies (projected to almost double through 2100), in which case the fixed cost of that infrastructure could be spread across more policies. However, if there are changes made to the program infrastructure to better handle the increase in policies (or for other reasons), those changes could have a positive or negative impact on the overall expense components.
  - Some portion of the expenses associated with the NFIP policies is also paid to the insurance companies which write policies for the NFIP. Any changes to this expense structure, to handle changes in the NFIP policyholder base, would also impact the average expense included in NFIP policies.

5.2.5 Change in Total Premium

The total change in premium for the NFIP is derived from combining the results of the change in loss cost with the change in premium due to the change in the number of policyholders. For the purposes of this analysis, it is assumed for Pre-FIRM policies that the NFIP can change rates 0.5% for every 1% of indicated loss cost change. For all other policies, it is assumed the NFIP can increase rates on a basis consistent with the increase in loss costs, and do so in a timely fashion.

Table 5-12. Total growth in premium after change in loss cost.

Epoch	No Rebuild	20% Rebuild	30% Rebuild
	(1)	(2)	(3)
Receded Shoreline			
2020	26%	21%	18%
2040	54%	44%	38%
2060	80%	62%	51%
2080	117%	84%	73%
2100	166%	110%	104%
Fixed Shoreline			
2020	29%	24%	21%
2040	67%	54%	47%
2060	107%	81%	66%
2080	166%	114%	94%
2100	250%	152%	138%

The overall change in premium ranges from 40% to 70% through the year 2040 and 100% to 250% through the year 2100. This increase is in today's dollars. It does not consider inflation level increases (such as increase in home values) which affect total premium. The total written premium for the NFIP in 2009 was $3.2 billion, which implies, in today's dollars, that the total annual written premium could grow to between $4.5 billion and $5.4 billion through 2040 and $6.4 billion and $11.2 billion through the year 2100.

From the estimated change in total premium and the growth in policies, it is possible to estimate the change in average premium per policy. As shown in Table 5-13, the average premium per policy will increase between 5% and 25% through year 2040 and 10% and 70% through the year 2100. In other words, if the current average premium for all policyholders is approximately $560 per year, then the average premium (in today's dollars) is estimated to increase to approximately $588 to $700 through the year 2040 and $616 to $952 through the year 2100. Even though, on average, this is approximately a 1% annual increase, it should be noted that there is additional variability between riverine and coastal zones, and likely from year to year.

5.2.6 Structures Lost to Erosion

Under the receded shoreline scenario, the coastal SFHA effectively experiences little to no increase in loss cost. This because the SFHA continues to move inland as sea level rises, which means policies within that group are effectively reset every epoch to the current distribution of risk classification. A certain group of structures from the prior epoch are effectively lost due to eroded shoreline and brought back into the

total analysis in an area outside of the SFHA. There is, however, the one-time cost of replacing the structures destroyed as the shoreline erodes. The cost for these structures has been estimated based on conclusions reached in the 2000 Heinz Center report. The cost of replacing these structures through 2100 is approximately 2% to 4% of the estimated premium through the same time period for the receded shoreline scenario. The total of these two costs is less than the estimated future costs under the stabilized shoreline scenario. This is because the stabilized shoreline can allow for high-risk structures to remain closer to the open ocean, resulting in a higher year-to-year expected loss cost.

Table 5-13. Growth in average premium per policy after change in loss cost.

Epoch	No Rebuild	20% Rebuild	30% Rebuild
	(1)	(2)	(3)
Receded Shoreline			
2020	12%	8%	6%
2040	19%	11%	6%
2060	25%	12%	5%
2080	33%	13%	6%
2100	44%	14%	11%
Fixed Shoreline			
2020	14%	10%	7%
2040	25%	15%	10%
2060	36%	19%	9%
2080	53%	23%	11%
2100	73%	25%	18%

5.2.7 Change in Catastrophic Events

The change in loss cost described above is considered to be at the expected loss cost level. Flood losses, by their nature, have a very high amount of variability. The NFIP is exposed to large swings in actual loss from year to year, as shown in the recorded loss experience. The climate change analysis is based on the expected changes in median flood parameters and does not address the magnitudes and frequencies of the inevitable spatial and temporal fluctuations around those medians. For example, a community might experience two large floods far exceeding its BFE in two consecutive years owing to random variability. The frequency of such events and the magnitudes of the larger floods are factors that will affect the variability of loss experience by the NFIP, costing more in loss dollars than the premium income can account for in a given year when the random fluctuations produce greater or

more numerous floods, and costing less during quiet periods when the fluctuations produce lower or fewer floods.

To the extent that the PELV curves used in the analysis consider the larger and less frequent events, such as a 500-year storm, the overall loss cost analysis would consider such events through the shift in the BFE. However, if the shift of evaluation at the 500-year level is faster or slower than the shift at the BFE level, the analysis could be biased in either direction. For example, if the BFE or 1% annual chance flood level increases 0.5 foot by 2020, but the 0.2% annual chance level increases by 1 foot, the overall analysis would be understated and the increase in loss cost would be greater than indicated above. However, if the BFE increases 0.5 foot for the 1% level and the 0.2% level increases only 0.25 foot, then the overall indications are overstated.

5.3 Summary of Findings

The estimates included in this analysis illustrate potential financial impacts of climate change on the NFIP. The findings presented in this report may be helpful to NFIP and NFIP stakeholders to consider in their strategic planning, consideration of long-term goals, and reform efforts.

As noted previously, the findings presented in this chapter are based on the median climate change analysis outputs and are generally presented for two scenarios: receded and fixed shorelines. These scenarios represent different assumptions underlying the impacts of climate change on the coast.

5.3.1 Demographic Findings

As noted above, the results of the economic analysis are based on the median change in the SFHA from the national climate change analysis. The climate change findings most significant to the economic analysis are growth in the SFHA and growth in population. The SFHA is expected to increase by approximately 40% to 45% and the population is expected to grow by approximately 70% through 2100. The combination of these two projections results in faster increases in population within the SFHA, which is expected to grow by 160% in the riverine SFHA and 60% (receded shoreline scenario) to 160% (fixed shoreline scenario) in the coastal SFHA.

5.3.2 Economic Findings

The economic analysis builds on the demographic findings in order to estimate overall growth in the NFIP in terms of the number of expected policies and the associated total premium. Additionally, as a measure of expected loss, the change in depth of the flood hazard area has been used to estimate an approximate change in average loss cost. The change in average loss cost can then be used to estimate the change in average premium (or cost to the policyholder) per policy.

In summary:

- The total number of policyholders participating in the NFIP is estimated to increase approximately 80% to 100% cumulatively through the year 2100. The range in this estimate is representative of the two scenarios considered for shoreline erosion.
- The total premium collected, before consideration of changes to SFHA depth and loss cost, will correspondingly increase by approximately 80% to 100%, depending upon the shoreline scenario considered. This increase is directly tied to the projected increase in the number of policyholders. Although this is a significant change, it should be noted that this represents only an approximately 1% change annually.
- The change in loss cost (i.e., the average expected loss associated with a policy) will increase between 20% and 90% through the year 2100, which is approximately 1% change or less per year. The loss cost is a measure of annual expected claim payments per $100 of insured value. In this analysis, the change in loss cost is representative of the overall change in expected losses, which is in addition to the change in expected losses due simply to the increase in the number of policyholders. The range in the change in loss cost is a result of several different scenarios considered, specifically, the two shoreline erosion scenarios discussed above and three different rebuilding assumptions.
- The average premium per policy will increase approximately 10% to 70% in today's dollars which is less than 1% per year. This estimate is less than the average estimated increase in loss cost only because it is assumed that NFIP will be able to increase rates in step with the increase in loss cost for only a portion of policies issued.
- The total annual aggregate program premium, after consideration of the change in loss cost and the increase in the number of policyholders, will increase approximately 100% to 250% in today's dollars by 2100. The total written premium for the NFIP in 2009 was $3.2 billion, which implies, in today's dollars, that the total annual written premium could grow to between $6.4 billion and $11.2 billion through the year 2100.
- Under the receded shoreline scenario, the estimated cost of all structures that are estimated to be destroyed due to the shoreline movement through 2100 is approximately 2% to 4% of the estimated total premium earned through 2100.
- More than 50%, and possibly as many as 75%, of the policies in 2100 will be considered "grandfathered" with respect to their floodplain depth risk classification.
  - This observation is based on the range of percentages shown in Tables 5-5, 5-6, and 5-7 under the various rebuilding and shoreline scenarios. This result is highly dependent on the rebuilding assumption in the analysis. The higher the rebuilding assumption, the fewer the number of policies that will be grandfathered. The 0% rebuilding assumption, while perhaps not a realistic scenario, does illustrate the worst-case scenario. Under the 30% rebuilding assumption, only about 30% of total premium in 2100 will be from policies rated according to the 2100 (i.e., correct at that time) BFE.

- This analysis assumes that all current (2010) policies are rated according to their correct classification.
- The estimate portion of policyholders consider to be "grandfathered" is based on the assumption that current ratemaking procedures and policies will not change over the course of the period covered in this study.

5.3.3 Discussion of Findings

The growth rate of policies and premium in the NFIP is faster than the growth rate of the general population. As the flood-hazard area expands, a larger percentage of the population is included in the flood-hazard area. In addition, population within this area is assumed to have a higher concentration of NFIP policyholders compared to areas outside the SFHA. This assumption is based on the current concentration factor (policies per population) of policies in and outside of the SFHA.

The growth rates of both premium and policy counts are also impacted by the shoreline erosion scenario selected. Under the receding shoreline scenario, the land area making up the coastal flood-hazard area remains approximately the same size through each future epoch. However, under the fixed shoreline scenario, the coastal flood-hazard area grows (in fact, at a much faster rate than the riverine SFHA). The growing coastal flood-hazard area, combined with a higher concentration of policies and higher average premium per policy, compounds the expected increase in the number of future policies and in total program premium.

The increase in average loss cost is impacted by two factors: the change in the SFHA depth and the shift in the risk classification of policies. The change in SFHA depth exposes an individual structure to greater frequency and severity of loss (assuming that the individual structure is not rebuilt or brought in line with current building standards). However, a structure in this situation would become "grandfathered" and continue to be rated at its original risk class[3]. The NFIP accounts for the increased risk associated with all policies within a class (e.g., zone) by averaging the expected loss cost across the entire class.

The analysis estimates this average change in loss cost across all policies as approximately 20% to 90% through the year 2100. This range of estimates is based on the different rebuilding assumptions considered in this analysis. The rebuilding assumptions are used to approximate the number of policies that are, for any reason, reset to the risk classification consistent with the epoch in which they are rebuilt. For example, the structure at 2 feet above the BFE could be "rebuilt" in 2020 to remain 2

[3] The individual structure would not change its "rated" height relative to the BFE for underwriting and premium calculations. In other words, if a structure is currently rated assuming it is 2 feet above the BFE, even if the BFE increases by 1 foot through 2020, the structure, under current policies, would be "grandfathered" and continue to be rated as if it is 2 feet above the BFE.

feet above the BFE (the BFE after change in depth of SFHA), resulting in no change to the structure's estimated risk. The rebuild assumptions can also serve as a proxy for an assumption reflecting limitations to the amount of time a policy can be grandfathered. As more policies are assumed to be rebuilt at each epoch, or fewer policies are allowed to remain grandfathered, the average increase in loss cost is reduced.

The average increase in premium per policy is approximately 10% to 70%, which is less than the average increase in loss cost. The increase in premium per policy is tempered because it is assumed that the NFIP will increase rates consistent with the full increase in loss cost for only a portion of policies. Specifically, it is assumed for Pre-FIRM policies, that the NFIP will change rates 0.5% for every 1% of indicated loss cost change. For all other policies, it is assumed that the NFIP will be able to increase rates 1:1 with the increase in loss cost. Under the scenarios that allow rebuilding, the number of Pre-FIRM structures does decrease and eventually becomes non-existent. This is because the analysis does not allow for new policies to be considered Pre-FIRM or for rebuilt policies to remain Pre-FIRM.

Under the receded shoreline scenario, though there is a one-time payout of insurance claims associated with structures that are lost due to erosion, this one-time payout is not as large as the increase in annual expected losses under the fixed shoreline scenario. This is because under the fixed shoreline scenario, structures remain in the current location, and expected annual loss for those structures continues to increase due to the increase in the water-level depth of the coastal floodplain. This results in a higher year-to-year expected loss cost.

5.3.4 Conclusions

The analysis findings based on using the median increase in the SFHA indicate that the NFIP will continue to grow and by 2100, will insure almost double the number of policyholders it does today. The NFIP has the opportunity now to plan for any potential issues or concerns related to the growth of the program and change in loss estimates. Although the average annual change in premium and losses over the 90 years included in this study is not significant, the cumulative impact will be. The NFIP will ultimately need to be able to administer a much large program, which may involve changes to the current structure. The increase in loss cost may be, on an incremental basis, easily incorporated into the rates charged. However, there is also expected to be increased variability in the total losses (claims) presented to the NFIP in any given year. Additionally, as the number of policies increase, particularly in flood-hazard areas, the NFIP could be exposed to much larger events (with respect to losses) than similar events would have produced in prior years. The swing in loss

payments made from year to year may be larger than the NFIP's current funding and borrowing structure accommodates.

The increase in loss cost estimates is significantly impacted by the current "grandfathering" programs. Under current ratemaking procedures, the NFIP annual rate review accounts for some portion of grandfathered policies when determining actuarial rates in total. As more policies become grandfathered because of increasing depth in SFHA, grandfathered policies may become a larger portion of the policy base. As this occurs, the long-term goal of having an actuarially sound program is jeopardized for two reasons: 1) within a specific rating class the exposures are becoming more heterogeneous, which is in conflict with generally accepted actuarial principles of differentiated risks and, 2) if the rate(s) for the ongoing risk class is such that the full-risk premiums are deemed to be unaffordable (politically or otherwise), at least one of the long-term goals of the NFIP (namely to offset taxpayer funded disaster relief) could be jeopardized.

Additionally, the disparity between grandfathered and non-grandfathered policies could lead to potential adverse selection between policyholders. Adverse selection generally occurs in insurance companies when a subset of the policyholders is charged rates lower than would be indicated by their true risk profile. These policyholders are effectively given a discount and would be more likely to purchase the insurance. Conversely, those policyholders charged a premium in excess of their true risk would gravitate to other insurers whose price is in line (i.e., lower) with respect to the insured's risk profile. For the NFIP, which relies in part on the widespread purchase of insurance to remain actuarially sound in total, if an increasing portion of policies are grandfathered and overall rates continue to increase, some policyholders may decide not to purchase flood insurance as a result of the cost. As the "less risky" policyholders find the insurance too costly relative to their risk (i.e., policyholders not in the SFHA) and choose not to insure, this would further accelerate the overall increase in loss cost for the remaining policyholders.

6.0

Summary of Findings and Technical Recommendations

6.0 Summary of Findings and Technical Recommendations

6.1 Summary of Technical and Economic Findings

The findings below are divided into technical and economic categories. Where appropriate, the findings are further subdivided according to riverine and coastal environments. The analyses for coastal areas were conducted for both *fixed* and *receding* shorelines so that separate estimates are presented, as appropriate. The indicated changes are typical values, only, for qualitative purposes.

6.1.1 Technical Findings

Riverine Environment – By the year 2100, the relative increase in the median estimates of the 1 percent annual chance floodplain (floodplain) depth and area (Special Flood Hazard Area or SFHA) in riverine areas is projected to average about 45% across the nation, with very wide regional variability. Depths and areas may increase by over 100% in some areas of the Northwest and in the vicinity of the Great Lakes, whereas smaller relative increases of about 20 to 40% may be typical of areas of the central and Gulf regions. Significant decreases in the median estimates of floodplain depth and SFHA are not anticipated in any region of the nation. As shown in Figure 4-16, there is significant variability in the 1 percent annual chance discharge about the median (50^{th} percentile) estimate. For example, use of the 25^{th} percentile indicates no increases in the SFHA for all areas of the country.

In populated areas of most interest to the NFIP, approximately 30% of these increases in the SFHA and base floodplain depth may be attributed to normal population growth, while the remaining portion represents the influence of climate change. The split is extremely variable from place to place and should not be construed as a definitive value. Depending upon the emissions scenario and population growth assumptions, the population component will be greater in highly developed areas, and substantially lower in undeveloped areas where climate change alone will dominate the composite total.

Coastal Environment – Assuming a *fixed* shoreline, the typical increase in coastal SFHA is projected to be about 55% by the year 2100, with very wide regional variability. The typical increase may range from less than 50% along the Pacific Coast to over 100% for portions of the Gulf of Mexico and the Atlantic coasts. Under the receding shoreline assumption, negligible change in coastal SFHA is projected. This is due to the fact that recession is assumed to compensate for the effects of sea level rise.

Riverine and Coastal Environments, Combined – As indicated above, the median increase in SFHA is projected to vary widely across the country. The national average increase in SFHA by the year 2100 may be very approximately:

- 40% for riverine areas and coastal areas if coastal recession is assumed; and
- 45% for riverine areas and coastal areas if fixed coastlines are assumed.

6.1.2 Economic Findings

Riverine and *Receding* Coastal Shorelines – The following economic estimates are subject to wide national variation, and so are qualitative only. Separate estimates are given for alternate shoreline assumptions, as indicated.

- The total number of NFIP insurance policies may increase by approximately 80% by 2100. The number of riverine policies may increase by about 100% and the number of coastal policies may increase by approximately 60%.
  - The increase in the number of polices is due in part to population growth and in part to the effect of climate change on the size of the SFHA.
  - Approximately 30% of the estimated increase in policies is due to population growth and approximately 70% is due to climate change.
- The average loss cost per policy may increase approximately 50% by the year 2100.
  - The cumulative increase may be approximately 10% to 15% through the year 2020 and 20% to 40% through the year 2080.
- Individual premiums per policy are expected to increase approximately 10% to 40% in today's dollars by the year 2100 in order to offset the projected increase in loss cost.
  - The difference between the expected change in premium compared with the expected change in loss cost reflects program limitations regarding pricing.
  - The cumulative increase would need to be approximately 5% to 10% through the year 2020 and 5% to 30% through the year 2080.
- The estimated increase in population in the coastal SFHA is expected to be about 60% by the year 2100.

Riverine and *Fixed* Coastal Shorelines

- The total number of NFIP policies may increase by approximately 100% by the year 2100. The number of riverine policies may increase by approximately 80% and the number of coastal policies may increase by 130%
- The average loss cost per policy may increase approximately 90% by the year 2100.
  - The cumulative increase may be approximately 10% to 15% through the year 2020 and 20% to 60% through the year 2080.

- Individual premiums per policy are expected to increase approximately 20% to 70% in today's dollars by the year 2100 in order to offset the projected increase in loss cost. This corresponds to a cumulative increase of about 0.6% per year.
  - The difference between the expected change in premium compared with the expected change in loss cost reflects program limitations regarding pricing.
  - The cumulative increase would need to be approximately 10% to 15% through the year 2020 and 10% to 50% through the year 2080.
- The estimated increase in population in the coastal SFHA is expected to be about 140% by the year 2100.

6.2 Summary of Technical Recommendations

The current climate study provides a high-level vulnerability assessment of the potential financial impacts of climate change on the NFIP at a national scale. This initial assessment of the impact of climate change may be used for preliminary planning purposes at a national level. However, it should be noted that present-day knowledge of climate change is limited and the forecasts of the current study have large uncertainties associated with them. The following technical recommendations are provided with the realization that climate change is an evolving science and that changes in climate happen with considerable regional variability.

1. Progress made by the scientific community in climate change science should be monitored on a regular basis and the current climate study should be updated or a new study should be conducted when climate models have a demonstrated skill in predicting future climate conditions. This would greatly improve the reliability of the predictions for short- and longer-term estimates of the impact of climate change on the NFIP.
2. To improve the accuracy of the economic analyses similar to the one conducted for the current climate study, NFIP data collection should be expanded to include
   - Accurate geospatial placement of policies and claims;
   - National inventory of geospatial locations of structures;
   - Elevation certificates linked to the National Flood Hazard Layer (NFHL) as well as policy and claim data;
   - Improvements in elevation data; and
   - Data regarding the distribution of property and of property values across floodplains.

     The last data item above is especially important for coastal areas because large condos and other high-value properties may be disproportionately located at or near the water's edge, which is also the zone of maximum flood hazard (VE Zones) and maximum erosion potential. Including these data will help improve economic estimates such as the cost per foot of erosion.

3. The Advisory Committee on Water Information has recently formed a climate change working group consisting of most of the Federal agencies working in the area of water resources. The scope of activities of this interagency working group may include, but not be limited to, 1) acceptable, realistic scenarios of anticipated impacts and exposure levels; and 2) technical approaches, data sources, degrees of error, and assumptions that may be acceptable. It should be noted that while the technical approach of a climate study conducted from the perspective of the NFIP is likely to be probabilistic in nature (the NFIP relies on probabilistic flood risk data), the actual probabilistic approach can differ (e.g., Monte Carlo method, Bayesian modeling) depending on the scope and intended use of a study.
4. The present study could be used as a basis to divide the country into several different regions for more detailed regional studies. Such divisions may be based on the forecast increases in the SFHA, population, number of policies, and cost of structures for short-term impacts (i.e., epoch 2020). The median and 75 percentiles could be used to analyze the potential risk that the NFIP may be subjected to.
5. The population projections in this study not only drive impervious area, in turn affecting rainfall-runoff equations, but are also used in the economic analysis to drive expected losses. The Intergovernmental Panel on Climate Change (IPCC) scenario-derived population assessments were used in this study and were appropriate in the context of the scope, intended use, and GAO mandate for this study. However, any future regional detailed studies should consider using U.S.-derived demographic projections. Spatial variations in population growth rates should also be considered.
6. Regional studies may be performed by taking the existing, nationwide hydrologic projections from the current study and applying those projections to existing, detailed hydraulic modeling studies performed at a local scale. The analysis would more accurately assess the potential effects of climate change for specific reaches, rivers, or regions by using preexisting information from FISs in those regions. For example, the current study estimated a statistical distribution of future possible flood flows based on global climate model (GCM) projections of extreme climate indicators. In data-rich areas (in terms of the availability of USGS stream gage data from the study), an estimated future distribution of base flood discharges could be passed through existing, detailed HEC-RAS modeling studies to obtain base floodplain boundaries that reflect a more detailed understanding of how climate change and population growth would impact flooding along a specific river. This may give an improvement in projected SFHAs with respect to the simplified assumptions used in the current study to relate flood discharges to the extents of flooding. In addition, uncertainty associated with the projections could be quantified by using projected discharges in HEC-RAS modeling studies to translate uncertainty in flood discharges to uncertainty in flood depth and in the extent of the SFHA.

   To further support regional analyses, the global circulation model results, such as projected daily rainfalls, may be processed using statistical downscaling or may

be linked with a regional climate model (RCM) to provide more detailed projections within a given region. The result provides higher-resolution climate forcing that can be linked to hydrologic impact models to quantify flood risks.

7. Due to scope and intended use of the current study, the nation's coastlines were divided into only 13 sea level rise regions. It is recommended that future studies consider further subdividing each of these regions to remove some of the variability inherent to such broad regions. This should especially be considered for the regions in the Pacific Northwest and Northern California.

   Any such subdivision should consider both erosion and sea level rise. Erosion remains a critical issue and, due to the numerous factors that contribute to erosion rates, a localized approach is needed in order to produce improved estimates. Similarly, in coordination with experts from NOAA, USGS, and local coastal communities, a more detailed assessment should be performed to verify historical relative sea level rise rates on a local basis. In addition, the effects of multi-decadal modes of ocean variability such as Pacific Decadal Oscillation or Atlantic Multi-decadal Oscillation on sea level rise rates should be further investigated as part of regionalization efforts.

8. The large-scale regression analysis technique that was used as part of this study could possibly be improved by coupling a macroscale hydrologic model such as the Variable Infiltration Capacity (VIC) model (available at http://www.hydro.washington.edu/Lettenmaier/Models/VIC/index.shtml) to the global climate model outputs. This would provide more accurate estimates of the impacts of climate change on flooding. It is anticipated that a land surface model such as VIC would greatly improve the ability to capture the major physical processes governing land-atmosphere interactions than regression modeling alone can do. In addition, land surface modeling would explicitly account for land cover, infiltration, snow, lakes, and rivers. Further improvement of the GCM results using statistical downscaling or dynamical downscaling with RCMs would support this effort by providing higher-quality precipitation data as an input to the VIC model.

9. A detailed assessment of variability should be performed as a part of any future study to capture the uncertainties associated with future projections. Such an assessment will increase the acceptability as well as the confidence level of the study projections. For example, an important source of variability not assessed in the present study was the variation inherent to the USGS stream gage data that were used as the basis for the riverine regression analysis.

10. Future studies should consider investigating and documenting the possibilities and magnitudes of systematic errors associated with study approach, which could not be performed within the scope of the current study. Existing flood data from FEMA's Mapping Information Platform (MIP) may be used for such investigations. For example, MIP data may be used to determine the error associated with the linear slope assumption for riverine overbank flooding. Similarly, the limitations of the plane beach assumption should be evaluated: Coastal areas terminated by

bluffs, for example, will not enlarge significantly, while areas terminated in very flat land could enlarge greatly.

11. Due to scope and intended use of the current study, it was assumed that change in affected population and structures will be proportional to change in SFHA. Population was taken to be uniformly distributed within the SFHAs and elsewhere across counties. The impact of non-uniform population distribution should be investigated in any future study or as a part of future improvement of the current study. This can be partly addressed by performing economic analyses at the Census Block level rather than at the county level.

Appendix A

Key Literature Review

Contributing authors

Joe Kasprzyk

Josh Kollat

Senanu Agbley

Steve Eberbach

Krista Conner

A Key Literature Review

A.1 Discussion of Sources

The literature review sought to set the scientific basis for the analysis of how changes in precipitation, temperature, storm activity, and sea-level rise affect flood frequency and intensity for coastal and riverine environments. Initially, a team of readers were assigned publications that gave a broad basis of the state of climate science. As the review continued, the team focused on targeted literature that provided a foundation for how to use published observations and predictions of climate signals to quantify flood impacts.

The first stage of the literature review focused on large reports that synthesized the state of the science of climate change and academic papers that gave examples of observed and predicted changes in the climate. In its Fourth Assessment Report, the Intergovernmental Panel on Climate Change (IPCC) outlined the science behind the warming of the climate system, illustrated observed effects of this warming on natural systems, and discussed possible mitigation strategies (IPCC, 2007). An important aspect of the report is its discussion of the uncertainties and geographic variability of climate change estimates. The literature review looked at the major contributions of the three working groups that reported on the physical science, climate impacts, and mitigation strategies associated with climate change, with a specific focus on the WGI (Working Group I) Physical Science Basis. Another set of synthesis reports studied was released by the U.S. Climate Change Science Program (CCSP). An example of these reports was the Synthesis and Assessment Product 3.3, which documents weather and climate extremes for the United States (CCSP, 2008a). The report gives evidence for observed increases in extreme temperature, droughts, and large rain events attributed to increases in carbon dioxide emissions. Using the large reports published by the IPCC and CCSCP, scientific papers were identified that would serve as the basis for the review team's conclusions. Throughout the literature review process, more than 100 peer-reviewed articles and reports pertaining to climate models, observed climate, and climate projections were reviewed.

A.2 Climate Change and Riverine Impacts

Projections of climate change generally show increases in temperature and intensification of precipitation patterns. Relevant to the riverine flooding analysis in this study, climate change could cause more severe rainstorms but also more intense and longer droughts. Scientists use Global Climate Models (GCMs) to

simulate the climate system, where mathematical models of atmospheric and ocean processes are used to test hypotheses about climate in the past and likely projections of future changes (CCSP, 2008a). Looking at the large number of reports published coupled with scientific papers that suggest changes in streamflow magnitude and timing (e.g., Lins and Slack, 1999; Milly et al., 2005) gave a clear picture of the science behind the climate inquiries. Especially important was the demonstrated framework of input data, model assumptions, and analysis of outputs that provided a basis for how the scientific community used observations and predictions of climate change to quantify its effects.

Beyond the set of general studies that examine the large-scale effects of climate change, the literature review was used to gain insight into specific scientific methods that would allow for the development of regression equations, sampling of the observed and predicted data, and inferences on changes in flood events. Examining a series of studies (Frich et al., 2002; Alexander et al., 2005; Tebaldi et al., 2006) resulted in familiarity with the concept of extreme climate indices (ECIs). These extreme indices are statistical metrics calculated from a daily time series such that changes in the indices could be used to demonstrate changes in climate extremes. Reviewing this literature allowed for comparison of different sets of indices and examination of coherent results from the studies. Because the projections of change required the use of GCM outputs, exploration of the extreme climate indices literature was coupled with discussion of the proper use of GCMs. A general overview of the usefulness of GCMs, including their strengths and weaknesses in simulating certain aspects of the climate system, were consulted (CCSP, 2008a). These targeted articles and reports provided a firm scientific basis for the methodology of the project and for linking the results and findings to the general body of scientific literature.

A.3 Emissions Scenarios

Projecting future climate requires assumptions about population growth, how the world economy will develop, and how land use changes (Arnell et al., 2004). The Special Report on Emissions Scenarios (SRES) created a series of equally plausible scenarios that represent formal assumptions for use in climate projections, grouped in different “families” named A1, B1, A2, and B2. These scenario families can be conceptualized using the quadrant system shown in Figure A-1.

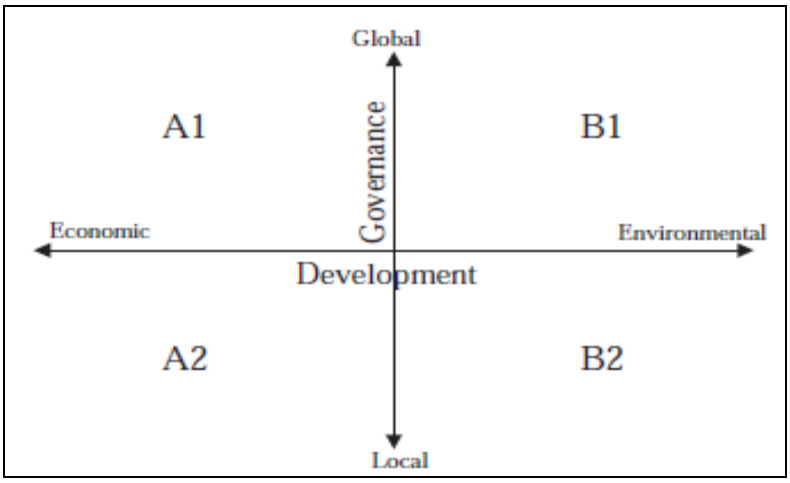

Figure A-1. Quadrant system to describe SRES scenario families (Arnell et al., 2004).

As shown in Figure A-1, scenario B1 represents environmentally focused development with a global sense of governance. Scenario B2 also represents environmentally focused development, but with more local governance. The population growth estimates for the A1 and B1 scenarios are "low," while the B2 scenario has "medium" growth and the A2 scenario has "high" growth. Additionally, the A1 family has a set of three separate scenarios that represent assumptions regarding energy use, ranging from fossil fuel-intensive energy use (A1FI) to mostly non-fossil fuel use (A1T), as well as a balanced approach (A1B).

In this study, three emissions scenarios were used: A1B, A2, and B1. These scenarios represent a reasonable range from low to high climate change assumptions, as well as the most GCM outputs available. The following brief summaries of the relevant scenarios are adapted from the discussion by Arnell et al. (2004). The A1B scenario assumes balanced energy use between fossil fuel and non-fossil fuel energy sources, high economic growth with fewer differences between world regions, and low population growth. The A2 scenario assumes a smaller amount of economic growth, but more rapid population change. The A2 scenario, using the quadrants approach of Figure A-1, assumes high economic growth but more local governance. The B1 scenario assumes low population growth and a more environmentally sustainable approach to economic growth. The scenarios are sampled equally from within the Monte Carlo sampling procedure to represent possible future conditions under climate change and population growth to 2100.

A.4 Extreme Climate Indices

GCM modeling groups needed to find innovative ways to share large datasets of their simulations of world climate with scientists and stakeholders. To circumvent transferring large daily estimates of climatic variables, these groups devised indices that would capture the extremes and important properties of the climate system in yearly values (Frich et al., 2002), referred to here as extreme climate indices (ECIs). One such value is the number of days in a given year that the temperature falls below a certain threshold. Alexander et al. (2005) created a gridded dataset of observed values for these ECIs using a set of 2,223 temperature gauges and 5,948 precipitation gauges. Tebaldi et al. (2006) did similar work with climate model projections of ECIs using 43 GCM runs across 10 separate GCMs for three SRES scenarios.

Published USGS regression analyses were used to relate the observed climate indices to the 1% chance flow for a set of USGS stream gauges across the United States. The three most statistically significant indices are defined in Table A-1.

Table A-1. Definitions of extreme climate indices (adapted from Frich et al., 2002).

Indicator	Description [Units]
Frost Days (FD)	Number of days with minimum temperature less than 0 degrees Celsius [days]
Consecutive Dry Days (CDD)	Maximum number of consecutive dry days, with precipitation less than 1 mm [days]
Maximum 5-Day Rainfall (R5D)	Maximum total precipitation in a 5-day period [mm]

A.5 Climate Change and Coastal Impacts

Evaluation of the impact of climate change on coastal flood hazards required collection of climate projections related to sea-level rise, changing storm frequency, and changing storm intensity. Global sea-level rise projections were obtained from Vermeer and Rahmstorf (2009). This publication proposed an extension of the semi-empirical approach developed by Rahmstorf et al. (2007), which incorporates an "instantaneous" sea-level response (e.g., heat uptake of the mixed surface layer of the ocean). Projected global sea-level rise ranges from 75 to 190 cm for the period 1990–2100 (see Figure A-2).

Scenario	Temperature range, °C above 1980–2000	Model average, °C above 1980–2000	Sea-level range, cm above 1990	Model average, cm above 1990
B1	1.4–2.9	2.0	81–131	104
A1T	1.9–3.8	2.6	97–158	124
B2	2.0–3.8	2.7	89–145	114
A1B	2.3–4.3	3.1	97–156	124
A2	2.9–5.3	3.9	98–155	124
A1FI	3.4–6.1	4.6	113–179	143

The temperatures used are taken from the simple model emulation of 19 climate models as shown in figure 10.26 of the IPCC AR4 (2); they represent the mean ± 1 SD across all models, including carbon cycle uncertainty. The sea-level estimates were produced by using Eq. 2 and 342 temperature scenarios and are given here excluding the uncertainty of the statistical fit, which is approximately ± 7% (1 SD).

Figure A-2. Temperature ranges and associated sea-level ranges by the year 2100 for different IPCC emission scenarios (Vermeer and Rahmstorf, 2009; the equation reference is to that paper).

There is continued uncertainty regarding whether observed changes in tropical cyclone characteristics such as frequency and intensity have exceeded changes anticipated through natural variability. In general, it is currently unclear whether human-induced climate change is having a discernible impact on tropical storm activity. Knutson et al. (2010) provides a comprehensive review of critical tropical cyclone-related publications. This publication reports a projected mean change in storm intensity for Northern Hemisphere storms of +9% and +8% for the Northern Atlantic by 2100. The mean change in storm frequency for Northern Hemisphere storms is projected at -12% and -8% for the North Atlantic by 2100. Results from Bender et al. (2010) and Emanuel et al. (2008) are consistent with these projections (see Table A-2). Estimates from Bender et al. (2010) were used in this study.

Similar uncertainty exists for estimates of future extra-tropical storm frequency and intensity. The literature generally predicts a decrease in the total number of extra-tropical cyclone events, but an increase in the number of intense events over the next century. Bengtsson et al. (2009) projects insignificant, slight increases in intensity of extra-tropical storms in the 21st century. Lambert and Fyfe (2006) projects decreases in the frequency of Northern Hemisphere extra-tropical storms as measured by total events (see Table A-3).

Table A-2. Summary of tropical storm projections obtained from key references.

Knutson et al. (2010)				
	Change in Storm Intensity		Change in Storm Frequency	
	Mean	Stdev	Mean	Stdev
Global	+8%	5	-18%	9
N. Hemisphere	+9%	5	-12%	10
N. Atlantic	+8%	6	-8%	30
Bender et al. (2010)				
	Change in Storm Intensity		Change in Storm Frequency	
	Mean	Stdev	Mean	Stdev
N. Atlantic	+10%	N/A	-33%	22
Emanuel et al. (2008)				
	Change in Storm Intensity		Change in Storm Frequency	
	Mean	Stdev	Mean	Stdev
N. Atlantic	+7%	34	+2%	39

Table A-3. Summary of extra-tropical storm projections obtained from key references.

Lambert and Fyfe (2006)		
	Change in Storm Frequency	
SRES	Mean	Stdev
B1	-4.3%	1.2%
A1B	-7.1%	1.4%
A2	-7.8%	1.6 %
Bengtsson et al. (2009)		
	Change in Storm Intensity*	
SRES	Mean	Stdev
A1B	+1%	1.4%

*Storm intensity projections are not yet available for Scenarios B1 and A2.

A.6 Population

The SRES scenarios are based on assumptions about population growth as one of the drivers of increased carbon emissions in the future climate. The SRES scenarios assumed that population growth percentages were constant spatially at the country scale – that is, the United States had a single growth model. Bengtsson et al. (2006)

provided a country-scale estimate for each of these SRES models, and these estimates were used in this study. A constant rate of growth spatially across the United States was used, but this growth rate changed in each year according to the assumptions of the specific SRES scenario.

These population growth models are available and would ideally be directly used in the regression to maintain consistency with the GCM extreme indices portion of the analysis. However, population was not used in the regression, and the only relevant variable that relates to changes in population (and therefore urbanization) is impervious area (IA).

There have been several studies in the literature that relate population to the amount of impervious area at a site, summarized by Exum et al. (2005). Each study used a regression technique to compare the population at a site to an estimate of its impervious area, and some of these studies were reported by Exum et al. (2005) and shown in Figure A-3.

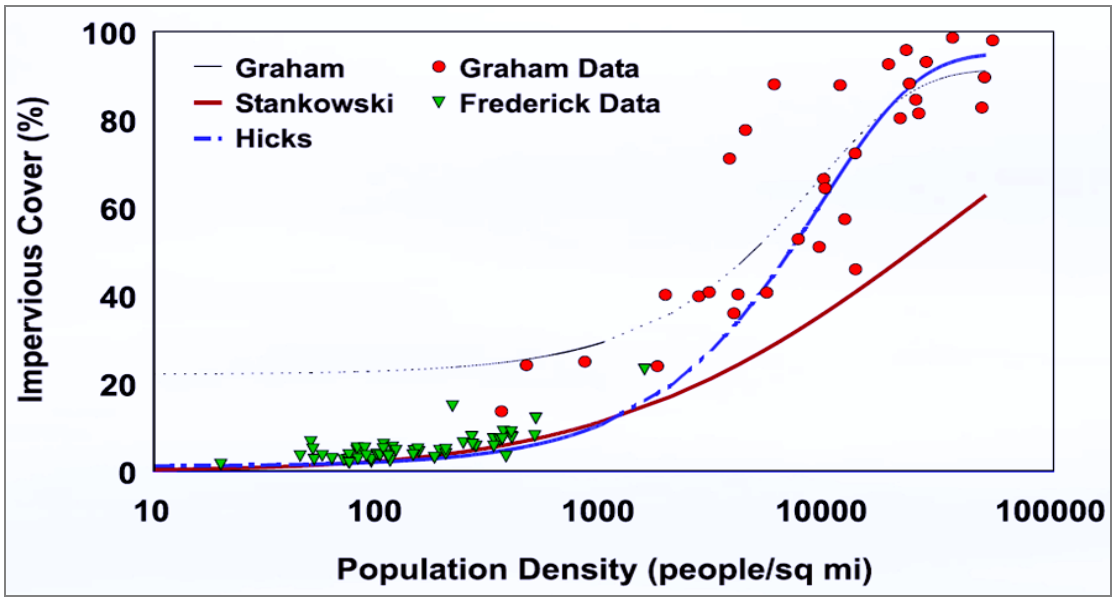

Figure A-3. Impervious cover versus population density for several studies (adapted from Exum et al., 2005).

The Hicks data set was used because it provides the best fit at both low and high percentages of impervious cover, as shown in the figure. The equation associated with the Hicks data set is:

$$IA = 95 - 94\exp(-0.0001094PD) \qquad \text{Equation (A-1)}$$

where IA is the percentage of impervious cover and PD is the population density at a site in people per square mile. One methodology for predicting future IA is as follows: The current IA is found on the vertical axis of the graph (Figure A-3), and the inverse of Equation (A-1) is used to find the "effective" population density at the site (i.e., the population density that corresponds with the Equation [A-1] estimate of IA). The SRES population growth model is used to find the percent change between the current estimated "effective" population and a future "effective" population. Finally, Equation (A-1) is used to find the future IA used in the regression.

Appendix B

Riverine Flood Methodology

Contributing authors

Wilbert O. Thomas, Jr.

Josh Kollat

Joe Kasprzyk

David Divoky

Art Miller

David Markwood

B Riverine Flood Methodology

B.1 Regression Analysis

B.1.1 Selection of USGS Gages

Regression analysis was applied to relate flood discharges, such as the 10 and 1percent annual chance floods, to watershed characteristics and climate indicators so that projections of the climate indicators could be used to estimate future changes in the flood discharges. Data on flood discharges and watershed characteristics were obtained from published reports and existing data files of the USGS. The objective was to select both rural and urban gaging stations with varying degrees of impervious area in the watershed so that future changes in flood discharges could be predicted based on population change and impervious area as well as climate change. The flood discharges at the gaging stations selected for analysis were not impacted by the effects of flood detention structures.

The limiting factor in the search for USGS gages was the number of urban gaging stations. There are a limited number of urban gaging stations where the USGS has published flood discharges that are based on at least 10 years of observed record or where the flood discharges are based on a calibrated watershed model. Data for about 200 urban stations meeting these criteria were obtained from USGS Water-Supply Paper 2207 (Sauer et al., 1983), which describes nationwide regression equations for estimating flood discharges for urban watersheds. Supplementary data were obtained from USGS reports on urban flood frequency that are posted on the following website: http://water.usgs.gov/osw/programs/nss/pubs.html. Urban flood discharges and watershed characteristics, including impervious area, were obtained from the data in USGS Water-Supply Paper 2207 (Sauer et al., 1983).

Alabama: USGS Water-Resources Investigations Report (WRIR) 82-683, Synthesized flood frequency of urban streams in Alabama

Florida: USGS WRIR 84-4004, Magnitude and frequency of floods from urban streams in Leon County, Florida

Georgia: USGS WRIR 95-4017, Flood-frequency relations for urban stream in Georgia—1994 update

Kentucky: USGS WRIR 97-4219, Estimation of peak-discharge frequency of urban streams in Jefferson County, Kentucky

Missouri: USGS WRIR 86-4322, Techniques for estimating flood-peak discharges from urban basins in Missouri

North Carolina: USGS WRIR 96-4084, Estimation of flood-frequency characteristics of small urban streams in North Carolina

South Carolina: USGS Scientific Investigations Report (SIR) 2004-5030, Estimating the magnitude and frequency of floods in small urban streams in South Carolina, 2001 http://pubs.usgs.gov/sir/2004/5030/

Tennessee: USGS WRIR 84-4110, Flood frequency and storm runoff of urban areas of Memphis and Shelby County, Tennessee and USGS WRIR 84-4182, Synthesized flood frequency of small urban streams in Tennessee

Texas: USGS WRIR 86-4069, The effects of urbanization on floods in the Austin metropolitan area, Texas

Wisconsin: USGS WRIR 86-4005, Estimating magnitude and frequency of floods for Wisconsin urban streams

Data for rural gaging stations were obtained from the USGS Streamflow and Basin Characteristics File (Dempster, 1983). This file contains flood discharges and watershed characteristics for approximately 13,000 unregulated rural gaging stations across the country. A criterion for selecting rural gaging stations was to limit the drainage area to 5,000 square miles. The original intent of the study was to define homogeneous regions of flood characteristics and watersheds larger than 5,000 square miles would generally cross regional boundaries. The rural watersheds less than 5,000 square miles were selected by establishing a 20- to 40-mile radius around urban areas as identified by the Environmental Systems Research Institute, Inc. The objective was to sample rural watersheds with similar watershed characteristics to the urban watersheds, with the exception of impervious area, and to obtain a reasonable mix of rural and urban watersheds so that impervious area would likely be significant in the regression equations. Impervious area is primarily a function of population growth and will be used to estimate the increase in flood discharges due to population growth.

The 2,357 urban and rural unregulated gaging stations selected for the study are given in Figure B1-1. The density of the gaging stations is greater in the east than the west because of the increased number of urban areas. Most of the urban stations are also in the eastern half of the country or along the west coast.

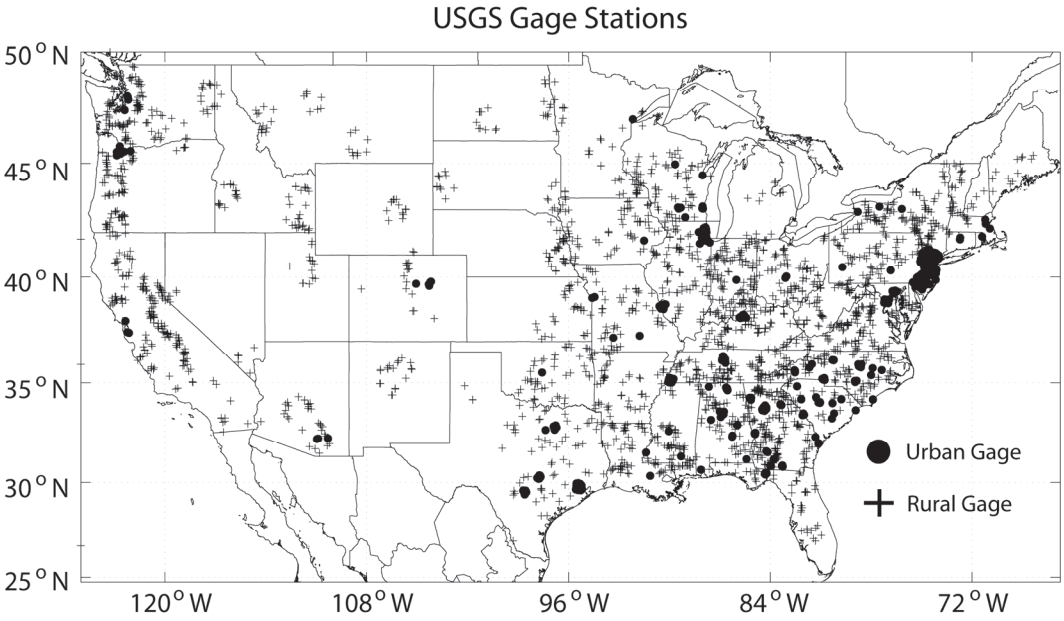

Figure B1-1. Locations of 2,357 USGS gaging stations – 384 urban (circles) and 1,973 rural (crosses) – used to develop the generalized regression relationship between $Q_{1\%}$, $Q_{10\%}$, watershed characteristics, and extreme climate indicators for observed conditions.

B.1.2 Characteristics of the USGS Gages

The following data were compiled at the selected 2,357 unregulated gaging stations in the conterminous United States:

- Drainage area of the watershed, in square miles;
- Channel slope, in feet per mile;
- Total channel length, in miles;
- Area of lakes and ponds (storage), in percent of the drainage area;
- Impervious area, in percent of the drainage area;
- Latitude and longitude of the gaging station, in decimal degrees; and
- 10- and 1-percent annual chance discharges, in cubic feet per second.

Of the 2,357 gaging stations, 384 stations are at urban watersheds where the impervious area of the watershed is greater than 1 percent. The 1% annual chance flood discharge was chosen because it is the base flood mapped by FEMA on Flood Insurance Rate Maps. The 10% annual chance flood discharge was chosen because the difference in elevation between the 10% and 1% annual chance floods is used by FEMA to determine flood insurance rates.

The watershed characteristics listed above were selected because these values are available in the USGS Streamflow and Basin Characteristics File (Dempster, 1983) for rural watersheds, in USGS Water-Supply Paper 2207 for urban watersheds, and in other urban reports posted on the USGS web site. The Streamflow and Basin Characteristics File and the USGS reports also include climatic characteristics such as the mean annual precipitation or the 2-year 24-hour rainfall. These climatic data were not compiled because the intent was to use observed extreme climate indicators for which future projections were available. The extreme climate indicators are described in the next section.

B.1.3 Observed Extreme Climate Indicators

A recent study published by Alexander et al. (2006) compiled a global gridded dataset of extreme climate indicators (ECIs) data using 2,223 temperature gages and 5,948 precipitation gages located throughout the world. In the United States specifically, quality controlled data were compiled for a suite of 27 ECIs available at over 2,600 gage locations for the period 1951–2003 to produce a gridded data resolution of 3.75° longitude by 2.5° latitude. Angular distance weighting was used to interpolate the gage estimates to the gridded resolution noted. These gridded data were downloaded from the UK's Met Office Hadley Centre website located at: http://hadobs.metoffice.com/hadex/index.html. The gridded, observed, extreme climate indicator data were then used to ECI values at each of the selected USGS gage locations using inverse distance weighting of the four closest gridded values.

Eight extreme climate indicators were evaluated for statistical significance in estimating the 10% and 1% annual chance flood discharges. Since some of the indicators are highly correlated and some have minimal variations across the conterminous United States, only three extreme climate indicators were used in the final regression analyses. The eight indicators are defined in Table B1-1.

Maps of the three extreme climate indicators that were determined to be important for this study (as a result of the regression analysis; the selected ECIs were chosen based on the amount of variance of the data that they explained independently of other candidate ECIs) are shown in Figure B1-2. The three extreme climate indicators selected were the number of frost days per year (FD), the number of consecutive dry days per year (CDD), and the maximum 5-day rainfall per year (R5D), shown in columns 1 through 3 of the figure, respectively. Quality controlled data were available for each of these three indices for the entire 53 year period over much of the U.S. Mean observed values of these indices for this period are shown in panels A through C of Figure B1-2. There was limited extreme climate indicator data

available for Alaska and there were no data available for Hawaii. Obtaining estimates of the observed extreme climate indicator values for the 1951–2003 period at each of the USGS gage locations provided a means of developing a regression relationship that utilized the extreme climate indicators as explanatory (predictor) variables related to flooding.

Table B1-1. Descriptions of the eight extreme climate indices proposed for use in this study (Tebaldi et al., 2006).

Indicator	Description	Units
FD	Total number of frost days, defined as the annual total number of days with absolute minimum temperature below 0 degrees Celsius.	days
GSL	Growing season length, defined as the length of the period between the first spell of five consecutive days with mean temperature above 5º Celsius and the last such spell of the year.	days
Tn90	Warm nights, defined as the percentage of times in the year when minimum temperature is above the 90th percentile of the climatological distribution for that calendar day.	%
R10	Number of days with precipitation greater than 10mm per year.	days
CDD	Annual maximum number of consecutive dry days.	days
R5d	Annual maximum 5-day precipitation total.	mm
SDII	Simple daily intensity index, defined as the annual total precipitation divided by the number of wet days.	mm d^{-1}
R95T	Fraction of total precipitation due to events exceeding the 95th percentile of the climatological distribution for wet day amounts.	%

B.1.4 Development of Regression Equations

Regression equations were developed for estimating the 10% and 1% annual chance flood discharges using the watershed characteristics and discharge data described earlier and observed estimates of the extreme climate indicators for the period 1951–2003. The objective in regression analysis is to have reasonably independent explanatory (predictor) variables. Preliminary regression analyses indicated that the means of the climatic indicators were slightly more significant than the median values, so the means of the ECIs for the period 1951–2003 were used in the regression analysis.

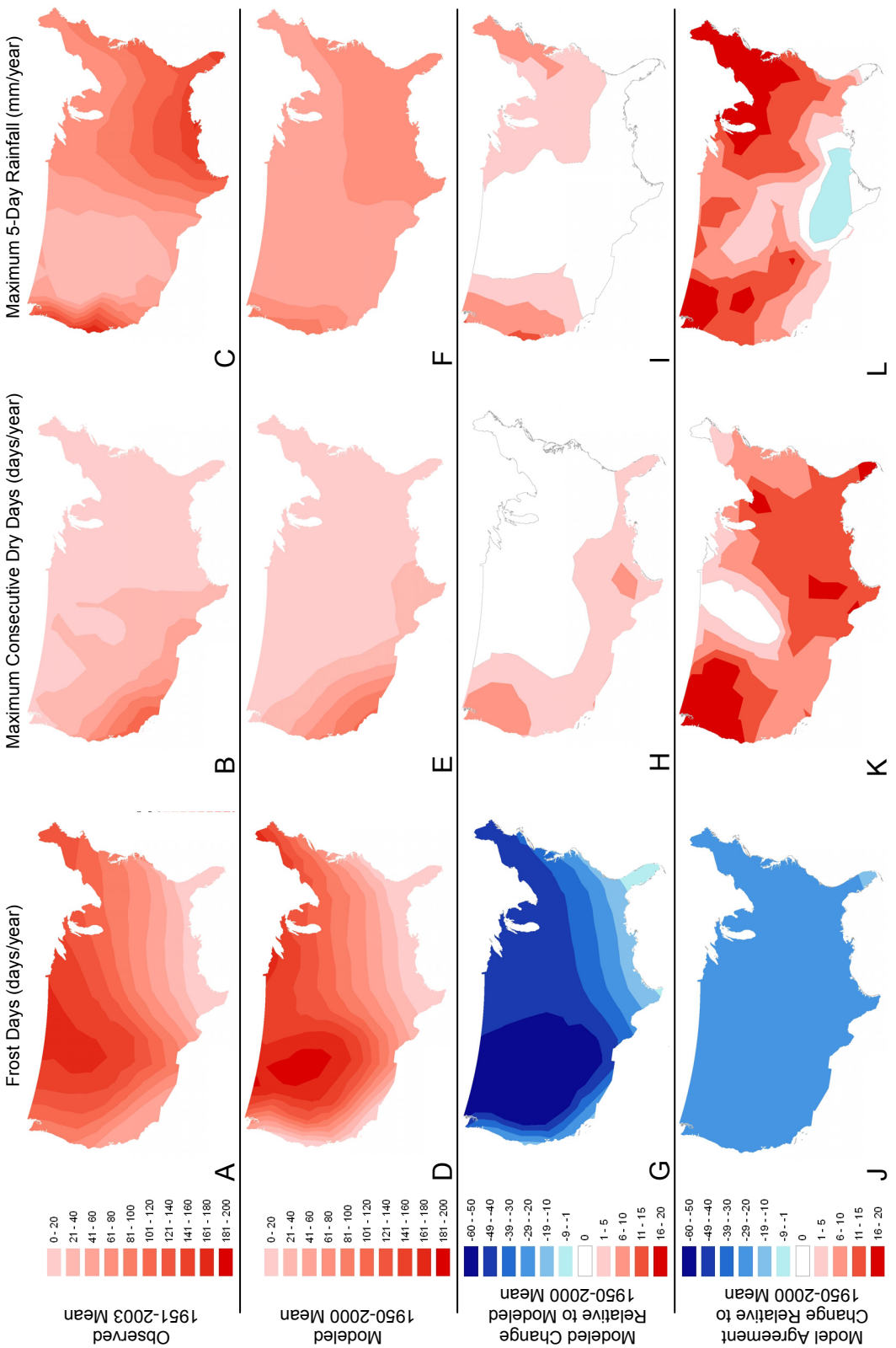

Figure B1-2. Observations and projections of the three climate indicators (FD, CDD, and R5D) used in this study. Maps A through C show mean observations for the period 1951 to 2003, respectively. Maps D through F show the multi-model, multi-scenario GCM mean for a similar time period (1950 to 2000). Maps G through I show the multi-model, multi-scenario GCM mean projected change in these three indices for the end of the century (2080 to 2099). Maps J through L show multi-model agreement for the projected change in the three indices for the end of the century, defined as the number of models predicting a positive change minus the number of models predicting a negative change. For the bottom two rows, red indicates hotter or dryer conditions, and blue indicates cooler or wetter conditions.

The ECIs were evaluated in the regression analysis and three were found to be statistically significant: number of frost days per year (FD), the maximum number of consecutive dry days per year (CDD), and the maximum 5-day rainfall per year (R5D). Some of the climate indicators were highly correlated and therefore not statistically significant in the regression analysis. A correlation matrix of the logarithms of the mean of the eight climate indicators for the 2,357 gaging stations is given in Table B1-2. The logarithms of the data were used because all data were transformed to logarithms for the linear regression analysis.

Table B1-2. Correlation coefficients of the logarithms of the mean values of the eight climate indicators at the gaging stations.

Variable	FD	GSL	Tn90	CDD	R10	R5D	R95T	SDII
FD	1.00	-0.42	0.18	-0.11	-0.32	**-0.73**	-0.27	**-0.79**
GSL		1.00	-0.37	-0.47	0.41	0.25	0.21	0.24
Tn90			1.00	0.41	-0.54	-0.27	0.12	-0.17
CDD				1.00	-0.68	-0.08	-0.02	-0.14
R10					1.00	**0.71**	0.16	0.64
R5D						1.00	0.46	**0.91**
R95T							1.00	0.32
SDII								1.00

The data in Table B1-2 indicate the following:

- SDII, the annual total precipitation divided by the number of days with precipitation greater than 1 mm, is highly correlated with both the number of frost days (FD) per year and the annual maximum 5-day rainfall per year (R5D). This explains why SDII is not significant in explaining the variation in the 10- and 1-percent annual chance flood discharges.
- R10, number of days with precipitation greater than 10 mm, is correlated with the annual maximum 5-day rainfall per year (R5D). Both variables are measures of rainfall. Because R5D has a greater variability and is more statistically significant, it was used in the regression equations. R5D is correlated with short-term rainfall data making this variable applicable to both small and large watersheds.
- The number of frost days (FD) per year and the annual maximum 5-day rainfall per year (R5D) are highly correlated but both are statistically significant in the regression analysis and were retained in the equations.

Two additional climate indicators – percentage of time when minimum temperature is above the 90th percentile of daily minimums (Tn90) and fraction of total precipitation exceeding the 95th percentile for wet days (R95T) – had minimal variation across the country. Tn90 varied from 9.96 to 10.90 percent and R95T varied from 0.17 to 0.28.

Therefore, these variables were not statistically significant because of the minimal range in values. The growing season length (GSL), which is the length of the period between the first spell of 5 consecutive days above 5 degrees Celsius and the last such spell, is not valid outside the mid-latitudes (Frich, 2002) and has significant variability from year to year at the same location. This variable is not a reliable explanatory variable. Although not shown in Table B1-2, channel length was highly correlated with drainage area (R^2 of 0.89) and was not included in the final regression equations.

Many regression analyses were performed using the Statistical Analysis System (SAS) to determine the statistically significant explanatory variables. All data were transformed to logarithms and a multiple linear regression analysis was performed. A constant of 1 was added to those variables that may have values close to zero. In terms of the untransformed data, this represents a power function relation between flood discharges and the watershed/climate indicators. The resulting 1% annual chance equation is:

$$Q_{1\%} = 1.321 * DA^{0.711} SL^{0.169} (ST+1)^{-0.332} (IA+1)^{0.188} (MFD+1)^{-0.206} (MCDD+1)^{-0.177} (MR5D+1)^{1.440} \quad \text{(B1-1)}$$

where $Q_{1\%}$ is the 1% annual chance flood discharge, in cubic feet per second;

DA is the drainage area of the watershed, in square miles;

SL is the channel slope, in feet per mile;

ST is the storage in the watershed as represented by the area of lakes and ponds, in percent of the drainage area;

IA is the impervious area, in percent of the drainage area;

MFD is the mean number of frost days per year for 1951–2003;

MCDD is the mean number of consecutive dry days per year for 1951–2003; and

MR5D is the mean of the annual maximum 5-day rainfall per year for 1951–2003, in millimeters.

The standard error of Equation (B1-1) is 58.8% and the R^2 value is 0.898. All the variables are significant at the 5-percent level implying there is less than a 5% chance of erroneously assuming the explanatory variables are significant when in fact they are not. Kollat et al. (2012) provide additional details on the development of the regression equations and split-sampling analyses to evaluate the predictive accuracy of the 1% annual chance equation.

The 10% annual chance equation is:

$$Q_{10\%} = 0.1093(DA)^{0.723}(SL)^{0.158}(ST+1)^{-0.339}(IA+1)^{0.222}(MFD+1)^{-0.044} \times (MCDD+1)^{-0.395}(MR5D+1)^{1.812} \quad \text{(B1-2)}$$

where $Q_{10\%}$ is the 10% annual chance flood discharge, in cubic feet per second, and all other variables are defined above.

The standard error of Equation (B1-2) is 57.4% and the R^2 value is 0.906. All the variables are significant at the 5-percent level except MFD. Note that the gage station estimates themselves also contain uncertainties (depending on record lengths, data variability, and so forth) not fully accounted for in this analysis. Consequently, it is recognized that the standard error is actually larger than estimated here, and could be reconsidered in future refinement of the work.

The means of the three extreme climate indicators for the period 1951–2003 were used in the regression analysis with the assumption that these data were fairly constant and representative of the observed or current climate conditions. This assumption was reasonable because the variation in FD, CDD, and R5D over the observed period 1951–2003 was small compared to the variation in these indicators over the projected period (2003–2100).

The gridded data for FD, CDD, and R5D as shown in Figure B1-2, were used in developing Equations (B1-1) and (B1-2). Regression analyses were also performed on the point data recorded at the individual temperature and precipitation stations (over 2,600 stations in the United States) used to develop the gridded data as described by Alexander and others (2006). The gridded data were more statistically significant and were better predictors than using the point data at the individual stations.

A plot of the predicted (Equation [B1-1]) versus observed $Q_{1\%}$ flood discharge (more precisely, versus the *published* values which here play the role of observations for purposes of comparison) is shown in Figure B1-3.

Figure B1-3 shows a total of 2,851 stations including outliers and unreliable values. As described earlier, the data were compiled from different USGS reports and databases and some of the $Q_{1\%}$ flood discharges are based on a minimum of only 10 years of data. In addition, some of the stations may be outliers due to watershed characteristics that are not accurate. These factors contributed to a large number of outliers. Because this was a nationwide analysis, a case-by-case investigation of each outlier station was not feasible and was not undertaken. Instead, a simple rule

was adopted by which the stations were censored on the basis of their residuals. The residuals, expressed as a ratio of the observed to predicted $Q_{1\%}$, were estimated and stations were censored if the residual or ratio was greater than 3.0 or less than 0.33. Experience has shown that when the observed and predicted values differ by a factor of three or more, then it is very likely that data point is an outlier that should probably not be included in the analysis. This simple censoring rule was appropriate owing to the scale of the present study (2,851 stations).

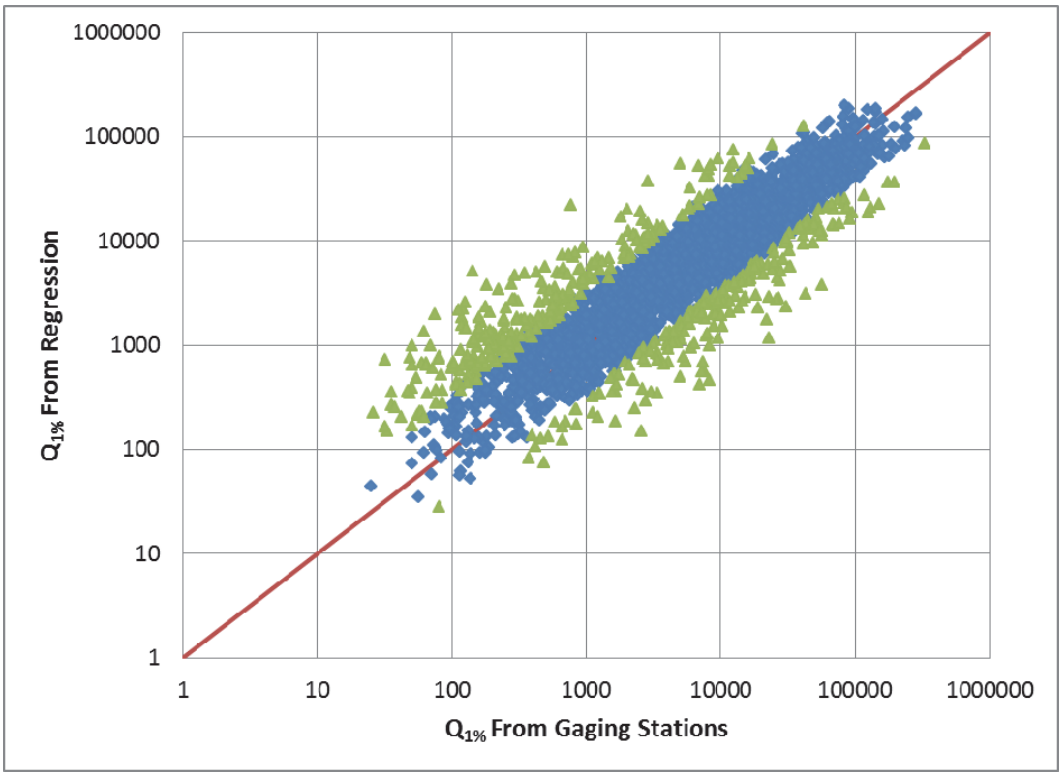

Figure B1-3. Scatter plot of the regression estimates versus the published values of $Q_{1\%}$ at 2,851 gaging stations. The points marked with the green triangles depart by more than a factor of three from the one-on-one line and were censored as a simple way to eliminate outliers in lieu of an infeasible case-by-case gaging station assessment; see the accompanying text. The 2,851 gaging stations were reduced to 2,357 stations used in the final analysis. Note that the trend is not significantly affected by this censoring, although variability is reduced.

As suggested by Figure B1-3, the censoring of stations with large residuals did not significantly affect the regression equations, but reduced the variability around the equation thereby reducing the estimate of the standard error. The original standard error based on 2,851 stations was over 100% and was considered unreasonable due to the inclusion of stations with large uncertainty in $Q_{1\%}$ and unusual watershed characteristics not accounted for in Equation (B1-1).

Equations (B1-1) and (B1-2) were developed for 2,357 stations across the conterminous United States. The equations are unbiased on a national basis but may be biased on a regional basis. The equations can be adjusted for regional bias but this is not necessary for this national study. The objective in using Equations (B1-1) and (B1-2) is to determine the percent increase in the 10% and 1% annual chance discharges as a result of future changes in the climate indicators or the impervious area. Whether or not the equations are corrected for regional bias does not impact the estimate of percent change in the 10% and 1% annual chance discharges. Equations (B1-1) and (B1-2) should not be used to predict climate change on a regional or statewide basis.

A major reason for developing nationwide equations was to have as large a variation in the independent variables as possible, particularly for the ECIs. The projections of future change in the ECIs are quite large under some of the scenarios and climate models. For Equations (B1-1) and (B1-2) to be applicable for future climate change, it was necessary to have a large variation in the observed climate indicators to avoid significant extrapolations of the equations. Test results indicated that significant extrapolation of the regression equations provided unreasonable estimates of $Q_{1\%}$. Table B1-3 provides summary statistics for the independent or explanatory variables used in the regression analysis.

Table B1-3. Summary statistics on the explanatory variables used in the regression analysis.

Variable	Mean	Standard deviation	Minimum	Maximum
Drainage area (mi^2)	268.96	603.49	0.02	4,927
Channel slope (ft/mi)	70.94	144.51	0.16	2,800
Storage (%)	1.65	5.03	0.00	74.00
Impervious area (%)	3.94	8.90	0	74.00
Frost days	97.58	36.34	13.87	184.53
Consecutive dry days	29.17	19.62	15.11	129.41
Maximum 5-day rainfall (mm)	115.68	26.13	40.50	184.28

B.2 Climate Model Projections

B.2.1 Climate Model Outputs

Climate model outputs utilized in the IPCC AR4 are hosted on the World Climate Research Programme's (WCRP's) Coupled Model Intercomparison Project phase 3 (CMIP3) multi-model dataset (see Meehl et al., 2007) located at: https://esg.llnl.gov:8443/index.jsp. Exploration of this database (in 2009) revealed the availability of extreme climate indicator outputs for 10 different GCMs across the three SRES scenarios explored in this study (B1, A1B, and A2). The availability of the three extreme climate indicators used in this study (FD, CDD, and R5D) is summarized in Table B2-1 where the number in each cell represents the number of ensemble realizations available for each model and scenario.

Table B2-1. Summary of extreme climate indicator availability.

Model	Country	Scenarios		
		B1	A1B	A2
CCSM3	USA	1	1	0
CNRM-CM3	France	1	1	1
GFDL-CM2.0	USA	0	1	1
GFDL-CM2.1	USA	0	1	1
INM-CM3.0	Russia	1	1	1
IPSL-CM4	France	1	1	1
MIROC3.2 Hi Res	Japan	1	1	0
MIROC3.2 Med Res	Japan	2	3	3
MRI-CGCM2.3.2	Japan	0	5	1
PCM	USA	4	4	4
Total		**43**		

In total, there were 43 model runs available containing the necessary extreme climate indicator outputs (11 for scenario B1, 19 for scenario A1B, and 13 for scenario A2). These outputs were obtained from the CMIP3 database and were processed using the Climate Data Operators (CDO) from the website of the Max Planck Institute for Meteorology. The CDO provide a set of tools for performing basic operations on the standard format (netCDF) output files generated by climate models such as regridding and basic statistical analysis. Since all climate models in Table B2-1 were run at differing spatial resolutions, all available outputs were remapped using distance-weighted averaging to a 3.75° longitude by 2.5° latitude grid resolution to match the resolution of the observed extreme climate indicators data set. In addition, 20-year statistical averages were calculated for each of five epochs

(2000–2019, 2020–2039, 2040–2059, 2060–2079, and 2080–2099) through the end of the century. The primary purpose of this processing step was to reduce the set of climate model output files to a format that could be easily processed in subsequent analysis steps.

B.2.2 Extreme Climate Indicator Projections

Following the processing of the climate model outputs, extensive data analysis was conducted in order to both confirm the validity of the processed data and to glean a more thorough understanding of the extreme climate indicator projections provided by the models. Figure B1-2 shows a summary of the analysis performed, including both an assessment of the multi-model mean projected change in each of the extreme climate indices as well as an assessment of agreement among the models. It should be noted that all analysis results are reported for scenario A1B only (the intermediate climate scenario), and are multi-model averages based on one run from each of the 10 models available. Change in an extreme climate indicator is expressed as a multi-model difference between the mean projection of the index and the modeled current conditions for the period 1950–2000. Model agreement is shown in panels J through L of Figure B1-2. Agreement is defined as the number of models that agree on a positive change in an indicator, minus the number of models that agree on a negative change in an indicator. Hence, high agreement on either a positive or negative change will be either blue or red respectively while no agreement (five models project a positive change while the other five project a negative change) will be indicated by white.

B.3 Fundamental Relationships

The purpose of this appendix is to derive how the effects of climate change and population are separated for the FEMA study. The notation used in the following sections is defined as follows.

Subscripts:

- c: current
- m: modeled (hence mc = modeled current conditions)
- p: projected (hence mp = modeled projection)
- rel: a relative percent change in some parameter over current conditions

Variables:

- D10: Flow depth associated with the 10% annual chance flooding event (10-year return period)

D100: Flow depth associated with the 1% annual chance flooding event (100-year return period)

FPA: Floodplain area associated with the flooded area between the Q100 and Q10 flows

FPD: Depth associated with flow in the floodplain defined here as the difference between D100 and D10

IA: Impervious area

Q10: Discharge associated with the 10% chance flooding event (10 year return period)

Q100: Discharge associated with the 1% chance flooding event (100 year return period)

T: Top width

B.3.1 Changes in the 100-Year Flow (Q100)

B.3.1.1 Equations

The main focus of the riverine portion of this study is in finding the ratio of the projected flow to the current flow, or in other words, the relative change in flow over current conditions (Equation [B3-1]).

$$\Delta Q100_{rel} = \frac{Q100_p}{Q100_c} \quad \text{(B3-1)}$$

Where $\Delta Q100_{rel}$ is the relative change in the Q100, $Q100_p$ is the projected Q100, and $Q100_c$ is the current Q100 measured at the USGS gauge.

Equation (B3-2) is used to find the $Q100_p$.

$$Q100_p = \frac{Q100_{mp}}{Q100_{mc}} Q100_c \quad \text{(B3-2)}$$

where $Q100_{mp}$ is the projected Q100 based on the regression equation, $Q100_{mc}$ is the current Q100 based on the regression equation (using the climate models' simulation of current conditions as input). This approach was used to correct for the possible bias in the climate models' simulations of current conditions.
Substituting Equation (B3-2) into Equation (B3-1) results in the relative change in Q100 that is dependent only on the projected flow (the mp subscript above) and the modeled current flow (mc), and that does not depend on the USGS-measured Q100c. This distinction is important: the purpose is to separate out the effects of climate change that are independent of impervious area (IA). Specifically, climate change effects are denoted with the subscript CL, and the impervious area effects

with IA. Using the portion of the regression equation that deals with climate indices results in:

$$\Delta Q100_{CL,rel} = \frac{Q100_{CL,mp}}{Q100_{CL,mc}} \quad \text{(B3-3)}$$

In other words, the relative change in Q100 with respect to climate is simply the ratio of the flow resulting from the regression equation using projected climate indices to the regression equation using current climate indices, with all other terms held constant.

The relative change is calculated in Q100 with respect to impervious area in (Equation [B3-4]). Note the substitution of the actual IA term here for clarity:

$$\Delta Q100_{IA,rel} = \frac{Q100_{IA,mp}}{Q100_{IA,mc}} = \frac{\left(IA_p + 1\right)^{0.188}}{\left(IA_c + 1\right)^{0.188}} \quad \text{(B3-4)}$$

The total relative change in Q100 is the product of the terms found in Equations (B3-3) and (B3-4):

$$\Delta Q100_{rel} = \Delta Q100_{CL,rel} \times \Delta Q100_{IA,rel} \quad \text{(B3-5)}$$

B.3.1.2 Computational Approach

1. Calculation of the relative change in Q100 due to the climate at each gage is completed (Equation [B3-3]).
2. Ordinary Kriging (see Appendix D.4) is used to find the corresponding value of $\Delta Q100_{CL,rel}$ at each grid cell (Equation [B3-3]).
3. "Effective" impervious area estimates for current and projected conditions are found using current and projected population density at each grid cell (the "Hicks" relationship between population density and IA).
4. Using the values calculated in step 3, $\Delta Q100_{IA,rel}$ is calculated at each grid cell.
5. The outputs are combined from steps 2 and 4 using Equation (B3-5) to find the $\Delta Q100_{rel}$ at each grid cell.

B.3.2 Calculating Changes in Flood Plain Depth (FPD)

B.3.2.1 Equations

The relative change in floodplain depth considers the difference between the 100-year depth and the 10-year depth as expressed in Equation (B3-6). This change is expressed as a ratio. To express the values as percent changes (as done previously) it is necessary to subtract 1 and multiply by 100%.

$$\Delta FPD_{rel} = \frac{D100_p - D10_c}{D100_c - D10_c} \quad \text{(B3-6)}$$

The depth (D) values in this study are a function of Q as expressed in Equation (B3-7):

$$D = 0.2158Q^{0.403} \quad \text{(B3-7)}$$

The calculation of the current D100 and D10 depths are straightforward calculations using the Q100 and Q10 observed at the USGS gages. The projected D100, however, uses the relative change in Q as shown in Equation (B3-8):

$$D100_p = 0.2158\left(\Delta Q100_{rel} \times Q100_c\right)^{0.403} \quad \text{(B3-8)}$$

Substitution of Equations (B3-8) and (B3-7) into 6 and will result in:

$$\Delta FPD_{rel} = \frac{\left(\Delta Q100_{rel} \times Q100_c\right)^{0.403} - \left(Q10_c\right)^{0.403}}{\left(Q100_c\right)^{0.403} - \left(Q10_c\right)^{0.403}} \quad \text{(B3-9)}$$

The change in floodplain depth is a function of the current observed Q100 and Q10, which are constant at each gage, and the $\Delta Q100_{rel}$, which was derived in section B.3.1.2. The terms in the numerator are separated and the separation of Equation (B3-5) is applied on the relative change to obtain:

$$\Delta FPD_{rel} = \left(\Delta Q100_{CL,rel}{}^{0.403} \Delta Q100_{IA,rel}{}^{0.403} \frac{\left(Q100_c\right)^{0.403}}{\left(Q100_c\right)^{0.403} - \left(Q10_c\right)^{0.403}} \right) - \left(\frac{\left(Q10_c\right)^{0.403}}{\left(Q100_c\right)^{0.403} - \left(Q10_c\right)^{0.403}} \right)$$

(B3-10)

B.3.2.2 Computational Approach

1. Perform steps 1 and 2 in section B.3.1.2 (find a kriged estimate of $\Delta Q100_{CL,rel}$ at each grid cell).
2. Perform steps 3 and 4 in section B.3.1.2 (find $\Delta Q_{IA,rel}$ at each grid cell).

3. Perform Ordinary Kriging to find an estimate of:

$$\frac{\left(Q100_c\right)^{0.403}}{\left(Q100_c\right)^{0.403}-\left(Q10_c\right)^{0.403}}$$ at each grid cell.

4. Perform Ordinary Kriging to find an estimate of:

$$\frac{\left(Q10_c\right)^{0.403}}{\left(Q100_c\right)^{0.403}-\left(Q10_c\right)^{0.403}}$$ at each grid cell.

5. Calculate Equation (B3-10) using the outputs from steps 1 through 4 above to obtain ΔFPD_{rel} at each grid cell.

B.3.3 Calculating Changes in the Flood Hazard Parameter (FHP)

B.3.3.1 Equations

The relative change in the "hazard parameter" relates the difference in the *projected* 100-year depth and 10-year depth to this difference under current conditions. The change is expressed as a ratio. The hazard parameter equation is shown in Equation (B3-11):

$$\Delta FHP_{rel}=\frac{D100_p-D10_p}{D100_c-D10_c} \quad \text{(B3-11)}$$

It should be noted that this equation is similar to the delta FPD expressed in Equation (B3-6). Each depth utilizes the D vs. Q relationship of Equation (B3-7). Equation (B3-12) shows the derivation of the D10p (similar to Equation [B3-8]):

$$D10_p=0.2158\left(\Delta Q10_{rel}\times Q10_c\right)^{0.403} \quad \text{(B3-12)}$$

That is, the projected D10 is related to the relative change in the Q10 and the current Q10 value. Substituting Equations (B3-8) and (B3-12) into (B3-11) yields:

$$\Delta FHP_{rel}=\frac{\left(\Delta Q100_{rel}\times Q100_c\right)^{0.403}-\left(\Delta Q10_{rel}\times Q10_c\right)^{0.403}}{\left(Q100_c\right)^{0.403}-\left(Q10_c\right)^{0.403}} \quad \text{(B3-13)}$$

Similar to the change in FPD, the change in FHP is related to current observed Q100 and Q10 (which are constant at each gage), the $\Delta Q100_{rel}$ that was derived in section B.3.1.2, and the $\Delta Q10_{rel}$, which is calculated in a similar manner to the 100-year flow, only using a different regression equation. Separating terms and applying

the separation of Equation (B3-5) to relative changes in both the Q10 and the Q100 results in Equation (B3-14). Note that the change in Q10 due to IA incorporates the exponent on the IA term in the Q10 relationship, which is different than the exponent from the Q100 relationship.

$$\Delta FHP_{rel} = \left(\Delta Q100_{CL,rel}{}^{0.403} \Delta Q100_{IA,rel}{}^{0.403} \frac{(Q100_c)^{0.403}}{(Q100_c)^{0.403} - (Q10_c)^{0.403}} \right) - \left(\Delta Q10_{CL,rel}{}^{0.403} \Delta Q10_{IA,rel}{}^{0.403} \frac{(Q10_c)^{0.403}}{(Q100_c)^{0.403} - (Q10_c)^{0.403}} \right) \quad \text{(B3-14)}$$

B.3.3.2 Computational Approach

1. Find a kriged estimate of $\Delta Q100_{CL,rel}$ at each grid cell.
2. Find $\Delta Q100_{IA,rel}$ at each grid cell.
3. Find a kriged estimate of $\Delta Q10_{CL,rel}$ at each grid cell.
4. Find $\Delta Q_{IA,rel}$ at each grid cell.
5. Perform Ordinary Kriging to find an estimate of: $\frac{(Q100_C)^{0.403}}{(Q100_C)^{0.403} - (Q10_C)^{0.403}}$ at each grid cell.
6. Perform Ordinary Kriging to find an estimate of: $\frac{(Q10_C)^{0.403}}{(Q100_C)^{0.403} - (Q10_C)^{0.403}}$ at each grid cell.
7. Calculate Equation (B3-14) using the outputs from steps 1–6 above to obtain ΔFHP_{rel} at each grid cell.

B.4 Monte Carlo Simulation Procedure

B.4.1 Monte Carlo Sampling Description

The purpose of the Monte Carlo sampling procedure is to aid in propagating the uncertainty associated with climate modeling and the uncertainty associated with developing the various regression relationships through to the final estimates of flooding impacts. This type of analysis then allows for an assessment of both the mean projected impact as well as the uncertainty associated with these projections.

The various sources of uncertainty quantified in the Monte Carlo sampling procedure include the following:

- Uncertainty associated with multiple climate models with possibly multiple runs available for each model.
- Uncertainty associated with multiple SRES scenarios (e.g., B1, A1B, A2).
- Uncertainty in the regression relationships among watershed characteristics, extreme climate indicators, and discharge.

These above mentioned sources of uncertainty were those identified by the project team as being quantifiable to a reasonable degree. Additional sources of uncertainty that were **not** included in the analysis include:

- Uncertainty in the relationship between impervious area and population density.
- Uncertainty associated with the regression relationship between discharge and flow depth.
- Uncertainty associated with the triangular wedge assumption used to translate projected changes in floodplain depth to changes in floodplain area.

The Monte Carlo sampling procedure is described in detail throughout the remainder of this appendix.

B.4.2 Detailed Monte Carlo Sampling Procedure

B.4.2.1 Initialize Grids

a) U.S. grid definition:

Longitude vertices = -163.125° W to -65.625° W
Latitude vertices = 23.75° N to 63.75° N
Number of cells: 27 cells longitude by 16 cells latitude
Cell sizes: 3.75° longitude by 2.5° latitude

b) Climate model output world grid:

Longitude vertices = -1.875° W to 178.125° E then -178.125° W to -5.625° W
Latitude vertices = -90.0° S to 87.5° N
Number of cells: 96 cells longitude by 72 cells latitude
Cell sizes: 3.75° longitude by 2.5° latitude

c) Map the U.S. grid into the climate model output world grid for climate data retrieval (i.e., for each cell in the U.S. grid, determine an index into the climate model output world grid).

d) Population projection grid:

Longitude vertices = -170.0° W to -60.0° W
Latitude vertices = 20.0° N to 70.0° N
Number of cells: 441 cells longitude by 201 cells latitude
Cell sizes: 0.25° longitude by 0.25° latitude

B.4.2.2 Read in Climate Model Projections and Population Projections

a) Read in climate model projections of extreme indices (FD, CDD, and R5D only) from the world grid into the U.S. grid for each epoch, scenario, and run that is available for each of the 10 models used.

b) Read in population projections for each epoch and scenario to the population grid defined above. These gridded population projections are not used to project changes in IA, but rather to project output at each gage location for possible future analysis. One possible use would be to combine maps of population growth with maps of change in flooding.

B.4.2.3 Monte Carlo Sampling Procedure

Important Equations:

Q regression equations:

$$Q10 = (0.1093)(DA^{0.723})(SL^{0.158})((ST+1)^{-0.339})((IA+1)^{0.222}) ((FD+1)^{-0.044})((CDD+1)^{-0.395})((R5D+1)^{1.812}) + \text{std error noise} \quad \text{(B4-1)}$$

Standard error: 0.2318 log units; $R^2 = 0.906$

$$Q100 = (1.321)(DA^{0.711})(SL^{0.169})((ST+1)^{-0.332})((IA+1)^{0.188}) ((FD+1)^{-0.206})((CDD+1)^{-0.177})((R5D+1)^{1.440}) + \text{std error noise} \quad \text{(B4-2)}$$

Standard error: 0.2368 log units; $R^2 = 0.898$

Gages: Loop through gage stations

Epochs: Loop through epochs

Scenarios: Loop through scenarios

MC Samples: Loop through Monte Carlo samples

For each sample:

1. Randomly sample each of the extreme indices projections from the various models and runs available. Note that models with multiple runs are weighted equally as those with only one run in the

sampling. For each sample, the three important indices (FD, CDD, and R5D identified from the regression analysis) are drawn independently from the various models and runs available. Independent draws were acceptable since the manner in which the discharge relationships are computed is such that the median is preserved correctly, although a small shift in means is introduced. Independent draws were also helpful in introducing a better account of variability in the results.

Q100 Calculations:

2. Estimate $Q100_{mc}$ from the regression relationship (Equation [B4-2]) using the indices sampled from the model outputs for this epoch and scenario and apply the standard error noise. This is the 100-year discharge associated with the modeled 1950–2000 conditions (mc).

3. Estimate $Q100_{mp}$ from the regression relationship (Equation [B4-2]) using the indices sampled from the model outputs for this epoch and scenario and apply the standard error noise. This is the 100-year discharge associated with the model projections for the epoch of interest (mp).

4. Calculate the projected $Q100_p$ representing the modeled change in discharge applied to the current observed $Q100_c$:

$$Q100_p = Q100_c \, (Q100_{mp}/Q100_{mc}) \qquad \text{(B4-3)}$$

Q10 Calculations:

5. Estimate $Q10_{mc}$ from the regression relationship (Equation [B4-2]) using the indices sampled from the model outputs for this epoch and scenario and apply the standard error noise. This is the 10-year discharge associated with the modeled 1950–2000 conditions (mc).

6. Estimate $Q10_{mp}$ from the regression relationship (Equation [B4-2]) using the indices sampled from the model outputs for this epoch and scenario and

apply the standard error noise. This is the 10-year discharge associated with the model projections for the epoch of interest (mp).

7. Calculate the projected $Q10_p$ representing the modeled change applied to the current observed $Q10_c$:

$$Q10_p = Q10_c\ (Q10_{mp}/Q10_{mc}) \qquad \text{(B4-4)}$$

MC Sampling: End

Scenarios: End

Statistics Calculations:

- Note: Statistics are now calculated on both the samples collected for each individual climate scenario and for the combined samples from all climate scenarios. This allows for either "lumped" or scenario based analysis.

1. Calculate the statistics of the $Q100_p$ sample distributions for this gage and epoch. These statistics include mean, median, and standard deviation, as well as every 1 percentile of the full sampling distribution.

2. Calculate the relative change in Q for each percentile of the distribution:

$$\Delta Q_{rel} = [(Q100_p/Q100_c)\text{-}1] * 100\% = [(Q100_p\text{-}Q100_c)/Q100_c] * 100\% \qquad \text{(B4-5)}$$

3. The distributions associated with $\Delta Q100_{rel}$ can then be to estimate changes in floodplain area (FPA) and flood hazard parameter (FHP) due to both climate change and population growth.

Epoch: End

- Output all of the data for this gage including the statistics that describe the FPD and Q100 distributions from the sampling (all epochs). Aside from the statistics of the distributions, all data associated with the gridded population projections, as well as the IA projections and populations estimated from these, are output. In addition, the statistics of the extreme indices projections sampled from the climate model outputs are saved as well.

Gages: End

B.5 Relating Depth to Discharge

B.5.1 Summary

To obtain differences between impacts of flood elevations, a simple relationship is needed to correlate depths of flow in a river (depth of flow in a channel cross section) to the discharge for flows extending into the overbank floodplains. Stream flows for the 2,357 USGS Stream Gage Stations were used to determine 1% annual chance exceedance and 10% annual chance exceedance floods (i.e., 100-year and 10-year return period flood events). The USGS published flood frequency analysis for these sites using Log-Pearson Type III analysis. These values were used in the present study to determine corresponding depths. The estimated 1% annual chance and 10% annual chance exceedance flood events were also predicted for the five epochs (2010–2019, 2020–2039,2040–2059, 2060–2079, and 2080–2099) using the Monte Carlo simulation procedure as discussed in a previous section. These flows were then converted to depths of flow by the following relationship.

$$D = 0.2158Q^{0.408}$$

B.5.2 Background

In order to convert flow to an elevation or depth, a relationship was developed following the procedures developed by Leopold and Maddock (1953) and Burkham (1977, 1978). Due to the scope of the study, it was imperative that a simple relationship be developed to represent a relationship that could be applied to the 2,357 USGS Stream Gage sites distributed across the U.S.

Leopold and Maddock laid some of the initial groundwork as reported in their classic study published in the USGS Water Supply Paper 252 and titled *The Hydraulic Geometry of Stream Channels and Some Physiographic Implications*. Leopold and Maddock found that hydraulic characteristics of velocity, width, and depth of flowing water vary with discharge as simple power functions at a given river cross section. In particular they found that the depth could be described by the following relationship:

$$D = aQ^f$$

where Q is the discharge and D is the mean depth of flow. The parameters *a* and *f* are numerical constants. Leopold and Maddock found that the average value for f computed using 20 river cross sections representing a large variety of rivers in the

Great Plains and the Southwest was equal to 0.40. However, no statistical analysis was performed on the data.

Burkham (1977) developed a simplified technique for determining depths for specific return period flows for natural channels. In his paper entitled *A technique for determining depths for T-year discharges in rigid-boundary channels*, he presented a simplified procedure to determine depth of flow as a function of discharge. He looked at discharges that will occur, on average, once in T years – i.e. 10 years, 50 years, 100 years – for natural channels (channels not significantly affected by manmade structures) having channel-control conditions and rigid boundaries. Channel-control conditions usually exist during relatively high flows in natural rigid boundary channels (i.e. in uniform flow where the Manning's equation is applicable). In developing the technique, he assumed the independent variables of (1) channel shape, (2) width at a reference elevation, (3) Manning's resistance coefficient, *n*, and (4) channel bottom slope or water surface slope.

Using Manning's equation, Burkham showed that the relation between depth, *D*, and discharge, *Q*, in a natural rigid channel could be expressed as a simple exponential function the same as Leopold and Maddocks' power function $D = aQ^f$ where a and f are functions of channel characteristics and channel shape. Burkham (1977) showed that the coefficient *a* is a function of channel slope and Manning's roughness coefficient *n* (i.e. $a = a(n / S^{1/2})$, and the exponent *f* is a function of channel shape. He noted that most natural channels' geometries can be represented by a parabolic shape, resulting in an exponent *f* of 0.46. He used data from Barnes (1967) to test his equation for depth and computed a standard error of the estimate for computed depths to be about 10%.

Burkham (1978) published a paper in which he developed a relationship between depth of flow and discharge. Similarly to Leopold and Maddock, Burkham found the "*f*" coefficient to be 0.42 having a standard deviation of 0.12. Burkham developed his relationship using 539 sites in seven states (Iowa, Maryland, Minnesota, New York, North Carolina, Ohio, and Wisconsin). He cautioned that the physiographic method is applicable only for natural channels having rigid boundaries.

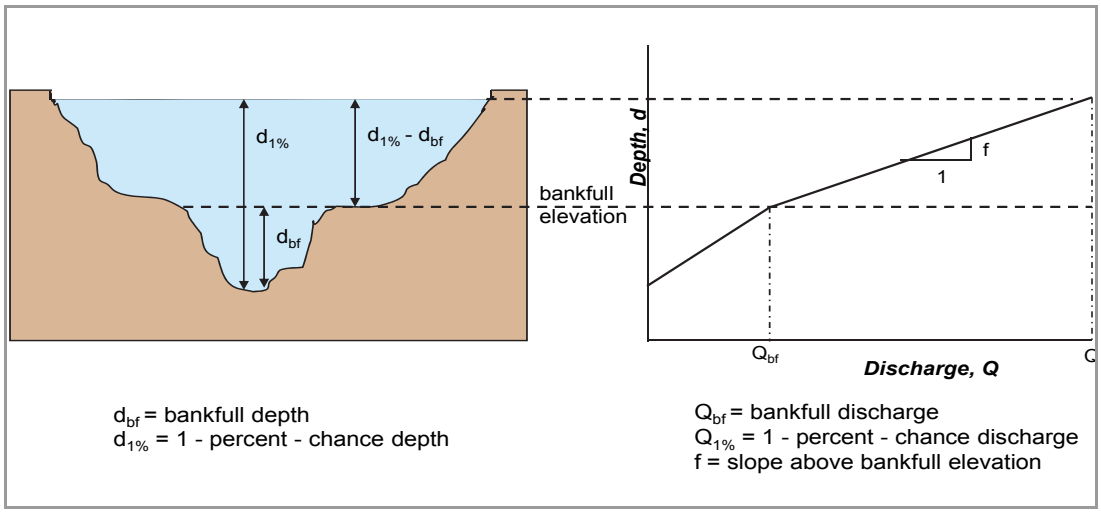

Figure B5-1. Estimating flood depths for overbank flows.

The HEC-RAS computer program was run to obtain output data for approximately 11,000 water surface profiles that were used to develop the relationship of D versus Q for out-of-bank flows as shown in Figure B5-1. The hydraulic models were obtained from the FEMA Mapping Information Platform (MIP) and represented FEMA regions 1, 3, 4, 5, 6, and 10.

In order to utilize the hydraulic models available from the MIP, the correlation of depth and discharge was developed between values unique to a specific profile for a given hydraulic model reach. The profiles used in the analyses were equal to or greater than the 10-year return period. Average depth and a reach-length weighted-average discharge were obtained for each profile, and a linear regression analysis was performed on the logarithms of these values.

Using the NFIP data available on the MIP was particularly desirable since the ultimate effort was to establish estimates of the impacts to the NFIP due to changing climate over the next century. Many of these model profiles contain anomalies from channel-control conditions, such as bridge crossings. These unwanted effects were diminished by considering the depth and discharge parameters on a reach-wide basis, and by the large quantity of data points collected.

The results of the regression analysis are given in the following equation.

$$D = 0.2158Q^{0.408}$$

The standard deviation was 0.19 and R^2 was 0.619. Figure B5-2 shows a histogram of the data and Figure B5-3 shows a scatter plot of the log D versus log Q.

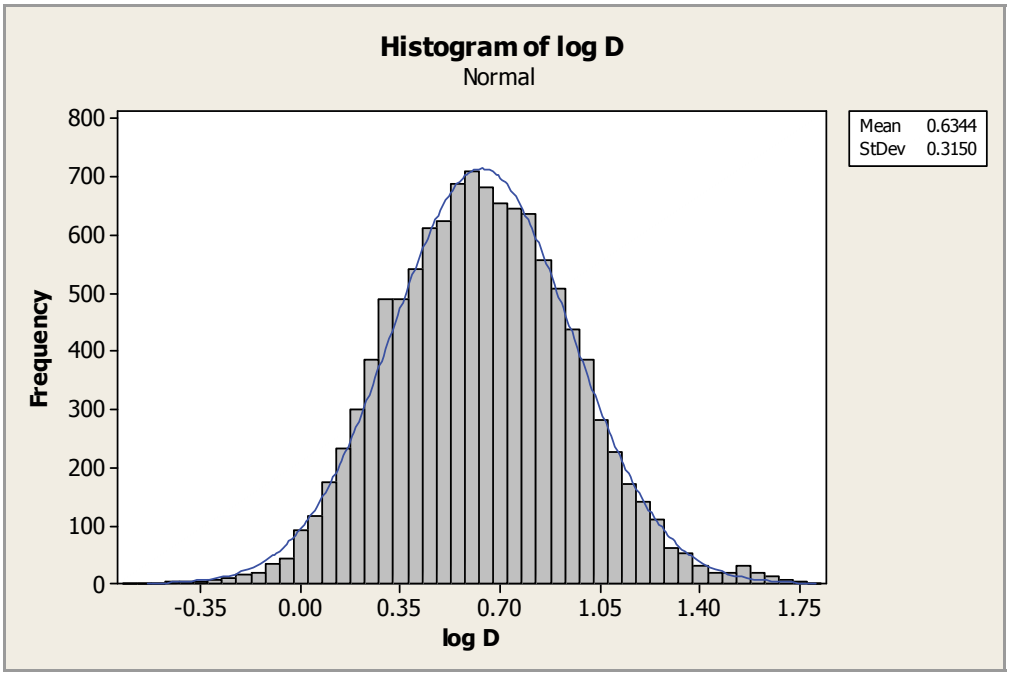

Figure B5-2. Histogram of log depth.

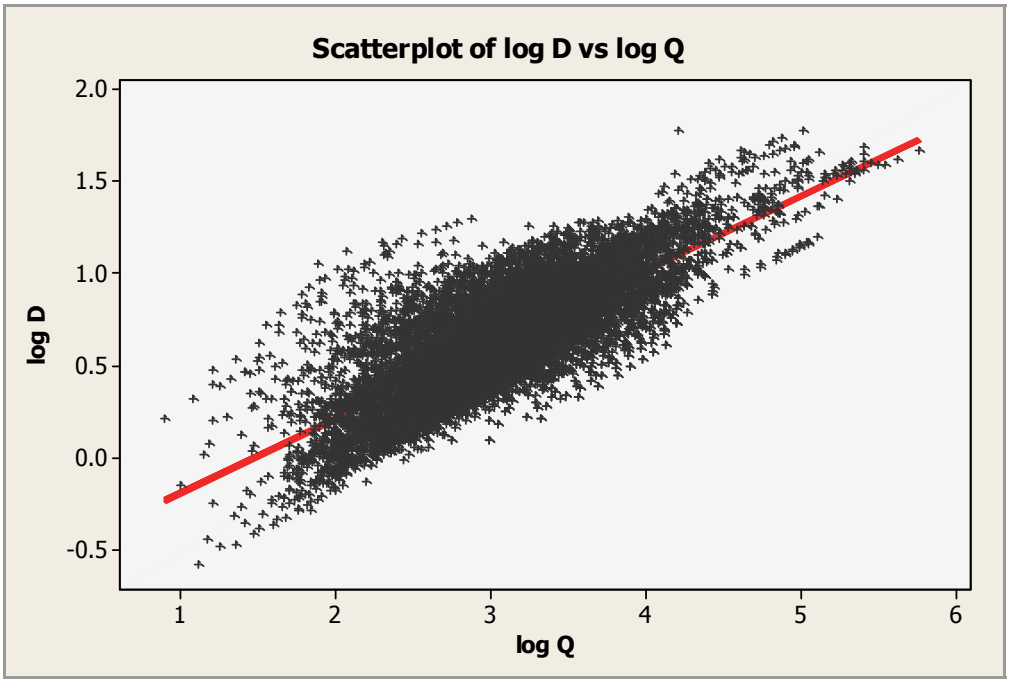

Figure B5-3. Plot of log depth vs. log discharge.

It is recognized that this simple expression does not include physically related parameters, such as channel slope, M ~~m~~anning's resistance coefficient ~~number~~, and so forth. However, an analysis showed that those factors become less significant for out of bank flows than for normal stream flows, and that little of the variance remains to be accounted for by them after Q, which itself implicitly reflects the effects of slope, friction, and other factors to an important degree. This is a matter that could be further addressed in future refinement of this study for individual regions for which data are available. For this national-scale study, the simple approach following Burkham (1977, 78) for relatively high flow rates was deemed most practical.

B.6 Relating the SFHA to Depth

B.6.1 Schematic Stream Cross Section

To convert a change in depth of flow to a change in top-width, a simple geometric relationship was developed using the properties of similar triangles. Figure B6-1 illustrates a typical cross section utilized in the HEC-RAS computer model, with specific features identified on the diagram. The cross section includes the main channel and an asymmetric flood plain, the SFHA. The "main channel" is delimited by the left "bank" and right "bank," marked "BL" and "BR." These banks identify the transition area between the main channel and the floodplain area. The current BFE for the 1% annual chance flood is shown by the middle horizontal line, and the future BFE (BFE_2) is shown by the upper line.

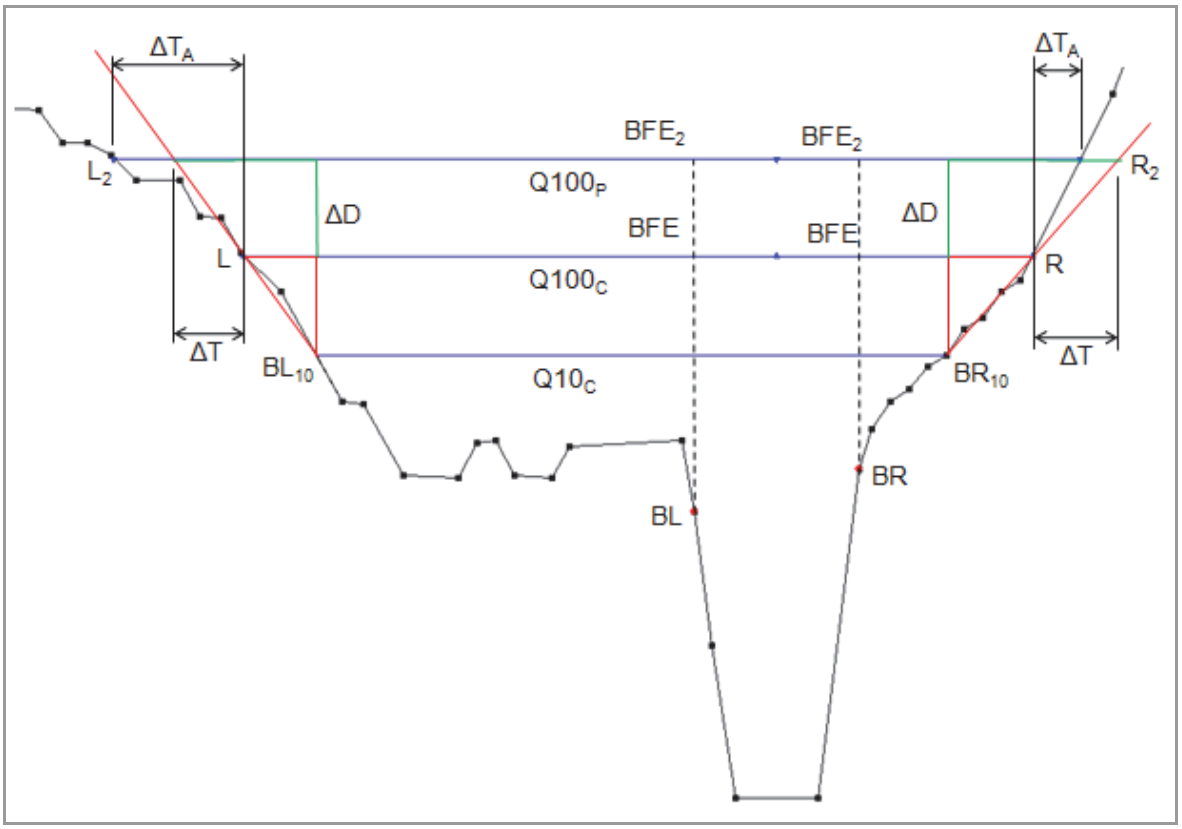

Figure B6-1. Cross section definition sketch.

B.6.2 Floodplain Wedge

The essential idea is to consider the floodplain on each side of the channel to be a simple triangular wedge as illustrated in Figure B6-2. A mean transverse slope would most likely differ on the two sides. It is assumed that small changes in the BFE will, to first order approximation, simply enlarge the SFHA in a proportional way. For example, a wedge extending from the right bank station into the right overbank zone is shown in Figure B6-1 as (BR, BFE, R), where R is the right-hand limit of the AE Zone. Similarly, the left wedge is shown as (BL, BFE, L). The wedges modified by climate change are shown as (BR, BFE_2, R_2), and as (BL, BFE_2, L_2) for the left side.

The left and right wedges are dissimilar triangles, since the total floodplain is asymmetric. However, on one side or the other, the current and future wedges are assumed to be similar triangles, so that the top half-width change from R to R_2, or L to L_2, is in strict proportion to the change from BFE to BFE_2 where the vertical datum is taken to be the chosen “bank” station (not a conventional datum such as NAVD).

B.6.3 Top-Width

The change in top-width needs to be determined to estimate the change in affected population and number of structures, and to determine policies that will be affected by the increase in discharge. FEMA maps the AE zone to include the "main channel" as shown in Figure B6-1. Therefore, estimates made of the changes in top-width that would include the "main channel" would be consistently biased to underestimate the effective change in the SFHA. Using the floodplain wedge, each side is treated appropriately according to its prevailing transverse slope (i.e., automatically excluding the "main channel" top-width).

B.6.4 Bank Stations

In computing water surface profiles utilizing HEC-RAS or a similar one-dimensional computer model, the selected bank stations that divide the "main channel" from the floodplain are not based upon any particular discharge frequency (i.e., 2-year return period). Therefore, utilizing the bank stations from HEC-RAS data files would require searching for detailed information such as that found in FEMA's Mapping Information Platform (MIP). The 10-year return period flows were available for the 2,357 U.S. Geological Survey Stream Gage sites that were used to develop the regression equations both for existing and predicted flows. The adopted procedure was to identify the associated 10-year elevations as a suitable proxy for the bank stations, noting that the only concern is the effective bank elevations – the actual stationing is not of interest. Also of note is that FEMA uses the Probability of Elevation (PELV) curves in conjunction with the Damage by Elevation (DELV) curves to determine flood insurance rates, and both of these curves are functions of the 10- and 100-year flood estimates. Thus Q_{10} and $Q_{1\%}$ are important parameters and are readily available (i.e., from the USGS gage records and from the MIP) for the HEC-RAS computer runs and can be used to determine the depth of flow and thus the SFHA.

B.6.5 Procedure

The procedure used to determine the change in top-width is as follows:

1. Determine the water surface elevations, WSEL, for the existing 10- and 100-year flood events.
2. Determine the water surface elevation for the new 100-year flood due to climate change.
3. Calculate the ΔT assuming the 10-year flood represents the bank stations and elevations using the equations given below. $WSEL_{100c}$ represents the water surface for the future 100-year flood event due to climate change.

Figure B6-2 illustrates the procedure.

$$\Delta T_{10yr\ Right} = \frac{(Right\ WSEL_{100}\ Station - Right\ WSEL_{10}\ Station)\ (WSEL_{100c} - WSEL_{100})}{WSEL_{100} - WSEL_{10}}$$

$$\Delta T_{10yr\ Left} = \frac{(Left\ WSEL_{100}\ Station - Left\ WSEL_{10}\ Station)\ (WSEL_{100c} - WSEL_{100})}{WSEL_{100} - WSEL_{10}}$$

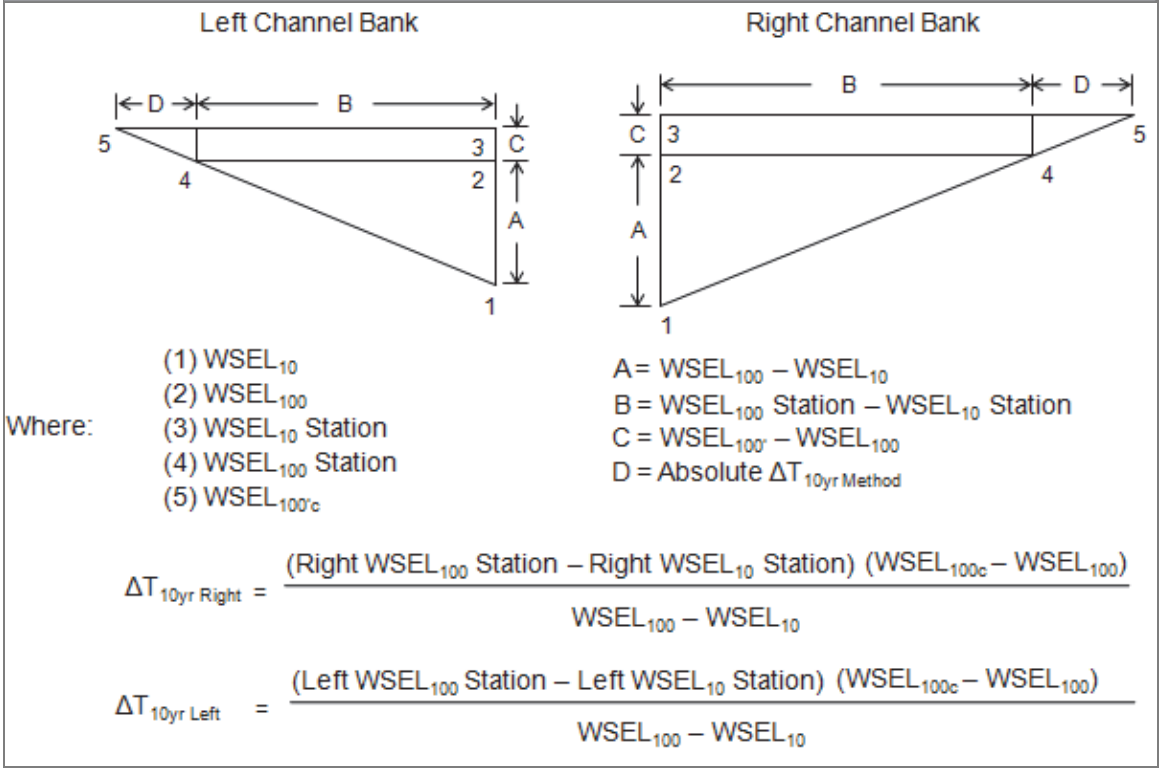

Where:

(1) $WSEL_{10}$
(2) $WSEL_{100}$
(3) $WSEL_{10}$ Station
(4) $WSEL_{100}$ Station
(5) $WSEL_{100'c}$

$A = WSEL_{100} - WSEL_{10}$
$B = WSEL_{100}$ Station $- WSEL_{10}$ Station
$C = WSEL_{100'} - WSEL_{100}$
D = Absolute $\Delta T_{10yr\ Method}$

$$\Delta T_{10yr\ Right} = \frac{(Right\ WSEL_{100}\ Station - Right\ WSEL_{10}\ Station)\ (WSEL_{100c} - WSEL_{100})}{WSEL_{100} - WSEL_{10}}$$

$$\Delta T_{10yr\ Left} = \frac{(Left\ WSEL_{100}\ Station - Left\ WSEL_{10}\ Station)\ (WSEL_{100c} - WSEL_{100})}{WSEL_{100} - WSEL_{10}}$$

Figure B6-2. Determination of the approximate change in top-width given a change in depth.

B.6.6 Validation of the Approximate Method

The FEMA Mapping Information Platform (MIP) was used to select 50 stream reaches having detailed flood studies determined using the computer program HEC-RAS. Cross section data were filtered to eliminate sections with bridges and culverts as well as significant ineffective flow areas. It was determined that these types of cross sections would distort the SFHA. The actual top-width changes computed using the HEC-RAS delineated bank stations were compared with estimated top-width changes from the 10-year proxy bank stations. The results are shown in Figures B6-3 and B6-4.

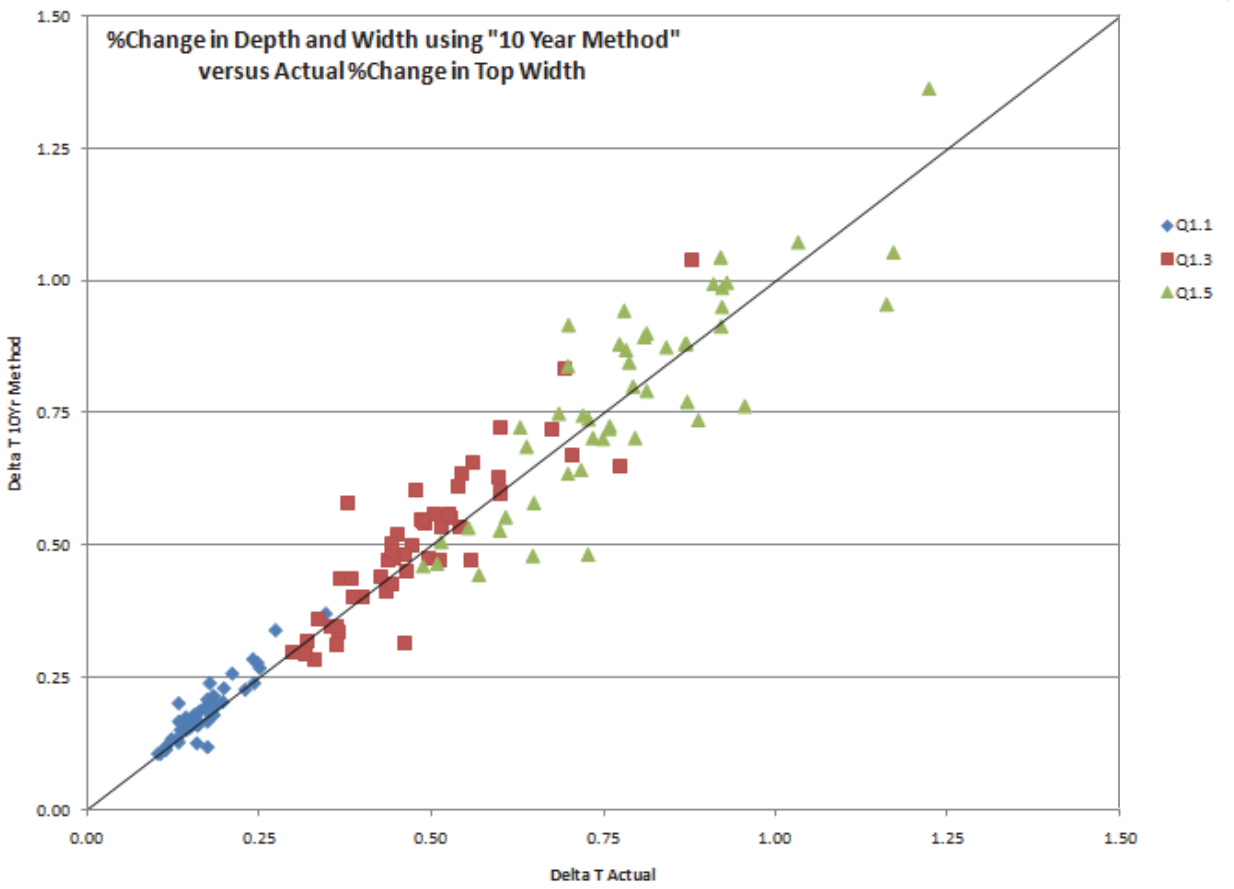

Figure B6-3. Percent change in top-width for 10-year flows versus actual change in top-width using bank stations in HEC-RAS.

In Figure B6-3, the 100-year present estimated flow was increased by 10, 30, and 50 percent in the HEC-RAS models to simulate flows affected by climate change (blue, red, and green respectively).

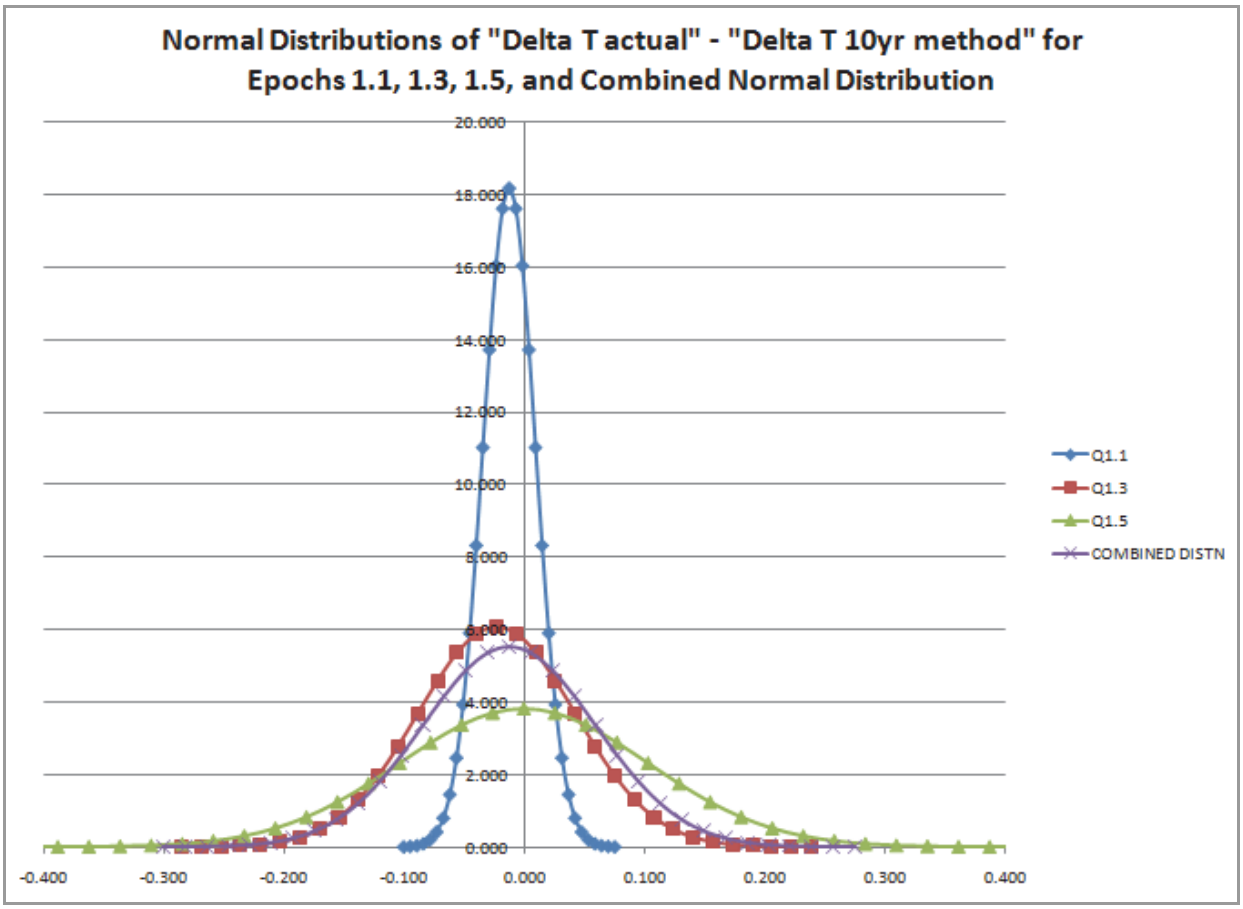

Figure B6-4. Normal distribution of Delta T actual minus Delta T 10-year method.

Figure B6-4 shows the difference Delta T actual minus Delta T 10-year method plotted as a normal distribution. As shown by the figure, there is a slight negative bias in the differences. Since the 10-year bank stations are generally outside the limits of the actual bank stations that are delineated in the HEC-RAS runs, the negative bias would be expected.

Appendix C

Coastal Flood Methodology

Contributing authors

Steve Eberbach

Senanu Agbley

David Divoky

C Coastal Flood Methodology

C.1 Sea Level Rise

Sea level rise (SLR) represents a persistent coastal hazard as well as an exacerbating factor during extreme coastal flooding. The chronic effects of SLR include the widespread, frequent, or permanent inundation of low-lying coastal areas over the long term. For example, it can be assumed that a one foot rise in sea level will generally inundate areas that have an elevation of one foot or less. This is certainly a simplified assumption since the dynamic processes that take place within shoreline systems result in shifts in the location and elevation of coastal landforms. Weiss and Overpeck (2006) and Titus and Wang (2008) are two well-documented sources of information on the potential for permanent inundation as a result of SLR.

This study focuses on the contribution of SLR to particular coastal flooding events. SLR enhances future coastal flood hazards relative to present conditions by increasing storm surge levels, wave heights, and coastal erosion rates. As it controls starting water surface elevations, SLR impacts all coastal inundation processes (including astronomic tide and tsunamis). The first step in accounting for these effects within the study was to subdivide the U.S. coastline into regions of relatively homogeneous rates of SLR. This regionalization provided the simplification needed to study approximately 95,000 miles of coastline throughout the U.S., and provided parameterization needed for Monte Carlo simulations. Thirteen regions were identified. Figures C-1 – C-3 identify Regions 1–10. Regions 11–13 (Alaska, Hawaii, and Puerto Rico, respectively) are not mapped, but are shown in Table C-1. Each region represents areas of similar historical trends in relative (i.e., local) SLR, as determined using data from the U.S. Geological Survey's (USGS) Coastal Vulnerability Index (CVI) (Thieler, et al. 1999–2000) and the National Oceanic and Atmospheric Administration's (NOAA) Center for Operational Oceanographic Products and Services (CO-OPS) (data available online). Within each region, the procedure outlined below was used to develop a range of SLR scenarios through the year 2100 at 20-year intervals, based on 1990 sea level conditions.

The relative sea level change data from the CVI were "derived from the increase (or decrease) in annual mean water elevation over time as measured at tide gauge stations along the coast. Relative sea level change data were obtained for 28 National Ocean Service (NOS) data stations and contoured along the coastline. These rates inherently include global eustatic sea level rise as well as local isostatic or tectonic land motion. Relative sea level change data are an historical record, and

thus show change for only recent time scales (past 50–100 years)." (Hammar-Klose and Thieler, 2001).

In addition to the SLR Regions, Figures C-1 through C-3 also identify the 27 original counties included in the *Evaluation of Erosion Hazards* (Heinz Center, 2000). These counties are highlighted because they served as the basis for the 2000 study, which investigated the impacts of coastal erosion on the National Flood Insurance Program. Significant information such as historical erosion rates and estimated property values were collected for this study and could assist in future evaluation of the impacts of coastal erosion under changing climate or sea level rise conditions.

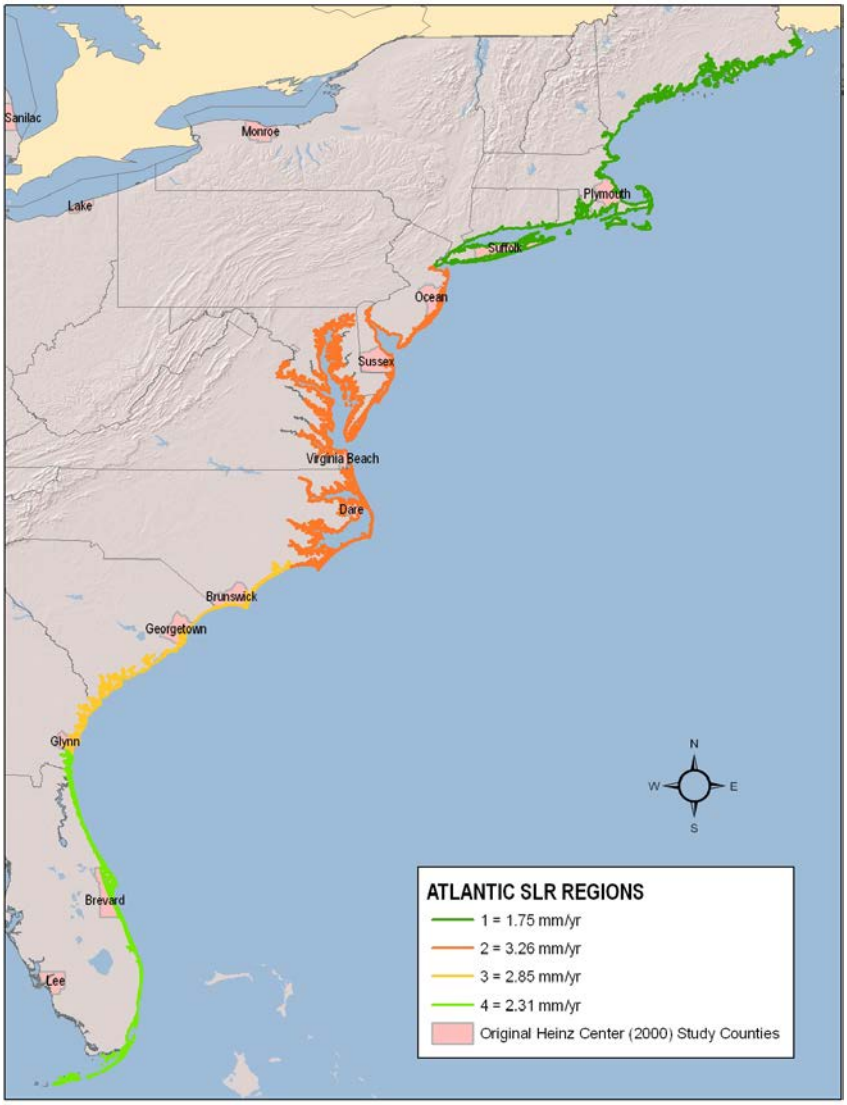

Figure C-1. Four Atlantic sea level rise regions (Regions 1–4) with mean relative SLR rates.

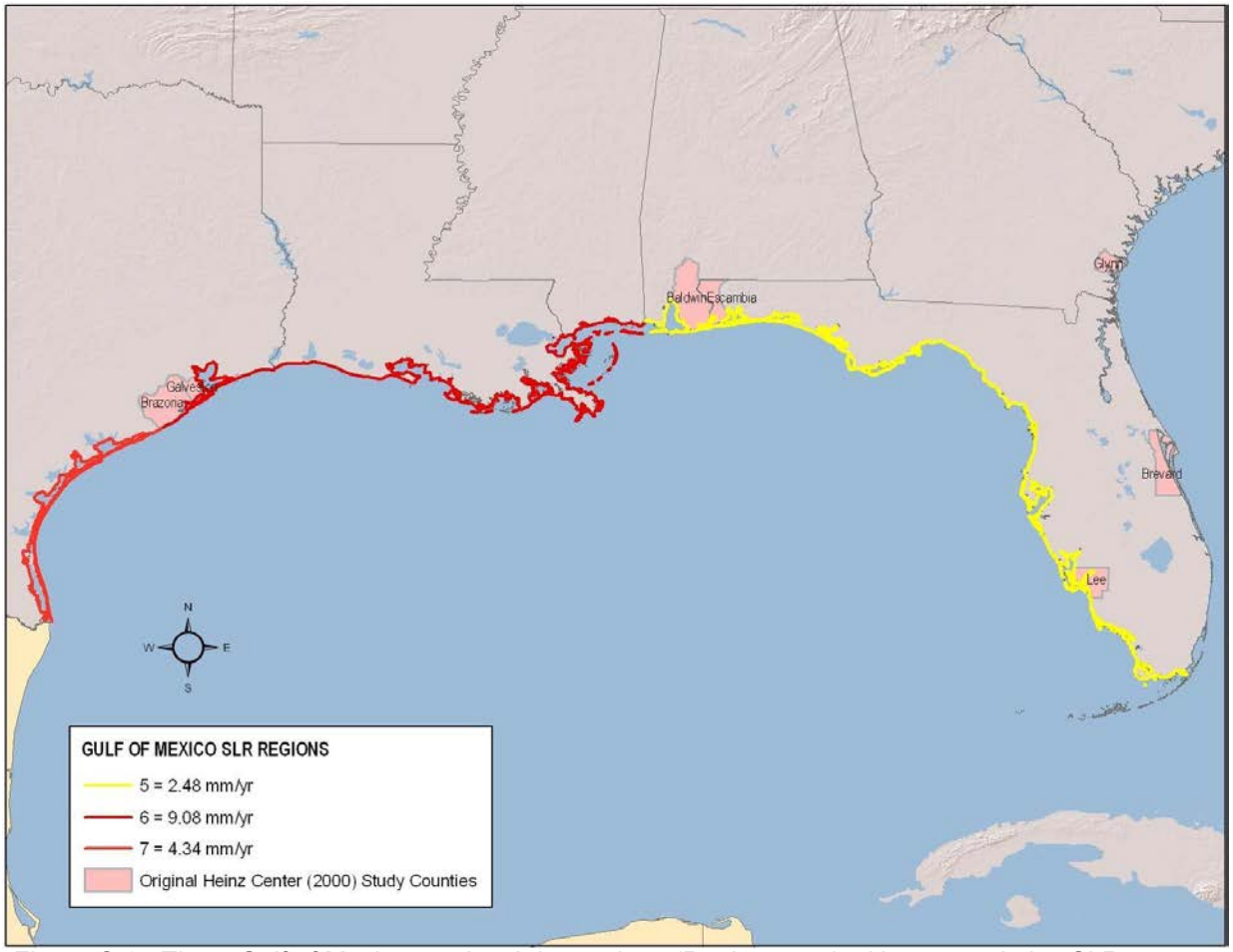

Figure C-2. Three Gulf of Mexico sea level rise regions (Regions 5–7) with mean relative SLR rates.

Figure C-3. Three Pacific sea level rise regions (Regions 8–10) with mean relative SLR rates.

Development of Regional, Historical, Relative SLR Rates

Regional, historical, relative SLR rates for each of the 13 SLR regions are shown in Table C-1. Values were calculated using a regional average approach. Except as noted, each of the 13 regions is reasonably homogeneous in terms of the rate of historical relative SLR. Region 9, for example, is an exception, with varying rates. However, since flood zones in that region are narrow and since the region is not a significant contributor to NFIP flood losses, the adopted CVI-based numbers are used here for consistency. A future localized study of Region 9 should adopt data with improved spatial resolution. The USGS CVI identifies the reach of coastline from the Alabama/Mississippi border west to the southern extent of Brazoria County, Texas, (Region 6) as an area where most relative SLR rates exceed 7.0 mm/yr. The CVI also identifies the section of coastline from the Mattole River, Humboldt County, CA, north to Crescent Bay, Clallam County, WA, (Region 9) as having relative SLR rates less than or equal to 0.0 mm/yr (see comment in Table C-1). Uplifting isostatic changes currently exceed eustatic SLR in this area.

Calculating a Range of Accelerated SLR Rates

The increase in sea level through 2100 is not expected to occur as a linear progression, but rather as a rate that may accelerate through time. The following formula developed by the NRC Marine Board (1987) represents accelerated SLR:

$$E(t) = \left(0.0012 + \left(M / 1000\right)\right)t + bt^2 \qquad \text{(C-1)}$$

Where, E = total relative sea level rise (meters) compared to 1990 sea level
t = time (years) since 1990
M = vertical land movement (mm/yr), where positive values of M are for decreasing land elevation
b = coefficient whose value is chosen to satisfy the requirement that E equals the correct (pre-assigned) eustatic sea level rise value at some time (*t*)

Eustatic sea level rise is represented by (0.0012)t while isostatic changes (i.e., local vertical land movement) is represented by (M/1000)t in Equation (C-1). This equation has been used previously by FEMA to establish projections of future sea level rise. In its report, *Projected Impact of Relative Sea Level Rise on the National Flood Insurance Program* (1991), FEMA assessed the impact of sea level rise on future flooding assuming 0.30m and 0.91m rise scenarios by the year 2100.

Table C-1. Average historical relative SLR rates for each of the 13 SLR regions identified in this study with the range of relative SLR rates extracted from each region.

Region	Extent of Region	Average Relative SLR Rate (mm/yr)	Range of Relative SLR Rates (mm/yr)
1	New England	1.75	0.9 to 2.75
2	Mid-Atlantic extending from NYC, NY south to Bogue Banks, NC	3.26	2.45 to 4.1
3	Bogue Banks, NC south to the Glynn County/Camden County, SC border	2.85	2.45 to 3.15
4	Glynn County/Camden County, SC border south to the Florida Keys	2.31	2.15 to 2.45
5	Florida Keys to Alabama/Mississippi border	2.48	1.8 to 4.4
6	Alabama/Mississippi border west to the southern extent of Brazoria County, TX	9.08	4.49 to 10.9
7	Southern extent of Brazoria County, TX to Mexico/US-TX border	4.34	3.7 to 6.89
8	Mexico/US-CA border north to the Mattole River, Humboldt County, CA	1.40	0.1 to 2.75
9	Mattole River, Humboldt County, CA north to Crescent Bay, Clallam County, WA	-0.99 ****	-1.9 to 0
10	Puget Sound east of Crescent Bay, Clallam County, WA to the Canada/US-WA border	0.57	0.05 to 0.9
11	Alaska	-9.93*	-12.69 to 2.76
13	Puerto Rico	1.34***	1.24 to 1.43

* Average of NOAA SLR rates at Juneau and Anchorage.

** Average of NOAA SLR rates from Nawiliwili, Mokuoloe, Honolulu, Kahului, and Hilo.

*** Average of NOAA SLR rates from San Juan and Magueyes Island.

**** Observed sea level trends available from NOAA tide stations (http://www.tidesandcurrents.noaa.gov/) show that there is substantial variability in historical sea level change rates throughout Region 9. Historical rates are greater than zero in some locations; particularly non-open coast areas. While it is recognized that the average relative SLR rate for Region 9 may not represent local changes as well as the average relative SLR rate does for other regions, it was agreed that CVI data should still be used in order to remain consistent with how values were calculated for SLR regions throughout the continental U.S.

Since the 1991 report was published, the observed global SLR rate from the period 1900–1999 has been revised to 1.7 mm/yr (Bindoff et al., 2007). It should be noted that recent observations have shown the rate of change between 1993 and 2003 was 3.1 mm/yr (Bindoff et al., 2007) and between 2003 and 2008 was 2.5 mm/yr (Cazenave et al., 2009). However, it is unclear whether these increased rates reflect decadal variability or are a long-term trend.

Therefore, the equation used in the 1991 FEMA SLR study is revised to:

$$E(t) = \left(0.0017 + \left(M\ /1000\right)\right)t + \ t^2 \qquad \text{(C-2)}$$

Equation (C-2) allows for the calculation of total relative sea level rise for each SLR region at any time (*t*) using an historical eustatic SLR rate of 1.7 mm/yr. Estimated rates of vertical land movement (*M*) needed for each of the 13 SLR regions are shown in Table C-2. These rates were determined by subtracting the historical rate of eustatic rise (1.7 mm/yr) from the regional relative SLR rates identified in Table C-1.

Table C-2. Summary of regional vertical land movement rates (M); subsidence (+), uplift (-).

Region	Relative SLR Rate (mm/yr)	Rate of Vertical Land Movement, M (mm/yr)
1	1.75	0.05
2	3.26	1.56
3	2.85	1.15
4	2.31	0.61
5	2.48	0.78
6	9.08	7.38
7	4.34	2.64
8	1.40	-0.30
9	-0.99	-2.69
10	0.57	-1.13
11	-9.93	-11.63
12	1.92	0.22
13	1.34	-0.36

Note that the effect of multi-decadal modes of ocean variability on sea level rates used in this study was not investigated. While these effects are not expected to have a notable influence on study results, further investigation is recommended as a future improvement to sea level rise regionalization. Based on the study methodology, detectable effects would result in modifications to rates of vertical land movement listed in Table C-2.

Using Equation (C-2), a range of sea level rise scenarios was determined for each 20-year interval in each of the 13 regions. A given sea level rise scenario for a selected 20-year epoch is ultimately dependent on the sea level condition at the year 2100 that is associated with expected global greenhouse gas emissions.

In order to evaluate Equation (C-2) for the constant *b*, an end condition sea level rise magnitude (*E)* must be chosen for a specified number of years in the future (*t*). The IPCC AR4 estimates that future changes in global sea level will range between 0.18 and 0.59 meters by the year 2100 (Bindoff et al., 2007). Observations indicate that SLR rates may be approaching the upper bounds of IPCC estimates due to potential increases in ice sheet melting (Vermeer and Rahmstorf, 2009). The U.S. Global Change Research Program's *Synthesis and Assessment Product 4.1* states that "thoughtful precaution suggests that a global SLR of 1 meter to the year 2100 should be considered for future planning and policy decisions" (CCSP, 2009). Using temperature increases estimated by the IPCC TAR, Rahmstorf et al. (2007) found that a eustatic rise of 0.5 to 1.4m by 2100 is possible. Figure C-4 summarizes these findings in more detail.

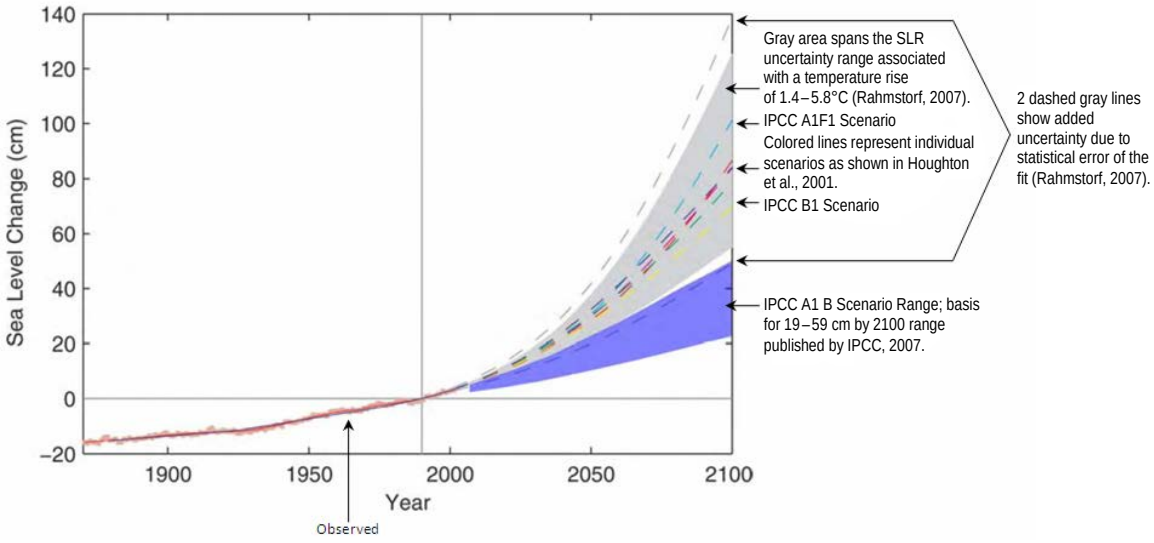

Figure C-4. Summary of observed and projected global sea level rise in centimeters, from Bindoff et al., 2007; Rahmstorf et al., 2007; and Houghton et al., 2001.

Since these publications, Vermeer and Rahmstorf (2009) proposed an extension of the semi-empirical approach developed by Rahmstorf et al. (2007) by incorporating "instantaneous" sea level response (e.g., heat uptake of the mixed surface layer of the ocean). This produced a revised projected range in global sea level rise of 0.81 to 1.79 m (0.79 to 1.9 m using 1 SD) for the period 1990 to 2100 (see Figure C-5 and Table C-3). These most recent projections are used as the basis for the upper bound of eustatic SLR in this study. In addition, note that Pfeffer et al. (2008) found that global sea level rise of 2 meters is possible under certain physical, glaciological

conditions and that other studies documenting even higher projections have been published.

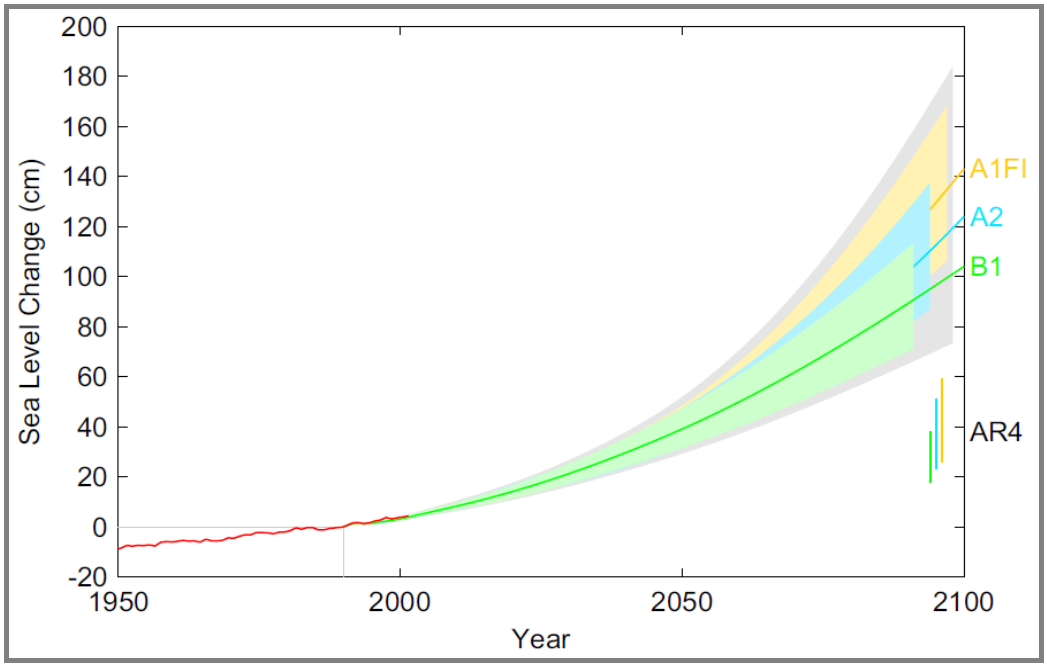

Figure C-5. Vermeer and Rahmstorf (2009) SLR projections from 1990 to 2100, based on IPCC AR4 temperature projections. Note that red line indicates observed SLR.

Table C-3. Summary of eustatic SLR projections compared to 1990 levels as they relate to the six SRES families.

Emissions Scenario	IPCC AR4 Projected SLR Ranges at 2100 (m)	Vermeer and Rahmstorf (2009) Projected SLR Ranges at 2100 (m)*	Vermeer and Rahmstorf (2009) Projected SLR Means at 2100 (m)*
B1	0.18 to 0.38	0.81 to 1.31	1.04
A1T	0.2 to 0.45	0.97 to 1.58	1.24
B2	0.2 to 0.43	0.89 to 1.45	1.14
A1B	0.21 to 0.48	0.97 to 1.56	1.24
A2	0.23 to 0.5	0.98 to 1.55	1.24
A1FI	0.26 to 0.59	1.13 to 1.79	1.43

* Sea level estimates were produced by using Equation (C-2) from Vermeer and Rahmstorf (2009) and 342 temperature scenarios and are shown in this table excluding uncertainty of the statistical fit, which is approximately +/- 7% (1SD).

As mentioned, global SLR scenarios used in this study were based on results from Vermeer and Rahmstorf (2009). With input from representatives from NOAA, FEMA, and the study review panel, it was agreed that these results represent some of the most commonly cited and agreed-upon SLR projections available from the climate science community. It is likely that these projections will be heavily considered in the IPCC Fifth Assessment Report to be finalized in 2014. In addition, results from Vermeer and Rahmstorf (2009) serve the overall study methodology well in that projections are provided for each of the six global greenhouse-gas emissions scenarios (SRES families). Using these eustatic rise estimates, a calculation is performed within the Monte Carlo simulation to determine the b constant that satisfies the specific SLR condition assigned. An example of the b coefficient calculation is shown in Table C-4.

It must be emphasized, however, that the acceleration of sea level rise adopted here is tentative and that, in fact, a very small *deceleration* has been reported in some studies; see, for example, Douglas (1992) and the recent discussion in Houston and Dean (2011). A recent paper by Nicholls et al. (2010) notes that while 0.5 to 2.0 m of eustatic rise during the twenty-first century (consistent with the projections shown in Figure C-5 and the values used in this study) represents a pragmatic range of possibility, it is nevertheless unlikely that values in the upper portion of the range will occur.

Table C-4. Example of calculation performed to determine b constant.

$E(t) = (0.0017 + (M/1000))t + bt^2$
ASSUMPTIONS: • 2100 eustatic SLR = 0.5 m compared to 1990 sea level; therefore, t = 110 yrs • 0.0017m/yr = 1.7mm/yr = historical rate of eustatic SLR at 1990 • Vertical land movement, M = 0 mm/yr; therefore $E(t)$ = 0.5 m
$E(t) = (0.0017)t + bt^2$
$0.5m = [(0.0017m/yr)*110yr] + (b*110yrs^2)$
$0.5m = 0.187m + (12100yrs^2*b)$
$0.313m = (12100yrs^2)*b$
$b = 0.0000258m*yrs^{-2}$

C.2 Storm Frequency

This section documents the procedures by which existing FEMA flood frequency curves were adjusted to account for projected changes in tropical and extra-tropical cyclone frequency.

C.2.1 Tropical Cyclone-Dominated Regions

Coastal flood hazard studies in tropical cyclone-dominated regions are based on the joint probability paradigm, that is, the maximum storm surge, η, produced by a tropical cyclone can be modeled as a function of a vector of storm parameters, $x = [x_1, ..., x_D]$:

$$\eta = \varphi(x), \tag{C-3}$$

where $\varphi(.)$ is a numerical model that operates on x. The storm parameters are, typically: the central pressure depression at landfall (a measure of the storm intensity), radius to maximum winds (a measure of the storm size), storm heading, forward speed, and the shoreline crossing point. The probability distribution of flood levels, $\Pr\{\eta_x > \eta\}$, is simply the integral of the joint probability distribution of the storm parameters over the storm sample space:

$$\Pr\{\eta_x > \eta\} = \int ... \int_{x \in X} f_X(x) H(\eta_x > \eta)\, dx, \tag{C-4}$$

where $f_X(.)$ is the joint probability distribution of the storm parameters, and $H(.)$ is a step function whose value is one or zero depending on the value of the argument (see Resio et al., 2010 and Toro et al., 2010b). The integral represents the probability that a storm will produce a surge elevation exceeding some arbitrary level, η. The rate at which this elevation is exceeded per year, the annual exceedance frequency distribution, $F(\eta)$, is computed as the product of the rate of storm occurrence per year, λ, and the joint probability distribution:

$$F(\eta) = \lambda \Pr\{\eta_x > \eta\} = \lambda \int ... \int_{x \in X} f_X(x) H(\eta_x > \eta)\, dx. \tag{C-5}$$

It is evident from Equation (C-5) that the effect of a change in storm frequency on $F(\eta)$ is independent of the detailed storm surge computations required to evaluate the multiple integral (see Resio et al., 2010 and Toro et al., 2010). Hence, given an existing storm surge frequency distribution and a relative change in storm frequency as a result of climate change, the storm surge frequency distribution in the new climate can be computed as follows:

$$F_2(\eta) = \frac{\lambda_2}{\lambda_1} F_1(\eta). \quad \text{(C-6)}$$

Subscript [1] denotes existing climate conditions and [2] denotes projected climate conditions. This procedure does not require any new hydrodynamic considerations. For example, consider that a Hurricane Katrina-type event produces a storm surge surface, $\eta_{x,y}$. This hydrodynamic response remains the same regardless of whether the event occurs once every 100 years or once every 400 years, provided all other parameters of the event remained the same. Since the return period (T) is approximately the inverse of the exceedance frequency distribution (i.e., $T = 1/F(\eta)$) Equation (C-6) can also be written as:

$$T_2 = \frac{\lambda_1}{\lambda_2} T_1. \quad \text{(C-7)}$$

Figure C-6 below illustrates the procedure for a 25% increment in storm frequency from year 2000 to year 2100 for some arbitrary flood frequency curve. In this hypothetical example, the 50-year (i.e., 0.02 exceedance probability) storm surge elevation is 14.35 feet. If the storm frequency were to increase by 25% at year 2100, then the average recurrence period for the same storm surge elevation would become 40 years (i.e., 0.02*1.25 exceedance probability). Similarly, as shown in Table C-5, the storm surge elevations having 100- and 500-year return periods in the new climate would have 80- and 400-year return periods.

Table C-5. Example of changes in recurrence intervals for a 25% increment in storm activity.

Storm Surge Elevation (ft)	Year 2000 Return Period (yrs)	Year 2100 Return Period (yrs)
14.35	50	40
16.73	100	80
21.63	500	400

As shown in Figure C-6, the existing storm surge elevations and the new return periods fully describe a new flood frequency curve that reflects the change in storm frequency. Storm surge elevations for other return periods in the new climate can either be read off the graph or found by log-linear interpolation:

$$y' = y_0 + (y_1 - y_0)\left[(\log x - \log x_0)/(\log x_1 - \log x_0)\right] \quad \text{(C-8)}$$

where $[y_0, y_1]$ is a pair of known surge elevations having return periods $[x_0, x_1]$, and x is the return period for which we want to find the corresponding surge elevation y'.

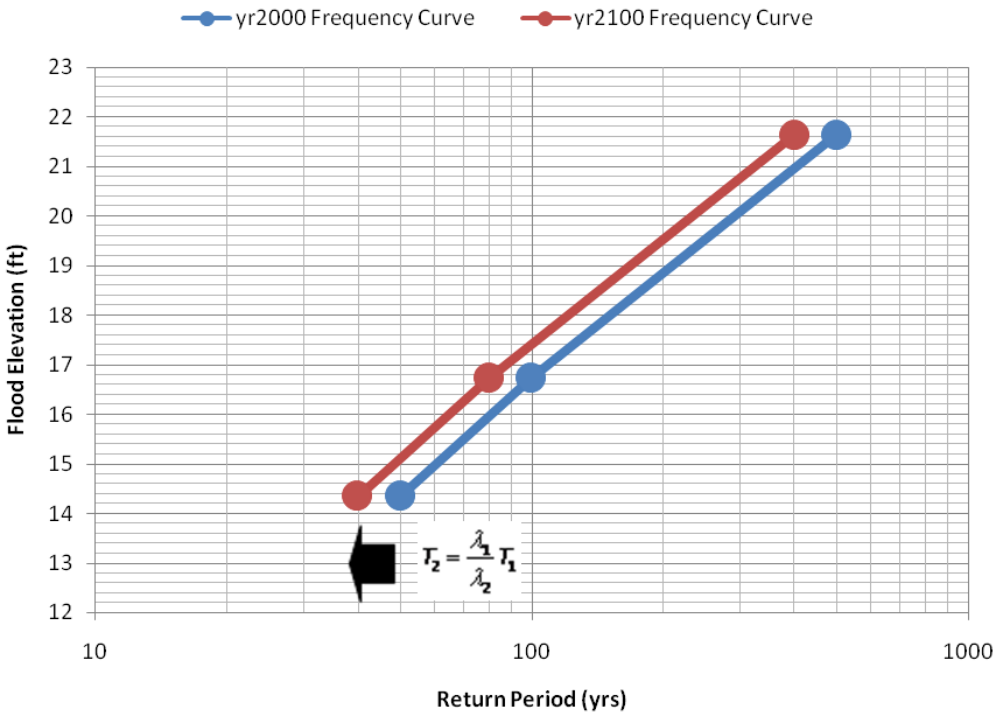

Figure C-6. Schematic illustrating the procedure for adjusting existing flood frequency curves for a change in storm frequency.

C.2.2 Extra-tropical Cyclone-Dominated Regions

Coastal flood hazard studies in extra-tropical cyclone-dominated regions follow parametric distribution fitting methods based on extreme value theory. The same results arrived at in the previous section apply here also; that is, annual flood level exceedance frequencies are directly proportional to the annual storm frequency.

C.3 Storm Intensity

This section documents the procedures by which existing FEMA flood frequency curves were adjusted to account for projected changes in tropical and extra-tropical cyclone intensity.

C.3.1 Tropical Cyclone-Dominated Regions

Figure C-7 from the HMTAP Mississippi study (Toro et al., 2010a), shows the pronounced linearity of storm surge versus the central pressure depression. This linearity is the basis for the simplified assumption relating changes in storm intensity, ΔP, to changes in storm surge elevations, η, in coastal regions where the dominant storm system influencing flood hazards are tropical cyclones. It is recognized that the assumption of linearity may fail at very high storm intensities owing to changes is ocean surface wave roughness and effective wind stress. However, the variation tends to remain linear in the range of intensities of interest for flood insurance studies. The surge-intensity relationship is of the form:

$$\eta = a + b\Delta P, \tag{C-9}$$

hence

$$\eta_2 = \eta_1 \frac{\Delta P_2}{\Delta P_1}, \text{ if } a = 0 \tag{C-10}$$

Subscript [1] denotes existing climate conditions and [2] denotes projected climate conditions. Figure C-8 illustrates the procedure for a 15% increment in storm intensity from year 2000 to year 2100 for some arbitrary flood frequency curve (details shown in Table C-6). Note that the example is for illustration only, and does not represent actual study values.

Table C-6. Changes in storm surge elevations for a 15% increment in storm intensity.

Return Period (yrs)	Frequency Adjusted Levels (ft)	Intensity Adjusted Levels (ft)
50	15.15	17.42
100	17.35	19.95
500	22.15	25.47

Although the variation is assumed to be linear, it does not necessarily follow that a given percentage change in ΔP causes an equal percentage change in surge, η, owing to the fact that the curves do not necessarily intercept the $y-$axis at zero. In order to estimate the error, ε, involved in the simplest assumption (which is that the relative change in η is the same as the relative change in ΔP), several curves (representing each major cluster of lines) from the figure were selected for a simple evaluation. The fits were made by fitting the intersections of the curves with the 38 and 98 mb lines, giving the values for a and b as shown in Table C-7.

Table C-7. Error in the relative change incurred by ignoring the intercept.

Curve	a	b	ε (%)
1	1.66	0.18	+12
2	-0.68	0.16	-5
3	-1.50	0.13	-15
4	-0.89	0.06	-21

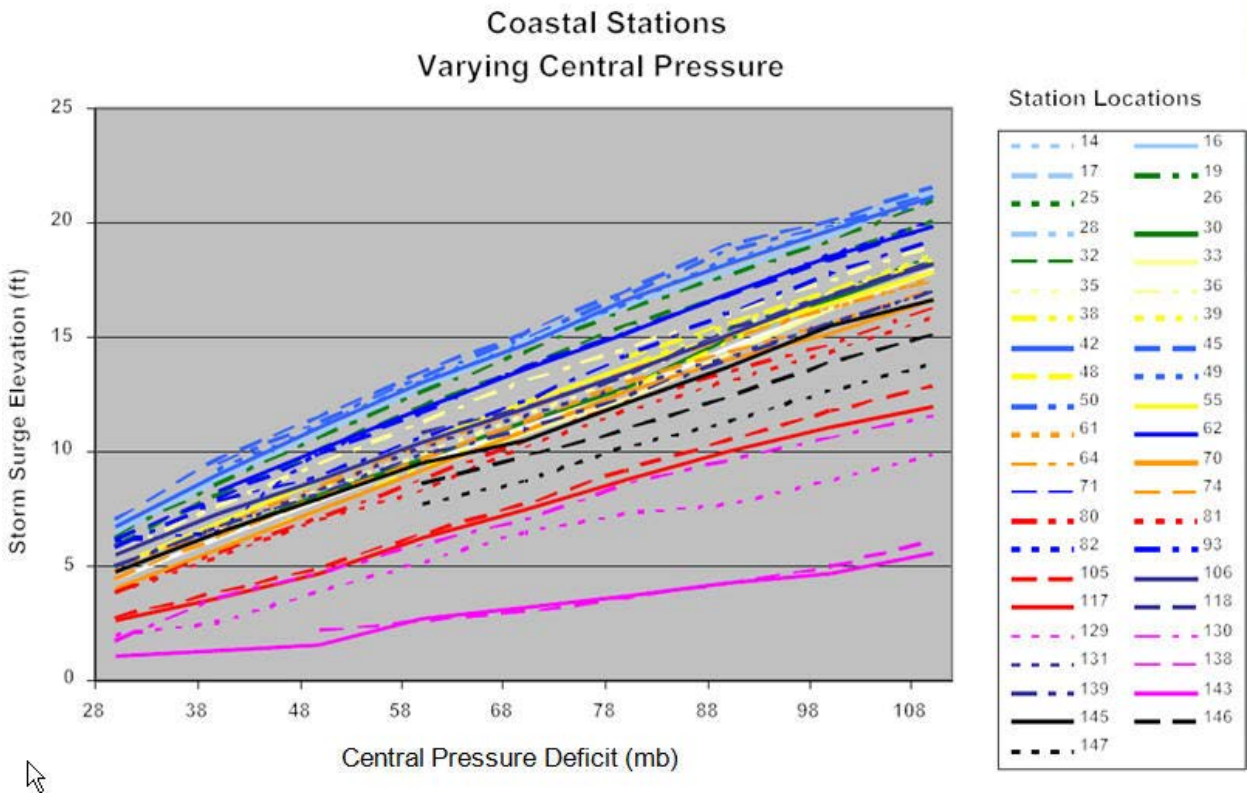

Figure C-7. Variation of storm surge elevations with the central pressure anomaly at different locations in Mississippi (from FEMA's HMTAP post-Katrina study).

The parameter a is the surge estimate associated with a zero strength storm, and as such would correspond to mean sea level for storm surge simulations conducted without tidal forcing. However, as seen in the table, the values are both positive and negative. For simplicity, let ΔP be represented as I, for intensity, and η by *S* for surge, and imagine that I changes from I_1 to I_2, for a relative change equal to R_I given by $(I_2 - I_1)/I_1$. The corresponding relative change of surge S, R_S, will be dS/S_I given by

$$R_S = \frac{dS}{S_I} = \frac{S_2 - S_1}{S_1} = \frac{a + bI_2 - (a + bI_1)}{a + bI_1} = \frac{b(I_2 - I_1)}{a + bI_1} \qquad \text{(C-11)}$$

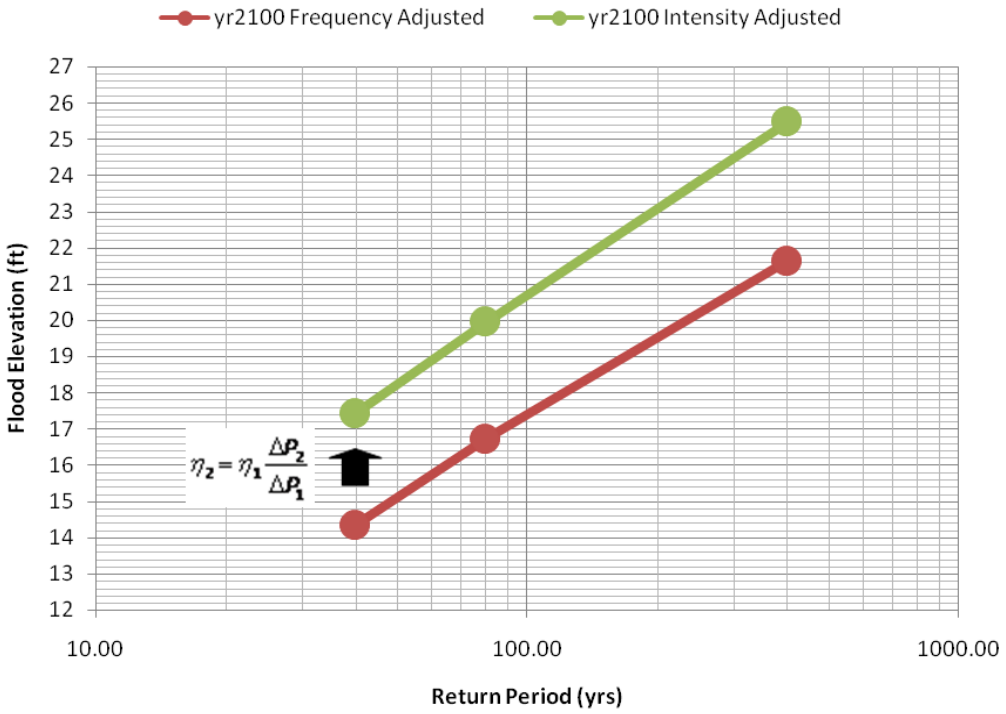

Figure C-8. Schematic illustrating the procedure for adjusting existing flood frequency curves for a change in storm intensity.

Imagine further that S is approximated by Z, obtained by neglecting a. Then a given relative change of I will equal the relative change in Z, R_Z, being just

$$R_Z = \frac{dZ}{Z_I} = \frac{Z_2 - Z_1}{Z_1} = \frac{bI_2 - bI_1}{bI_1} = \frac{dI_1}{I_1}. \qquad \text{(C-12)}$$

The relative change of Z can be compared with the relative change in S by taking the ratio of the right-most sides of these two equations

$$\frac{R_Z}{R_S} = \frac{dI}{I_1}\frac{a + bI_1}{bdI} = 1 + \frac{a}{bI_1} \equiv 1 + \varepsilon, \qquad \text{(C-13)}$$

where ε can be considered the error in the relative change incurred by ignoring a. To estimate this error, a representative value of I is needed, characteristic of 100-year surge conditions. As a first guess, imagine that a value of 78 mb is chosen. This choice, with the estimated values of a and b, gives the final column shown in the table above. Note that the indicated errors are not the errors in surge height, but are only the percentage errors in the estimated relative change owing to a change in storm intensity. In other words, if the relative change in surge was 10%, a 20% error

in this would mean an estimated surge change of 12% (or of 8%) rather than 10%. Note that some of the curves will have positive and some will have negative error terms, so that the approximation does not necessarily imply a systematic error. Given new storm surge elevations, the accompanying wave height, H , and wave crest elevation above the stillwater surge level, H_C, are related by :

$$H_C = 0.7\left(H\right) = (0.7(0.78d)) = 0.546d = 0.546\eta\,, \tag{C-14}$$

In this expression, 0.78 is the breaking factor and *d* is the water depth which, at the shoreline, is equal to the surge elevation. The expression assumes that the wave crest accounts for 70% of the wave height. The wave crest elevation above the stillwater surge is mapped as the BFE in FEMA's flood maps and is sensitive to local wave damping by vegetation and blockage by structures. As a simple assumption in this study, the wave crest addition has been taken to be a fixed fraction of the flood depth, and therefore to remain in geometric similitude across the coastal SFHA. See the additional discussion in Section C.4.

C.3.2 Extra-tropical Cyclone-Dominated Regions

In coastal regions where extra-tropical cyclones are the dominant storm system affecting the coastline, the primary flood hazard may not be wind and pressure driven storm surge, but may equally be due to processes such as wave runup and overtopping. The surge component is assumed to behave as for tropical storm zone, with elevations proportional to wind speed squared (ΔP in the earlier hurricane discussion is roughly proportional to the square of wind speed). The wave fields developed by extra-tropical cyclones tend to be fully developed due to the long storm durations and large wind fetches that characterize these systems. The Pierson-Moskowitz wave spectrum is the model wave spectrum commonly adopted for fully developed seas. Given this parameterization for fully developed seas, the significant wave height (H) is proportional to the wind speed (U) squared (Liang, 1998):

$$H \propto U^2 \tag{C-15}$$

so that

$$H_2/H_1 = U_2^{\,2}/U_1^{\,2} \tag{C-16}$$

Additionally, the significant wave height is proportional to the square of the peak wave period and hence to the deepwater wavelength (L) (Liang, 1998):

$$H \propto T^2 \tag{C-17}$$

so that

$$H_2/H_1 = T_2^2/T_1^2 = L_2/L_1\,, \tag{C-18}$$

since $L = gT^2/2\pi$. Substitution of these relationships into a representative wave runup (R) formulation (TAW, 2002) gives

$$R = \gamma \frac{m}{\sqrt{H/L}} H\,, \tag{C-19}$$

where γ subsumes several coefficients, including roughness, and m represents the slope of the profile, respectively. This yields a simple transfer function that relates a change in storm intensity (wind speed in this case) to a change in wave runup elevation:

$$R_2 = R_1 \frac{H_2}{H_1} = R_1 \frac{U_2^{\,2}}{U_1^{\,2}}. \tag{C-20}$$

Given a flood frequency relationship based on wave runup elevations and a relative change in wind speeds between two climate conditions, the procedure for adjustment follows the approach illustrated in Figure C-8. Storm surge in extratropical zones is assumed to vary in the same manner.

Reviewing this and the prior section dealing with tropical storms, one sees that there is no essential distinction between them, with both surge and runup being estimated directly from projected changes in storm intensity (wind speed squared or central pressure depression). Consequently, a single rule applies to all areas without the need to distinguish between them.

C.4 Inland Extent of Flooding

The previous sections document procedures by which existing FEMA flood frequency curves are adjusted to account for projected changes in sea level, storm frequency, and storm intensity. These flood frequency relationships exist only for locations on the shoreline; however, it is necessary to also quantify the potential effect of climate change on the inland extent of flooding. The scale of the current project precludes an attempt to quantify the potential effects of climate change on floodplain extents via detailed, site-specific hydrodynamic simulations. Following the FEMA sea level rise study conducted in 1991, simple geometric arguments were adopted to qualify the potential impact of projected climate change on the inland extents of flooding. Figure C-9 provides an illustration of this approach. It is assumed that the average slope

over the coastal SFHA does not change, so that if the storm surge at the coast increases from y to z as shown in the figure, then the inland extent of flooding will change from a to b. This assumption of proportionality exactly mirrors the assumption made for riverine overbank flooding. In the coastal case, there is an additional flood component: the wave crest elevation above the surge as discussed with Equation (C-14). This additional elevation is taken to be a fixed fraction (about 55%) of the surge flood depth (surge level minus ground level). Consequently, the wave component does not enlarge the SFHA since the surge flood depth goes to zero at the inland limit of the SFHA.

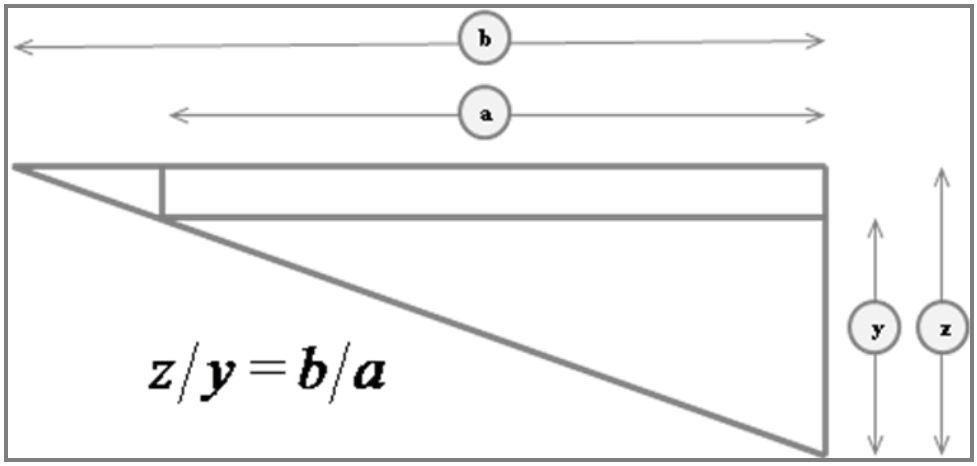

Figure C-9. Schematic showing the characterization of the landward extents of flooding (b and a) based on simple rules of proportionality with coastal flood levels y and z.

The scope of the study precludes direct modeling of the influence of local landforms and morphology on storm surge potential. Based on the study framework however, the use of existing FIS data indirectly captures typical countywide characteristics such as sheltered vs. open coast landforms, which influence storm surge hazard potential. Localized characteristics not already reflected in existing flood elevations are considered to have a minor effect on aggregated nationwide estimates of percent change in coastal floodplain area or flood elevations.

C.5 Monte Carlo Simulation Procedure

This section documents the Monte Carlo simulation procedure used to produce probabilistic estimates of the potential impact of climate change on coastal flood elevations and floodplain extents. The procedure incorporates the uncertainty in the various input parameters into the output so that a range of probable outcomes and the corresponding likelihoods are identified.

Climate change impacts on flood elevations and floodplain extents were computed, for several hundred thousand simulations, using the procedures described in the previous sections. Probabilistic estimates were obtained by randomly sampling inputs for each calculation from probability distributions assumed for each of the climate change variables listed below:

- global sea level,
- storm frequency, and
- storm intensity.

The outputs are aggregated for each coastal county at the end of five 20-year time periods starting from year 2020. Figure C-10 illustrates the Monte Carlo simulation procedure. Each climate change variable was assumed to possess a Gaussian distribution with the means and variances indicated in the literature section. Since projections for climate change variables were available for only the end of year 2100, projections (y') for all other epochs (x) were linearly interpolated based on years 2000 (x_0) and 2100 (x_1), values (y_0) and (y_1) respectively, as follows:

$$y' = y_0 + (y_1 - y_0)\left[(x - x_0)/(x_1 - x_0)\right]. \quad \text{(C-21)}$$

The existing flood frequency data for each coastal county were sourced from Flood Insurance Study (FIS) texts available from the FEMA Map Service Center. The flood frequency curve for each county was characterized by adopting the median values of the 10-, 50-, 100-, and 500-year return periods. Each FIS text reported values for at least two of these return periods. Wherever values for certain return periods were missing, the data were filled in by log-linear interpolation as illustrated in Equation (C-8). Figure C-11 shows example results of the simulations for a typical site. .

The Monte Carlo simulation procedure is summarized in the pseudo-code below:

Initialize Data Arrays:
    Read climate change projection data for emission scenarios [B1, A1B, A2]
    Read flood frequency data for U.S. coastal counties
Counties: Loop over U.S. coastal counties [J=1, …, numCounties]
    Epochs: Loop over epochs [K=1, …, numEpochs]
        Samples: Loop over maximum number of samples [L=1, …, numSamples]
            Randomly sample emission scenario [M=B1, A1B, A2]
            Go to [100] or [200] depending on storm climate classification for [J]
            [100]: Approach for tropical cyclone-dominated regions
                Add Gaussian variation to sea level projection for [J, K, M]
                Adjust frequency curve for projected sea level rise

Add Gaussian variation to frequency projection for [K, M]
Adjust frequency curve for change in storm frequency
Add Gaussian variation to intensity projection for [K, M]
Adjust frequency curve for change in storm intensity
Compute % changes in BFE, FHA, and FHP

[200]: Approach for extra-tropical cyclone-dominated regions
Add Gaussian variation to sea level projection for [J, K, M]
Adjust frequency curve for projected sea level rise
Add Gaussian variation to frequency projection for [K, M]
Adjust frequency curve for change in storm frequency
Add Gaussian variation to intensity projection for [K, M]
Adjust frequency curve for change in storm intensity
Compute % changes in BFE, FHA, and FHP

Samples: End of loop
Sort data arrays for % changes in BFE, FHA, and FHP
Find 10^{th}, 25^{th}, 50^{th}, 75^{th}, and 90^{th} percentiles

Epochs: End of loop

Counties: End of loop

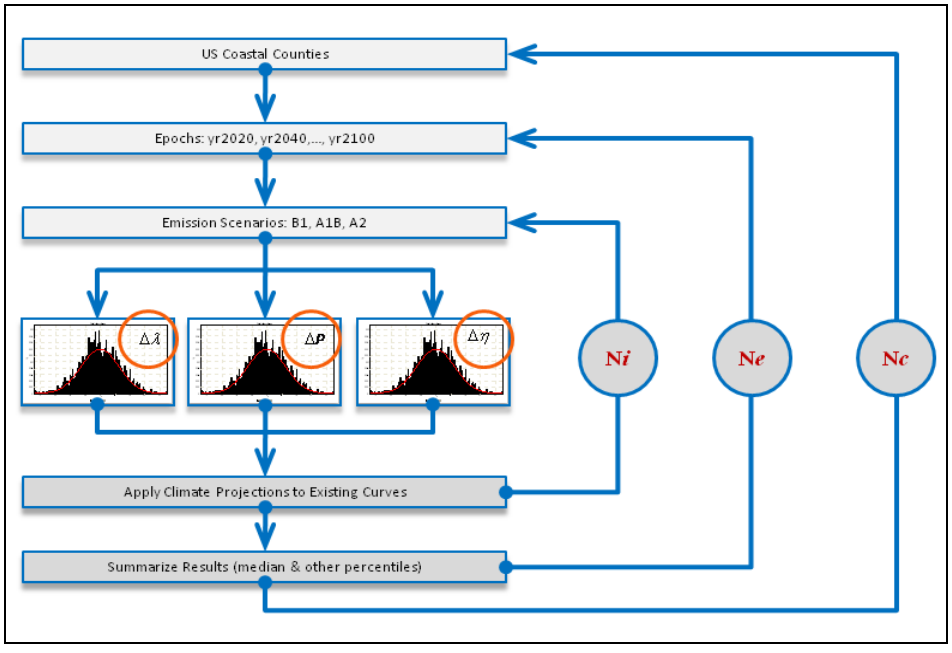

Figure C-10. Schematic of the Monte Carlo simulation procedure.

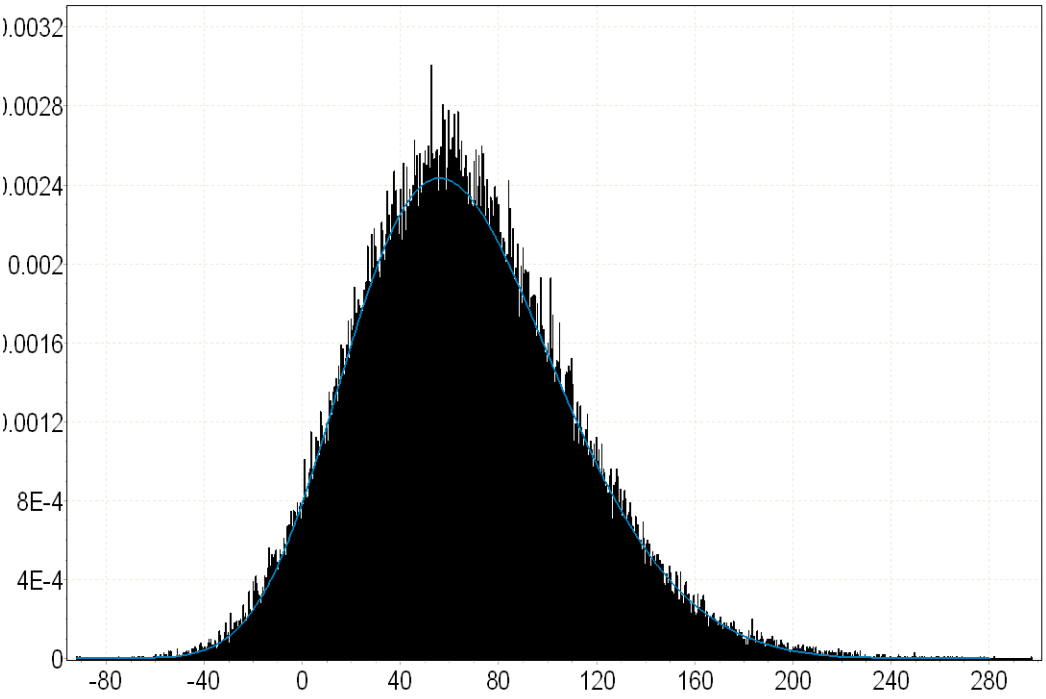

Figure C-11. Percentage changes in the BFE for a typical site at year 2100.

Appendix D

Demographic Analysis

Contributing authors

Ray Yost

Kevin Coulton

Susan Phelps

D Demographic Analysis

D.1 Notation Summary

ΔFPA_{rel} – Relative percent change in floodplain area over current conditions

ΔHP_{rel} – Relative percent change in FHF (flood hazard factor) over current conditions

D.2 Estimating Current SFHA and Affected Population

Much of the demographic analysis used in this study was based on earlier work performed by AECOM for FEMA for both riverine and coastal areas. Among the primary demographic data sources used in that work were U.S. Census Block Group data from the 2000 Census, USGS Hydrologic Unit Code (HUC) 12 watershed data rolled up to Level 8, (July 2009), and FEMA participating community data through July 2009. The Census Block Groups, as shown in Figure D-1, are irregular in size and shape, but have a relatively even distribution of population. Figure D-2 shows national coverage of the HUC 8 watersheds.

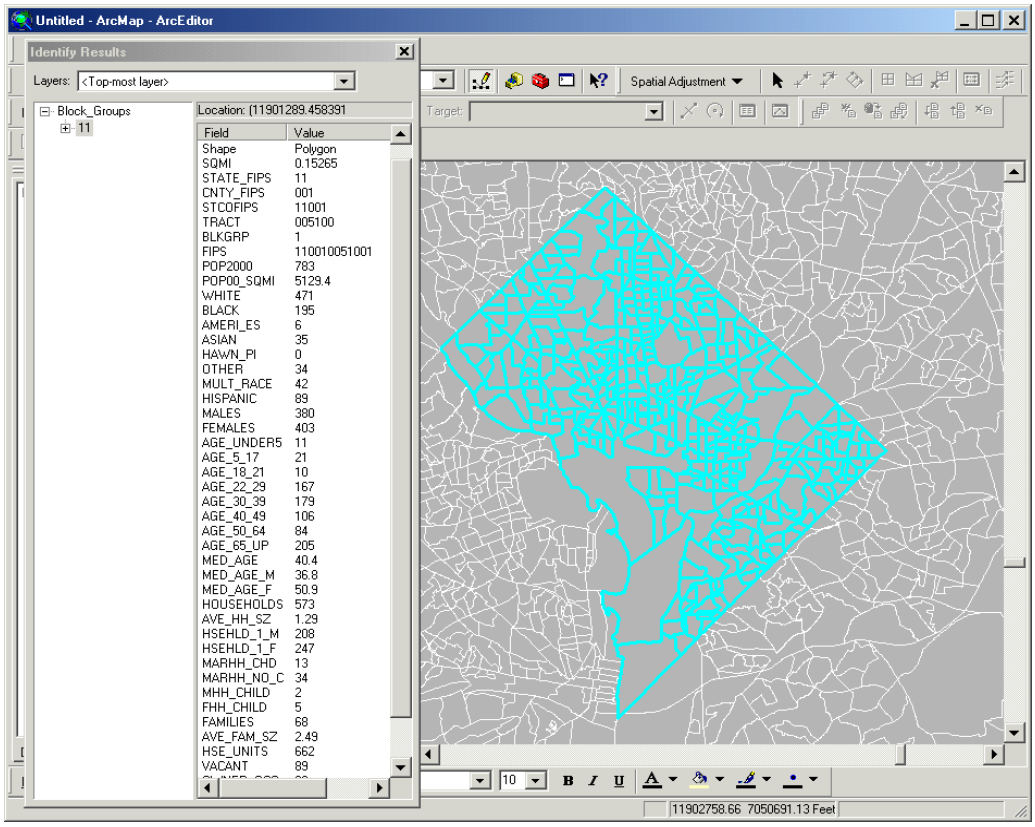

Figure D-1. Illustration of typical local Census Block coverage.

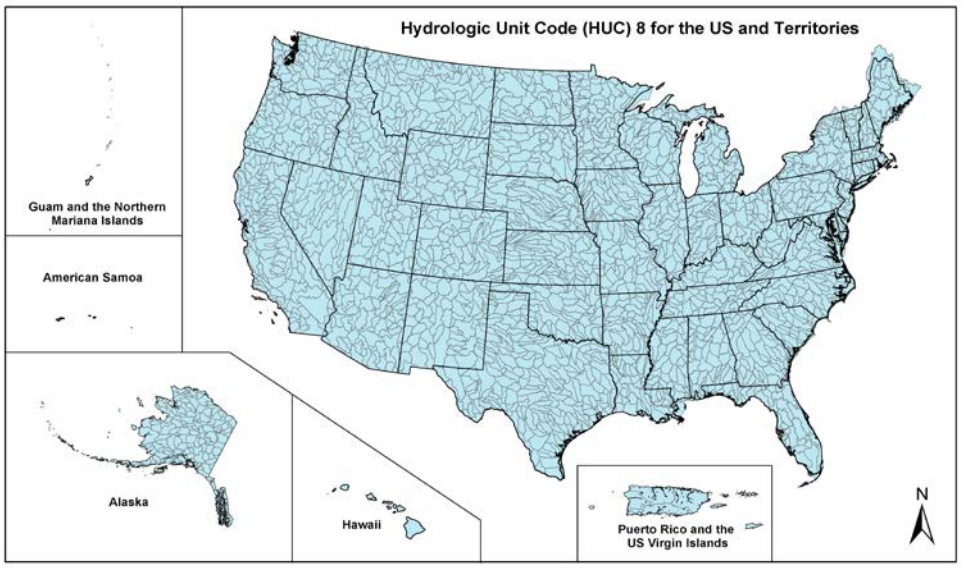

Figure D-2. Illustration of HUC 8 watershed coverage.

FEMA data sources included the National Flood Hazard Layer (NFHL) through April 2009, Q3 data that consists of flood zones only, as digitized from flood insurance rate maps, and legacy data licensed from First American. Illustrative examples of coverage of these three sources are shown in Figures D-3 through D-5. Additional related information was obtained from the USGS 100K National Hydrography Dataset for streams.

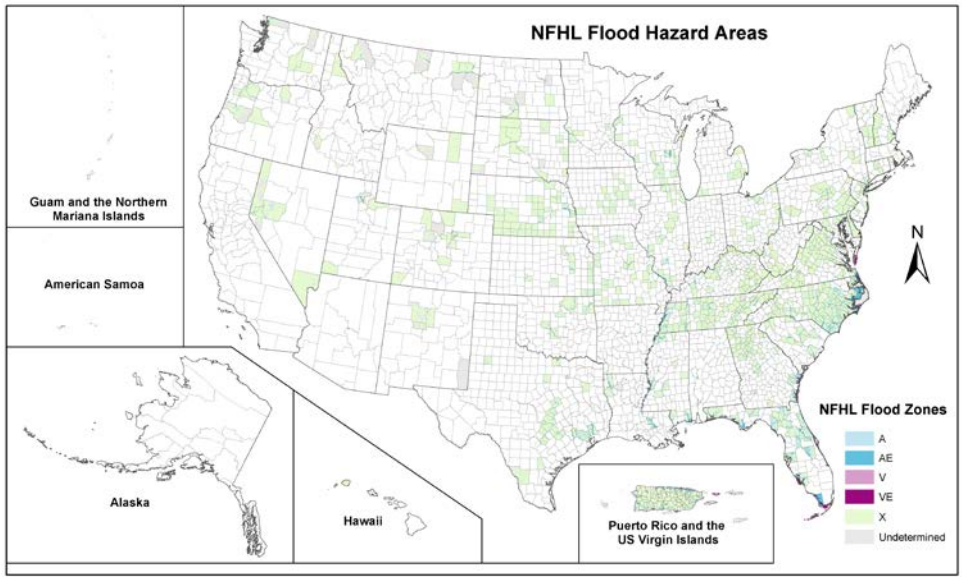

Figure D-3. Illustration of FEMA's NFHL coverage.

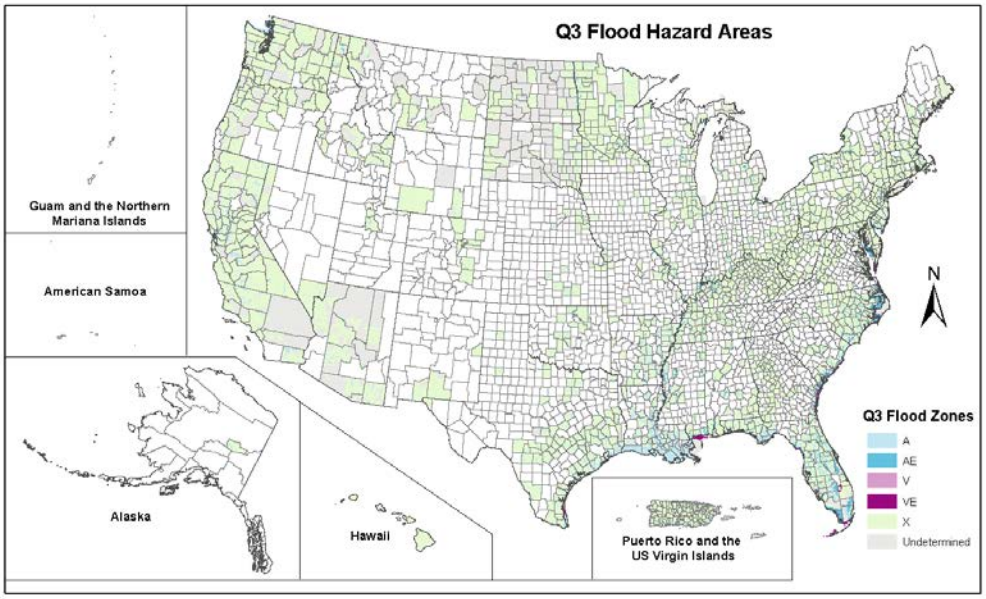

Figure D-4. Illustration of FEMA's Q3 coverage from digitized flood maps.

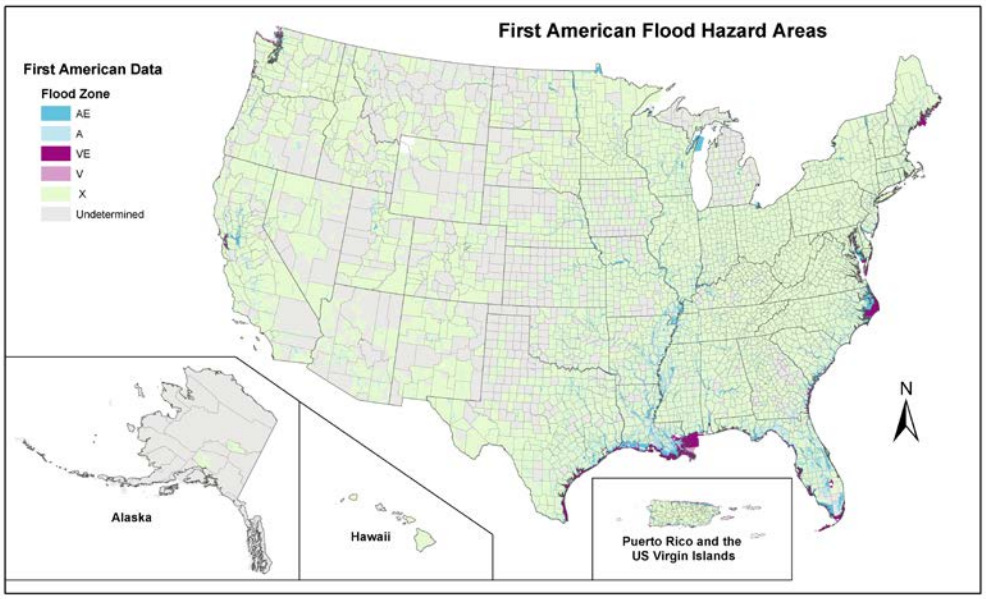

Figure D-5. Illustration flood hazard zones from First American data.

Information regarding flood insurance policies and loss distributions was obtained from Federal Insurance Administration 2008 policy data, single-loss claims data (cumulative from 1978–2008), 2007 Repetitive Loss Claims data, and Repetitive Loss Properties data (derived from 2007 Repetitive Loss Claims). Figure D-6 shows the corresponding national distributions of policies and losses.

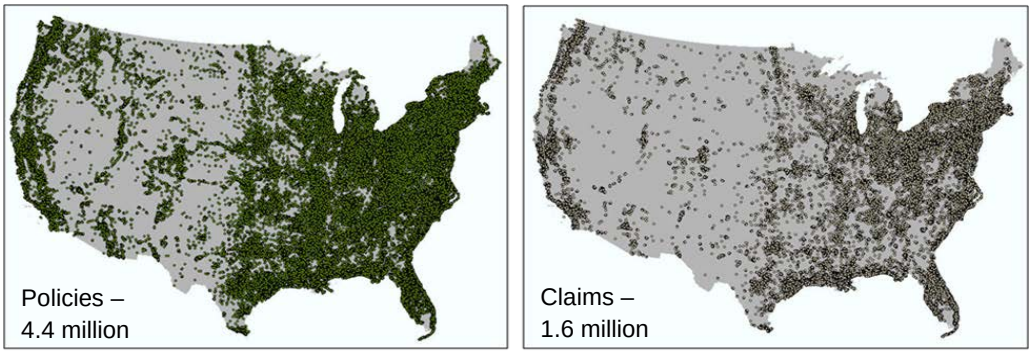

Figure D-6. Distributions of flood insurance policies and cumulative claims at 2008.

It might be noted that these distributions mimic the distributions of available USGS stream gage data discussed in Appendix B, both following population patterns. Consequently, although hydrologic data are less dense in some western areas, those are also the areas for which exposure is proportionally less.

Data for population and housing units (current) were taken from 2009 projections provided by Spatial Insights, Inc., and Applied Geographic Solutions, Inc. (AGS). This information was used in conjunction with flood zone data to estimate current population and housing units within the 1% floodplain. Population projections through 2019 (not considering the longer term projections through 2100 discussed elsewhere) was also taken from Spatial Insights, Inc., and AGS. Finally, supporting information was obtained from FEMA on Federally Declared Disaster Areas based on county-wide declarations from 1959 – July 2009. The primary results of this demographic task were summarized in spreadsheet form as shown in the small extract of Figure D-7.

FIPS	SQMI ZONE 0.2% ANNUAL CHANCE FLOODING	SQMI ZONE 1% ANNUAL CHANCE FLOODING	SQMI ZONE A	SQMI ZONE A1-A30	SQMI ZONE A99	SQMI ZONE FLOODWAY	SQMI ZONE UNKNOWN	SQMI ZONE V	SQMI ZONE V1-V30	SQMI ZONE VE	SQMI ZONE X	FLOOD ZONE TOTAL AREA
060014090004	0	0.15447	0.01196	0.07251	0	0	0	1.90462	0.01053	0.02845	0.05996	5.63316
060014204001	0	0	0	0.0153	0	0.36781	0	0	0.02929	0	0	0.49808
060014220003	0	0	0	0.10454	0	0	0.17893	0	0.04282	0	0.00406	0.87355
060014334003	0.0056	0.13272	0	0.00002	0	0	0	0	0.00023	0.58653	0.3511	1.10835
060014415031	0.00243	0.58281	0.02358	12.18288	0.5134	0	0.00318	0	1.41361	0	0.01219	21.4935
060014415032	0	0.01992	0.13783	5.02869	0	0	0.04207	0	0.00004	0	0.03204	8.12163
060133580005	0	0	0.99726	0.00335	0	0	0.00148	0	0.03671	0	0	2.99127
060133591011	0	0	0.00001	0.15127	0	0	0.22679	0	0.01376	0	0	1.71593
060133800001	0.03954	0	0.00383	0.00047	0	0	0	0	0.00004	0.30742	0.55018	0.90148
060411011001	0	2.4502	0.01949	0.27643	0	0	0.02042	4.18058	5.43505	0.13424	1.26639	13.49852
060411043001	0.1268	0.2745	0.00398	3.23538	0	0.00127	0	0	0.07889	0.05028	0.06614	4.12327
060411060012	0	0.02168	0.0007	2.919	0	0	0.06748	0	0.10922	0.00021	0.00179	4.71106

Figure D-7. Sample extract of demographic nationwide flood zone data.

As can be seen, data are given for each spatial unit identified by a unique FIPS code (Federal Information Processing Standard, a five-digit number that uniquely identifies counties and county equivalents within the U.S.) including, in this sample, land areas located within each flood zone type. Other portions of the spreadsheet contain exactly similar breakdowns for population, policies, structures, and loss data.

D.3 Separating Coastal from Riverine Areas

The work summarized in the preceding section includes all flooding sources, both riverine and coastal. Current FEMA NFIP regulations do not distinguish between mapped coastal and riverine AE zones; they are combined as one zone. In order to account separately for flood hazards in those distinct zones, a second analysis was undertaken by AECOM for FEMA prior to the present study, to segregate coastal demographic data from the lumped national data.

Building upon the prior work, it was first necessary to develop a systematic method to separate the coastal and riverine AE Zones and delineate this new boundary line onto the digital flood hazard database. The details of this task can be found in a recent paper, “An Estimate of the U.S. Population Living in 100-Year Coastal Flood Hazard Areas,” by Crowell, et al (*Journal of Coastal Research*, March 2010). In brief, the methods used involved simplified assumptions permitting an approximate delineation of the coastal-riverine break to be made. These included selection of the point at which the first downstream riverine BFE had been defined, or at the downstream limit of a riverine floodway with the particular method dependent on the

quality of the available flood hazard data. GIS unions were then performed to spatially combine the coastal flood hazard areas identified in this way with the Census Block group population data from the prior work, resulting in separate demographic data spreadsheets for riverine and coastal flood hazard areas.

D.4 Riverine Kriging Analysis

In order to estimate the financial impact of climate and population change to the country as a whole, spatially continuous projections of change in FPA are required. The Monte Carlo sampling procedure (Appendix B) resulted in estimates of change in FPA at each of the 2,357 USGS gage locations chosen. These point estimates were then used as a basis from which to produce spatially continuous smoothed maps of change using Ordinary Kriging (OK). OK generated a spatially continuous random field based on actual data at nearby locations. It represents a linear least squares estimation approach whereby the mean is local (but unknown) and based on the data being used in estimating a point. Optimal weighting of the actual data are determined by solving a set of linear equations that make use of the modeled semi-variogram (spatial correlation between data values) to ensure that estimates are unbiased. In addition, by nature of the Kriging equations, the Kriging variance can also be obtained for an estimation location, providing a means of assessing the uncertainty associated with the interpolation estimate. For additional details on OK and Kriging in general, refer to Goovaerts (1997).

The first step in the Kriging analysis was to perform a variogram analysis to determine an appropriate variogram model for each data set interpolated. Albers equal-area conic projection was used prior to the variogram analysis to project the data for the lower 48 states within the window defined by 65° W to 130° W longitude by 24° N to 51° N latitude. Tables D-1 and D-2 contain summaries of the variogram analysis, including the variogram model selection, the parameters associated with each of those models for different percentiles of both of the ΔQ100 and ΔQ10 distributions, and the two kriged constants identified in Appendix B. Note that the range values associated with each model reflect spatial distance normalization where the long dimension of the U.S. data window (65° W to 130° W longitude) was normalized to 1.0. Following the variogram analysis, OK was performed on the 10^{th}, 25^{th}, 50^{th}, 75^{th}, and 90^{th} percentiles of the ΔQ100 and ΔQ10 distributions for each epoch of interest using the models described in Tables D-1, D-2, and D-3.

The OK was performed over a 0.25°-latitude-by-0.25°-longitude grid that encompassed the lower 48 states using moving windows that incorporated a

maximum of eight of the closest data points in an estimate. The kriged estimates associated with the 50th percentile (or median) projected change in FPA over current conditions for the period 2080–2099 are shown in Figure D-8. The Kriging variance associated with these estimates is shown in Figure D-9. The kriged estimates associated with the 50th percentile (or median) projected change in FHP over current conditions for the period 2080–2099 are shown in Figure D-10. Kriging variance associated with this map would be spatially similar, albeit different in magnitude due to the actual data being estimated. Similar Kriging estimates were produced for the 10th, 25th, 50th, 75th, and 90th percentile projections for both ΔFPA_{rel} and ΔFHP_{rel} for each epoch.

Following the Kriging analysis, estimates of ΔFPA_{rel} and ΔFHP_{rel} for each percentile of the distribution were linearly interpolated to the years 2020, 2040, 2060, 2080, and linearly extrapolated to the year 2100 (recall that 20-year epochs – 2000-2019, 2020-2039, etc. – were used in the analysis up to this point). These data were subsequently utilized with the demographic data to produce financial impact estimates that are reported on later in this appendix. It should also be noted that the results presented in this section represent the riverine portion of the analysis only and do not yet incorporate the coastal analysis.

Table D-1. Summary of variogram models and parameters selected for each epoch and the 10th, 25th, 50th, 75th, and 90th percentiles of the ΔQ100 distribution.

	Epoch	Model	Nugget	Sill	Range
ΔQ100_10% Climate Only	2000-2020	Gaussian	0.18	3.17	0.85
	2020-2040	Gaussian	0.14	1.96	0.49
	2040-2060	Gaussian	0.27	3.1	0.40
	2060-2080	Gaussian	0.31	9	0.39
	2080-2100	Gaussian	0.77	15.1	0.40
ΔQ100_25% Climate Only	2000-2020	Gaussian	0.46	13.3	1.09
	2020-2040	Gaussian	0.37	5.48	0.52
	2040-2060	Gaussian	0.7	8.3	0.42
	2060-2080	Gaussian	0.9	23.5	0.40
	2080-2100	Gaussian	2	41.6	0.43
ΔQ100_50% Climate Only	2000-2020	Gaussian	1.2	94.5	1.73
	2020-2040	Gaussian	1.1	17.8	0.57
	2040-2060	Gaussian	2.1	25.4	0.45
	2060-2080	Gaussian	2.8	69.3	0.43
	2080-2100	Gaussian	6.1	130.6	0.46
ΔQ100_75% Climate Only	2000-2020	Gaussian	3.3	5619	7.70
	2020-2040	Gaussian	3.4	60.2	0.63
	2040-2060	Gaussian	6.1	80.2	0.48
	2060-2080	Gaussian	9.3	207.5	0.45
	2080-2100	Gaussian	18.5	418.9	0.50
ΔQ100_90% Climate Only	2000-2020	Gaussian	8.1	64787	15.70
	2020-2040	Gaussian	9.2	182	0.69
	2040-2060	Gaussian	16.4	231	0.52
	2060-2080	Gaussian	27.3	564	0.48
	2080-2100	Gaussian	50.7	1223	0.54

Table D-2. Summary of variogram models and parameters selected for each epoch and the 10th, 25th, 50th, 75th, and 90th percentiles of the ΔQ10 distribution.

	Epoch	Model	Nugget	Sill	Range
ΔQ10_10% Climate Only	2000-2020	Gaussian	0.3	3	0.60
	2020-2040	Gaussian	0.1	4	0.43
	2040-2060	Gaussian	0.2	7	0.40
	2060-2080	Gaussian	0.5	16	0.37
	2080-2100	Gaussian	1	21	0.37
ΔQ10_25% Climate Only	2000-2020	Gaussian	0.8	8	0.65
	2020-2040	Gaussian	0.3	10	0.45
	2040-2060	Gaussian	0.8	17	0.43
	2060-2080	Gaussian	2	40	0.43
	2080-2100	Gaussian	4	52	0.35
ΔQ10_50% Climate Only	2000-2020	Gaussian	0.7	35	0.70
	2020-2040	Gaussian	0.7	28	0.45
	2040-2060	Gaussian	1	46	0.40
	2060-2080	Gaussian	2	115	0.40
	2080-2100	Gaussian	5	150	0.35
ΔQ10_75% Climate Only	2000-2020	Gaussian	5	100	0.70
	2020-2040	Gaussian	3	90	0.55
	2040-2060	Gaussian	5	130	0.45
	2060-2080	Gaussian	10	300	0.42
	2080-2100	Gaussian	25	450	0.40
ΔQ10_90% Climate Only	2000-2020	Gaussian	15	320	0.80
	2020-2040	Gaussian	10	200	0.50
	2040-2060	Gaussian	15	330	0.45
	2060-2080	Gaussian	20	750	0.42
	2080-2100	Gaussian	70	1200	0.42

Table D-3. Summary of variogram models and parameters for the two kriged constants described in Appendix B. These constants were required in order to estimate changes in FPA and HP.

	Model	Nugget	Sill	Range
Q10c/(Q100c-Q10c)	Gaussian	2.99	1.81	0.41
Q100c/(Q100c-Q10c)	Spherical	2.99	1.81	0.41

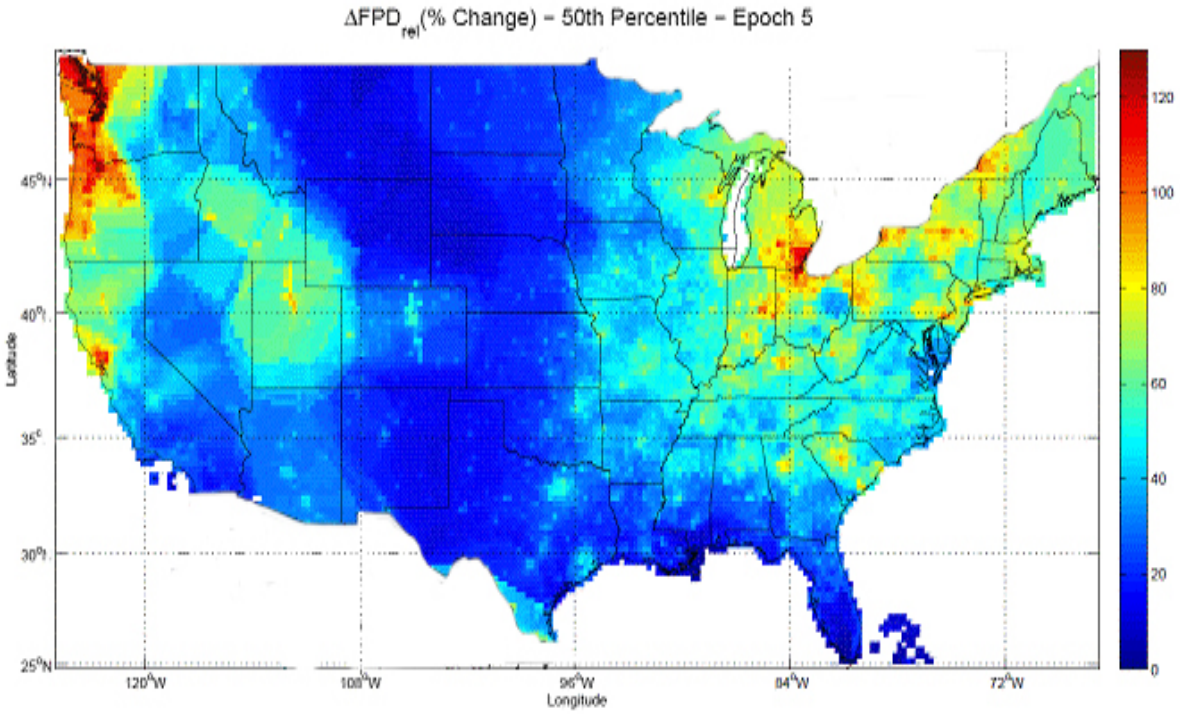

Figure D-8. Spatially continuous ordinary Kriging estimates of the 50th percentile (or median) change in FPD (or equivalently, the change in FPA) over current conditions for the time period 2080–2099. Estimates produced in areas of Mexico and Canada should be ignored as they are the result of extrapolating from gage locations from within the U.S. Estimated changes in FPA toward the end of the century range from little to no change in the Midwest, to more than 100 percent change in the Pacific Northwest and highly urbanized areas of the Northeast.

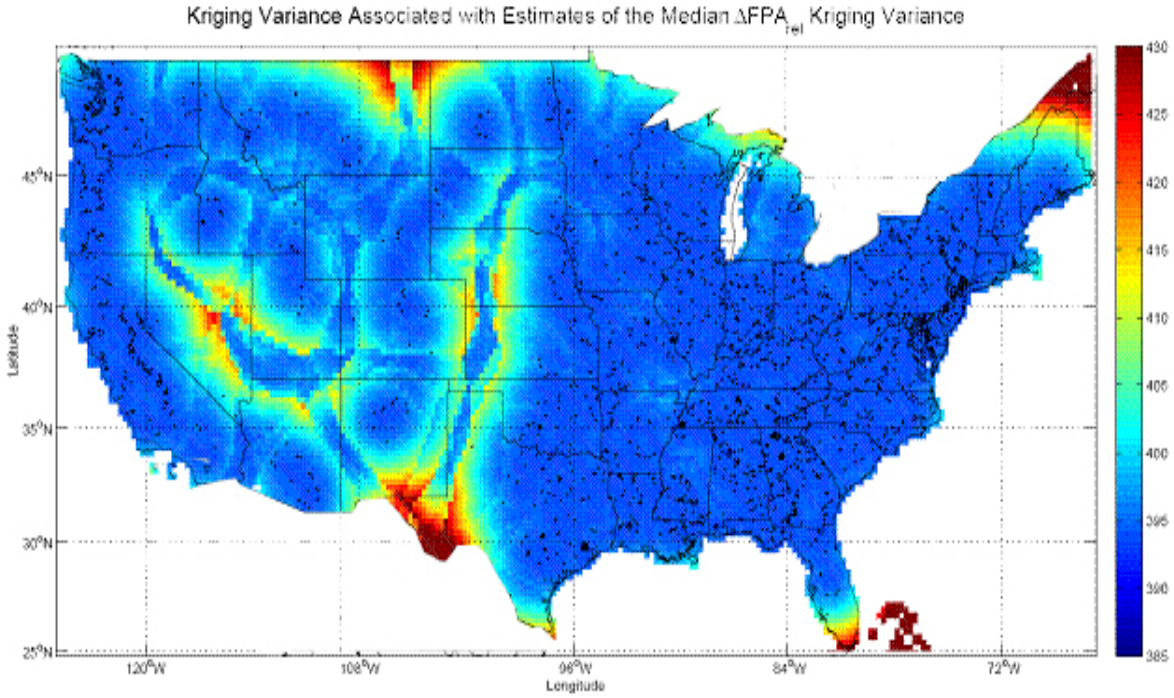

Figure D-9. Kriging variance associated with ordinary Kriging estimation of the 50th percentile change in FPA over current conditions for the time period 2080–2099. While the actual Kriging variance values will change for other parts of the FPA distribution and other variables such as the HP, the relative spatial characteristics of the Kriging variance will remain similar. In other words, there is high Kriging variance in parts of the West and Midwest where USGS gage locations are sparse. In addition, areas of very high Kriging variance in Mexico and Canada are the result of spatial extrapolation in those regions.

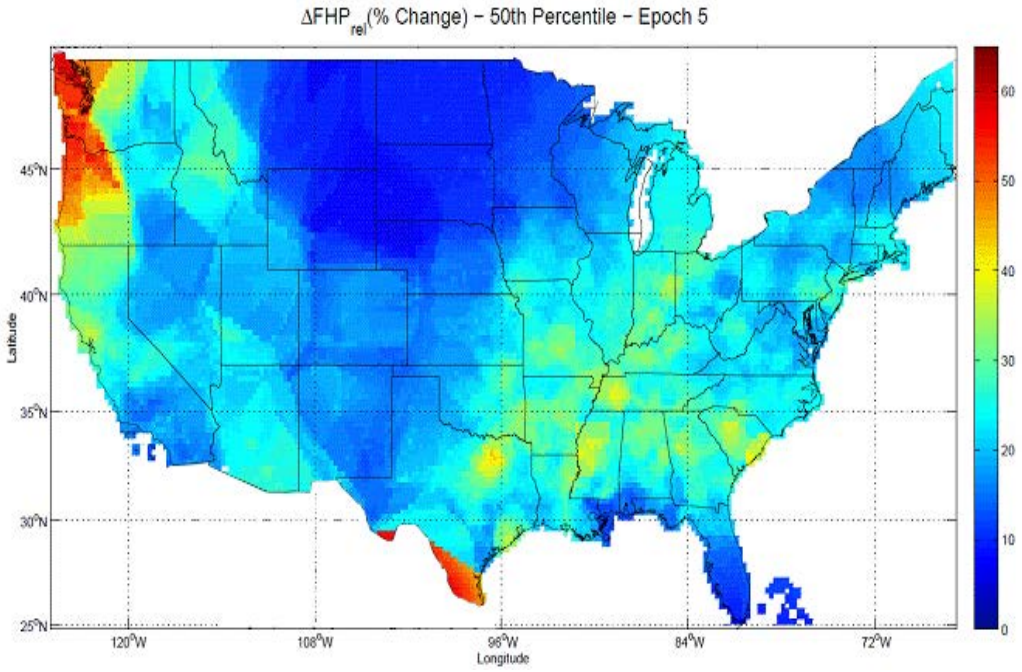

Figure D-10. Spatially continuous ordinary Kriging estimates of the 50th percentile (or median) change in FHP over current conditions for the time period 2080–2099. Estimates produced in areas of Mexico and Canada should be ignored as they are the result of extrapolating from gage locations from within the U.S. Estimated changes in FHP toward the end of the century range from little to no change in the Upper Midwest, to more than 50 percent change in much of the Pacific Northwest. Many urban areas of the South Central U.S. are predicted to change by as much as 40 percent.

D.5 GIS Analysis at County Scale

The Kriging analysis just summarized produced a spatially continuous set of estimates of changes in flood factors over the nation. In order to proceed from that information to an evaluation of impact, it is necessary to connect the climate/flood change data with the demographic data. Although this could have been done at the level of the Census Block data, such extremely fine resolution would not be consistent with the general degree of approximation and resolution inherent in the physical data and the study methods. Instead, it was decided to work at a county level. This means that counties, with their associated population, policies, claims, and so forth, for each flood zone type, would be the basic unit used for aggregation to the national level. It is important to emphasize here – as is done elsewhere in this report – that although the analysis proceeded from this level of resolution, the findings are *not* to be interpreted as valid at this level. There is a great deal of uncertainty in the analysis that makes any particular local estimate highly unreliable. However, if it is true that the methods are not seriously biased, then variations from

place to place are expected to be self-canceling in the overall national projections that form the ultimate findings of this study.

The steps involved in attaching climate/flood change data to counties were as follows. First, for a given parameter such as flood hazard area, the change in that parameter (at a particular epoch) was tabulated at the centroids of each interpolated 0.25 degree grid cell, such as:

Latitude	Longitude	Percent Change
49.37500	-124.37500	33.57226
49.12500	-124.37500	33.58073
48.87500	-124.37500	33.78965
48.62500	-124.37500	28.79691
48.37500	-124.37500	28.80398

Working with a U.S. county GIS dataset, it was then straightforward to determine which counties contained each of these points, so that the corresponding percent parameter changes were also assigned to those counties. The number of points falling within a particular county varies widely, according to the size of the county, with some small counties not enclosing any grid points.

The value of parameter change assigned to a county was the simple average of the several points contained within the county. In the event that a county unit contained no parameter points, a spatial join was performed to assign the percent change value of the nearest grid centroid to that null county centroid.

This procedure produced a final dataset with an averaged percent change value for every county or county equivalent area of the nation. This information, in turn, was connected to the demographic data spreadsheet discussed earlier to provide estimates of change for all counties.

A small sample portion of the result is in illustrated in Figure D-11. The data are arranged by county, with five rows for each, corresponding to the five epochs of interest. Columns show changes in the flood parameters of interest at the five standard percentiles. A map showing a sample of the national results (for change in flood area: illustrative only) for the counties is shown in Figure D-12. Keep in mind, however, that county-resolution values are only intended as an intermediate computational stage leading to the national aggregate estimates. They should not be construed as individual findings of the study.

FEMA Region	State	County	FIPS	County Population (2009 Projection)	Total 1% Floodplain Area (sq. miles)	Population in 1% Floodplain (for 2009)	Epoch	ΔFPD_{rel} & ΔFPA_{rel}					Current population in Riverine Floodplain (%)	Projected population in riverine floodplain (% of projected county population)					ΔHP_{rel}				
								10%	25%	50%	75%	90%		10%	25%	50%	75%	90%	10%	25%	50%	75%	90%
4	Alabama	Autauga	1001	50833	95.88	8069	2020	-277	-170	16	318	743	16	0	0	18	66	100	-56	-33	9	77	173
4	Alabama	Autauga	1001	50833	95.88	8069	2040	-274	-165	26	333	768	16	0	0	20	69	100	-55	-30	13	84	184
4	Alabama	Autauga	1001	50833	95.88	8069	2060	-273	-164	28	337	774	16	0	0	20	69	100	-53	-27	19	92	196
4	Alabama	Autauga	1001	50833	95.88	8069	2080	-273	-164	28	338	776	16	0	0	20	70	100	-50	-24	23	100	209
4	Alabama	Autauga	1001	50833	95.88	8069	2100	-272	-162	32	344	785	16	0	0	21	70	100	-49	-21	28	107	219
4	Alabama	Baldwin	1003	175086	381.96	40449	2020	-208	-130	8	229	541	20	0	0	21	66	100	-58	-35	5	69	160
4	Alabama	Baldwin	1003	175086	381.96	40449	2040	-207	-127	12	235	551	20	0	0	22	67	100	-57	-34	7	74	167
4	Alabama	Baldwin	1003	175086	381.96	40449	2060	-207	-127	11	236	552	20	0	0	22	67	100	-56	-32	10	77	173
4	Alabama	Baldwin	1003	175086	381.96	40449	2080	-207	-128	10	235	551	20	0	0	22	67	100	-55	-31	12	81	179
4	Alabama	Baldwin	1003	175086	381.96	40449	2100	-207	-127	12	237	556	20	0	0	22	67	100	-54	-29	15	85	185
4	Alabama	Barbour	1005	29511	84.04	2742	2020	-237	-147	12	268	629	9	0	0	10	34	68	-57	-33	8	74	169
4	Alabama	Barbour	1005	29511	84.04	2742	2040	-234	-142	20	280	648	9	0	0	11	35	69	-55	-31	12	80	178
4	Alabama	Barbour	1005	29511	84.04	2742	2060	-234	-142	21	282	652	9	0	0	11	35	70	-53	-28	16	87	189
4	Alabama	Barbour	1005	29511	84.04	2742	2080	-234	-142	20	282	652	9	0	0	11	35	70	-52	-26	20	94	198
4	Alabama	Barbour	1005	29511	84.04	2742	2100	-234	-140	23	286	657	9	0	0	11	36	70	-51	-24	23	99	206
4	Alabama	Bibb	1007	21709	32.11	1113	2020	-283	-173	18	326	761	5	0	0	6	22	44	-56	-33	9	77	174
4	Alabama	Bibb	1007	21709	32.11	1113	2040	-279	-167	28	343	787	5	0	0	7	23	45	-55	-30	14	84	185
4	Alabama	Bibb	1007	21709	32.11	1113	2060	-278	-166	30	347	794	5	0	0	7	23	46	-52	-26	19	93	197
4	Alabama	Bibb	1007	21709	32.11	1113	2080	-278	-165	32	349	797	5	0	0	7	23	46	-50	-23	24	101	210
4	Alabama	Bibb	1007	21709	32.11	1113	2100	-276	-163	36	356	809	5	0	0	7	23	47	-48	-20	29	108	221
4	Alabama	Blount	1009	57468	36.99	3268	2020	-323	-198	21	373	870	6	0	0	7	27	55	-56	-33	9	77	173
4	Alabama	Blount	1009	57468	36.99	3268	2040	-319	-192	30	388	895	6	0	0	7	28	57	-55	-30	14	85	185
4	Alabama	Blount	1009	57468	36.99	3268	2060	-318	-190	35	396	907	6	0	0	8	28	57	-52	-26	20	95	201
4	Alabama	Blount	1009	57468	36.99	3268	2080	-316	-187	39	404	919	6	0	0	8	29	58	-49	-22	27	106	217
4	Alabama	Blount	1009	57468	36.99	3268	2100	-314	-183	46	415	936	6	0	0	8	29	59	-47	-18	32	114	230

Figure D-11. Sample extract from the final demographic and flood/climate change data file.

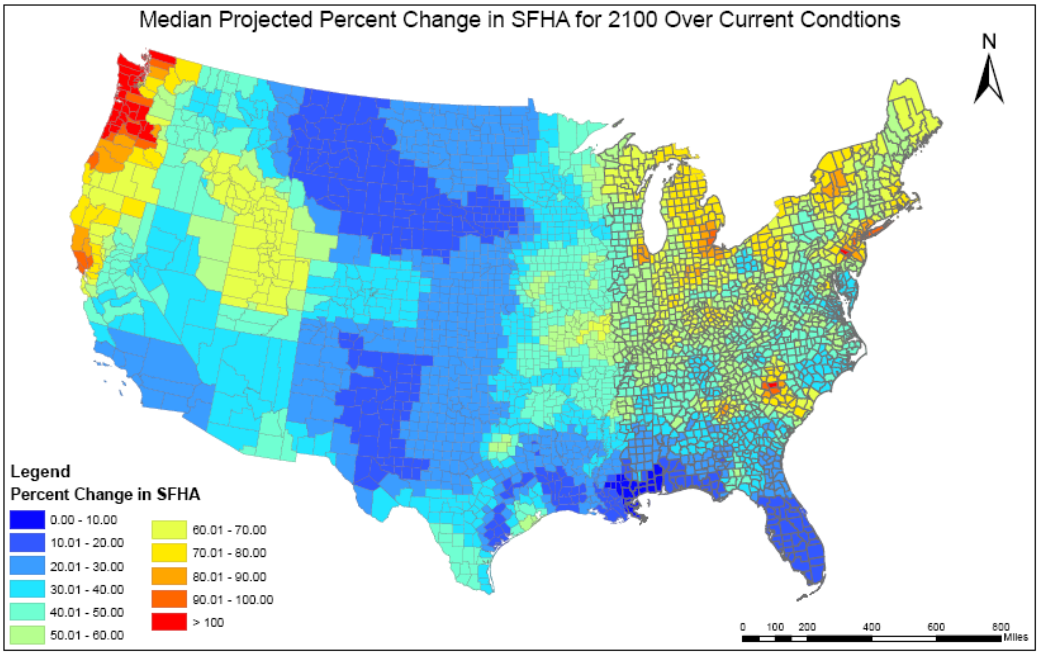

Figure D-12. Sample of intermediate county level estimates of SFHA change at 2100.

Appendix E

Index of Economic Analysis Exhibits

Contributing authors

Susan Pino, ACAS, MAAA, ARM

Joshua Merck

E Index of Economic Analysis Exhibits

This appendix lists the supporting exhibits that illustrate the economic analysis described in Chapter 5.0. The economic analysis calculations were performed separately for each county included in this study and therefore a full set of riverine and coastal analysis exhibits listed below would repeat for each county. The summary exhibits combine the results of the analysis exhibits from each county. In the supplementary materials provided to FEMA, we have included one set of these exhibits that illustrate the calculations of an example county (i.e., not actual data).

Summary Exhibits

Exhibit 1 – Exhibit 1 shows the summary of results compiled from the individual county analysis

- Sheet 1 – Assumption summary
- Sheet 2 – Summary of policy, population, and premium growth
- Sheet 3 – Summary of SFHA growth
- Sheet 4 - Detailed summary of riverine and coastal policy growth
- Sheet 5 – Summary of premium by risk classification
- Sheet 6 – Summary of estimated premium after loss cost adjustment
- Sheet 7 – Summary of estimated premium growth rates after loss cost adjustment
- Sheet 8 – Summary of estimated average premium by policy
- Sheet 9 – Countrywide estimate of change in loss cost
- Sheet 10 – Total riverine estimated change in loss cost
- Sheet 11 – Riverine Pre- and Post-FIRM estimated change in loss cost
- Sheet 12 – Riverine PRP and non-PRP estimated change in loss cost
- Sheet 13 – Total coastal estimated change in loss cost
- Sheet 14 – Coastal Pre- and Post-FIRM estimated change in loss cost
- Sheet 15 – Coastal PRP and non-PRP estimated change in loss cost

Riverine Analysis Exhibits

Exhibit 2 – Riverine Analysis Exhibits

- Sheet 1 – Assumption summary
- Sheet 2 – Projected growth in policies in the SFHA
- Sheet 3 – Projected growth in policies outside the SFHA
- Sheet 4 – Projected total future policies and premium
- Sheet 5 – Projected total future policies by risk classification
- Sheet 6 – Projected future policies in the SFHA by risk classification
- Sheet 7 – Projected future policies outside the SFHA by risk classification
- Sheet 8 – Average future premium by risk classification for all policies
- Sheet 9 – Average future premium by risk classification for policies within the SFHA
- Sheet 10 – Average future premium by risk classification for policies outside the SFHA
- Sheet 11 – Estimated change in loss cost for all policies
- Sheet 12 – Estimated change in loss cost for polices in the SFHA
- Sheet 13 – Estimated change in loss cost for policies outside the SFHA
- Sheet 14 – Estimated change in future damage factors

Exhibit 3 – Development of change in damage factors for riverine policies. This set of exhibits would additionally be repeated at each future epoch. Only one epoch is shown for illustrative purposes.

- Sheet 1 – Estimated damage factors for each policy group (Pre-FIRM, Post-FIRM, PRP, Non-PRP)
- Sheet 2 – Summary of PELV curve probabilities by structure height relative to BFE
- Sheet 3 – Summary of DELV arrays
- Sheets 4 to 16 – Multiplication of PELV probabilities times DELV arrays for each structure type

Coastal Analysis Exhibits

Exhibit 4 – Coastal Analysis Exhibits

- Sheet 1 – Assumption summary
- Sheet 2 – Projected growth in policies in the SFHA

- Sheet 3 – Projected growth in policies outside the SFHA
- Sheet 4 – Projected total future policies and premium
- Sheet 5 – Projected total future policies by risk classification
- Sheet 6 – Projected future policies in the SFHA by risk classification
- Sheet 7 – Projected future policies outside the SFHA by risk classification
- Sheet 8 – Average future premium by risk classification for all policies
- Sheet 9 – Average future premium by risk classification for policies within the SFHA
- Sheet 10 – Average future premium by risk classification for policies outside the SFHA
- Sheet 11 – Estimated change in loss cost for all policies
- Sheet 12 – Estimated change in loss cost for polices in the SFHA
- Sheet 13 – Estimated change in loss cost for policies outside the SFHA
- Sheet 14 – Estimated change in future damage factors

Exhibit 5 – Development of change in damage factors for coastal policies. This set of exhibits would additionally be repeated at each future epoch. Only one epoch is shown for illustrative purposes.

- Sheet 1 – Estimated damage factors for each policy group (Pre-FIRM, Post-FIRM, PRP, Non-PRP)
- Sheet 2 – Summary of PELV curve probabilities by structure height relative to BFE
- Sheet 3 – Summary of DELV arrays
- Sheets 4 to 16 – Multiplication of PELV probabilities times DELV arrays for each structure type

Appendix F
Study Notation

Contributing author

Joe Kasprzyk

F Study Notation

F.1 Monte Carlo Output Files and Variables

Study output was separated into several output files. Each file and the variables it contains are described in the sections below.

F.1.1 USGageEIs.csv

This file contains the current and projected extreme indices used in the regression analysis. Each of the items below explains each column, with the file tag first, and the description following. For each extreme index, several values are given and will be explained here in general terms. Consider frost days as an example. The first part of the file tag represents the index; here "fd" stands for frost days. The next part of the identifier describes how the index was calculated, and the third part of the identifier represents the statistical property of the value such as whether it is a min, max, standard deviation, and so forth.

fd_C describes the current observed value for frost days, that is, it is the mean of the 50-year observed record for this index.

The fd_MC variables stand for "modeled current" conditions. Each climate model was run for an experiment with 20th century climate forcings to ascertain the model's predictive skill. Since each model represents a different conceptual picture of the climate system, these predictions of 20th century conditions differ. The minimum (fd_MC_Min), maximum (fd_MC_Max), mean (fd_MC_Mean), and standard deviation (fd_MC_std) of the ensemble of values of this variable were reported. The ensemble comes from having multiple climate models and multiple runs of some of these models, and each run has extreme index outputs for the current 1953–2003 period.

In a similar manner, the fd_MP variables give predictions of "modeled predicted" conditions. Each climate model was run for experiments out to 2100, and now in addition to the fact that there are multiple models and model runs, there are multiple emissions scenarios also being tested. This collection of models, runs, and scenarios yields a distribution of predicted values for each extreme index. The actual values of interest are 10-year averages for each epoch, which are reported here. Similar to the modeled current data, min (fd_MP_Min), max (fd_MP_Max), mean (fd_MP_Mean), and standard deviation (fd_MP_std) are reported for each variable.

The several extreme indices in the file are listed below. The full set of nine outputs is written here for frost days, but omitted for each other variable. For this and all lists in the report, the units are given in square brackets after the description.

StationID: USGS Station ID.

Epoch: Epoch of time, between 1 and 5.

fd_C: Observed current frost days [days].

fd_MC_Min: Minimum of climate model prediction of current frost days [days].

fd_MC_Max: Maximum of climate model prediction of current frost days [days].

fd_MC_Mean: Mean of climate model prediction of current frost days [days].

fd_MC_std: Standard deviation of climate model prediction of current frost days [days].

fd_MP_Min: Minimum of climate model prediction of projected frost days, at a given epoch [days].

fd_MP_Max: Maximum of climate model prediction of projected frost days, at a given epoch [days].

fd_MP_Mean: Mean of climate model prediction of projected frost days, at a given epoch [days].

fd_MP_std: Standard deviation of climate model prediction of projected frost days, at a given epoch [days].

cdd_[indicators]: Consecutive dry days (with all nine variables as above) [days].

r5d_[indicators]: Maximum 5-day rainfall (with all nine variables as above) [mm].

F.1.2 USGageInfo.csv

This file contains the observed info for each gage. Note that each value is repeated for each of the five epochs, even though the values will be the same for a given gage for all five epochs.

The variables are defined as follows:

StationID: USGS Station ID

Type: Country. Note that while this data field can be expanded for future studies in multiple countries, all the gages in this study are in the United States (U.S.).

Long.: Longitude. These values are negative in the Western Hemisphere.

Lat.: Latitude.

DA: Drainage area [square miles].

Sl: Channel slope [feet/mile].

Storage: Water storage area as a percent of the drainage area [%].

Epoch: Epoch of time, between 1 and 5. Note that this is irrelevant in this file under the current study assumptions. That is, each of the above values never changes in time. In future studies, values such as storage could change in the future due to assumptions of land cover change, new reservoirs, etc.

F.1.3 USGagePopandIA.csv

This file contains population and impervious area used in the regression with some extra information for later analysis. The following explanation will be for scenario B1, but the calculations are similar for the other scenarios.

A gridded population density observation at the year 1990 is available at each site ("Pop_1990(peop/mi^2)"), but it is not used to estimate changes in impervious area. Instead, national growth models for each scenario are input to a relationship between population and impervious area to obtain a scaled increased impervious area relative to the observed value at each gage.

The following method calculates projections of impervious area. Use the Hicks IA-Population equation (see Appendix A), and given observed impervious area ("IA_C(%)") solve for a gage's corresponding "effective" population ("PopEff_C(peop/mi^2)"). This effective population does not have much bearing on the actual population at the site other than its usefulness in being paired with the Hicks equation to project impervious area in the future. Using this effective population, use the population growth model from scenario B1 (the other scenarios are calculated in a similar manner, only using a different growth model) to project a population at each epoch ("PopEff_P_B1(peop/mi^2)"). Given the new population at the desired epoch, the Hicks equation is used to calculate a new impervious area percentage ("IA_P_B1(%)"). As with the other categories P represents projections and C represents current conditions.

The variables are defined as follows:

StationID: USGS Station ID.

Epoch: Epoch of time, between 1 and 5.

Pop_1990(peop/mi^2):	Population at 1990. Not used in regression, but helpful for later analysis [persons / sq. mi.].
Pop_2010_A1B1(peop/mi^2):	Projected population at 2010, used by applying the growth model of scenarios A1 and B1 to the 1990 population. Not used in regression, but helpful to see whether the 1990 population and population growth model is accurate in predicting current population conditions [persons / sq. mi.].
Pop_P_B1(peop/mi^2):	Projected population at a given epoch for scenario B1. Not used in regression [persons / sq. mi.].
Pop_P_A1B(peop/mi^2):	Projected population at a given epoch for scenario A1B. Not used in regression [persons / sq. mi.].
Pop_P_A2(peop/mi^2):	Projected population at a given epoch for scenario A2. Not used in regression [persons / sq. mi.].
PopEff_C(peop/mi^2):	Current effective population, calculated using the Hicks equation from observed current impervious area [persons / sq. mi.].
PopEff_P_B1(peop/mi^2):	Projected effective population at a given epoch, calculated by applying the B1 growth model to PopEff_C [persons / sq. mi.].
PopEff_P_A1B(peop/mi^2):	Projected effective population at a given epoch, calculated by applying the A1B growth model to PopEff_C [persons / sq. mi.].
PopEff_P_A2(peop/mi^2):	Projected effective population at a given epoch, calculated by applying the A2 growth model to PopEff_C [persons / sq. mi.].
IA_C(%):	Current impervious area [percent of drainage area].
IA_P_B1(%):	Projected impervious area at a given epoch, calculated by applying the Hicks equation to PopEff_P_B1 [percent of drainage area].
IA_P_A1B(%):	Projected impervious area at a given epoch, calculated by applying the Hicks equation to PopEff_P_A1B [percent of drainage area].
IA_P_A2(%):	Projected impervious area at a given epoch, calculated by applying the Hicks equation to PopEff_P_A2 [percent of drainage area].

F.1.4 USGageQ10Dist.csv and USGageQ100Dist.csv

The files USGageQ10Dist.csv and USGageQ100Dist.csv give distributional estimates for Q10 and Q100 respectively, similar to the D100 relative change distributions discussed earlier (see section F.1.1).

The files contain the USGS Station ID ("StationID") and Epoch ("Epoch") similar to the other files. The distributional estimates that are reported in these files represent relative changes in flow as described by Equation (F-1), where Q represents either Q10 or Q100, and the # represents the percentile being calculated:

$$Q\_P\_\# = [(Qp - Qc) / Qc] * 100\% \quad \text{(F-1)}$$

where Qp represents the projected flow, and Qc represents the current flow. To calculate Qp, Equation (F-2) is used, using the modeled projected (Qmp) and modeled current (Qmc) flow where inputs to the regression equation come from the climate model.

$$Qp = Qc (Qmp / Qmc) \quad \text{(F-2)}$$

The purpose of Equation (F-2) is to express Qp as a "scaled" multiplier of Qc, that is, if the modeled projected flow is twice as large as the modeled current flow, the final projected flow will be twice the current flow. In this manner, the approach will work even if the climate models greatly over or under predict the current conditions.

The manner in which Equation (F-1) is defined means that there is a theoretical lower limit for Q_P (that is, a bound for Q_P_0 can be predicted). If the modeled minimum Qp is zero, the limit of Equation (F-1) is negative 100 percent. This makes sense, since, zero flow is in essence a change of negative 100 percent.

The output files have columns with percentiles of these distributions, at 2 percentile intervals.

F.1.5 USGageQStats.csv

This file provides statistics from input and output to the Monte Carlo analysis, for Q10, Q100, and other variables. The following list will provide descriptions of each variable, with separate sections describing the types of variables.

StationID:	USGS Station ID.
Epoch:	Epoch of time, between 1 and 5.

F.1.5.1 Q10 Variables

Q10_C(cfs): Observed current Q10 [cfs].

Q10_MC_Mean(cfs): Mean of the climate model prediction of current Q10. Note that the values for this variable differ slightly as a function of the epoch. This is due to the fact that the sampling of climate indices for input to the regression equation is done separately for each epoch, thus changing the estimate of the mean at each calculation [cfs].

Q10_MC_Mean(%): Percent difference between the observed Q10 and the Q10 predicted by the models (see Equation [F-3], just below). A negative value here means that the models say that the flow is less than the observed [percent].

Q10_MC_Mean(%) = (Q10_MC_Mean(cfs) - [Q10_C(cfs))/Q10_C(cfs)] (F-3)

Q10_MP_Mean(cfs): Mean of unscaled climate model predictions of Q10, at a given epoch. This is a raw value from the climate models that is not scaled relative to the observed current conditions [cfs].

Q10_MP_Mean(%): Percent difference between the observed Q10 and the Q10 predicted by the models, for a given epoch. This is a percent difference calculated in a similar manner to Equation (F-3), where the Q10_MP_Mean(cfs) with the Q10_C are compared. A negative value here means that the model prediction is lower than the current value, but it does not mean that the model is actually predicting a decrease. This is because the projection to the current conditions has not yet been scaled (to correct for bias between the climate model prediction and the observation) [percent].

Q10_P_Median(cfs): Median of scaled climate model predictions of Q10, at a given epoch. Here, the value is scaled using Equation (F-2) [cfs].

Q10_P_Median(%): Percent difference between the observed Q10 and the scaled Q10 predicted from the models (Q10_P_Median(cfs), see above), for a given epoch [percent].

Q10_P_Mean(cfs): Mean of scaled climate model predictions of Q10, at a given epoch. Here, the value is scaled using Equation (F-2) [cfs].

Q10_P_Mean(%): Percent difference between the observed Q10 and the scaled Q10 predicted from the models (Q10_P_Mean(cfs), see above), for a given epoch [percent].

Q10_P_Std(cfs): Standard deviation of scaled climate model predictions of Q10, at a given epoch [cfs].

Q10_P_Std(%): Percent difference between the observed Q10 and the scaled Q10 predicted from the models (Q10_P_Std(cfs), see above), for a given epoch [percent].

F.1.5.2 Q100 Variables

This set of variables is similar to that described in Section F.1.6.1, only with Q100 instead of Q10. Recall that for each major variable predicted in this study, there are four different variable types: C is the observed current conditions; MC is the modeled current conditions (climate model predictions of current extreme indices as the input to the regression); MP is the modeled "unscaled" predicted conditions (climate model predictions of future extreme indices as input to the regression); and P is the scaled predictions based on climate model output, calculated as:

(C value)*(MP value/MC value)

For the specific definitions, please see section F.1.6.1.

F.2 Regression Equations

The following regression equations were developed for estimating the 100-year and 10-year flood discharges.

100-year equation in log linear form:

log Q100 = 0.12097 + 0.711 * log(DA) + 0.169 * log(SL) – 0.332 * log(STOR+1) + 0.188 * log(IA+1) – 0.206 *log(MFD+1) – 0.177 * log(MCDD+1) + 1.440 * log(MRx5+1)

100-year equation in power function form:

Q100 = 1.321 * DA0.711 SL0.169 (STOR+1)-0.332 (IA+1)0.188 (MFD+1)-0.206 (MCDD+1)-0.177 (MRx5+1)1.440

R^2 = 0.898, Standard error = 0.23679 log units = 58.8 percent
10-year equation in log linear form:

log Q10 = -0.96155 + 0.723 * log(DA) + 0.158 * log(SL) – 0.339 * log(STOR+1) + 0.222 * log(IA+1) – 0.044 * log(MFD+1) – 0.395 * log(MCDD+1) + 1.812 * log(MRx5+1)

10-year equation in power function form:

Q10 = 0.1093 * DA0.723 SL0.158 (STOR+1)-0.339 (IA+1)0.222 (MFD+1)-0.044 (MCDD+1)-0.395 (MRx5+1)1.812
R^2 = 0.906, Standard error = 0.23184 log units = 57.4 percent

Where

Q100 =	100-year discharge, in cfs
Q10 =	10-year discharge, in cfs
DA =	drainage area, in square miles
SL =	channel slope, in feet per mile
STOR =	water storage areas as a percentage of the drainage area
IA =	impervious area as a percentage of the drainage area
MFD =	mean number of frost days per year
CDD =	mean of the maximum number of consecutive dry days per year
MRx5 =	mean of the maximum 5-day rainfall for a given year

Appendix G

References

G References

Alexander, L. V., X. Zhang, T. C. Peterson, J. Caesar, B. Gleason, A. M. G. Klein Tank, M. Haylock, D. Collins, B. Trewin, F. Rahimzadeh, A. Tagipour, K. Rupa Kumar, J. Revadekar, G. Griffiths, L. Vincent, D. B. Stephenson, J. Burn, E. Aguilar, M. Brunet, M. Taylor, M. New, P. Zhai, M. Rusticucci, J., and L. Vazquez-Aguirre. 2006. Global Observed Changes in Daily Climate Extremes of Temperature and Precipitation. Journal of Geophysical Research. Vol. 111.

Arnell, N. W. 2004. "Climate and Socio-Economic Scenarios for Global-Scale Climate Change Impacts Assessments: Characterizing the SRES Storylines." Pp. 3-20 in Global Environmental Change. Vol. 14.

Barnes, H.H., Jr. 1967. Roughness Characteristics of Natural Channels. Pp. 213 in the United States Geological Survey, Water Supply Paper 1849.

Bender, M., T. Knutson, R. Tuleya, J. Sirutis, G. Vecchi, S. Garner, and I. Held. 2010. "Modeled Impact of Anthropogenic Warming on the Frequency of Intense Atlantic Hurricanes." Science.

Bengtsson, L., K. Hodges, and N. Keenlyside. 2009. "Will ExtraTropical Storms Intensify in a Warmer Climate?" Pp. 2276-2301 in Journal of Climate. Vol. 22.

Bengtsson, M., Shen, Y., and Oki, T. 2006. "A SRES-based gridded global population dataset for 1990-2100." Pp. 113-131 in Population and Environment. Vol. 28.

Bindoff, N.L., J. Willebrand, V. Artale, A. Cazenave, J. Gregory, S. Gulev, K. Hanawa, Le Quéré, S. Levitus, Y. Nojiri, C.K. Shum, L.D. Talley, and A. Unnikrishnan. 2007. Observations: Oceanic Climate Change and Lea level. Climate Change 2007: The Physical Science Basis. Pp. 385-432 in the Fourth Assessment Report of the Intergovernmental Panel on Climate. Contribution of Working Group I. New York, NY and Cambridge, United Kingdom: Cambridge University Press.

Bruun, P. 1962. Sea Level Rise as a Cause of Shore Erosion. Pp. 117-130 in the Journal of Waterways and Harbors Division, ASCE. Vol. 88.

Burkham, D.E. 1978. Accuracy of Flood Mapping. Pp. 515-527 in the Journal of Research, United States Geological Survey.

Burkham, D.E. 1977. A Technique for Determining Depth for T-year Discharges in Rigid Boundary Channels. Pp. 77-83 in the United States Geological Survey Water-Resources Investigations Report.

Cazenave, A. 2008. Sea Level Budget Over 2003–2008: A Reevaluation From GRACE Space Gravimetry, Satellite Altimetry and Argo, Glob. Planet. Change. DOI:10.1016/j.gloplacha.2008.10.004.

Climate Change Science Program (CCSP). 2009. Coastal Sensitivity to Sea-Level Rise: A Focus on the Mid-Atlantic Region. A Report by the United States CCSP and the Subcommittee on Global Change Research. United States Environmental Protection Agency, Washington D.C.
Available at http://www.climatescience.gov/Library/sap/sap4-1/final-report/default.htm.

Climate Change Science Program (CCSP). 2008a. Climate Models: An Assessment of Strengths and Limitations. A Report by the United States CCSP and the Subcommittee on Global Change Research. Department of Energy, Office of Biological and Environmental Research, Washington, D.C.

Climate Change Science Program (CCSP). 2008b. Weather and Climate Extremes in a Changing Climate. Regions of Focus: North America, Hawaii, Caribbean, and U.S. Pacific Islands. A Report by the United States CCSP and the Subcommittee on Global Change Research. Department of Commerce, National Oceanic and Atmospheric Administration (NOAA) National Climatic Data Center, Washington, D.C.
Available at http://www.climatescience.gov/Library/sap/sap3-3/default.php.

Crowell, M., and S. P. Leatherman, eds. 1999. “Coastal Erosion Mapping and Management.” P. 196 in the Journal of Coastal Research. Vol 28 (Special Issue).

Crowell, M., K. Coulton, C. Johnson, J. Westcott, D. Bellomo, S. Edelman, and E. Hirsch. March, 2010. An Estimate of the U.S. Population Living in 100-Year Coastal Flood Hazard Areas. Journal of Coastal Research.

Dempster, G.R. 1983. "Streamflow/Basin Characteristics Retrieval." Pp. 31 in the United States Geological Survey WATSTORE User's Guide. Vol 4.

Douglas, B.C. 1992. "Global Sea Level Acceleration." Pp. 12699-12706 in Journal of Geophysical Research, Vol. 97, Issue C8, DOI: 10.1029/92JC01133.

Emanuel, K., R. Sundararajan, and J. Williams. 2008. Hurricanes and Global Warming: Results from Downscaling IPCC AR4 Simulations. Bulletin of the American Meteorological Society.

Exum, L., S. Bird, J. Harrison, and C. Perkins. 2005. "Estimating and Projecting Impervious Cover in the Southeastern United States." United States Environmental Protection Agency (EPA) Report No. EPA/600/R-05/061, EPA. Washington, D.C.

Federal Emergency Management Agency. 1991. Projected Impact of Relative Sea Level Rise on the National Flood Insurance Program. Washington, D.C.: FEMA.

Frich, P., L. Alexander, P. Della-Marta, B. Gleason, M. Haylock, A. Klein Tank, and T. Peterson. 2002. "Observed Coherent Changes in Climatic Extremes During the Second Half of the Twentieth Century." Pp. 193-212 in Climate Research. Vol. 19.

Goovaerts, P. 1997. Geostatistics for Natural Resources Evaluation, New York, NY: Oxford University Press.

H. John Heinz III Center for Science, Economics, and the Environment. April, 2000. Evaluation of Erosion Hazards. Washington, D.C. Available online at http://www.heinzctr.org/publications/index.shtml.51: 21527–21532 from Proceedings of the National Academy of Sciences.

Hayes, T.L. and D.A. Neal. 2010. Actuarial Rate Review In Support of the Recommended October 1, 2010, Rate and Rule Changes. Washington, D.C.: FEMA. Available online at http://www.fema.gov/library/viewRecord.do?id=4277.

Houghton, J.T. Climate Change 2001: The Scientific Basis. Cambridge, United Kingdom: Cambridge University Press.

Houston, J.R. and R.G. Dean. 2011. "Sea Level Acceleration Based on U.S. Tide Gauges and Comparison to Global Gauge Results." Accepted for publication in the Journal of Coastal Research.

Intergovernmental Panel on Climate Change (IPCC). 2007. Climate Change 2007: Synthesis Report. Contribution of Working Groups I, II and III to the Fourth Assessment Report of the Intergovernmental Panel on Climate Change (IPCC), Geneva, Switzerland.
Available at http://www.ipcc.ch/ipccreports/ar4-syr.htm.

Kennedy, E.J. 1985. "Discharge Ratings at Gaging Stations." Pp. 59 in Book 3, Techniques of Water-Resources Investigations of the United States Geological Survey.

Knutson, T., J. McBride, J. Chan, K. Emanuel, G. Holland, C. Landsea, I. Held, J. Kossin, A.K. Srivastava, and M. Sugi. 2010. Tropical Cyclones and Climate Change. Nature Geoscience.

Kollat, J.B., J.R. Kasprzyk, W.O. Thomas, Jr., A.C. Miller, and D. Divoky. 2012. Estimating the Impacts of Climate Change and Population Growth on Flood Discharges in the United States. Journal of Water Resources Planning and Management, American Society of Civil Engineers, Vol. 138, No. 5, September 1, 2012, pp. 442-452.

Lambert, S. and J. Fyfe. 2006. Changes in Winter Cyclone Frequencies and Strengths Simulated in Enhanced Greenhouse Warming Experiments. Results from the models participating in the Intergovernmental Panel on Climate Change (IPCC) diagnostic exercise. Climate Dynamics.

Leopold, L.B. and T. Maddock. 1953. "The Hydraulic Geometry of Stream Channels and Some Physiographic Implications." Pp. 57 in the United States Geological Survey Professional Paper 252.

Liang, A.K. 1998. "An Introduction to Ocean Waves." Guide to Wave Analysis and Forecasting. Ed. Geneva, Switzerland. World Meteorological Organization.

Lins, H, and J. Slack. 1999. "Streamflow Trends in the United States." Pp. 227-230 in Geophysical Research Letters.

Meehl, G. A., C. Covey, T. Delworth, M. Latif, B. McAvaney, J. F. B. Mitchell, R. J. Stouffer, and K. E. Taylor. 2007. "The WCRP CMIP3 Multi-Model Dataset: A New Era in Climate Change Research." Pp. 1383-1394 in the Bulletin of the American Meteorological Society. Vol. 88.

Milly, P. C. D., R. Wetherald, K. Dunne, and T. Delworth. 2002. "Increasing Risk of Great Floods in a Changing Climate." Pp. 514-517 in Nature. Vol 415.

Nakicenovic, N. 2000. A Special Report on Emissions Scenarios from Working Group III of the Intergovernmental Panel on Climate Change (IPCC). Cambridge University Press. Available at http://www.grida.no/publications/other/ipcc_sr/?src=/climate/ipcc/emission/index.htm.

National Oceanic and Atmospheric Administration: Center for Oceanographic Products and Services (NOAA CO-OPS). Data available online at: http://tidesandcurrents.noaa.gov.

Nicholls, R.J., N. Marinova, J.A. Lowe, S. Brown, P. Vellinga, D. de Gusmão, J. Hinkel, and R.S.J. Tol. 2010. "Sea-level rise and its possible impacts given a 'beyond 4°C world' in the twenty-first century." Pp. 161-181 in Phil. Trans. R. Soc. A (2011) Vol. 369, DOI: 1098/rsta.2010.0291. Available at http://www.ecoshock.org/transcripts/RoySoc%204D%20Sea%20Level.pdf

Pfeffer. 2008. Kinematic Constraints on Glacier Contributions to 21st Century Sea-Level Rise. Pp. 1340-1343 in Science. Vol. 321. DOI: 10.1126/science.1159099.

PricewaterhouseCoopers LLP. 1999. Study of the Economic Effects of Charging Actuarially Based Premium Rates for Pre-FIRM Structures. Washington, D.C.: FEMA. Available online at http://www.fema.gov/library/viewRecord.do?id=2555.

Rahmstorf, S. 2007. A Semi-Empirical Approach to Projecting Future Sea-Level Rise. Pp. 368-370 in Science. Vol. 315. DOI: 10.1126/science.1135456.

Resio, D. T., J. L. Irish, and M.A. Cialone. 2009. "A Surge Response Function Approach to Coastal Hazard Assessment – Part 1: Basic Concepts." Natural Hazards.

Sauer, V.B., W. Thomas, V. Stricker, and K. Wilson. 1983. "Flood Characteristics of Urban Watersheds in the United States." Pp. 63 in the United States Geological Survey Paper 2207.

Tebaldi, C., K. Hayhoe, J. Arblaster, and G. Meehl. 2006. "Going to the Extremes: An Intercomparison of Model-Simulated Historical and Future Changes in Extreme Events." Pp. 185-211 in Climatic Change. Vol. 79.

Thieler, E.R., J. Williams, and E. Hammar-Klose. 1999–2000. National Assessment of Coastal Vulnerability to Sea-Level Rise. Woods Hole Field Center, Woods Hole, MA. Available at http://woodshole.er.usgs.gov/project-pages/cvi.

Titus J.G., and J. Wang. 2008. Maps of Lands Close to Sea Level along the Middle Atlantic Coast of the United States: An Elevation Data Set to Use While Waiting for LIDAR. Section1.1 in Background Documents Supporting Climate Change Science Program Synthesis and Assessment Product 4.1. EPA 430R07004. United States Environmental Protection Agency, Washington, D.C.

Toro, G., D.T. Resio, D. Divoky, A.W. Niedoroda, and C.W. Reed. 2010a. "Efficient Joint Probability Methods for Hurricane Surge Frequency Analysis." Journal of Ocean Engineering.

Toro, G., A.W. Niedoroda, C.W. Reed, and D. Divoky. 2010. "Quadrature-Based Approach for the Efficient Calculation of Surge Hazard." Journal of Ocean Engineering.

Vermeer, M. and S. Rahmstorf. 2009. Global Sea Level Linked to Global Temperature. Pp. 21527-21532 in Proceedings of the National Academy of Sciences. Vol. 106: 51.

Weiss, J.L., and J.T. Overpeck. 2006. Climate Change and Sea Level: Maps of Susceptible Areas. Department of Geosciences, University of Arizona. Available at http://www.geo.arizona.edu/dgesl/index.html.

Wuebbles, D.J., K. Hayhoe, and J. Parzen. 2010. "Introduction: Assessing the effects of climate change on Chicago and the Great Lakes." Pp. 1-6 in Journal of Great Lakes Research, Vol 36, Supplement 2.